

---

**Pacific Northwest  
National Laboratory**

Operated by Battelle for the  
U.S. Department of Energy

# Results of Detailed Hydrologic Characterization Tests— Fiscal and Calendar Year 2005

F. A. Spane  
D. R. Newcomer

February 2008



Prepared for the U.S. Department of Energy  
under Contract DE-AC05-76RL01830

---

## DISCLAIMER

This report was prepared as an account of work sponsored by an agency of the United States Government. Neither the United States Government nor any agency thereof, nor Battelle Memorial Institute, nor any of their employees, makes **any warranty, express or implied, or assumes any legal liability or responsibility for the accuracy, completeness, or usefulness of any information, apparatus, product, or process disclosed, or represents that its use would not infringe privately owned rights.** Reference herein to any specific commercial product, process, or service by trade name, trademark, manufacturer, or otherwise does not necessarily constitute or imply its endorsement, recommendation, or favoring by the United States Government or any agency thereof, or Battelle Memorial Institute. The views and opinions of authors expressed herein do not necessarily state or reflect those of the United States Government or any agency thereof.

PACIFIC NORTHWEST NATIONAL LABORATORY

*operated by*

BATTELLE

*for the*

UNITED STATES DEPARTMENT OF ENERGY

*under Contract DE-AC05-76RL01830*

Printed in the United States of America

Available to DOE and DOE contractors from the  
Office of Scientific and Technical Information,

P.O. Box 62, Oak Ridge, TN 37831-0062;

ph: (865) 576-8401

fax: (865) 576 5728

email: reports@adonis.osti.gov

Available to the public from the National Technical Information Service,  
U.S. Department of Commerce, 5285 Port Royal Rd., Springfield, VA 22161

ph: (800) 553-6847

fax: (703) 605-6900

email: orders@nits.fedworld.gov

online ordering: <http://www.ntis.gov/ordering.htm>

## **Results of Detailed Hydrologic Characterization Tests— Fiscal and Calendar Year 2005**

F. A. Spane  
D. R. Newcomer

February 2008

Prepared for the U.S. Department of Energy  
under Contract DE-AC05-76RL01830

Pacific Northwest National Laboratory  
Richland, Washington 99352

## **Abstract**

This report provides the results of detailed hydrologic characterization tests conducted within selected Hanford Site wells during fiscal and calendar year 2005. Detailed characterization tests performed included groundwater-flow characterization, barometric response evaluation, slug tests, in-well vertical groundwater-flow assessments, and a single-well tracer and constant-rate pumping test. Hydraulic property estimates obtained from the detailed hydrologic tests include hydraulic conductivity, transmissivity, specific yield, effective porosity, in-well lateral and vertical groundwater-flow velocity, aquifer groundwater-flow velocity, and depth-distribution profiles of hydraulic conductivity. In addition, local groundwater-flow characteristics (i.e., hydraulic gradient and flow direction) were determined for a site where detailed well testing was performed. Results obtained from these tests provide hydrologic information that supports the needs of Resource Conservation and Recovery Act waste management area characterization as well as sitewide groundwater monitoring and modeling programs. These results also reduce the uncertainty of groundwater-flow conditions at selected locations on the Hanford Site.



## Summary

The U.S. Department of Energy's Hanford Groundwater Monitoring Project, managed by Pacific Northwest National Laboratory, examines the potential for offsite migration of contamination within aquifer systems underlying the Hanford Site. An important characterization element that helps define the migration of contamination is the analysis of hydrologic tests, which provide estimates of hydraulic properties for the tested aquifer systems. Information gained from analyzing hydrologic tests is important when evaluating aquifer-flow characteristics (i.e., groundwater-flow velocity) and transport travel time, which are key parts of effective groundwater monitoring and modeling. Obtaining representative hydraulic-property information for the unconfined aquifer beneath the Hanford Site can be complicated by temporal changes in the water-table elevation and associated aquifer thickness. In particular, earlier hydrologic tests in the 200-West and 200-East Areas may reflect overlying, hydrogeologic units that are no longer saturated and are not part of the current groundwater flow system. Obtaining current information on hydraulic properties of the aquifer provides a way to assess the reliability and/or representativeness of earlier data and provides up-to-date information that can be used for effective groundwater monitoring and modeling.

This report presents test results obtained from the detailed hydrologic characterization program of the unconfined aquifer system conducted for the Hanford Groundwater Monitoring Project during fiscal (FY) and calendar year (CY) 2005. Hydrologic tests conducted as part of the detailed program include the following:

- slug testing (9 completed wells tested)
- discrete depth interval slug testing (3 boreholes tested; with a total of 14 discrete-depth interval tests)
- tracer-dilution tests (1 well tested)
- tracer-pumpback tests (1 well tested)
- constant-rate pumping tests (1 well tested)
- vertical flow, in-well assessment (3 wells tested).

Hydrologic test results conducted during FY and CY 2005 for eight wells tested in the 200-West Area reflect hydrogeologic Unit 5 of the Ringold Formation (gravel Unit E). For the one well tested in the 200-East Area, results are associated with hydrogeologic Unit 1 of the Hanford formation (sand and gravel dominated facies). Hydraulic-property estimates obtained from the detailed hydrologic tests include hydraulic conductivity, transmissivity, specific yield, effective porosity, in-well lateral and vertical groundwater-flow velocity, aquifer groundwater-flow velocity, and vertical depth distribution of hydraulic conductivity. In addition, local groundwater-flow characteristics (i.e., hydraulic gradient, flow direction) were determined for the one site where detailed tracer testing was performed. Pertinent results from the FY and CY 2005 detailed characterization program are summarized in the following paragraphs.

Slug-test results for completed wells provided hydraulic-conductivity estimates that ranged from 3.8 to 17.7 m/day for the eight 200-West Area wells, and averaged 96.9 m/day for the one 200-East Area

well. These results are consistent with previously reported slug-test values for the Ringold Formation and Hanford formation within the 200-West and 200-East Areas, respectively. Examination of selected depth-discrete slug-test characterization results for three 200-West Area locations (299-W11-25B, 299-W14-11, and 299-W22-47) indicates no distinct areal depth-profile pattern for hydraulic conductivity that is consistent for all borehole sites. In most cases, a relatively uniform vertical distribution/depth profile was exhibited at each test location.

Analysis of the constant-rate pumping test results for well 299-W22-47 indicates a transmissivity, hydraulic conductivity, and specific yield value of 1116 m<sup>2</sup>/day, 16.5 m/day, and 0.3, respectively. The specific yield estimate is considered to be less certain than the transmissivity and hydraulic conductivity estimates because of the relatively short duration (i.e., ~4 hr) allotted for the pumping test. A comparison of the slug-test-derived hydraulic conductivity estimate at well 299-W22-47 (average type-curve analysis value;  $K = 17.3$  m/day) with the value obtained from the constant-rate pumping test ( $K = 16.5$  m/day) indicates a very close correspondence. This close correspondence exhibited between slug and pumping test estimates is consistent with previous test comparisons at the Hanford Site and falls within the error range commonly reported for slug tests in aquifer characterization studies (i.e., within a factor of ~2 or less in comparison to pumping test-derived values).

In-well, upward vertical groundwater-flow conditions were measured within three completed wells (299-W11-25B, 299-W14-11, and 299-W22-47) using electromagnetic borehole flowmeter surveys. The cause of the observed, in-well vertical flow conditions is not known, but may be the result of either 1) proximity to local discharge, 2) heterogeneous formation conditions along the well screen, or 3) effects from neighboring well-pumping/-sampling or remedial action activities. The existence of vertical flow is not necessarily reflective of actual groundwater-flow conditions within the surrounding aquifer, but its presence implies a vertical flow gradient and has implications pertaining to the representativeness of groundwater samples collected from such monitor-well facilities.

Based on the low in-well vertical groundwater-flow rates exhibited at well 299-W22-47 (i.e., 0.005 to 0.011 m/min, it was the selected as the site for detailed tracer-dilution and pumpback testing. The tracer-dilution test results indicated an average in-well lateral groundwater-flow velocity ( $v_w = 0.13$  m/day), and the observed tracer dilution depth profile patterns corroborated the presence of a slight upward in-well vertical groundwater-flow condition. Results from the tracer-pumpback test provided estimates for effective porosity and aquifer groundwater-flow velocity of 0.294 and 0.093 m/day (~34 m/year), respectively. However, because of the relatively small radial distance effectively characterized by this test (i.e., ~0.2 m), these property values may be considered to be only qualitative estimates for the surrounding aquifer.

Quantitative groundwater-flow characterization provided groundwater-flow direction and hydraulic gradient information during the tracer-dilution test period. This was based on trend-surface analysis of water-table elevation data for selected monitoring wells surrounding well 299-W22-47. The analysis results indicated a consistent east-southeasterly groundwater-flow direction and a hydraulic gradient of 0.00165 m/m. These groundwater-flow characteristics are consistent with conditions reported for this general area of the Hanford Site.

## **Acknowledgments**

Several Pacific Northwest National Laboratory staff members contributed to the hydrologic tests presented in this report. In particular, Kirk Cantrell provided laboratory and field support for the tracer tests. Alex Mitroshkov performed laboratory bromide analyses on discrete water samples collected during tracer-pumpback tests. Bruce Williams identified hydrogeologic units tested at the well sites. The field-testing personnel and test equipment support provided by Duratek Federal Services, Inc. is also acknowledged.

In addition, Pacific Northwest National Laboratory staff members contributed significantly to this report's preparation. Paul Thorne and Wayne Cosby provided technical peer review and editorial comments, respectively. Thanks are also extended to Jon Fruchter and Stuart Luttrell (now with Fluor Hanford, Inc.) for providing project funding support.





## Acronyms

CY	calendar year
DOE	U.S. Department of Energy
DOE/RL	U.S. Department of Energy/Richland Operations
EBF	electromagnetic borehole flowmeter
FY	fiscal year
I.D.	inside diameter
KGS	Kansas Geological Survey
MSL	mean sea level
NAVD88	North American Vertical Datum of 1988
O.D.	outside diameter
PDT	Pacific Daylight Time
PNNL	Pacific Northwest National Laboratory
PST	Pacific Standard Time
RCRA	Resource Conservation and Recovery Act
SST	single-shell tank
WMA	Waste Management Area



## Nomenclature

- $A$  = cross-sectional area within well screen;  $L^2$   
 $b$  = aquifer thickness;  $L$   
 $C$  = tracer concentration in the test interval at time,  $t$ ;  $M$  per  $L^3$   
 $C_D$  = well slug-test-response damping parameter; dimensionless  
 $C_o$  = initial tracer concentration in well at the start of the test;  $M$  per  $L^3$   
 $C_t$  = average tracer concentration in well at test termination;  $M$  per  $L^3$   
 $g$  = acceleration due to gravity;  $L/T^2$   
 $\Delta h_w$  = water-level change over the last hour;  $L$   
 $\Delta h_{ai}$  = barometric pressure change over the last hour;  $L$   
 $\Delta h_{ai-1}$  = barometric pressure change from 2 h to 1 h previous;  $L$   
 $\Delta h_{ai-n}$  = barometric pressure change from  $n$  hours to  $(n-1)$  hour previous;  $L$   
 $H_o$  = theoretical slug-test stress level;  $L$   
 $H_p$  = projected or observed slug-test stress level;  $L$   
 $H_{p-out}$  = projected initial slug-test stress level for outer zone analysis;  $L$   
 $I$  = hydraulic gradient; dimensionless  
 $K$  = hydraulic conductivity;  $L/T$   
 $K_D$  = vertical anisotropy ( $K_v/K_h$ ); dimensionless  
 $K_h$  = hydraulic conductivity in the horizontal direction;  $L/T$   
 $K_{hx}/K_{hy}$  = horizontal anisotropy; dimensionless  
 $K_{snd}$  = hydraulic conductivity of sandpack;  $L/T$   
 $K_v$  = hydraulic conductivity in the vertical direction;  $L/T$   
 $L_e$  = effective well water-column length;  $L$   
 $L_s$  = well-screen length;  $L$   
 $m$  = saturated thickness of test interval within well-screen section;  $L$   
 $M_i$  = initial tracer mass emplaced in well;  $M$   
 $M_r$  = tracer mass recovered during pumpback;  $M$   
 $M_w$  = tracer mass in well and sandpack at time of pumpback;  $M$   
 $M_{50\%}$  = 50% of the tracer mass within the aquifer;  $M$   
 $n$  = number of hours that lagged barometric effects are apparent; dimensionless  
 $n_e$  = effective porosity; dimensionless  
 $Q$  = pumping rate;  $L^3/T$   
 $Q_{avg}$  = average pumping rate;  $L^3/T$   
 $Q_w$  = in-well lateral groundwater discharge within the well test interval;  $L^3/T$   
 $r_c$  = well casing radius;  $L$   
 $r_{eq}$  = equivalent well casing radius;  $L$   
 $r_{eq-in}$  = equivalent well casing radius for inner-zone analysis;  $L$   
 $r_{eq-out}$  = equivalent well casing radius for outer zone analysis;  $L$   
 $r_{obs}$  = radial distance from pumped well to monitor-well location;  $L$   
 $r_{snd}$  = sandpack radius;  $L$   
 $r_t$  = equivalent radius of tracer measurement system;  $L$

$r_w$  = radius of pumping well; L  
 $R_e$  = effective test radius parameter; as defined by Bouwer and Rice (1976); L  
 $s$  = drawdown; L  
 $s'$  = drawdown corrected for aquifer dewatering; L  
 $S$  = storativity; dimensionless  
 $S_s$  = specific storage; 1/L  
 $S_y$  = specific yield; dimensionless  
 $T$  = transmissivity;  $L^2/T$   
 $t$  = time; T  
 $t_d$  = tracer dilution or drift time; T  
 $t_p$  = pumping time required to recover 50% of the tracer; T  
 $t_t$  = total elapsed tracer time, equal to  $t_d + t_p$ ; T  
 $V$  = well volume over measurement section;  $L^3$   
 $V_w$  = test interval well volume;  $L^3$   
 $v_a$  = groundwater-flow velocity within aquifer; L/T  
 $v_v$  = vertical groundwater-flow velocity within well; L/T  
 $v_w$  = lateral groundwater-flow velocity within well; L/T  
 $v_{wz}$  = lateral groundwater-flow velocity for individual depths within well; L/T  
 $X_{0n}$  = regression coefficients corresponding to time lags of 0 to n hours; dimensionless  
 $Y_o$  = slug-test stress level; L  
 $\sigma$  = dimensionless unconfined aquifer parameter, equal to  $S/S_y$   
 $\infty$  = groundwater-flow distortion factor; dimensionless, common range 0.5 to 4

# Contents

Abstract .....	iii
Summary .....	v
Acknowledgments.....	vii
Acronyms.....	ix
Nomenclature.....	xi
1.0 Introduction.....	1.1
2.0 Hydrogeologic Setting .....	2.1
2.1 Hydrogeology of the 200-West Area.....	2.1
2.2 Hydrogeology of the 200-East Area .....	2.4
3.0 Detailed Test Characterization Methods.....	3.1
3.1 Slug Tests .....	3.1
3.1.1 Over-Damped Test Analysis Methods.....	3.4
3.1.2 High-Permeability/Under-Damped Analysis Methods.....	3.11
3.1.3 Drill-and-Test Boreholes .....	3.13
3.2 Single-Well Tracer Tests .....	3.17
3.2.1 Tracer-Dilution Tests.....	3.17
3.2.2 Tracer-Pumpback Tests .....	3.19
3.2.3 In-Well Vertical Flow Assessment.....	3.21
3.3 Constant-Rate Pumping Tests.....	3.24
3.3.1 Test Methods and Equipment .....	3.24
3.3.2 Barometric Pressure Effects Removal .....	3.24
3.3.3 Unconfined Aquifer Dewatering Drawdown Correction.....	3.25
3.3.4 Diagnostic Analysis and Derivative Plots .....	3.26
3.3.5 Type-Curve-Matching Analysis Methods.....	3.28
3.3.6 Straight-Line Analysis Methods .....	3.29
3.4 Groundwater-Flow Characterization .....	3.29
4.0 Slug-Test Results .....	4.1
4.1 Completed Well Slug-Test Characterizations.....	4.1
4.1.1 Well 299-E33-49 .....	4.1
4.1.2 Well 299-W11-46 .....	4.4
4.1.3 Well 299-W14-11 .....	4.5
4.1.4 Well 299-W15-83 .....	4.5

4.1.5	Well 299-W15-94 .....	4.8
4.1.6	Well 299-W15-152 .....	4.12
4.1.7	Well 299-W19-47 .....	4.16
4.1.8	Well 299-W22-47 .....	4.16
4.1.9	Well 299-W22-80 .....	4.19
4.2	Borehole Test/Depth Interval Characterizations.....	4.24
4.2.1	299-W11-25B .....	4.24
4.2.2	299-W14-11 .....	4.32
4.2.3	299-W22-47 .....	4.41
5.0	Tracer-Dilution Test Results: Well 299-W22-47 .....	5.1
6.0	Tracer-Pumpback Test Results: Well 299-W22-47 .....	6.1
7.0	Constant-Rate Pumping Test Results: Well 299-W22-47 .....	7.1
8.0	Groundwater-Flow Characterization Results.....	8.1
8.1	Ambient, In-Well Vertical Flow Characterization .....	8.1
8.1.1	Well 299-W14-11 .....	8.1
8.1.2	Well 299-W22-47 .....	8.3
8.1.3	Well 299-W22-80 .....	8.5
8.2	Lateral Groundwater-Flow Conditions: Well 299-W22-47.....	8.7
9.0	Conclusions.....	9.1
9.1	Slug and Pumping Test Results .....	9.1
9.2	Single-Well Tracer Test Results .....	9.3
10.0	References.....	10.1
Appendix A.	Selected Analysis Figures for Test/Depth Intervals: Boreholes 299-W11-25B, 299-W14-11, and 299-W22-47	
Appendix B.	Summary of Recent Slug-Test Characterization Results for Completed Wells Within the General 200-West Area	

## Figures

1.1. Location Map of Wells Tested During Fiscal and Calendar Year 2005 .....	1.3
2.1. Stratigraphic Relationships of Various Hydrogeologic Units.....	2.2
2.2. Hydrogeologic Cross Section Through 200-West and 200-East Areas .....	2.3
3.1. Diagnostic Slug-Test-Response Types .....	3.5
3.2. Predicted Slug-Test Response for Nonelastic Formation, Elastic Formation, and High Hydraulic Conductivity Sand-Pack Conditions .....	3.6
3.3. Predicted Slug-Test Response: Negative Finite-Thickness Skin Conditions .....	3.9
3.4. Predicted Slug-Test Derivative Response: Negative Finite-Thickness Skin Conditions.....	3.9
3.5. Predicted Slug-Test Response: Positive Finite-Thickness Skin Conditions .....	3.10
3.6. Effects of Hydraulic Conductivity on Predicted Under-Damped Slug-Test Response .....	3.12
3.7. General Pneumatic Slug-Test System Using Dual-Wall Drill Casing System.....	3.14
3.8. Visualization of Slug-Test-Response System Using a Dual-Wall Drill Casing System .....	3.15
3.9. Example of Test-System Oscillatory Response Superimposed on Over-Damped, Slug-Test Recovery .....	3.16
3.10. Hypothetical Tracer-Dilution Pattern Indicative of Vertical In-Well Downward Flow .....	3.22
3.11. Characteristic Log-Log Drawdown and Drawdown Derivative Plots for Various Hydrogeologic Formation and Boundary Conditions.....	3.27
4.1. High-K, Critically-Damped Slug-Test Analysis Plot for Well 299-E33-49 .....	4.4
4.2. Selected Slug-Test Analysis Plots for Well 299-W11-46.....	4.6
4.3. Selected Slug-Test Analysis Plots for Well 299-W14-11.....	4.7
4.4. Heterogeneous Formation Slug-Test Response Exhibited for Well 299-W15-83.....	4.8
4.5. Selected Slug-Test Type-Curve Analysis Plots for Well 299-W15-83: Inner-Zone Analysis.....	4.9
4.6. Selected Slug-Test Analysis Plots for Well 299-W15-83: Outer Zone Analysis .....	4.10
4.7. Heterogeneous Formation Slug-Test Response Exhibited for Well 299-W15-94.....	4.11
4.8. Selected Slug-Test Type-Curve Analysis Plots for Well 299-W15-94: Inner-Zone Analysis .....	4.11



4.9. Selected Slug-Test Analysis Plots for Well 299-W15-94: Outer Zone Analysis .....	4.13
4.10. Heterogeneous Formation Slug-Test Response Exhibited for Well 299-W15-152.....	4.14
4.11. Selected Slug-Test Type-Curve Analysis Plots for Well 299-W15-152: Inner-Zone Analysis .....	4.14
4.12. Selected Slug-Test Analysis Plots for Well 299-W15-152: Outer Zone Analysis .....	4.15
4.13. Heterogeneous Formation Slug-Test Response Exhibited for Well 299-W19-47.....	4.17
4.14. Selected Slug-Test Type-Curve Analysis Plots for Well 299-W19-47: Inner-Zone Analysis .....	4.17
4.15. Selected Slug-Test Analysis Plots for Well 299-W19-47: Outer Zone Analysis .....	4.18
4.16. Combined Slug-Test Analysis Plots for Well 299-W22-47.....	4.20
4.17. Predicted Slug-Test Type-Curve Response Plots for Well 299-W22-80.....	4.21
4.18. Comparison of Low-Stress, Slug-Test-Response Plots for Well 299-W22-80.....	4.22
4.19. Combined Slug-Test Analysis Plots for Well 299-W22-80.....	4.23
4.20. Well 299-W11-25B Location Map .....	4.25
4.21. Hydraulic Conductivity Profile at Borehole 299-W11-25B .....	4.29
4.22. Well 299-W14-11 Location Map.....	4.33
4.23. Hydraulic Conductivity Profile at Borehole 299-W14-11 .....	4.37
4.24. Well 299-W22-47 Location Map.....	4.42
4.25. Hydraulic Conductivity Profile at Borehole 299-W22-47 .....	4.45
5.1. Average Tracer-Dilution Test Results Within Well 299-W22-47 .....	5.3
6.1. Tracer-Pumpback Test Results for Well 299-W22-47 .....	6.2
7.1. Barometric Pressure and Associated Well Water-Level Response during a 21-Day Baseline Monitoring Period at Well 299-W22-47.....	7.3
7.2. Barometric Response Analysis Plot for Well 299-W22-47 .....	7.4
7.3. Drawdown and Recovery Test Data Comparison for Pumping Well 299-W22-47.....	7.4
7.4. Type-Curve and Derivative Plot Analysis of Recovery Test Data for Pumping Well 299-W22-47 .....	7.5
8.1. Map of 200-West Area Wells Surveyed with the Electromagnetic Borehole Flowmeter .....	8.2

8.2. Well 299-W14-11 EBF Ambient Survey Results: Measured Vertical Flow-Rate Profile (top), and Calculated Differential Lateral Flow-Rate Profile (bottom) .....	8.4
8.3. Well 299-W22-47 EBF Ambient Survey Results: Measured Vertical Flow-Rate Profile (top), and Calculated Differential Lateral Flow-Rate Profile (bottom) .....	8.6
8.4. Well 299-W22-80 EBF Ambient Survey Results: Measured Vertical Flow-Rate Profile (top), and Calculated Differential Lateral Flow-Rate Profile (bottom) .....	8.8
9.1. Hydraulic Conductivity Histogram for Recently Tested 200-West Area Wells.....	9.2

## Tables

1.1. New and Recently Constructed RCRA Wells Characterized in Fiscal and Calendar Year 2005 .....	1.2
1.2. Pertinent As-Built Information for Wells Tested During Fiscal and Calendar Year 2005 .....	1.4
3.1. Detailed Hydrologic Characterization Elements .....	3.1
4.1. Completed Well Slug-Test Characteristics .....	4.2
4.2. Completed Well Slug-Test Results .....	4.3
4.3. Slug-Test Characteristics for Selected Test/Depth Intervals at 299-W11-25B .....	4.26
4.4. 299-W11-25B Test/Depth Interval Slug-Test Analysis Results .....	4.28
4.5. Slug-Test Characteristics for Selected Test/Depth Intervals at 299-W14-11 .....	4.34
4.6. 299-W14-11 Test/Depth Interval Slug-Test Analysis Results.....	4.36
4.7. Slug-Test Characteristics for Selected Test/Depth Intervals at 299-W22-47 .....	4.43
4.8. 299-W22-47 Test/Depth Interval Slug-Test Analysis Results.....	4.44
6.1. Tracer-Pumpback Test Summary for Well 299-W22-47.....	6.2
7.1. Constant-Rate Pumping Test Summary .....	7.1
8.1. Summary of Ambient EBF Flowmeter Survey Results .....	8.3
8.2. Groundwater-Flow Characterization Analysis Results.....	8.9

## 1.0 Introduction

The Hanford Groundwater Monitoring Project managed by Pacific Northwest National Laboratory (PNNL) assesses the potential for onsite and offsite migration of contamination within the shallow, unconfined, aquifer system and the underlying, upper, basalt-confined aquifer system at the Hanford Site. As part of this activity, detailed hydrologic characterization tests are conducted within wells at selected Hanford Site locations to provide hydraulic property information and groundwater-flow characterization for the unconfined aquifer. Results obtained from these characterization tests provide hydrologic information that supports the needs of the *Resource Conservation and Recovery Act* (RCRA) (42 USC 6901) facility hydrogeologic characterization and sitewide groundwater monitoring and modeling programs. These results also reduce the uncertainty of groundwater-flow conditions at selected locations on the Hanford Site.

This report is the sixth of a series that provides the results of detailed hydrologic characterization tests conducted within recently constructed Hanford Site wells completed within the unconfined aquifer system. In the previous five reports, Spane et al. (2001a, 2001b, 2002, 2003) and Spane and Newcomer (2004) presented the results of hydrologic characterization tests conducted during Fiscal Year (FY) 1999, 2000, 2001, 2002, and 2003, respectively. In this report, results of tests conducted during FY and Calendar Year (CY) 2005 are provided. The various characterization elements employed in FY and CY 2005, as part of the detailed hydrologic characterization program, include the following:

- slug tests—to evaluate well-development conditions and provide preliminary hydraulic-property information (e.g., hydraulic conductivity) for the design of subsequent hydrologic tests
- tracer-dilution tests—to determine the vertical distribution of hydraulic conductivity and/or groundwater-flow velocity within the well-screen section and to identify vertical flow conditions within the well column
- tracer-pumpback tests—to characterize effective porosity and average, aquifer, groundwater-flow velocity
- constant-rate pumping tests—to provide quantitative hydraulic property information (e.g., transmissivity, hydraulic conductivity, storativity, specific yield) when conducted in concert with tracer-pumpback phase and analysis of drawdown and recovery data
- in-well vertical flow surveys—to assess in-well vertical flow conditions within the well-screen section
- barometric-response evaluation—to compare the characteristics of well response to barometric fluctuations, estimate vadose zone transmission characteristics, and remove barometric pressure effects from hydrologic test responses

- groundwater-flow characterization—to quantify the direction of groundwater flow and hydraulic gradient conditions.

Newly constructed and existing RCRA wells selected for characterization during FY and CY 2005 are listed in Table 1.1. The RCRA wells are all constructed of 10.16-centimeter-diameter stainless-steel casing with wire-wrapped stainless-steel screens and sand pack. These wells were constructed either to replace older wells that are going dry because of the declining water table (e.g., 200-West Area) or for additional monitoring well areal coverage. Most wells tested are screened across the water table and penetrate approximately the top 3 to 10 meters of the aquifer. One of the test wells (299-W22-47) was selected to provide detailed hydraulic characterization information within the Waste Management Area (WMA) SST-S-SX. Figure 1.1 shows the location of the wells tested during FY and CY 2005 in relationship to the 200-West and 200-East Areas of the Hanford Site. The alignment of the hydrogeologic cross-section discussed in Chapter 2 is also shown in the figure. Boundaries of the various RCRA waste management areas are presented on site maps contained in Hartman et al. (2006). Table 1.2 provides pertinent as-built and well-completion information for the identified test wells. This report presents the results of hydrologic characterization conducted at these well sites during FY and CY 2005.

**Table 1.1.** New and Recently Constructed RCRA Wells Characterized in Fiscal and Calendar Year 2005

Well	RCRA Waste Management Area
299-E33-49	SST B-BX-BY
299-W11-25B	SST T
299-W11-46	SST T
299-W14-11	SST TX-TY
299-W15-83	LLWMA-4
299-W15-94	LLWMA-4
299-W15-152	LLWMA-4
299-W19-47	SST U
299-W22-47	SST S-SX
299-W22-80	SST S-SX
SST = Single-shell tank.	

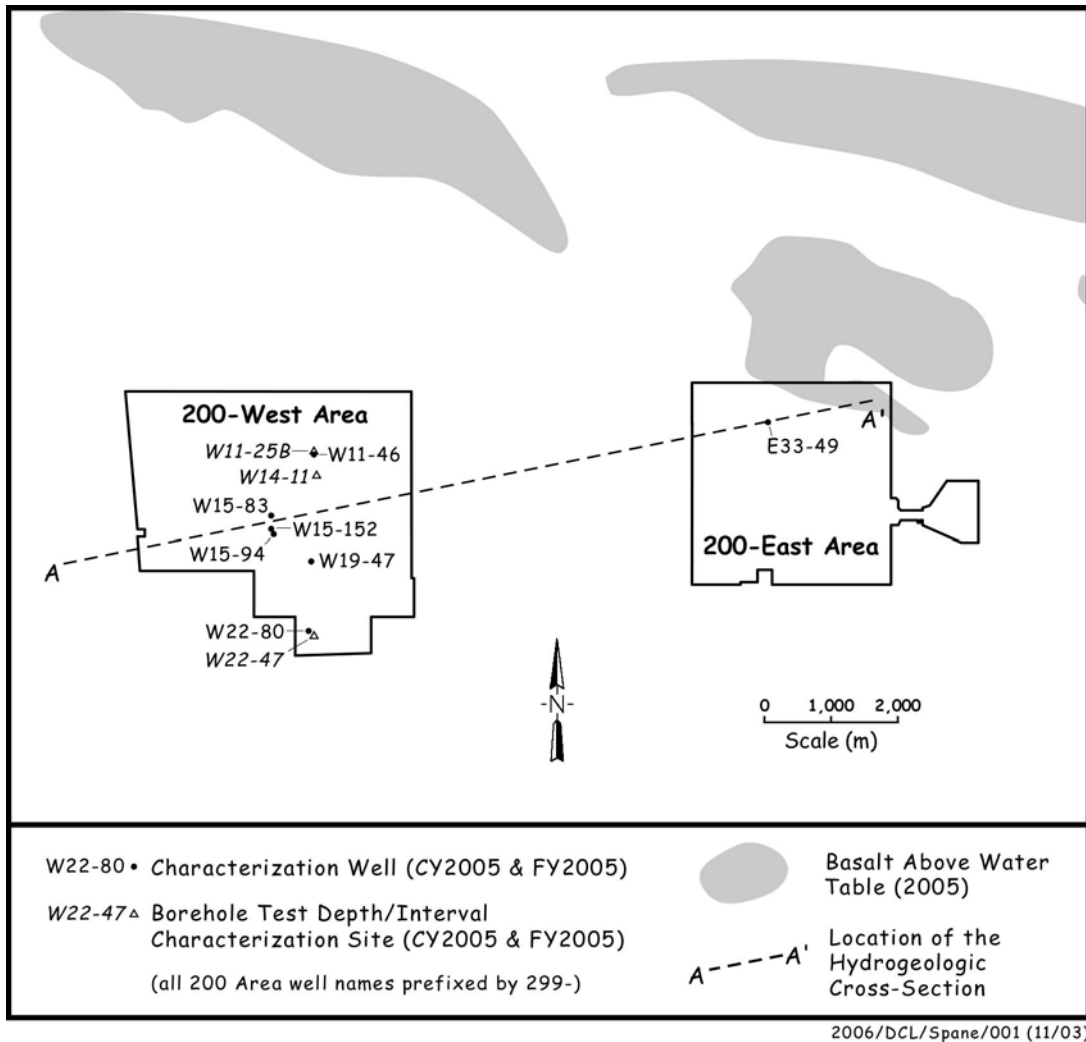


**Figure 1.1.** Location Map of Wells Tested During Fiscal and Calendar Year 2005

**Table 1.2.** Pertinent As-Built Information for Wells Tested During Fiscal and Calendar Year 2005

<b>Well</b>	<b>Ground Surface/Brass-Cap Elevation, m, MSL (NAVD88)</b>	<b>Well-Screen Depth Below Ground Surface/Brass Cap, m</b>	<b>Saturated Well-Screen Section, m, MSL (NAVD88)</b>
299-E33-49	203.24	80.31–86.41	122.12–116.83 (5.29) <sup>(a)</sup>
299-W11-46	210.12	80.28–86.38	129.84–123.74 (6.10) <sup>(b)</sup>
299-W14-11	204.38	79.76–82.81	124.62–121.57 (3.05) <sup>(c)</sup>
299-W15-83	208.95	71.63–82.30	136.45–126.65 (9.80)
299-W15-94	209.41	71.96–82.63	136.86–126.78 (10.08)
299-W15-152	209.41	72.51–82.61	136.90–126.80 (10.10)
299-W19-47	205.55	69.20–79.87	135.87–125.68 (10.19)
299-W22-47	205.53	69.70–80.37	135.61–125.16 (10.45)
299-W22-80	199.97	62.49–73.17	135.79–126.80 (8.99)
<p>(a) Number in parentheses is saturated thickness within the well-screen interval; it reflects conditions at time of slug testing.</p> <p>(b) Water table is located 6.45 m above top of well screen.</p> <p>(c) Water table is located 11.00 m above top of well screen.</p> <p>MSL = mean sea level.</p> <p>NAVD88 = North American Vertical Datum of 1988.</p>			

## 2.0 Hydrogeologic Setting

Major hydrogeologic units within the sediments above the basalt bedrock in the 200-West and 200-East Areas include the Ringold Formation and the overlying, informally named, Hanford formation. The less extensive Cold Creek Unit occurs between these formations in some places. Lindsey (1995) has stratigraphically divided the Ringold Formation into different facies associations based on geologic characteristics and depositional environment. The facies classifications and depositional environments of post-Ringold sediments, including the Cold Creek Unit and the Hanford formation, are discussed in DOE (2002). In addition to this geologic classification system, a hydrogeologic-based classification system was developed (Thorne et al. 1993; Cole et al. 2001) to support consolidated groundwater-modeling studies of the Hanford Site. This system is also based on the Ringold facies classification of Lindsey (1995), but subdivides units based on texture with less emphasis on the time of deposition. A comparison of the two classifications is shown in Figure 2.1. The major classification system difference in the vicinity of the 200 Areas is the grouping of the lower sand-dominated portion of Lindsey's (1995) upper Ringold with Ringold gravel Units E and C to form hydrogeologic model Unit 5 with the overlying fine-grained upper Ringold sediments forming model Unit 4. A general west-to-east cross section in Figure 2.2 shows the hydrogeologic units underlying the 200-West and 200-East Areas. Figure 1.1 shows the surface trace of the cross section in relationship to the test wells described in this report.

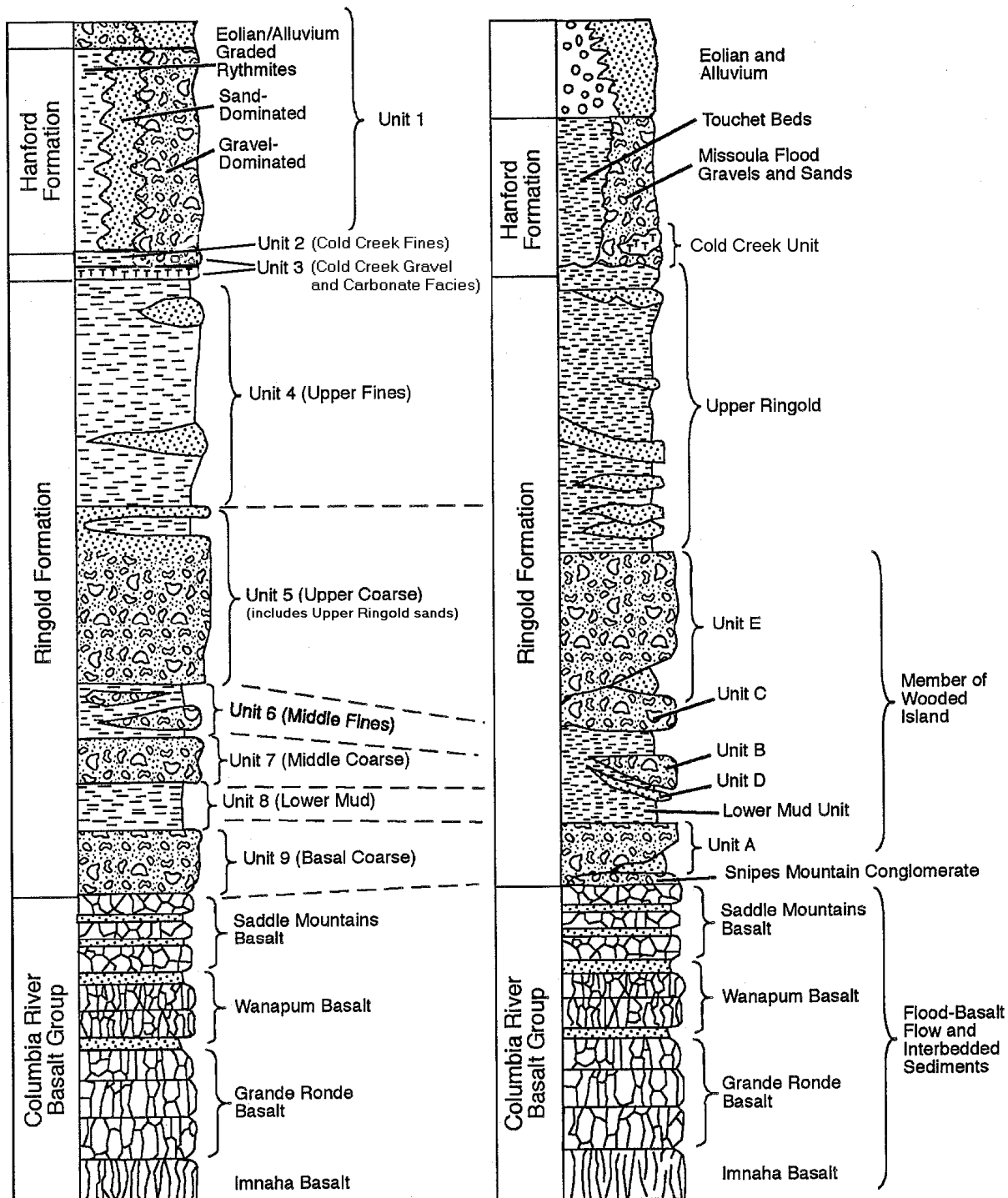
The brief hydrogeologic description for the 200-West and 200-East Areas presented below is taken primarily from Spane et al. (2003), which is based on the following reports: Graham et al. (1984), Lindsey et al. (1992), Connelly et al. (1992a, 1992b), Thorne et al. (1993), Lindsey (1995), and Williams et al. (2000).

### 2.1 Hydrogeology of the 200-West Area

The aquifer system above the basalt bedrock in the 200-West Area comprises two aquifer systems: an unconfined aquifer and an underlying, locally confined aquifer. The unconfined aquifer lies almost entirely within the Ringold Unit E gravel (Unit 5) and is composed of fluvial, gravel-dominated sediments with a fine-sand matrix. The FY and CY 2005 results for test wells located in the 200-West Area reflect the Ringold Unit E gravel (Unit 5). Sediment within this hydrogeologic unit exhibits variable degrees of cementation, ranging from partially to well-developed. Cemented zones up to several meters thick and extending laterally over several hundred meters have been identified in the 200-West Area. Thin, laterally discontinuous, sand and silt beds also are intercalated in the gravelly deposits.

The lower Ringold mud (Unit 8), consisting of overbank and lacustrine deposits, underlies the unconfined aquifer. This mud unit is continuous over all but the northeast corner of the 200-West Area (Reidel and Chamness 2007). It is also generally absent just north of the 200-West Area. The lower mud unit generally thickens and dips to the south and southwest. The top of the mud unit, which has an irregular surface, forms the lower boundary of the unconfined aquifer in the 200-West Area.

The lower mud separates the unconfined aquifer from an underlying confined aquifer, which is composed of the Ringold Unit A gravel (Unit 9). This unit is composed of fluvial gravels with lesser



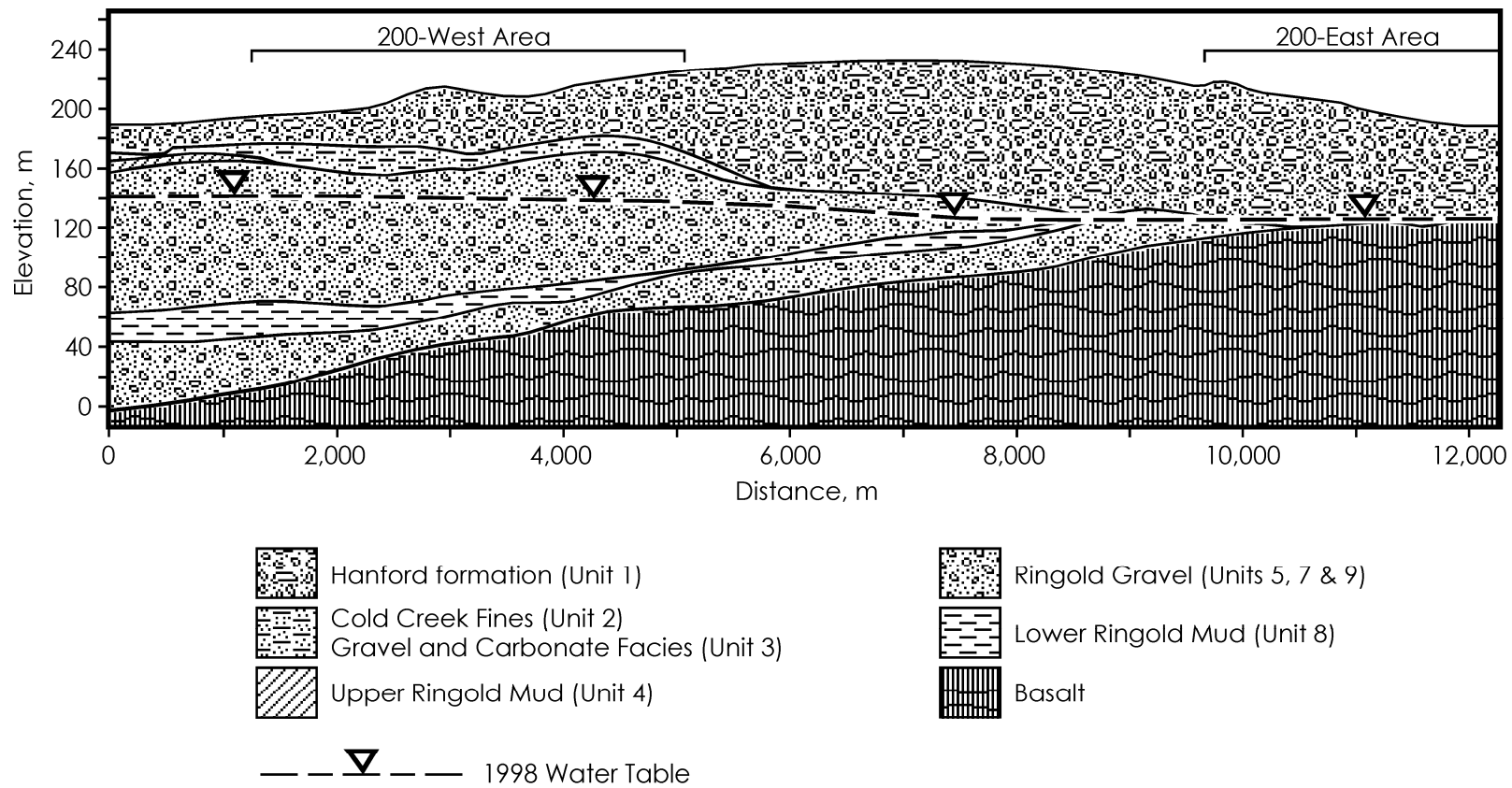
After Thorne et al. (1993)

Not to Scale

After Lindsey (1995)

**Figure 2.1.** Stratigraphic Relationships of Various Hydrogeologic Units





2004/DCL/Spaue/002 (07/27)

**Figure 2.2.** Hydrogeologic Cross Section Through 200-West and 200-East Areas (adapted from Spaue et al. 2003)

amount of intercalated sands and silts. This basal unit, which lies directly above the basalt bedrock, thickens and dips to the south and southwest. The uppermost basalt formation beneath the 200-West Area is the Saddle Mountains Basalt.

## **2.2 Hydrogeology of the 200-East Area**

As in the 200-West Area, the aquifer system above the basalt in the 200-East Area consists of the unconfined aquifer and, in some places, a locally confined aquifer that underlies the discontinuous lower Ringold mud (Unit 8). The unconfined aquifer within the 200-East Area lies within the Hanford formation (Unit 1) and/or Ringold Formation gravel units E, C, and A (Units 5, 7, and 9) (see Figure 2.1). In the northern part of the 200-East Area, the unconfined aquifer is thin in locations where the basalt surface forms subsurface highs. In these locations, the unconfined aquifer lies almost entirely within the Hanford formation (Unit 1). Most wells recently tested within the 200-East Area (Spane et al. 2001a, 2001b, 2002, 2003) and Spane and Newcomer (2004) are reflective of either the Hanford formation or reworked Ringold gravel Unit E sediments. Some or all of these undifferentiated gravel- and sand-dominated sediments may represent reworking of the Ringold Formation deposits by either ancestral Columbia River or Missoula flood events, which removed fine-grained material, decreased consolidation, and increased permeability of the sediments. Because of the preponderance of unconsolidated gravel and sand deposits, this unit generally exhibits higher permeabilities than older, non-reworked hydrogeologic units within the Ringold Formation.

The lower boundary of the unconfined aquifer in the 200-East Area is defined by the top of the lower Ringold mud (Unit 8), the top of a fine-grained subunit within Ringold gravel unit A (Unit 9B), or the top of relatively impermeable basalt. However, the basalt flow top associated with the uppermost basalt flow may be brecciated and form part of the unconfined aquifer as reported in Spane and Newcomer (2004). To the north of the 200-East Area, the lower Ringold Formation units and underlying upper basalt flows were extensively eroded by the Missoula floods at the time the Hanford formation was deposited. Previous reports have indicated that direct hydrogeologic communication between the unconfined and underlying, upper, basalt-confined aquifer is likely in these areas (Gephart et al. 1979; Graham et al. 1984; Spane and Webber 1995).

The Ringold lower mud (Unit 8), which forms the confining mud unit separating the overlying, unconfined aquifer from the underlying, locally confined, aquifer within Ringold gravel unit A (Unit 9), is composed primarily of low-permeability, fluvial overbank, paleosol, and lacustrine silts and clay, with minor amounts of sand and gravel. As indicated in Figure 2.1, Ringold gravel unit A (Unit 9) is composed of local subunits. Unit 9B consists of poorly characterized silt- to clay-rich zones and represents a relatively thin, low-permeability, local confining unit within the basal Ringold gravel. Confining Units 8 and 9B extend above the regional water table east of the 200-East Area near the 216-B-3 Pond.

## 3.0 Detailed Test Characterization Methods

This report provides the results of detailed hydrologic characterization tests conducted within selected Hanford Site wells during FY and CY 2005. Detailed characterization tests performed included groundwater-flow characterization, barometric response evaluation, slug tests, single-well tracer tests (tracer-dilution, tracer-pumpback, and in-well vertical flow surveys), and constant-rate pumping tests. Table 3.1 provides a summary of the various hydrologic characterization elements. More in-depth descriptions of the methods used to analyze slug tests, various single-well tracer tests, and constant-rate pumping tests are provided in the following sections and are taken primarily from Spane et al. (2002 and 2003) and Spane and Newcomer (2004).

### 3.1 Slug Tests

Because of their ease of implementation and relatively short duration, slug tests are commonly used to provide initial estimates of hydraulic properties (e.g., range and spatial/vertical distribution of hydraulic conductivity,  $K$ ). Because of the small displacement volumes employed during slug tests, hydraulic properties determined using this characterization method are representative of conditions relatively close

**Table 3.1.** Detailed Hydrologic Characterization Elements

Element	Activities	Results <sup>(a)</sup>
Groundwater-flow characterization	Trend-surface analysis of well water-level data	Quantitative determination of groundwater-flow direction and hydraulic gradient
Barometric response evaluation	Well water-level response characteristics to barometric changes	Aquifer-/well-model identification, vadose zone property characterization, correction of hydrologic test responses for barometric pressure fluctuations
Slug test	Multistress-level tests conducted at each well site	Local $K_h$ , $T$ of aquifer surrounding well site
Tracer-dilution test	Monitoring dilution of administered tracer at injection well site	Determination of $v_w$ and vertical distribution of $K_h$
Tracer-pumpback test	Pumping/monitoring of recovered tracer and associated pressure response in monitor wells	Local- to intermediate-scale $n_e$ and $v_a$
In-well vertical flow surveys	In-well flow measurements using an electromagnetic borehole flow meter or inferred from monitoring the vertical movement of tracer within the well screen	Determination of $v_v$ within the monitor-well–screen section
Constant-rate pumping test	Pumping/monitoring of pressure response in monitor wells	Intermediate to large-scale, $K_h$ , $K_v/K_h$ , $K_{hx}/K_{hy}$ , $T$ , $S$ , $S_y$
(a) Note: See Nomenclature for definitions.		

to the well. For this reason, slug-test results are commonly used to design subsequent hydrologic tests having greater areas of investigation (e.g., slug interference [Novakowski 1989; Spane 1996; Spane et al. 1996], constant-rate pumping tests [Butler 1990; Spane 1993]).

Slug tests conducted as part of the FY and CY 2005 detailed characterization program were performed by removing a slugging rod (withdrawal test) of known displacement volume. Slug-withdrawal tests were employed rather than slug-injection tests (i.e., by rapidly immersing the slugging rod) because of their reported superior results for unconfined aquifer tests where the water table occurs within the well-screen section (e.g., Bouwer 1989). At all test sites, two different size slugging rods were used to impart varying stress levels for individual slug tests. The slug tests were repeated at each stress level to assess the reproducibility of the test results. Comparison of the normalized slug-test responses is also useful to evaluate stress-dependent, non-linear test well conditions. Evidence of stress dependence for tests within low to intermediate permeability formations may indicate the effectiveness of well development and the presence of near-well heterogeneities and dynamic skin conditions, as noted in Butler et al. (1996). Dynamic skin conditions refer to the non-repeatability of test responses conducted at a particular stress level. This non-repeatability of test response is commonly associated with changing formational conditions near the well caused by incomplete well development. As described in Butler (1998), hydraulic property characterization results obtained from wells exhibiting stress dependence should be viewed with caution; with more credence given to test responses exhibiting less lagged response characteristics (e.g., tests conducted at lower stress levels). Conversely, wells exhibiting repeatable slug-test responses at different stress levels indicate a stable or static formation condition surrounding the well and suggest that the well has been effectively developed.

Based on volumetric relationships, the two different size slugging rods theoretically impart a slug-test stress level of 0.458 meter (low-stress tests) and 1.117 meters (high-stress tests) within a 0.1016-meter inside diameter well. However, for conditions where wells are screened across the water table, as for most of the Hanford Site wells tested in FY and CY 2005 and where the well-screen sand pack has a relatively high permeability, the actual stress level imposed on the test formation may be lower than the theoretical stress level. This is due to the added pore volume of the sand pack at the time of test initiation. For these situations, the actual slug-test stress level is determined by projecting the observed early test response back to the time of test initiation. For test situations where the water-table is within the well-screen section and where the theoretical slug-test stress level,  $H_o$ , is greater than the observed or projected stress level,  $H_p$ , an equivalent well radius,  $r_{eq}$ , must be used instead of the actual well-casing radius,  $r_c$ , in the various analytical methods. The  $r_{eq}$  can be calculated by using the following relationship presented in Butler (1998)

$$r_{eq} = r_c \left( \frac{H_o}{H_p} \right)^{1/2} \quad (3.1)$$

The previous discussion is particularly relevant and applicable for tests performed within formations possessing low to intermediate permeabilities. For test formations exhibiting very high permeabilities (e.g.,  $> 50$  m/d), this relationship may not be utilized due to the uncertainty of actual applied stress,  $H_o$ . The uncertainty occurs because of the finite time required to remove the slugging rod (i.e.,  $\sim 1$  sec) and the

associated test recovery that occurs during the removal process. For high-permeability test formation situations, the observed maximum  $H_o$  is commonly used, and  $r_{eq}$  assumed to be equal to  $r_c$ .

As discussed in Butler (1998), water levels within a well can respond in one of three ways to the instantaneously applied stress of a slug test. As shown in Figure 3.1, these response model patterns are 1) an over-damped response, where the water levels recover in an exponentially decreasing recovery pattern, 2) an under-damped response, where the slug-test response oscillates above and below the initial static, with decreasing peak amplitudes with time, and 3) critically-damped, where the slug-test behavior exhibits characteristics that are transitional to the over- and under-damped response patterns. Factors that control the type of slug-test-response model exhibited within a well include a number of aquifer properties (hydraulic conductivity) and well-dimension characteristics (well-screen length, well-casing radius, well-radius, fluid-column length) and can be expressed by the response damping parameter,  $C_D$ , which Butler (1998) reports for unconfined aquifer tests as

$$C_D = \frac{\left(\frac{g}{L_e}\right)^{1/2} r_c^2 \ln\left(\frac{R_e}{r_w}\right)}{2KL} \quad (3.2)$$

where  $g$  = acceleration due to gravity

$L_e$  = effective well water-column length

$r_c$  = well casing radius; i.e., radius of well water-column that is active during testing

$R_e$  = effective test radius parameter; as defined by Bouwer and Rice (1976)

$r_w$  = well radius

$K$  = hydraulic conductivity of test interval

$L$  = well-screen length.

Given the multitude of possible combinations of aquifer properties, well casing dimensions, and test interval lengths, no universal  $C_D$  value ranges can be provided that describe slug-test-response conditions. However, in considering various test site conditions that might be encountered at newly constructed Hanford Site RCRA monitoring wells (i.e., with a saturated well-screen length,  $L = 10.67$  m and well casing radius,  $r_c = 0.051$  m), the following **general** guidelines on slug-test-response prediction are provided:

- $K \leq 27$  m/day:  $C_D > 2$  = over-damped response
- $K = 27 - 54$  m/day:  $C_D 1 - 2$  = critically-damped response
- $K \geq 54$  m/day:  $C_D < 1$  = under-damped response

An over-damped test response generally occurs within test wells monitoring low to moderately high-permeability formations (e.g., Ringold Formation) and is indicative of test conditions where frictional forces (i.e., resistance of groundwater flow from the test interval to the well) are predominant over test system inertial forces. For over-damped slug tests, two different methods were used for the slug-test analysis: the semiempirical, straight-line analysis method described in Bouwer and Rice (1976) and Bouwer (1989) and the type-curve-matching method for unconfined aquifers presented in Butler (1998).

A detailed description of over-damped, slug-test-analysis methods is presented in Section 3.1.1. Analysis details and results of slug tests exhibiting over-damped response characteristics at monitor wells tested during FY and CY 2005 are provided in Chapter 4.

Under-damped test-response patterns are exhibited within stress wells where inertial forces are predominant over formation frictional forces. This commonly occurs in wells with extremely long well fluid columns (i.e., large water mass within the well column) and/or that penetrate highly permeable aquifers (e.g., Hanford formation). Tests exhibiting under-damped behavior should be conducted with very small stress levels, i.e.,  $H_0 \ll L$ , as originally noted in Van der Kamp (1976) and restated in Butler (1998). For standard Hanford Site RCRA wells exhibiting under-damped test conditions, the maximum stress level used for such test sites should not generally exceed  $\sim 1/10$  of the saturated well-screen length. Methods for analyzing unconfined aquifer tests exhibiting high-permeability under-, over-, or critically-damped characteristics include techniques described in Springer and Gelhar (1991), Butler (1998), McElwee and Zenner (1998), Butler and Garnett (2000), Zurbuchen et al. (2002), and Butler et al. (2003). Because of the ease provided by a spreadsheet-based approach, the analysis method presented in Butler and Garnett (2000) has been used in previous characterization reports by the authors (e.g., Spane and Newcomer 2004) to analyze all tests exhibiting under-damped response behavior (i.e., high permeability/oscillatory pattern). No well tests conducted during FY and CY 2005 exhibited true formational under-damped behavior. A detailed description of under-damped slug-test analysis methods, however, is presented in Section 3.1.2 for analytical completeness.

Critically-damped test responses are indicated by stress well water-level responses that are transitional to the over- and under-damped test conditions, as shown in Figure 3.1. They typically occur in wells that monitor test formations exhibiting relatively high hydraulic conductivity. As noted in Butler (1998), distinguishing between over- and critically-damped slug-test responses may be difficult in some cases (i.e., because of test signal noise) when examined on arithmetic plots. Proper model identification may be enhanced, however, when semi-log plots are used, i.e., log head versus time. Critically-damped slug tests exhibit a diagnostic concave-downward pattern when plotted in semi-log plot format. This is in contrast to over-damped response behavior, which displays either a linear or concave upward pattern. Slug tests exhibiting critically-damped test response can be analyzed with the same analytical methods used for under-damped tests. Generally, the analysis method presented in Butler and Garnett (2000) was used for all tests exhibiting critically-damped response behavior.

### **3.1.1 Over-Damped Test Analysis Methods**

The following sections provide a detailed discussion of analytical methods and considerations for slug tests exhibiting over-damped responses.

#### **3.1.1.1 Bouwer and Rice Method**

The Bouwer and Rice method is a well-known technique and is widely applied for analyzing slug tests. A number of analytical weaknesses, however, limit the successful application of the Bouwer and Rice method for analyzing slug-test responses. These weaknesses constrain its application to slug-test responses that exhibit steady-state flow, isotropic conditions, no well-skin effects, and no elastic (storage) formation response. Unfortunately, these limitations are commonly ignored, and the Bouwer and Rice

method is applied to slug-test responses that do not meet the test-analysis criteria. A more detailed discussion on the analytical limitations of the Bouwer and Rice method is provided in Hyder and Butler (1995), Brown et al. (1995), and Bouwer (1996).

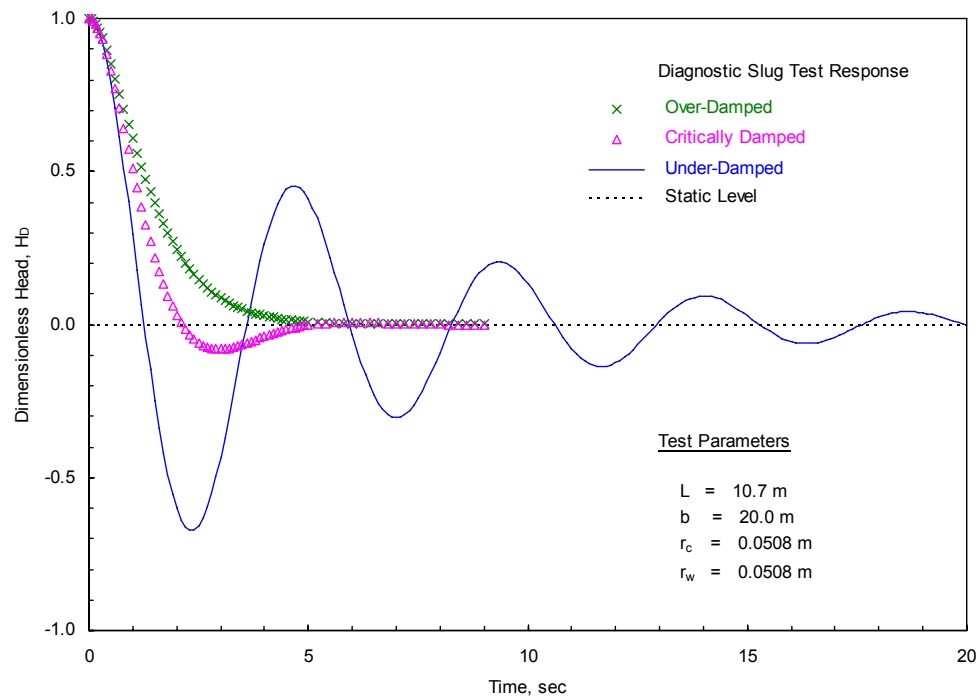


**Figure 3.1.** Diagnostic Slug-Test-Response Types

For slug tests exhibiting elastic storage response, it should be noted that improved estimates can be obtained if analysis criteria specified in Butler (1996, 1998) are observed. Figure 3.2 shows the predicted, normalized, slug-test response for three well/aquifer-test conditions: 1) nonelastic formation, 2) elastic formation, and 3) elastic formation with high-K sandpack effects. The test responses were calculated using the Kansas Geological Survey (KGS) model described in Liu and Butler (1995) for the given test conditions listed in Figure 3.2. As shown, the presence of elastic aquifer storage (i.e., specific storage,  $S_s$ ) and effects of a high-permeability sand pack cause curvilinear test responses (concave upward) that deviate from the predicted linear, nonelastic formation response. When this diagnostic curvilinear response is exhibited in the slug-test response, Butler (1996, 1998) recommends that the late-time test analysis be employed (i.e., the normalized head segment between 0.3 and 0.2) when using the Bouwer and Rice (1976) method. As shown in Figure 3.2, the two elastic curvilinear test responses over the specified late-time segment closely parallel the nonelastic test-formation response. This indicates that quantitative estimates for  $K$  can be obtained using the Bouwer and Rice method over a wide range of test-response conditions (nonelastic or elastic formation, high-K sandpack effects) if the proper analysis criteria are applied.

Because of its semi-empirical nature, analytical results obtained using the Bouwer and Rice method (i.e., in contrast to results obtained using the type-curve-matching method) may be subject to error. Bouwer and Rice (1976) indicated that the  $K$  estimate, using their analysis method, should be accurate to within 10% to 25%. Hyder and Butler (1995) state an accuracy level for the Bouwer and Rice method

within 30% of actual for homogeneous, isotropic formations, with decreasing levels of accuracy for more complex well/aquifer conditions (e.g., well-skin effects). For these reasons, greater credence is generally afforded the analytical results obtained using the type-curve-matching approach, which has a more rigorous analytical basis.

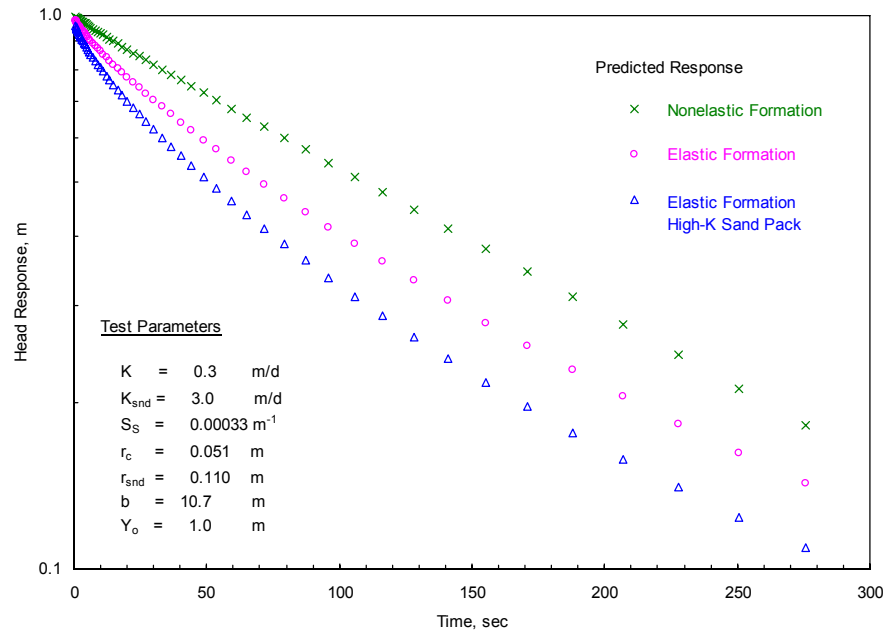


**Figure 3.2.** Predicted Slug-Test Response for Nonelastic Formation, Elastic Formation, and High Hydraulic Conductivity Sand-Pack Conditions

### 3.1.1.2 Type-Curve Method

Because the type-curve method can use all or any part of the slug-test response in the analysis procedure, it is particularly useful for analyzing unconfined aquifer tests. The method also does not have any of the aforementioned analytical weaknesses of the Bouwer and Rice method. To facilitate the standardization of the slug-test type-curve analyses, a set of initial analysis parameters was assumed:

- a vertical anisotropy,  $K_D$ , value of 1
- a specific storage,  $S_s$ , value of  $0.00001 \text{ m}^{-1}$
- an assumption that the well-screen interval below the water table was equivalent to the test-interval section.

To standardize the slug-test type-curve-matching analysis for all slug-test responses, a  $K_D$  value of 1 was assumed. As noted in Butler (1998), this is the recommended value to use for slug-test analysis when setting the aquifer thickness to the well-screen length. Previous investigations by F. A. Spane (author) have indicated that single-well slug-test responses are relatively insensitive to  $K_D$ ; therefore, the use of an assumed (constant) value of 1 over a small well-screen section (i.e.,  $\leq 10$  meters long) within an aquifer



having a thickness of  $\geq 10$  meters is not expected to have a significant impact on the determination of hydraulic conductivity,  $K_h$ , from the type-curve-matching analysis.

To facilitate the unconfined aquifer slug-test type-curve analysis, an  $S_s$  value of  $0.00001 \text{ m}^{-1}$  was used for all initial analysis runs. After initial matches were made through adjustments of transmissivity,  $T$ , additional adjustments of  $S_s$  were then attempted to improve the overall match of the test-response pattern. In most test cases, slight modifications (i.e., increasing  $S_s$ ) were made to the input  $S_s$  values to improve the final analysis type-curve matches. However, other factors influence the shape of the slug-test curve (e.g., skin effects,  $K_D$ ). For this reason, the  $S_s$  estimate obtained from the final slug-test analyses is considered to be of only qualitative value and should not be used (as in the case for  $K_h$ ) for quantitative applications.

For the slug-test analysis, the well-screen interval below the water table (rather than the sandpack interval) was used to represent the test interval. This was based on the assumption that the formation materials within the screened interval have a higher permeability than the sandpack; therefore, test-response transmission is expected to propagate faster laterally from the well screen to the surrounding test formation than vertically within the sandpack zone. In reality, only small differences exist between individual well-screen and sandpack-interval lengths (i.e., compared to the aquifer-thickness relationship) and, subsequently, no significant differences in analysis results would be expected. This assumption is consistent with recommendations listed in Butler (1996).

The type-curves analyses presented in this report were generated using the KGS program described in Liu and Butler (1995). The KGS program is not strictly valid for the boundary condition, where the water table occurs within the well screen. However, a comparison of slug-test type curves generated from converted pumping-test-type curves (as described in Spane 1996), which accounts for this boundary effect, indicates very little difference in predicted responses when compared to the KGS model results. Because of this close comparison and the fact that the KGS program calculates slug-test responses directly and can be applied more readily for analyzing the slug-test results, it was used as the primary type-curve-analysis method in this report.

### **3.1.1.3 Heterogeneous Formation Analysis**

Inherent in the analytical methods discussed above is the assumption that the test interval is homogeneous. A number of formation heterogeneities, however, can exert significant influence on slug-test response. Recognized heterogeneous formation conditions affecting slug-test response include multi-layers of varying hydraulic properties within the well-screen section, the presence of linear boundaries, and radial variation of hydraulic properties with distance from the well (i.e., radial boundaries).

The effects of multi-layer conditions within the test interval have been examined previously by Butler et al. (1994) and Butler (1998). These studies indicate that the presence of multi-layers of varying hydraulic properties cannot be distinguished from the pattern of the slug-test response. For well screens that fully penetrate a heterogeneous, multi-layer aquifer, the hydraulic conductivity estimated from the slug test will be an arithmetic average of the thickness-weighted  $K_h$  values of the individual layers. For well screens that partially penetrate the upper-part of a multi-layer aquifer, the hydraulic conductivity

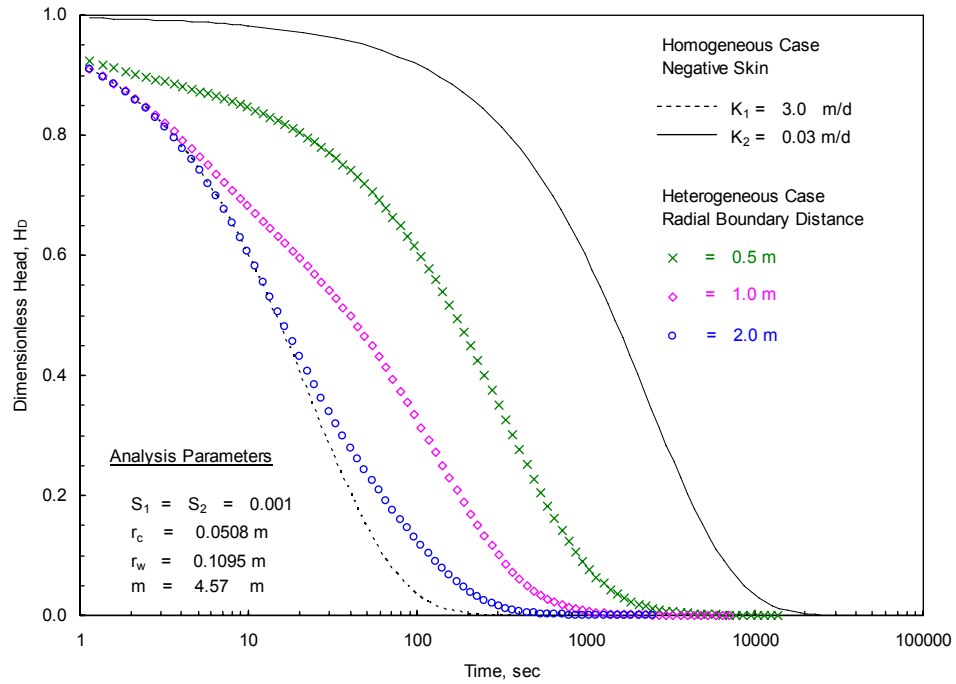
estimated from the test also will represent a thickness-weighted arithmetic average, as long as significant vertical leakage does not occur from layers underlying the test interval.

The effects of linear boundaries on slug-test response have been examined previously by Karasaki et al. (1988) and Guyonnet et al. (1993). These effects are largely dependent on the nature of the boundary (i.e., no-flow or constant-head), proximity to the test well, and the storage characteristics of the aquifer and well. As a generalization, Guyonnet et al. (1993) state that no-flow boundaries cause the slug-test response to deviate from and delay recovery, while constant-head boundaries cause the slug test to recover faster than that predicted for a corresponding unbounded system response. Karasaki et al. (1988) accounts for the presence of linear boundaries within the slug-test response by employing image-well theory. The effect of linear boundaries is very similar to that imposed by radial boundaries, which is discussed in the following paragraphs.

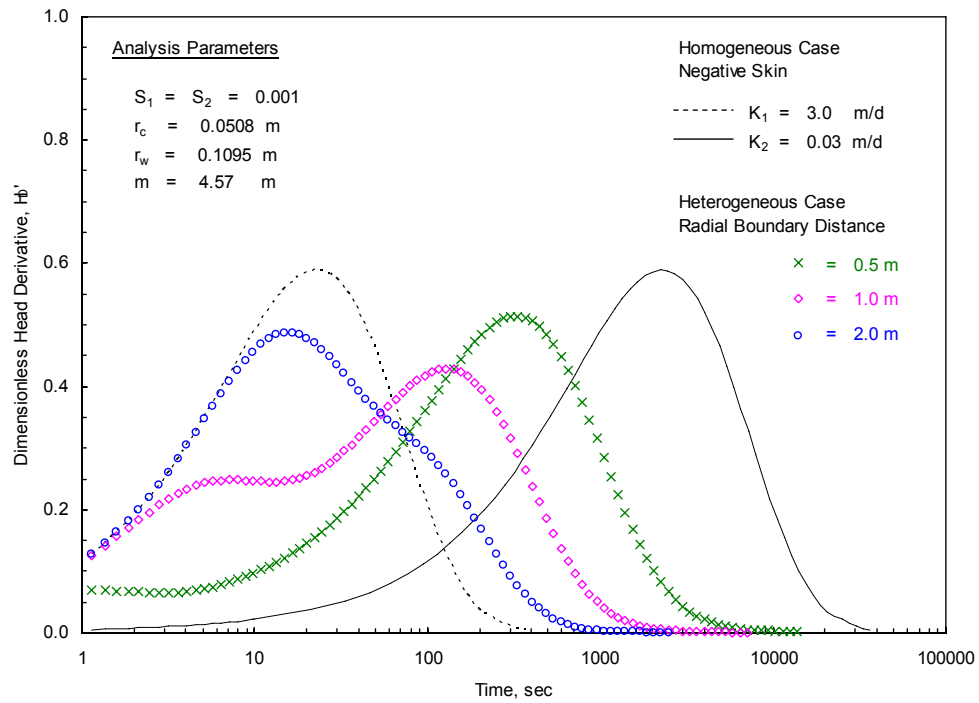
The effects of radial variations of hydraulic properties surrounding the test well have been investigated previously in studies examining slug tests in the presence of finite-thickness skin (e.g., Moench and Hsieh 1985). A finite-thickness skin is essentially a radial boundary condition surrounding a fully penetrating well where the inner zone has significantly different hydraulic properties than the outside zone. A negative skin refers to the case where  $K_h$  of the inner zone is much greater than that of the outer zone (i.e.,  $K_1 \gg K_2$ ), while a positive skin denotes the opposite condition (i.e.,  $K_1 \ll K_2$ ). The effects of a radial boundary on slug-test response are largely a function of the contrast in  $K_h$  for the inner and outer zone, the storage characteristics, and the radial distance from the well to the boundary.

Figure 3.3 shows the predicted slug-test responses for a negative finite-thickness skin condition, where the inner zone has a  $K_h$  100 times greater than the outer zone, for various selected radial boundary distances (0.5, 1, 2 meters). The test responses were generated using the KGS program referenced in Section 3.1.2, which can account for finite-thickness well-skin conditions. For comparison purposes, homogeneous slug-test responses (i.e., no radial boundary) for the  $K_h$  representative solely of the inner and outer zones also are provided. For this example, the storativities,  $S$ , for both zones are set equal and representative of elastic formation conditions ( $S_1 = S_2 = 0.001$ ). An examination of Figure 3.3 indicates several important features. During early-test times, all the radial boundary examples follow the inner-zone response (i.e., homogeneous formation response), with the duration of coincidence being directly associated with distance to the radial boundary. The presence of the radial boundary is exhibited by the departure from inner-zone response, where the test response becomes flatter (recovery rate decreases) and transitions to a combined composite test response, reflective of the hydraulic properties inside and outside the radial boundary. Recognizing whether radial flow boundaries are present within the slug-test response may be difficult unless the transition-period segments of the test are distinct. Recognizing the presence of radial boundaries, however, is more apparent when slug-test derivative plots are employed.

Figure 3.4 shows the predicted slug-test derivative responses for the same test conditions presented in Figure 3.3. As shown, radial boundaries for the distances greater than 0.5 meter are denoted by a derivative pattern exhibiting multiple peaks or a stair-step pattern, which is in contrast to the smooth, single-peak derivative pattern exhibited by homogeneous formations. For radial distances extremely close (e.g., <0.5 meter) or far (e.g., >5 meters) from the test well, the presence of boundaries may not be detected within the test response.



**Figure 3.3.** Predicted Slug-Test Response: Negative Finite-Thickness Skin Conditions



**Figure 3.4.** Predicted Slug-Test Derivative Response: Negative Finite-Thickness Skin Conditions

Figure 3.5 shows the predicted slug-test responses for a positive finite-thickness skin condition, where the inner zone has a  $K_h$  0.01 times that of the outer zone, for the same selected radial boundary distances (0.5, 1, 2 meters) and test conditions examined for the negative skin case (only the  $K_h$  values for the inner and outer zones are reversed). As for the previous negative-skin example, during early-test times, the various heterogeneous responses follow the inner-zone response (i.e., homogeneous formation response), with the duration of coincidence being directly associated with distance to the radial boundary. The presence of the radial boundary is exhibited by the departure from inner-zone response, where the test response becomes steeper (recovery rate increases), with test recovery becoming reflective of a combined composite test response reflective of the hydraulic properties inside and outside the radial boundary. The increased steepness in test response due to the presence of a radial boundary (positive-skin) becomes more apparent when type-curve analysis methods are used (i.e., in comparison to the Bouwer and Rice method). As discussed in Butler (1998), the analysis of slug tests affected by positive-skin conditions often requires the use of homogeneous formation-type curves with unrealistically low storativity values (i.e., to match the entire test response). For this reason, Butler (1998) recommends the use of type-curve analysis for slug tests to detect whether positive skin-radial boundaries are present within the test response.

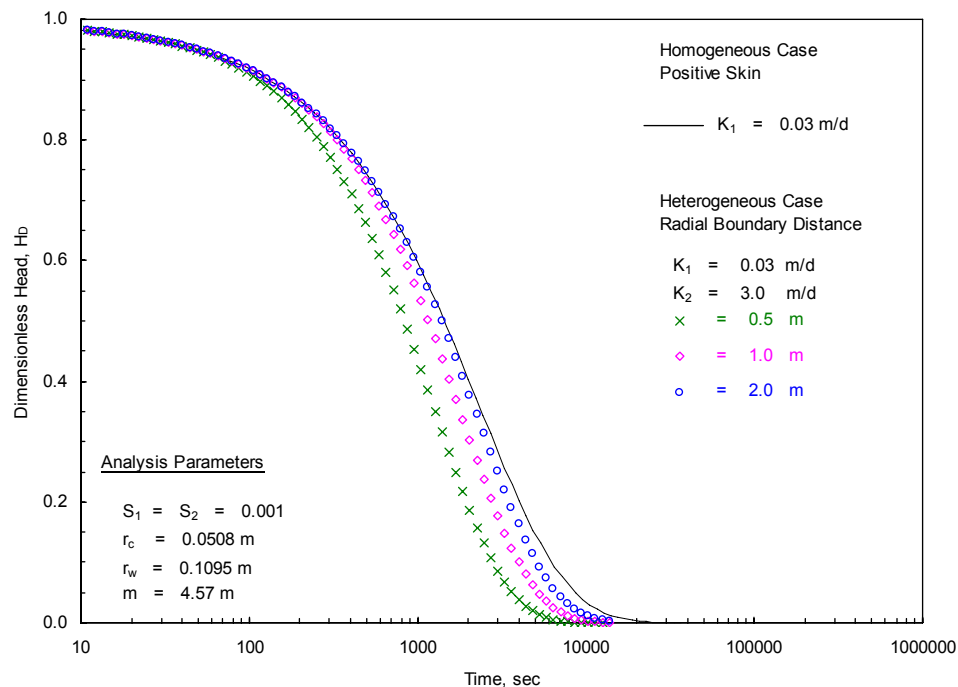


**Figure 3.5.** Predicted Slug-Test Response: Positive Finite-Thickness Skin Conditions

Only one of the completed wells (well 299-W26-14) tested during FY and CY 2005 exhibited effects of heterogeneous formation-radial boundary conditions (i.e., higher  $K$  inner zone). No composite slug-test-response analysis (i.e., using  $K_h$  values for the inner and outer zones) was attempted, however, using the finite-thickness skin solution available within the KGS program (as shown in Figure 3.3, Figure 3.4, and Figure 3.5). This is due to the non-uniqueness of the analytical solution (i.e., similar test responses can be derived using different combinations of  $K$ ,  $S$  and skin/inner-zone thickness). For the test

exhibiting heterogeneous formation behavior, the inner and outer-zone test responses were analyzed independently using the homogeneous formation analysis approach. (Note: this is a departure from the composite analysis approach used in Spane et al. (2001b) to analyze three test wells exhibiting heterogeneous formation response conditions). For the outer-zone test response, which is more representative of actual formation/aquifer conditions, the homogeneous formation analysis procedure outline in Butler (1998) was used. This procedure is similar to the method described in Section 3.1 to calculate the actual stress level,  $H_p$ . For a homogeneous formation analysis of the outer-zone test response, the early-time test data reflecting the higher permeability inner zone is ignored and an initial, outer-zone test stress level ( $H_{p-out}$ ) is calculated by projecting the observed, outer-zone test data back to the time of test initiation. For test conditions where the water-table occurs within the well-screen section, an equivalent well radius,  $r_{eq-out}$ , must be used instead of the actual well-casing radius,  $r_c$ , in the various analytical methods used for the outer-zone analysis. The  $r_{eq-out}$  is calculated by using Equation 3.1, substituting  $H_{p-out}$  for  $H_p$  in the equation.

### 3.1.2 High-Permeability/Under-Damped Analysis Methods

Slug-test response within highly permeable formations is commonly influenced by processes (e.g., inertial) that are not accounted for in the previously discussed analytical methods. For Hanford Site conditions, high-permeability formation conditions can be expected when test responses are under- or critically-damped and exhibit any or all of the following characteristics:

- complete recovery within 10 seconds
- oscillatory recovery pattern
- overly-steep type-curve recovery and heightened derivative plot pattern
- concave downward Bouwer and Rice plot.

Slug tests exhibiting these response characteristics cannot be analyzed quantitatively using the Bouwer and Rice (Section 3.1.1.1) or type-curve (Section 3.1.1.2) methods. As noted previously, methods that can be employed for analyzing unconfined aquifer tests exhibiting high-permeability characteristics include methods described in Springer and Gelhar (1991), Butler (1998), McElwee and Zenner (1998), McElwee (2001), Butler and Garnett (2000), and Zurbuchen et al. (2002). Because of the ease provided by a spreadsheet-based approach, the test analysis method presented in Butler and Garnett (2000) was used for tests exhibiting high-permeability response characteristics, i.e., under- or critically-damped. The technique employs a type-curve generating/matching procedure wherein the analyst:

- first, generates a test type-curve response (based on test/well input parameters) that matches the general recovery amplitudes for peaks and troughs exhibited by the observed slug-test-response pattern by adjusting the response damping parameter,  $C_D$ , and then
- adjusts the generated type curve response using the modulation factor for matching the oscillatory period exhibited by the observed slug-test response.

In most test cases, the exhibited test-response period is largely controlled by the test and well characteristics (e.g.,  $r_c$ ,  $r_w$ ,  $L$ ,  $L_e$ ) while the recovery amplitudes exhibited by the test peaks and troughs is

highly dependent on test formation permeability. Figure 3.6 shows the effect of test formation permeability on the recovery amplitudes of peaks and troughs as well as the duration of oscillatory response. As indicated, lower test interval permeabilities exhibit more rapidly damped response patterns while higher test interval permeabilities are denoted by less amplitude attenuation and longer test-response durations.

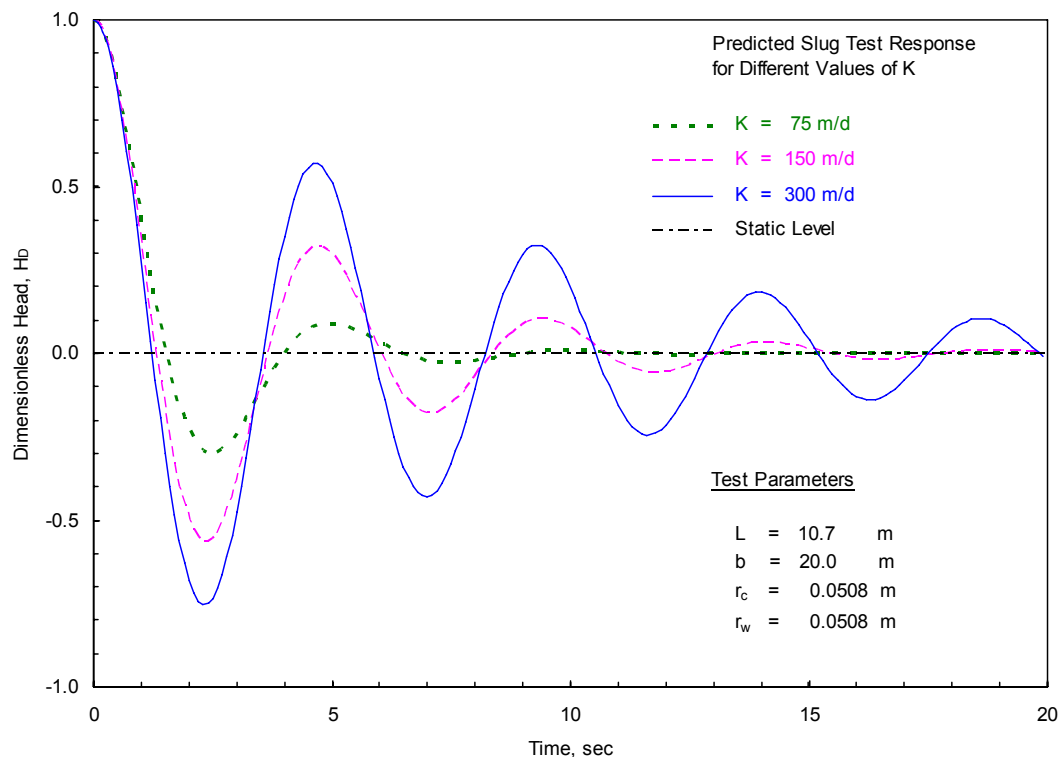


**Figure 3.6.** Effects of Hydraulic Conductivity on Predicted Under-Damped Slug-Test Response

Similar analysis procedures are used for tests exhibiting critically-damped behavior. The only difference is the number of match points for the generated test simulation to the observed test response. These match points are commonly limited to only one peak and trough as well as the recovery point to static, pre-test conditions. FY and CY 2005 test well 299-E33-49 is an example of a well exhibiting critically-damped behavior. Analysis results for this well characterization are discussed in Chapter 4.

It should be noted that the High-K analysis method requires that the pressure sensor used during testing be located in close proximity to the water-table surface, as discussed in Zurbuchen et al. (2002), Butler et al. (2003), and Chen and Wu (2006). This is due to the effects of water-column acceleration within the well. For these situations, tests conducted having a pressure sensor depth of  $>2$  m below the water-column surface may produce a lower K estimate over actual conditions. This is due to damping effects imposed by the exhibited fluid-column acceleration.

### 3.1.3 Drill-and-Test Boreholes

The previous analytical discussion pertains to slug tests conducted in completed wells with standard single-casing systems. For slug tests conducted within “drill-and-test” boreholes during the active borehole drilling phase, a packer/well-screen assembly is lowered on a test-casing string to the current borehole bottom/depth, and the drill-casing is retracted a prescribed length exposing the surrounding formation to the installed well-screen. The inflatable packer is inflated within the drill casing, effectively isolating the exposed test interval from the overlying annular zone between the test-casing string and drill casing. It is also assumed that the drill casing provides an effective seal with the contacted formation, limiting hydraulic communication with overlying formations during testing.

All slug tests conducted within the three drill-and-test boreholes during FY and CY 2005 (i.e., well 299-W11-25B, 299-W14-11, and 299-W22-47) were drilled using a dual-wall drill casing system. The use of a dual-casing system, theoretically, allows hydraulic communication between the drill-casing annular area and underlying well-screen/test interval (note: this assumes that the drilling bit orifices at the bottom of the drill casings were not clogged with drill cutting debris, which could effectively seal the drill casing annular zone from contributing to associated test responses). The dual-wall casing used for borehole advancement and testing at the three sites had the following inside diameter/outside diameter (I.D./O.D.) dimensions: outer casing 0.216/0.229 m; inner casing 0.152/0.165 m.

A 20-slot, well-screen section was attached below the packer to maintain an open section for testing after retracting the drill casing. For testing at all three borehole sites, one standard packer/well-screen assembly was used: 3.05-m well-screen. In most cases, a strain-gauge, 0 to 69 kPa (0 to 10 psig) pressure transducer was installed within the test-casing string to monitor downhole test-interval response before and during slug testing. Figure 3.7 shows a schematic of the deployed test system within a dual-wall drill casing system, as prepared for conducting pneumatic slug tests. Pneumatic slug tests conducted at these test sites required the use of a surface wellhead assembly for sealing the test-casing string, thereby isolating the test interval from the overlying inner, drill-casing section. This wellhead isolation is required to contain the administered compressed air that is used to pneumatically depress the fluid columns to designed slug-test stress levels, as discussed in Section 2. Salient features of the well-head assembly include:

- a sealed, pass-through connection allowing for passage of downhole pressure transducer and cable to be used to measure test-interval pressure response within the test-casing string
- an outside pressure probe connection that allows direct measurement of the air/gas pressure within the test-casing below the surface seal
- a connection to allow compressed air to be introduced directly to the inside of the testing-string casing
- surface wellhead valves for the rapid release of the compressed air within the testing-string casing, which allows for the *immediate* initiation of slug-test application.

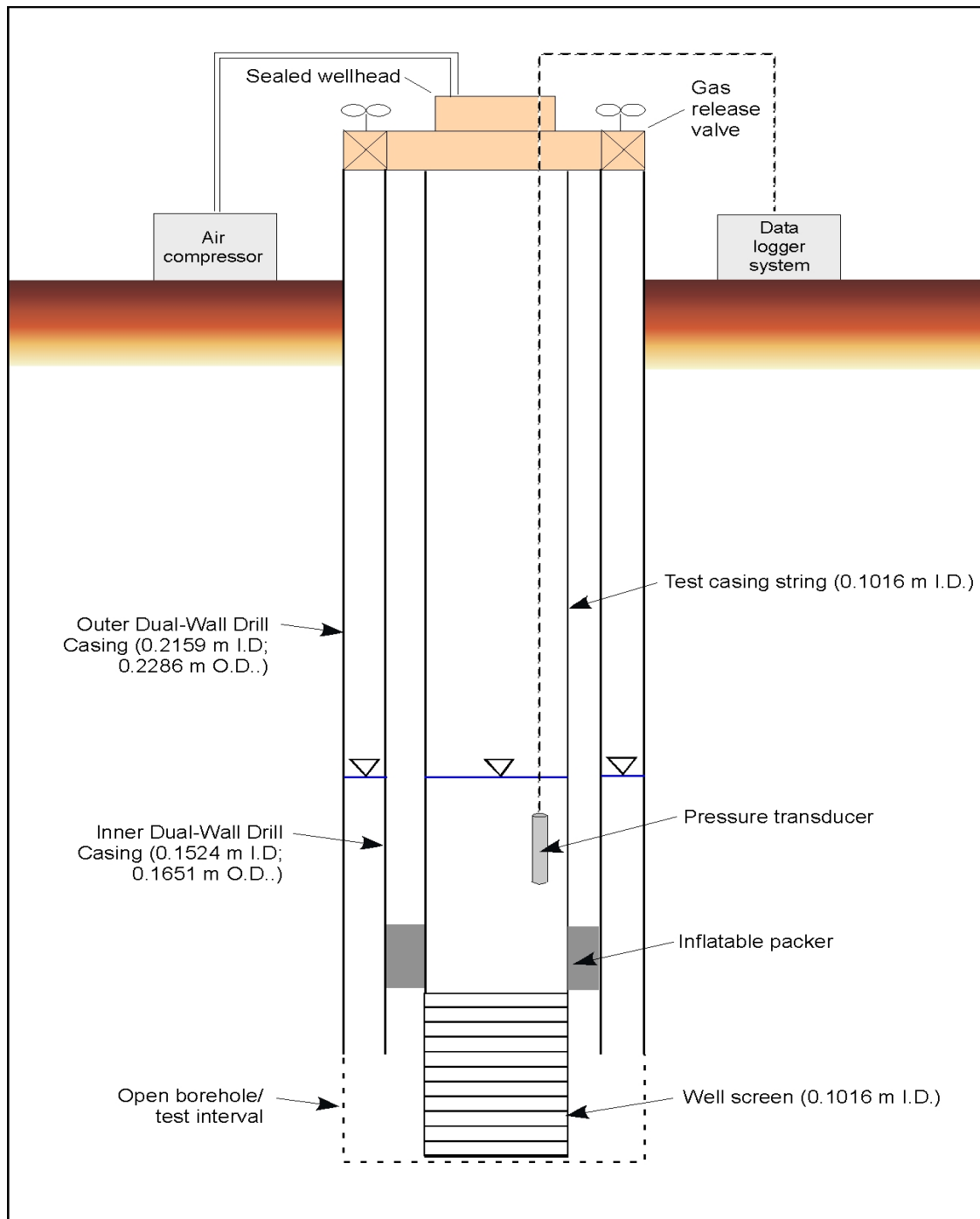


**Figure 3.7.** General Pneumatic Slug-Test System Using Dual-Wall Drill Casing System



The use of the dual-wall drill casing to add “complexity” to the slug-test analysis by the presence of an annular zone between the dual walls of the drill casing, which is also potentially communicative with the underlying test interval (as indicated in Figure 3.7). The presence of two connected test system areas (i.e., within the 0.1016 m I.D. testing string and within the dual-wall drill casing annular area) to respond to the initiated slug-test response can be visualized as a “u-tube” test system that is connected to the test formation (see Figure 3.8). As noted in Spane (1996), the slug-test-response time,  $t$ , is directly related to the square of the radius of the area where the water-level response occurs,  $r_c^2$ , and can be expressed in the form of the relationship below:

$$t = \frac{S r_c^2}{T} \quad (3.3)$$

where  $S$  is the test interval storativity, and  $T$  is the test interval transmissivity.

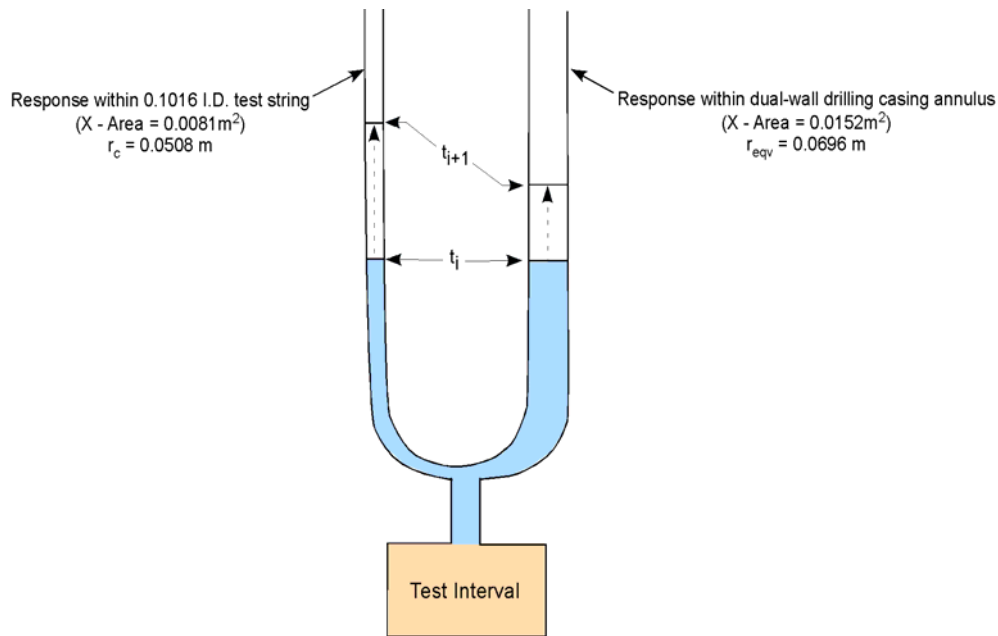


**Figure 3.8.** Visualization of Slug-Test-Response System Using a Dual-Wall Drill Casing System

Slug-test-response occurring in such a dual-area test system is a function not only of the hydraulic properties within the test interval, but also water-level (head) imbalances that occur between the two test system areas because of inertial effects and recovery rate differences within the dual-area test system (as indicated in Equation 3.3). As shown in Figure 3.9 for a test conducted in borehole 299-W11-25B, water-level recovery imbalances within the dual-area test system create an oscillatory behavior that is expected to be most pronounced during the early phases of test recovery and would diminish with lowering recovery rates exhibited later during the tests. This is particularly true at the time of test initiation, when pressure head imbalances are the maximum between the two test-system areas. Because the cross-sectional area within the dual-wall annulus is larger than within the test string (i.e., 0.0152 m<sup>2</sup> vs. 0.0081

$\text{m}^2$ ), recovery within the larger annular zone would noticeably lag behind that within the smaller testing string during the early slug-test-response period. Since the test-interval response pressure is only measured within the smaller testing string ( $r_c = 0.0508 \text{ m}$ ), the initial test recovery (i.e.,  $\leq 3 \text{ sec}$ ) should be reflective of recovery solely within the smaller testing string. The mass imbalance in water-level recovery (pressures) between the dual-wall area and the testing string (inertial effects) would cause recovery to perceptively slow within the testing string, which is controlled by the test-interval hydraulic properties, and then oscillate against a common recovery trend back to static level conditions. The duration or persistence of the superimposed oscillations is mainly a function of the test-interval hydraulic property characteristics and the casing friction within the test casing system. General observations of test results indicate that the imposed oscillatory behavior is quickly dampened by test intervals having moderate transmissivities but can persist for long periods of the test recovery for test intervals exhibiting low transmissivity conditions (e.g.,  $T \leq 5 \text{ m}^2/\text{day}$ ;  $L = 3.05 \text{ m}$  and  $K = 1.6 \text{ m/day}$ ).

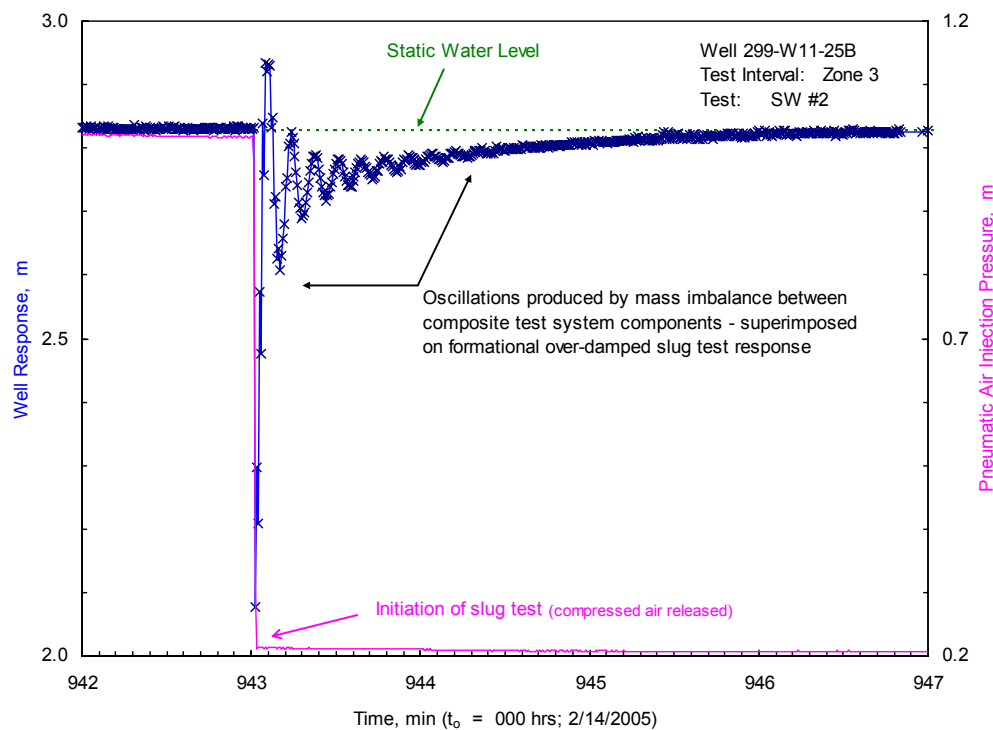


**Figure 3.9.** Example of Test-System Oscillatory Response Superimposed on Over-Damped, Slug-Test Recovery

Previous tests conducted in dual-casing test systems at other neighboring 200-West Area borehole locations have indicated that for average background, an over-damped, slug-test response exhibiting this type of early-time, superimposed test system oscillatory behavior can be predicted if an average radius ( $r_{\text{avg}} = 0.0685 \text{ m}$ ) calculated from the two test-system areas is used for the casing radius,  $r_c$ , in the analytical solutions. For the testing string and dual-wall drilling casing used at the three boreholes with the dual-drill casing system, the following test system test radii analysis relationships apply:

$r_c$  = radius of testing string; (0.0508 m)  
 $r_{an}$  = equivalent radius of the annular zone between the dual-wall drill casing; (0.0696 m)  
 $r_{eqv}$  = equivalent radius of the total test system:  $(r_c^2 + r_{an}^2)^{1/2}$ ; (0.0861 m)  
 $r_{avg}$  = average test system radius:  $(r_c + r_{eqv})/2$ ; (0.0685 m).

To analyze the results of tests exhibiting this type of oscillatory behavior superimposed on formational over-damped (exponential decay) or critically-damped (transitional) test-response characteristics, a two-step analysis procedure was employed. First, to remove the effects of the artificially imposed test-system oscillations, a central-point moving average was applied to the observed test data. The central-point moving average “length” that was most effective in removing the early-time, oscillatory response was equal to  $\frac{1}{2}$  the observed test oscillatory period. The smoothed test data using the central-point moving average scheme represents the test response that is reflective of the “average” test system to the imposed stress, and it was then analyzed using the Butler and Garnett (2000) analysis method described previously for either over- or critically-damped tests. As noted previously, the well casing radius value of 0.0685 m used in test analyses represents the average radius,  $r_{avg}$ , for the two regions within the test system where slug-test response occurred (i.e. within the testing string and annular area between the dual-wall drill casing).

## 3.2 Single-Well Tracer Tests

Single-well tracer tests can provide information on groundwater-flow characteristics (e.g., flow velocity) and aquifer properties (i.e., vertical distribution of K, effective porosity,  $n_e$ ). During FY and CY 2005, a single-well tracer test was conducted at well 299-W22-47 and included a tracer-dilution and tracer-pumpback test. Performance and analysis methods for the various single-well tracer test elements are described in the following sections.

### 3.2.1 Tracer-Dilution Tests

For the tracer-dilution test, a bromide solution of known concentration was mixed within the well-screen section. The decline of tracer concentration (i.e., “dilution”) with time within the well screen was monitored directly using a vertical array of bromide-specific ion-electrode sensors located at known depth intervals. The sensors were calibrated in the laboratory with standards of known bromide concentration before and following the performance of the tracer-dilution test. Based on the dilution characteristics observed, the vertical distribution (i.e., heterogeneity) of hydraulic properties and/or in-well flow velocity can be estimated for the formation section penetrated by the well screen. The presence of vertical flow within the well screen can also be identified from the sensor/depth-dilution-response pattern. A description of the performance and analysis of tracer-dilution test characterization investigations is provided in Halevy et al. (1966), Hall et al. (1991), and Hall (1993).

Essential design elements of a tracer-dilution test include establishing a known, constant tracer concentration within the test section by mixing or circulating the tracer solution in the wellbore/test interval and monitoring the decline of tracer concentration with time within the test interval.

The decline in tracer concentration within the wellbore can be analyzed to ascertain the hydraulic gradient,  $I$  (if the formation's  $K$  is known) or the test-interval  $K$  (if the hydraulic gradient is known) using the following analytical expression:

$$\ln \left( \frac{C}{C_o} \right) = \frac{-(Q_w t)}{V_w} \quad (3.4)$$

where  $C$  = concentration of the tracer in the test interval at time,  $t$   
 $C_o$  = initial concentration of the tracer at the start of the test  
 $Q_w$  = in-well lateral groundwater discharge within the well-test interval  
 $V_w$  = isolated test interval well volume.

For test-analysis purposes, Equation 3.4 is commonly rewritten to calculate the groundwater-flow velocity within the well,  $v_w$ , as follows:

$$v_w = \frac{d(\ln C)/dt}{-A/V} \quad (3.5)$$

where  $A$  is the cross-sectional area within well screen,  $L^2$ , and  $V$  is the well volume over the measurement section,  $L^3$ .

As shown by Halevy et al. (1966), to take into account the cross-sectional/well-measurement volume effects of the emplaced in-well tracer-measurement system (downhole probe, cables), Equation 3.5 can be rewritten as

$$v_w = \frac{d(\ln C)/dt}{-[2r_w / \pi(r_w^2 - r_t^2)]} \quad (3.6)$$

where  $r_w$  is the radius of well screen,  $L$ , and  $r_t$  is the equivalent radius of tracer-measurement system,  $L$ .

It should be noted that the calculated  $v_w$  is not the groundwater-flow velocity within the aquifer,  $v_a$ . The  $v_w$  is related to actual groundwater velocity within the aquifer by the following relationship:

$$v_w = v_a n_e \infty \quad (3.7)$$

where  $n_e$  is the effective porosity, dimensionless, and  $\infty$  is the groundwater-flow-distortion factor, dimensionless, with a common range of 0.5 to 4.

Various aspects of conducting tracer-dilution tests (i.e., test design, influencing factors) have been discussed previously by a number of investigators (e.g., Halevy et al. 1966; Freeze and Cherry 1979). Following completion of the tracer-dilution test, the tracer can be recovered from the formation by pumping and the results analyzed to assess the effective porosity within the test interval. Tracer-pumpback tests are discussed in the following section.

Some investigators have noted differences in hydraulic property estimates obtained with tracer-dilution techniques and other test methods (e.g., Drost et al. 1968; Kearn et al. 1988). These differences were attributed, in some cases, to distortions in the flow field caused by increased (or decreased) permeability near the well.

Analysis details and results for the tracer-dilution test conducted at well 299-W22-47 are provided in Chapter 5.

### **3.2.2 Tracer-Pumpback Tests**

Detailed procedures to conduct standard, single-well, conservative tracer tests are provided in Pickens and Grisak (1981) and Molz et al. (1985). The tracer pumpback includes the following basic test procedure:

- emplace a conservative tracer (bromide) within the well/aquifer system
- define a prescribed residence (drift) time for the tracer to be dispersed within the aquifer
- withdraw the tracer from the well/aquifer system by pumping at a constant rate
- monitor tracer concentrations at the test well (bromide sensor/flow cell) and collect discrete groundwater samples for quantitative laboratory analysis.

The tracer-testing program relied on natural groundwater flow to emplace the tracer and did not include actual injection of the bromide tracer into the surrounding aquifer. Because of the relatively small area represented by the well (i.e., in comparison to the aquifer) and volumes of tracer involved, the results obtained from these tracer tests may be more susceptible to wellbore effects (e.g.,  $\infty$  and possible down-gradient dead zone).

For the tracer-pumpback tests, a constant-rate pumping test is initiated after the average tracer concentration decreases (i.e., is diluted) to a sufficient level within the well screen (usually a one-to-two order of magnitude reduction from the original tracer concentration). The objective of the pumpback test is to capture the tracer that has moved from the well into the surrounding aquifer. Tracer recovery is monitored qualitatively by measuring the tracer concentration at the surface using a bromide sensor/flow cell installed in the discharge line. Discrete samples are collected at the surface at preselected times for quantitative laboratory tracer analysis.

The time required to recover the center of tracer mass from the aquifer provides information concerning  $n_e$  and  $v_a$ .  $n_e$  is a primary hydrologic parameter that controls contaminant transport. Analytical methods available for the analysis of single-well, tracer injection/withdrawal tests include (in addition to the previously cited references) Güven et al. (1985), Leap and Kaplan (1988), and Hall et al. (1991). The procedure to analyze the tracer-pumpback results is based on a rearrangement of the equations presented in Hall et al. (1991), which combines the basic pore velocity groundwater-flow equation (Equation 3.8) with the regional advective flow-velocity equation (Equation 3.9) describing tracer-drift and -pumpback tests as reported in Leap and Kaplan (1988).

$$v_a = \frac{K I}{n_e} \quad (3.8)$$

$$v_a = \frac{[(Q t_p)/\pi n_e b]^{1/2}}{t_t} \quad (3.9)$$

Combining and rearranging results in

$$v_a = \frac{Q t_p}{\pi b t_t^2 K I} \quad (3.10)$$

and

$$n_e = \frac{\pi b t_t^2 K^2 I^2}{Q t_p} \quad (3.11)$$

where  $v_a$  = advective groundwater-flow velocity within the aquifer; L/T

$n_e$  = effective porosity; dimensionless

$K$  = hydraulic conductivity; L/T

$I$  = local hydraulic gradient; dimensionless

$b$  = aquifer thickness; L

$Q$  = tracer-pumpback rate; L<sup>3</sup>/T

$t_p$  = pumping time required to recover the center of mass of tracer emplaced into the aquifer

$t_t$  = total elapsed time equal to sum of the tracer drift time,  $t_d$ , (time from tracer emplacement to start of recovery pumping) and  $t_p$ .

The  $K$  values used in Equations 3.10 and 3.11 were determined from analysis of constant-rate pumping tests for the test well (i.e., during the tracer pumpback). The estimate for  $I$  was determined using trend-surface analysis of water-level elevation measurements from nearby wells as described in Section 3.4. The  $b$  value was calculated directly from geologic information obtained for the well or a projection from known geologic relationships at nearby wells.

Several steps were required to calculate the time required to recover the tracer center of mass emplaced into the aquifer. The bromide concentration versus time profile during the pumpback test was determined by laboratory analysis of discrete samples collected closely over time. The mass of tracer recovered with time was calculated, based on integrating the product of the exhibited tracer concentration profile and observed pumping rate during the test. The  $t_p$  value, to the center of mass, was calculated by dividing the tracer mass recovered by the actual tracer mass transported into the aquifer. To calculate the actual tracer mass within the aquifer, the mass within the well-screen column and surrounding well sand-pack at the start of the pumpback test was subtracted from the initial mass emplaced in the well. The mass within the well screen was determined by multiplying the known well-screen volume by the average

concentration, which was calculated by the final readings of the bromide sensors used during the tracer-dilution test. The sensors were removed generally within 2 hours of initiation of the tracer pumpback; therefore, their final readings are representative of initial pumpback conditions. For calculating the tracer mass within the sandpack, the study assumed that the tracer concentration was the same as observed within the well screen. Sandpack volumetric calculations were based on available as-built information, a porosity of 25%, and the assumption that 50% of the sandpack (i.e., the downgradient side) would be occupied by the tracer.

The mathematical relationship to calculate half the tracer mass recovered during the pumpback,  $M_{50\%}$ , which is the mass used to calculate the center of mass recovery time,  $t_p$ , then can be expressed as:

$$M_{50\%} = \frac{0.50 (M_r - M_w)}{M_i - M_w} \quad (3.12)$$

where  $M_r$  is the mass of tracer recovered during the tracer pumpback,  $M_i$ ;  $M_w$  is the mass of tracer within well screen and well sandpack at the beginning of the tracer pumpback,  $M_i$ ; and  $M_i$  is the mass of tracer initially emplaced in the well,  $M_i$ .

The  $t_p$  also was corrected (reduced) to account for the transit time of the pumped water from the pump intake to the land surface (i.e., the location where laboratory samples were collected).

Analysis details and results for tracer-pumpback tests conducted at each of the selected test wells are provided in Chapter 6.

### 3.2.3 In-Well Vertical Flow Assessment

Assessment of ambient, in-well vertical flow conditions is important from a perspective of evaluating the representativeness of the well for hydrochemical and contaminant characterization applications as well as for potential impact on the performance of tracer-dilution tests. The potential bias and adverse impacts of vertical in-well flow on hydrochemical characterization have been examined in detail by Reilly et al. (1989), Church and Granato (1996), and Elci et al. (2001) and will not be discussed in this report. Because tracer-dilution testing is an integral part of detailed hydrologic test characterization previously conducted at the Hanford Site (Spane et al. 2001a, 2001b, 2002, 2003; Spane and Newcomer 2004) and performed at well 299-W22-47 during CY 2005, the recognition and quantification of ambient, in-well flow will be discussed in this report section.

In previous site investigations, the presence of in-well vertical flow conditions was quantified using three different test methods: tracer-dilution pattern analysis, vertical flow-tracer tests, and electromagnetic borehole flowmeter (EBF) surveys. As previously reported in Spane et al. (2001a, 2001b), close corroboration was exhibited between the three test methods. Budgetary constraints commonly limit the application of all three in-well vertical flow assessment methods within individual wells. During FY and CY 2005, one well (299-W22-47) was characterized using the tracer-dilution test method, while three wells (299-W14-11, 299-W22-47, and 299-W22-80) were tested using the EBF survey method. No vertical flow tracer tests were conducted during the characterization period.

As discussed in Section 3.2.1, the successful performance of tracer-dilution tests requires that lateral groundwater-flow conditions exist within the well fluid column. The presence of vertical flow, however, is indicated during the initial phases of tracer dilution if a systematic, “stair-step,” tracer-dilution pattern is exhibited for the respective depth settings of the bromide sensor. Figure 3.10 illustrates a hypothetical tracer-dilution pattern for various depths for a downward vertical flow condition within the well screen. As shown, the pattern evolves with time (after the tracer has been uniformly mixed within the well-screen section), as a result of the downward flow/mixing of nontracer groundwater. As shown in Figure 3.10, the pattern is characterized by a progressive extension of a constant tracer concentration for the sensors at greater depths, followed by a rapid decline of tracer on arrival of the downward flow mixture of tracer and nontracer groundwater. During late test times, the tracer versus depth profiles exhibit a parallel-linear pattern. In-well vertical flow,  $v_v$ , can be calculated by using the arrival time of the tracer/nontracer groundwater mixture front at the various known sensor depth settings.

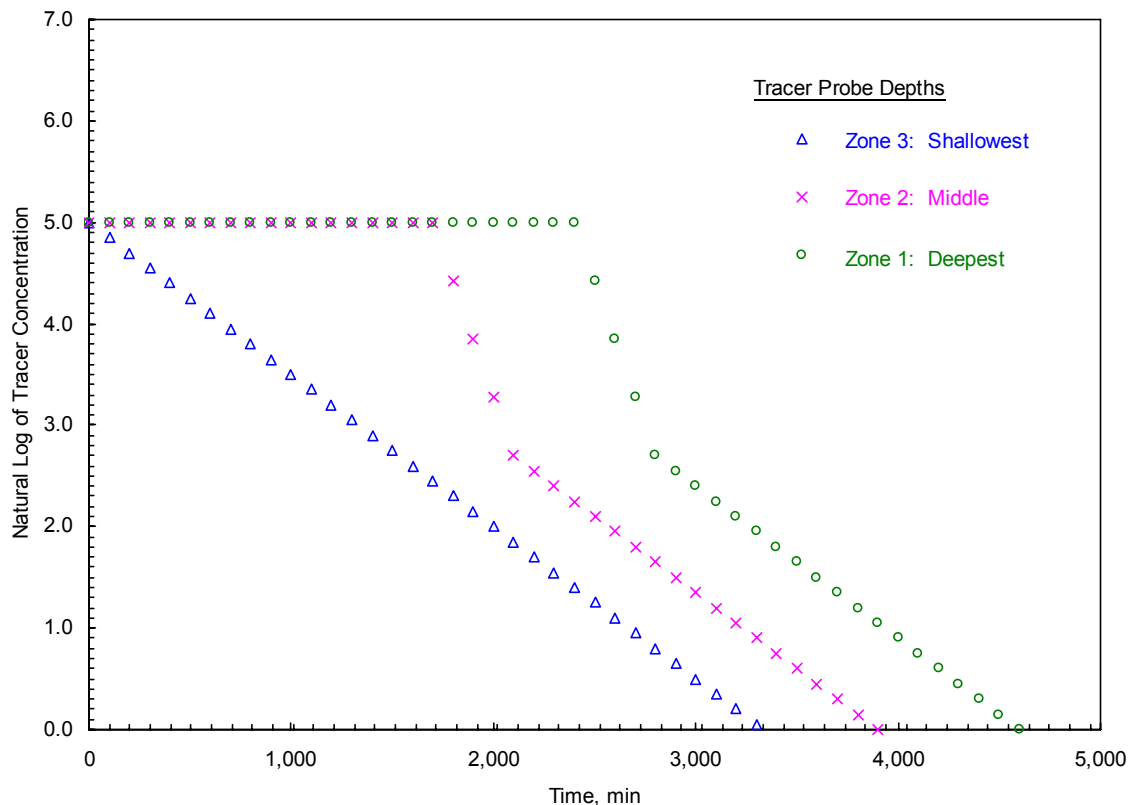


**Figure 3.10.** Hypothetical Tracer-Dilution Pattern Indicative of Vertical In-Well Downward Flow

Briefly stated, the EBF method measures in-well vertical flow indirectly, based on Faraday’s Law of Induction, which states that the voltage induced by a conductor moving at right angles through a magnetic field is directly proportional to the velocity of the conductor moving through the field. In this analogy, flowing water within the well is the conductor, the electromagnet within the EBF generates a magnetic



field, and the EBF electrodes are used to measure the induced voltage of the flowing water within the system. For sign convention, upward flow represents a positive voltage signal, and downward flow represents a negative voltage signal.

The EBF system consists of an electromagnet and two electrodes positioned 180 degrees apart inside a hollow cylinder within the equipment assembly. The inside diameter of the hollow cylinder is 0.0254 m (1 in.), and the outside diameter of the probe cylinder is 0.0508 m (2 in.). The probe is connected to an electronics box at the surface using an insulated/jacketed cable. The downhole electrodes transmit a voltage signal that is directly proportional to the vertical velocity of water (acting as the conductor) within the hollow cylinder of the EBF assembly. A surface computer records the voltage signal and converts the signal to an in-well flow-rate measurement.

An inflatable packer is used to channel in-well flow through the EBF measurement cylinder and to minimize bypass flow between the probe and the surrounding well screen. The inflatable packer consists of a rubber sleeve attached to a stainless steel assembly, which is sealed on its ends with hose clamps. The EBF probe cylinder is placed inside the stainless steel assembly. The packer and fittings of the assembly are checked for gas leaks in the field before lowering the assembly into the well. An in-well profile of ambient, in-well vertical flow is developed by systematically raising and lowering the EBF to known depth intervals, inflating the packer assembly, and recording stabilized flowmeter readings. At each measurement depth setting, inflation of the packer was controlled using compressed nitrogen gas, a regulator, and inflation tubing. After inflating the packer, the integrity of the packer seal was qualitatively checked by lifting the attached EBF equipment cable to verify packer tension and stability within the well-screen section. In-well flow conditions were allowed to stabilize generally for a period of 5 to 10 minutes to dissipate any disturbances caused by movement of the packer/probe assembly within the well screen. After recording the flow measurement, the packer was deflated using a vented surface valve, the EBF probe was then raised slowly to the next depth, and the measurement procedure was then repeated.

EBF flowmeter measurements are generally made in succession from bottom to top of the well screen. Zero flow points within the well are measured in the sump section below the bottom of the well screen at the beginning and at the top of the water column at the end of the EBF survey, respectively. These measurements provide a known zero-flow reference for the ambient flow measurements and account for uncertainty associated with drift that may occur during the survey. For consistency, all ambient flow measurements were corrected to the zero flow point measured at the top of the water column. A more detailed description of the EBF instrument system and field test applications are provided in Young et al. (1998) and Waldrop and Pearson (2000).

Results of in-well ambient vertical flow assessments based on the tracer-dilution test and EBF surveys conducted during FY and CY 2005 are presented in Chapter 8. A discussion of the previous in-well vertical flow characterizations and method comparisons are presented in Spane et al. (2001a, 2001b, 2002, 2003) and Spane and Newcomer (2004).

### **3.3 Constant-Rate Pumping Tests**

Drawdown and recovery water levels were measured during tracer-pumpback tests for the one 200-West Area well selected for detailed hydrologic characterization (299-W22-47). Diagnostic analysis of the test responses was first conducted to determine aquifer/test system characteristics and to identify whether the test data display infinite-acting radial flow behavior. The drawdown and recovery phases of constant-rate discharge were then analyzed by type-curve fitting of log-log plots and, if appropriate, by straight-line analysis of semilogarithmic data plots of water-level change versus time. Test performance and methods used to analyze the results obtained from constant-rate testing are described in this section. Analysis details and results for the selected test well are provided in Chapter 7.

#### **3.3.1 Test Methods and Equipment**

A 3-hp Grundfos® submersible pump was used to remove water during each pumping test. Flow rates were monitored with a surface turbine flowmeter (inside diameter 0.025 meter, Arad®, model #555061). Flow was adjusted manually using a gate valve to maintain constant-rate conditions. During the initial minutes of pumping (e.g., first 3 minutes), “instantaneous” flow rates were determined by measuring the time required for 19 liters of flow to register on the flow-meter dials. Flow-meter totalizer readings were recorded every 5 to 20 minutes during pumping. Druck, Inc., 0 to 10 psig, differential pressure transducers (model # PDCR® 1830-8388) were used to monitor water levels in the pumping well and the nearby monitor wells during the test. The transducers were vented at the surface to compensate automatically for atmospheric pressure fluctuations. Pressure transducer measurements were recorded using a Campbell Scientific, Inc. model CR-10X™ data logger.

Because tracer recovery also was being monitored during the tracer-pumpback test, part of the discharged groundwater was routed through a flow-through cell containing a bromide-selective ion probe, and a sampling port was used to collect water for laboratory analysis of the bromide tracer. These devices were located downstream from the flowmeter. The discharged water during the pumping test was collected in a tank truck for subsequent disposal at an effluent disposal facility.

#### **3.3.2 Barometric Pressure Effects Removal**

The analysis of well water-level responses during hydrologic tests provides the basis to estimate hydraulic properties that are important to evaluate groundwater-flow velocity and transport characteristics. Barometric pressure fluctuations, however, can have a discernible impact on well water-level measurements. Although the pressure transducers were vented to compensate for changes in barometric pressure, barometric pressure fluctuations also can cause changes in the water level in a well. This response effect is commonly ascribed to confined aquifers; however, wells completed within unconfined aquifers may also exhibit associated responses to barometric changes (Weeks 1979; Rasmussen and Crawford 1997). Water levels in unconfined aquifers typically exhibit variable time-lagged responses to barometric fluctuations. This time-lag response is caused by the time required for the barometric pressure change to be transmitted from land surface to the water table through the vadose zone, as compared to the instantaneous transmission of barometric pressure through the open well.

To determine the significance of barometric effects, well water-level responses were monitored during an extended baseline period after the constant-rate discharge test was terminated, and they were compared to the corresponding barometric pressure changes. Barometric pressures were obtained from the Hanford Meteorology Station (located immediately east of the 200-West Area) where they are recorded hourly. The barometric responses were then analyzed and removed from the recorded water levels using the multiple-regression deconvolution techniques described in Rasmussen and Crawford (1997) and Spane (1999, 2002). This technique relies on a least-squares fit of the water-level change to the corresponding barometric pressure change and time-lagged earlier barometric pressure changes. As noted in Spane (1999), under prevalent conditions in the 200-West and East Areas, no significant difference in removal efficiency was derived in using data collected at higher recording frequencies (e.g., 15 minutes). Therefore, data collected at a 1-hour frequency were used in the process of removing barometric pressure effects from the pumping test conducted at well 299-W22-47.

Because barometric changes were recorded at a constant 1-hour frequency, the relationship between water level and barometric change can be represented as follows:

$$\Delta h_w = X_0 \Delta h_{ai} + X_1 \Delta h_{ai-1} + X_2 \Delta h_{ai-2} + \dots + X_n \Delta h_{ai-n} \quad (3.12)$$

where  $\Delta h_w$  = water-level change over the last hour  
 $\Delta h_{ai}$  = barometric pressure change over the last hour  
 $\Delta h_{ai-1}$  = barometric pressure change from 2 hours to 1 hour previous  
 $\Delta h_{ai-n}$  = barometric pressure change from n hours to (n-1) hour previous  
 $X_0 \dots X_n$  = regression coefficients corresponding to time lags of 0 to n hours  
n = number of hours that lagged barometric effects are apparent.

After calculating  $X_0 \dots X_n$ , simulated well water levels associated with the hourly barometric responses were calculated from the above equation for the baseline period. The results were then compared to the actual observed well water-level response for a “goodness of fit” evaluation. To remove barometric effects from water levels recorded during the constant-rate discharge test, a simulated well water-level response was calculated based on the hourly barometric changes that were observed over the test period. The predicted barometric-induced response was then subtracted from the recorded pumping test water-level measurements. Analysis techniques described in the following section were then applied to the data after removal of barometric effects. A discussion of the barometric response analysis performed in association with the pumping test conducted at well 299-W22-47 is presented in Chapter 7.

### 3.3.3 Unconfined Aquifer Dewatering Drawdown Correction

In thin aquifers where drawdown represents a significant percentage of the total saturated thickness, corrections for dewatering the unconfined aquifer are required to account for the decrease in associated aquifer transmissivity. Jacob (1963) provided an equation to correct drawdown data obtained for pumping tests within thin unconfined aquifers. The corrected drawdown,  $s'$ , which accounts for aquifer dewatering, can be calculated using the following relationship:

$$s' = s - \left( \frac{s^2}{2b} \right) \quad (3.13)$$

where  $s$  is the observed drawdown, and  $b$  is the initial saturated aquifer thickness.

For most previously tested Hanford Site well locations, the drawdown represented only a small part of the total aquifer thickness (e.g., 200-West Area). This was also the case for well 299-W22-47 that was tested during FY and CY 2005. For this test well, a maximum drawdown data correction of less than 0.001 m is indicated ( $s = 0.3$  m;  $b = 67.6$  m). For this reason, the drawdown correction as described in Equation 3.13 is largely inconsequential and was not employed in the pumping test analysis for well 299-W22-47.

### 3.3.4 Diagnostic Analysis and Derivative Plots

Log-log plots of water level versus time have traditionally been used for diagnostic purposes to examine pumping-test drawdown data. More recently, the derivative of the water level or pressure has also been used (Bourdet et al. 1989; Spane 1993) as a diagnostic tool. The use of derivatives has been shown to improve significantly the diagnostic and quantitative analysis of various hydrologic test methods (Bourdet et al. 1989; Spane 1993). The improvement in test analysis is attributed to the sensitivity of pressure derivatives to various test/formation conditions. Specific applications for which derivatives are particularly useful include the following:

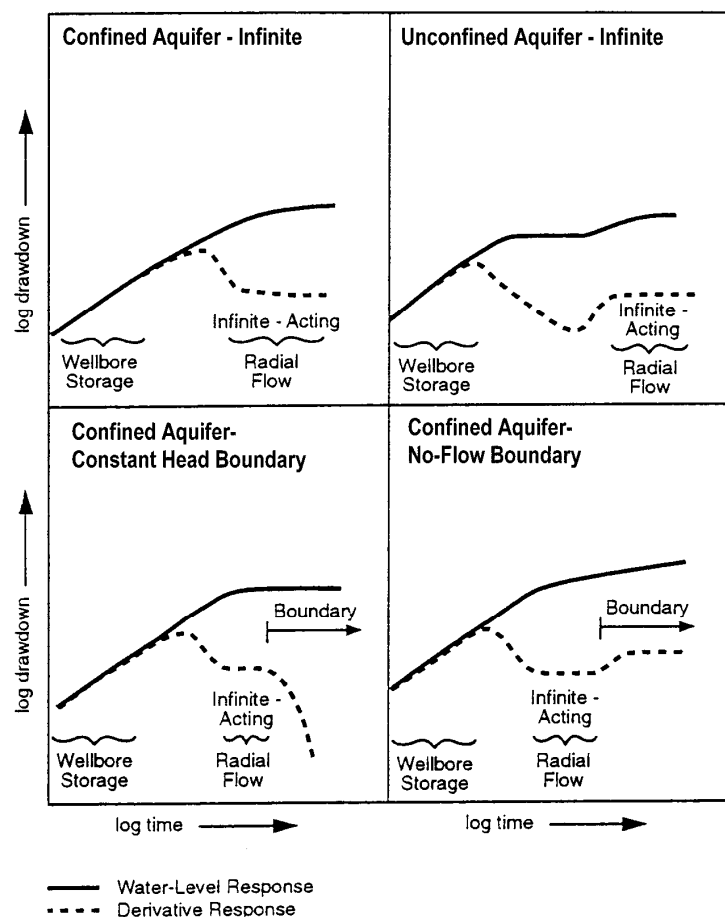
- determining formation-response characteristics (confined or unconfined aquifer) and boundary conditions (impermeable or constant head) that are evident within the test data
- assisting in selecting the appropriate type-curve solution through combined type-curve/derivative plot matching
- determining when infinite-acting, radial flow conditions are established and, therefore, when straight-line analysis methods are applicable.

Figure 3.11 shows log-log drawdown and derivative responses that are characteristic of some commonly encountered formation conditions. As shown, early test data within a pumped well are largely dominated by wellbore storage/skin effects, which are indicated by a steep, upward-trending derivative. The derivative normally decreases during the transition from wellbore storage to radial flow and stabilizes at a constant value when infinite-acting, radial flow conditions are established. The stable derivative reflects the straight line on the semilog plot for infinite-acting radial flow. Unconfined aquifers and formations exhibiting double-porosity characteristics (e.g., fractured media) may show two stable derivative sections at the same vertical position separated by a “valley” that represents the transition from one storage value to the other. Diagnostic derivative plots are also useful to identify boundary effects.

A linear, no-flow boundary has a distinctive derivative pattern. If radial flow occurs before the influence of the boundary is established, a stable/flat derivative (radial-flow condition) will occur for a time, which is then followed by an upward shift to double the original value (no-flow boundary).

Constant-head boundaries display a downward trend in the derivative, which may be preceded by a stable derivative if radial flow conditions occur before the boundary effect becomes dominant. For the diagnostic and test analysis aspects of this report, derivative responses were calculated using the DERIV program described in Spane and Wurstner (1993).

For the pumping test conducted as part of the FY and CY 2005 detailed hydrologic characterization test, the derivative of the water level with respect to the natural logarithm of time was calculated and plotted on composite log-log plots of drawdown and recovery versus time. Diagnostic and analysis results of the log-log plot of water-level and the associated derivative response for the constant-rate pumping test conducted at well 299-W22-47 are provided in Chapter 7.



**Figure 3.11.** Characteristic Log-Log Drawdown and Drawdown Derivative Plots for Various Hydrogeologic Formation and Boundary Conditions

### 3.3.5 Type-Curve-Matching Analysis Methods

Type-curve-matching methods (Theis 1935; Hantush 1964; Neuman 1972, 1974, 1975) are commonly used to analyze pumping test responses. For this study, unconfined aquifer pumping test-type curves were generated using the WTAQ3 computer program described by Moench (1997). WTAQ3 can be used to generate type curves that represent a wide range of test and aquifer conditions, including partially penetrating wells, confined or unconfined aquifer models, well-skin effects, and wellbore storage at both the stress (pump) and observation (monitor) well locations. The type-curve-generation program also allows for noninstantaneous release (drainage-delay factor) of water from the unsaturated zone during the pumping test. However, this was found to not be a significant factor in the analysis; therefore, the type curves used in the analyses for this report all reflect an instantaneous release of water, which was the approach used by Neuman (1972, 1974, 1975).

In the type-curve-matching procedure, the log-log drawdown or recovery data and its associated derivative response for an individual well were matched simultaneously with dimensionless type-curve responses generated using WTAQ3 (Moench 1997) and the associated derivative plots obtained with the DERIV program (Spane and Wurstner 1993). The dimensionless responses depend on the assumed values of sigma,  $\sigma = S/S_y$ , and vertical anisotropy,  $K_D = K_v/K_h$ . For initial type-curve-matching runs, the values for  $\sigma$  and  $K_D$  were set at 0.001 and 0.10, respectively. Minor adjustments were made to the initial  $K_D$  value to improve dimensionless curve matches of the data and associated derivative response patterns. The predicted response also is influenced by the assumed storativity,  $S$ , value because of its effect on wellbore storage. After an appropriate dimensionless match to the observed test data was obtained, dimensional curves were generated using the given well/test conditions (e.g., well radius, radial distance to observation well, average pumping rate) and making adjustments to aquifer properties ( $T$ ,  $S_y$ ) until the best match with the observed data was obtained. (Note that adjusting  $S_y$  also changes the value of  $S$  because  $\sigma$  was held constant.)

Type-curve-matching methods are normally applied to observation well data and not to pumping wells because of the additional head losses that commonly occur at the pumped well. However, in previous analyses of test responses for the new RCRA wells in the 200-West Area (as reported in Spane 2001a, 2001b, and 2002), the fitting of type curves to stress-well responses resulted in approximately the same  $T$  as fitting type curves to the observation well data. This suggests a high efficiency of the stress well, which incorporates a screen and sand pack in a relatively low-permeability aquifer. Therefore, little head loss appears to be associated with the movement of water into the well during pumping. Because of the similarities in well construction and development activities, it is assumed that the use of type-curve analysis of observed drawdown responses at the pumping well tested during FY and CY 2005 is also appropriate. While this method is expected to provide quantitative estimates for  $T$  and  $K_h$ , estimates obtained for  $K_D$  and  $S_y$  based solely on pumping well data analysis are considered to be only qualitative values. This is attributed primarily to the relative insensitivity of pumping well type curves to  $K_D$  and the relatively short-duration of pumping tests normally conducted on the Hanford Site (e.g., 240 to 360 min).

### **3.3.6 Straight-Line Analysis Methods**

For straight-line analysis methods, the rate of change of water levels within the well during draw-down and/or recovery is analyzed to estimate hydraulic properties. Because well effects are constant with time during constant-rate tests, straight-line methods can be used to analyze quantitatively the water-level response at both pumping and observation wells. The semilog, straight-line analysis techniques commonly used are based on either the Cooper and Jacob (1946) method (for drawdown analysis) or the Theis (1935) recovery method (for recovery analysis). These methods are theoretically restricted to the analysis of test responses from wells that fully penetrate nonleaky, homogeneous, isotropic, confined aquifers. Straight-line methods, however, may be applied under nonideal well and aquifer conditions if infinite-acting, radial flow conditions exist. Infinite-acting, radial flow conditions are indicated during testing when the change in pressure, at the point of observation, increases in proportion to the logarithm of time. As discussed above, the use of diagnostic derivative methods (Bourdet et al. 1989) makes it easier to identify the portions within the test data where straight-line analysis is appropriate. As will be discussed in Chapter 7, derivative analysis of the observed test responses indicated that infinite-acting, radial flow conditions were not established at well 299-W22-47 during the constant-rate pumping test. The use of straight-line analysis methods, therefore, is appropriate for this test.

## **3.4 Groundwater-Flow Characterization**

To support the detailed hydrologic characterization program, groundwater-flow direction and hydraulic gradient conditions were calculated at the various test sites during the period of tracer testing. Groundwater-flow direction and hydraulic gradient were determined using the commercially available WATER-VEL (In-Situ, Inc. 1991) software program. Water-level elevations from neighboring, representative wells were used as input with the WATER-VEL program to calculate groundwater-flow direction and hydraulic gradient conditions. The program uses a linear, two-dimensional trend surface (least squares) to randomly locate hydraulic head or water-level elevation input data. This method is similar also to the linear approximation technique described by Abriola and Pinder (1982) and Kelly and Bogardi (1989). Reports that demonstrate the use of the WATER-VEL program for calculation of groundwater-flow velocity and direction on the Hanford Site include Gilmore et al. (1992) and Spane (1999). Details and results for a groundwater-flow characterization conducted at well 299-W22-47 are presented in Section 8.2.

## **4.0 Slug-Test Results**

Multiple slug tests were conducted at the nine identified completed wells and three multi-depth test interval well sites during FY and CY 2005. The slug tests were initiated either mechanically by rapidly removing a slugging rod of known volume from the well-screen section or pneumatically by releasing compressed gas used to depress the well water-column within the test casing system. For standard mechanical slug-test characterizations, two different size slugging rods were used during the testing program at each well to impose different stress levels on the test section. The stress levels for the two slugging rods are calculated to impose a slug-withdrawal test response of 0.458 m (low-stress tests) and 1.117 m (high-stress tests) within a 0.1016-m inside diameter well. For pneumatic tests, no set pressures were utilized; however, the highest stress level employed was generally  $\geq 2$  times the lowest test stress used during the test characterization.

As noted in Butler (1996), differences exhibited between slug tests conducted at different stress levels can be used to evaluate stress-dependent, non-linear test well effects (e.g., dynamic skin, turbulent head loss), which are unrelated to aquifer characteristics. Methods used to analyze the slug-test results are described in Section 3.1. Table 4.1 summarizes the diagnostic slug-test-response characteristics exhibited at the respective test well locations. As indicated, eight test sites exhibited over-damped, homogeneous or heterogeneous formation conditions. For these diagnostic test conditions, the analytical methods presented in Section 3.1.1 (i.e., Bouwer and Rice or type-curve methods) are the appropriate methods used for test analysis. For the test well site exhibiting critically-damped test responses, the High-K analysis method described in Section 3.1.2 was used. As noted in Section 3.1.2, the High-K analysis method requires that the pressure sensor utilized during testing be located in close proximity to the water-table surface. This is due to the effects of water-column acceleration within the well. Because of testing constraints at this site, the pressure sensor was located  $>2$  m below the water-column surface for most tests performed. As a result, hydraulic conductivity derived for this well site may be lower than the actual formation hydraulic conductivity, due to damping effects imposed by the exhibited fluid-column acceleration. A summary list of the hydraulic properties determined from slug testing is provided in Table 4.2. A description of the performance and analysis of slug tests conducted at each well site is provided below.

### **4.1 Completed Well Slug-Test Characterizations**

Slug-test characterization was conducted at nine test well-site locations after final well construction activities were completed. Analytical results and pertinent test information for the completed well slug tests are discussed in the following section.

#### **4.1.1 Well 299-E33-49**

The well-screen test interval is located immediately above the Saddle Mountains Basalt (the base of the unconfined aquifer at this location) and consists of unconsolidated sediments of the Hanford formation (Unit 1). The borehole geology log for this well indicates that the Hanford formation test



section (i.e., 81.12 to 86.41 m below ground surface [bgs]) generally consists of a sandy gravel unit composed of 60% gravel, 30 to 35% sand, and 5 to 10% silt.

**Table 4.1.** Completed Well Slug-Test Characteristics

Test Well	Test Parameters		Hydrogeologic Unit Tested	Diagnostic Response
	Aquifer Thickness <sup>(a)</sup> (m)	Test Interval Saturated Thickness (m)		
299-E33-49	5.29	5.29	Hanford formation (Unit 1)	Critically-Damped
299-W11-46	49.9	6.10	Ringold Formation (Unit 5)	Over-Damped/Elastic Response
299-W14-11	52.1	3.05	Ringold Formation (Unit 5)	Over-Damped/Elastic Response
299-W15-83	63.5	9.80	Ringold Formation (Unit 5)	Over-Damped/Heterogeneous Formation Response
299-W15-94	62.9	10.08	Ringold Formation (Unit 5)	Over-Damped/Heterogeneous Formation Response
299-W15-152	66.4	10.10	Ringold Formation (Unit 5)	Over-Damped/Heterogeneous Formation Response
299-W19-47	62.9	10.19	Ringold Formation (Unit 5)	Over-Damped/Heterogeneous Formation Response
299-W22-47	67.6	10.45	Ringold Formation (Unit 5)	Over-Damped/Critically-Damped
299-W22-80	68.6	8.99	Ringold Formation (Unit 5)	Over-Damped
Note: For all test wells, $r_c = 0.051$ meter; $r_w = 0.110$ meter (see Nomenclature for definitions). Unit number in parentheses indicates the relevant groundwater-flow model layer, as described in Thorne et al. (1993). (a) Determined either from actual site drill/depth information or from projection from neighboring wells.				

Seven standard slug tests (three low and four high stress tests) were conducted on September 20, 2005. All slug tests exhibited critically-damped (transitional response) behavior, which is indicative of moderate to high-permeability aquifer conditions. Because of the exhibited critically-damped response behavior, the High-K analysis method presented in Butler and Garnett (2000) and Butler et al. (2003) (see Section 3.1.4) was used to analyze the slug tests at well 299-E33-49.

Because of the existing high-permeability test-interval conditions, very small test responses were observed for the low-stress tests (test response <0.05 m, with recovery <6 sec). Due to the larger test responses produced, better analytical results were obtained for the high-stress tests. As discussed in Butler et al. (2003), for tests conducted in high-permeability formations, the pressure sensor should be situated in close proximity to the top of the well water-column to avoid well acceleration effects. For the slug-test characterization conducted at well 299-E33-49, the pressure sensor was situated within 0.5 meters of the top of the well water-column for only two of the high-stress slug tests. For the remaining tests, the pressure sensor was situated at a standard depth of ~2.3 meters below the top of the well water-column. For the above reasons, hydraulic property characterization for the well-screen

interval was limited to the two high-stress slug tests conducted with the pressure probe positioned near the top of the water column.

**Table 4.2.** Completed Well Slug-Test Results

Test Well	Bouwer and Rice Analysis Method	Type-Curve Analysis Method		High-K Analysis Method <sup>(b)</sup>	
	Horizontal Hydraulic Conductivity, $K_h$ <sup>(a)</sup> (m/day)	Horizontal Hydraulic Conductivity, $K_h$ <sup>(a)</sup> (m/day)	Specific Storage, $S_s$ (m <sup>-1</sup> )	Horizontal Hydraulic Conductivity, $K_h$ <sup>(a)</sup> (m/day)	Dimensionless Damping Parameter, $C_D$
299-E33-49	NA	NA	NA	85.8–108.0 <sup>(b)</sup> (96.9)	0.60–0.75
299-W11-46	2.72–2.99 (2.87)	3.67–3.89 (3.78)	5.0E-4–7.0E-4	NA	NA
299-W14-11	7.49–8.19 (7.84)	10.8	1.0E-3–5.0E-4	NA	NA
299-W15-83	Inner Zone: 9.34–11.7 (10.5) Outer Zone: 4.22–4.40 (4.31)	Inner Zone: 9.94–13.0 (11.5) Outer Zone: 5.36	1.0E-04 5.0E-6	NA	NA
299-W15-94	Inner Zone: 9.22–13.9 (11.6) Outer Zone: 4.44–4.54 (4.49)	Inner Zone: 11.7–14.7 (13.2) Outer Zone: 5.83	5.0E-6–5.0E-5 5.0E-6	NA	NA
299-W15-152	Inner Zone: 23.9–31.3 (27.6) Outer Zone: 11.4–13.6 (12.5)	Inner Zone: 30.2–34.8 (32.5) Outer Zone: 17.7	5.0E-6–1.0E-4 1.0E-6 to 1.0E-4	NA	NA
299-W19-47	Inner Zone: 11.4–17.1 (14.3) Outer Zone: 3.71–4.23 (3.97)	Inner Zone: 15.1–21.6 (18.4) Outer Zone: 4.10–4.75 (4.43)	1.0E-6–5.0E-5 1.0E-6–5.0E-5	NA	NA
299-W22-47	13.5	17.3	1.0E-6	NA	NA
299-W22-80	9.72–10.2 (9.96)	13.0	1.0E-5–4.0E-5	NA	NA
Note: see Nomenclature for definitions.					
Number in parentheses is the average value for all tests.					
(a) Assumed to be uniform within the well-screen test section. For tests exhibiting a heterogeneous formation response, only outer zone analysis results are considered representative of <i>in situ</i> formation conditions.					
(b) Standard analytical methods are not valid. Results are based on the High-K analysis method presented in Butler and Garnett (2000).					

An example of a High-K analysis plot for one of the two tests analyzed for this well is shown in Figure 4.1. As indicated, a critically-damped (single-oscillatory) response is exhibited with a rapidly damped recovery to static conditions (i.e., recovery within ~6 seconds). Similar response characteristics were exhibited for the other high-stress test. Estimates for K ranged from 85.8 to 108.0 m/day and averaged 96.9 m/day for the two high-stress tests.

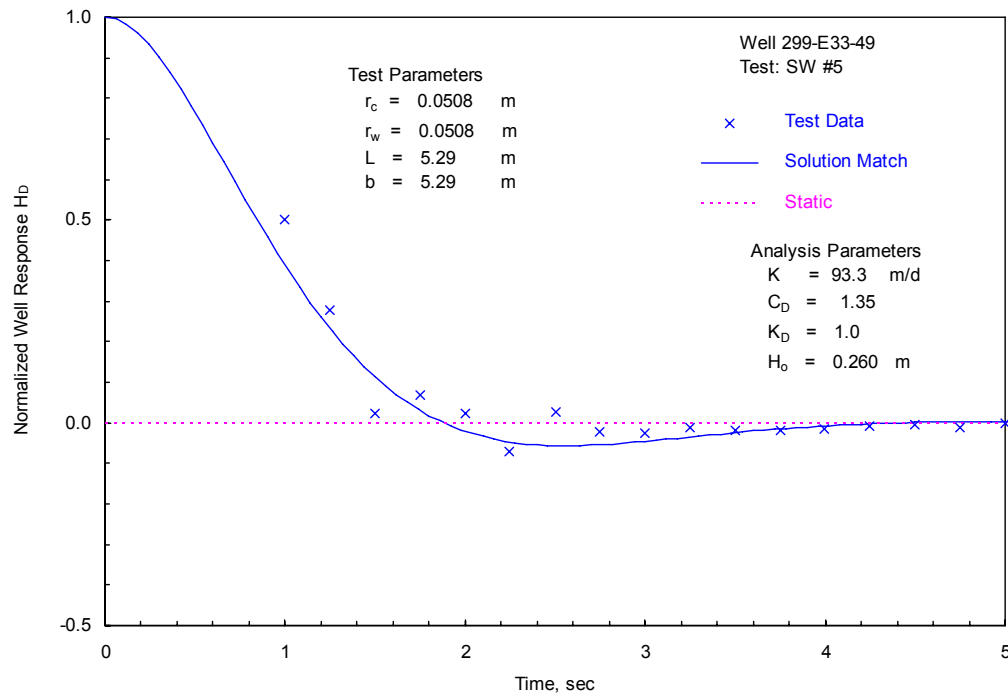


**Figure 4.1.** High-K, Critically-Damped Slug-Test Analysis Plot for Well 299-E33-49

#### 4.1.2 Well 299-W11-46

At the time of testing, the well-screen test interval, which consisted of unconsolidated sediments of the Ringold Formation (Unit 5), was located approximately 6.45 m below the unconfined aquifer water-table surface. The borehole geology log for this well indicates that the Ringold Formation test section (i.e., 80.28 to 86.38 m bgs) generally consists of a silty sandy to sandy gravel unit, which grades to a sand near the base of the test interval. The overlying sandy gravel unit is composed of 55 to 70% gravel, 20 to 35% sand, and 10% silt.

A total of four slug tests (two low and two high stress) were conducted on September 21, 2005. A comparison of the normalized, high- and low-stress slug-test responses indicates essentially identical behavior, which indicates linear test behavior and suggests that the well had been fully developed. Examination of the individual slug-test responses also indicates an elastic (concave upward) response displayed on the Bouwer and Rice analysis plot in Figure 4.2. The elastic response requires that late-time analysis be employed (i.e., the normalized head segment between 0.3 and 0.2) when using the Bouwer and Rice (1976) method, as recommended in Butler (1996, 1998). A test method comparison of  $K$  estimates indicates that consistently lower results (~25% lower) were obtained for the Bouwer and Rice method. For the Bouwer and Rice method, estimates for  $K$  ranged from 2.72 to 2.99 m/d (average 2.87 m/d), while the type-curve method provided estimates between 3.67 and 3.89 (average 3.78 m/d) for both stress-level tests. Selected examples of the analysis plots for this well are shown in Figure 4.2.

### 4.1.3 Well 299-W14-11

At the time of testing, the well-screen test interval, which consisted of unconsolidated sediments of the Ringold Formation (Unit 5), was located approximately 11.00 m below the unconfined aquifer water-table surface. The borehole geology log for this well indicates that the Ringold Formation test section (i.e., 79.76 to 82.81 m bgs) generally consists of a sandy gravel unit, which is composed of 60% gravel, 35% sand, and 5% silt.

A total of five slug tests (two low and three high stress) were conducted on September 20, 2005. A comparison of the normalized, high- and low-stress slug-test responses indicates essentially identical behavior, which indicates linear test behavior and suggests that the well had been fully developed. Examination of the individual slug-test responses also indicates an elastic (concave upward) response displayed on the Bouwer and Rice analysis plot in Figure 4.3. The elastic response requires that late-time analysis be employed (i.e., the normalized head segment between 0.3 and 0.2) when using the Bouwer and Rice (1976) method, as recommended in Butler (1996, 1998). A test method comparison of K estimates indicates that consistently lower results (~30% lower) were obtained for the Bouwer and Rice method. For the Bouwer and Rice method, estimates for K ranged from 7.49 to 8.19 m/d (average 7.84 m/d), while the type-curve method provided an identical analysis estimate value of 10.8 m/d for both stress-level tests. Selected examples of the analysis plots for this well are shown in Figure 4.3.

### 4.1.4 Well 299-W15-83

At the time of testing, the well-screen interval included the upper 9.80 m of the unconfined aquifer and consisted of unconsolidated sediments of the Ringold Formation (Unit 5). The borehole geology log for this well indicates that the Ringold Formation test section (i.e., 72.50 to 82.30 m bgs) generally consists of a sandy gravel unit, which varies in composition from 50 to 80% gravel, 15 to 50% sand, and 0 to 10% silt.

A total of four slug tests (two high and two low stress) were conducted on October 5, 2005. All slug-test responses indicated a heterogeneous formation behavior, with a higher permeability zone located in proximity to the well screen, as indicated by a rapid recovery rate at early test times. This transitions to a slower recovery rate for the surrounding lower permeability material (exemplified on the type-curve response plot in Figure 4.4). A comparison of the normalized, high- and low-stress, slug-test responses indicates a slight delay in the early-test, time-response behavior for the high-stress tests, which is attributable to higher turbulence that occurred for these tests. For this reason, the low-stress test results are believed to provide more representative estimates for the inner-zone region close to the well screen. Nearly identical behavior was evident for tests conducted at a particular stress level, suggesting that the well had been developed sufficiently to establish stable skin conditions.

Slug tests exhibiting heterogeneous formation test response can be analyzed quantitatively using the homogeneous formation analysis approaches described in Chapter 3. For the homogeneous formation analysis, the type-curve method estimates for K ranged between 9.94 and 13.0 m/day (average 11.5 m/day) for both stress-level tests for the higher permeability inner zone (example analysis figure

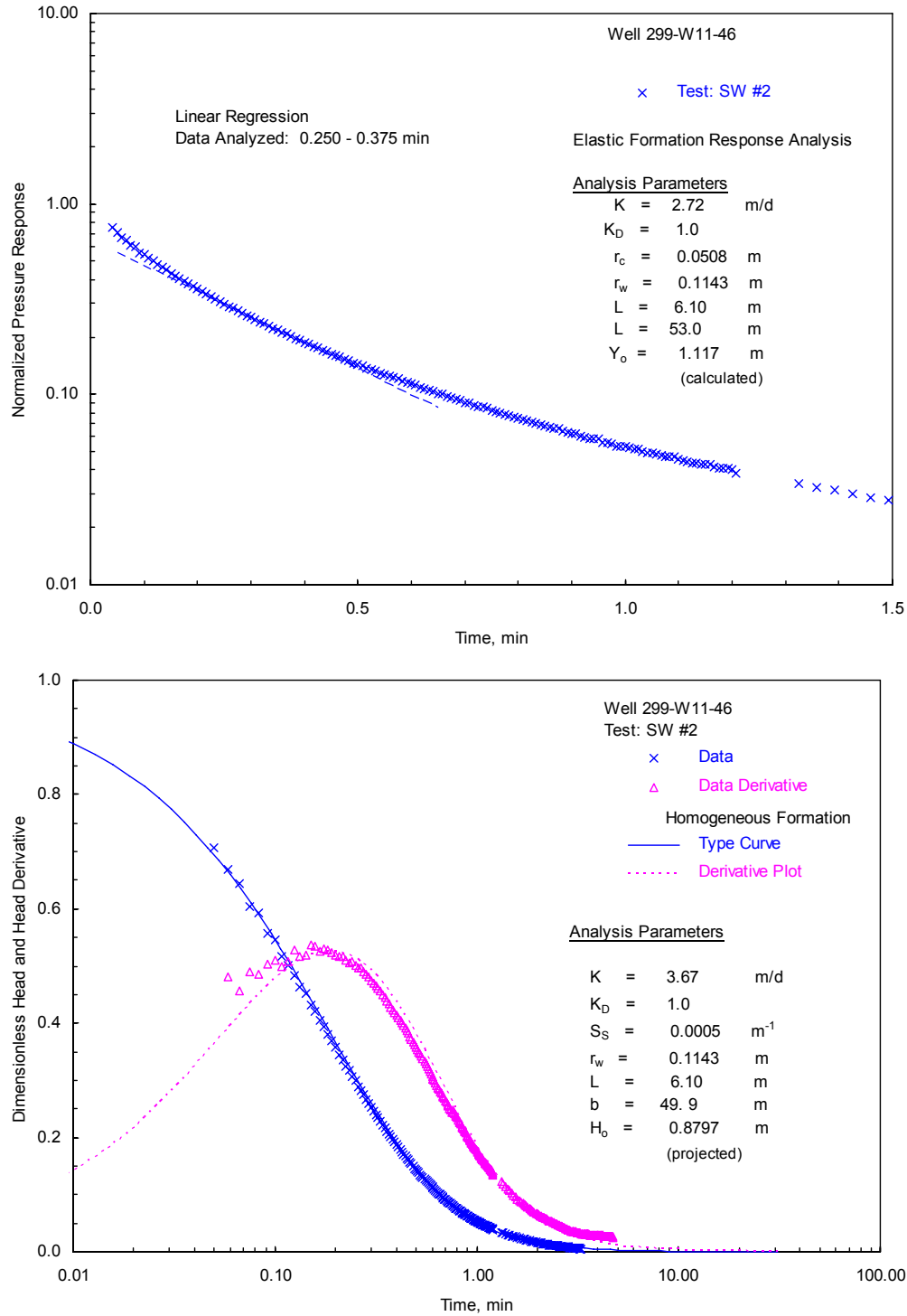


**Figure 4.2.** Selected Slug-Test Analysis Plots for Well 299-W11-46 (Bouwer and Rice method [top] and type-curve method [bottom])

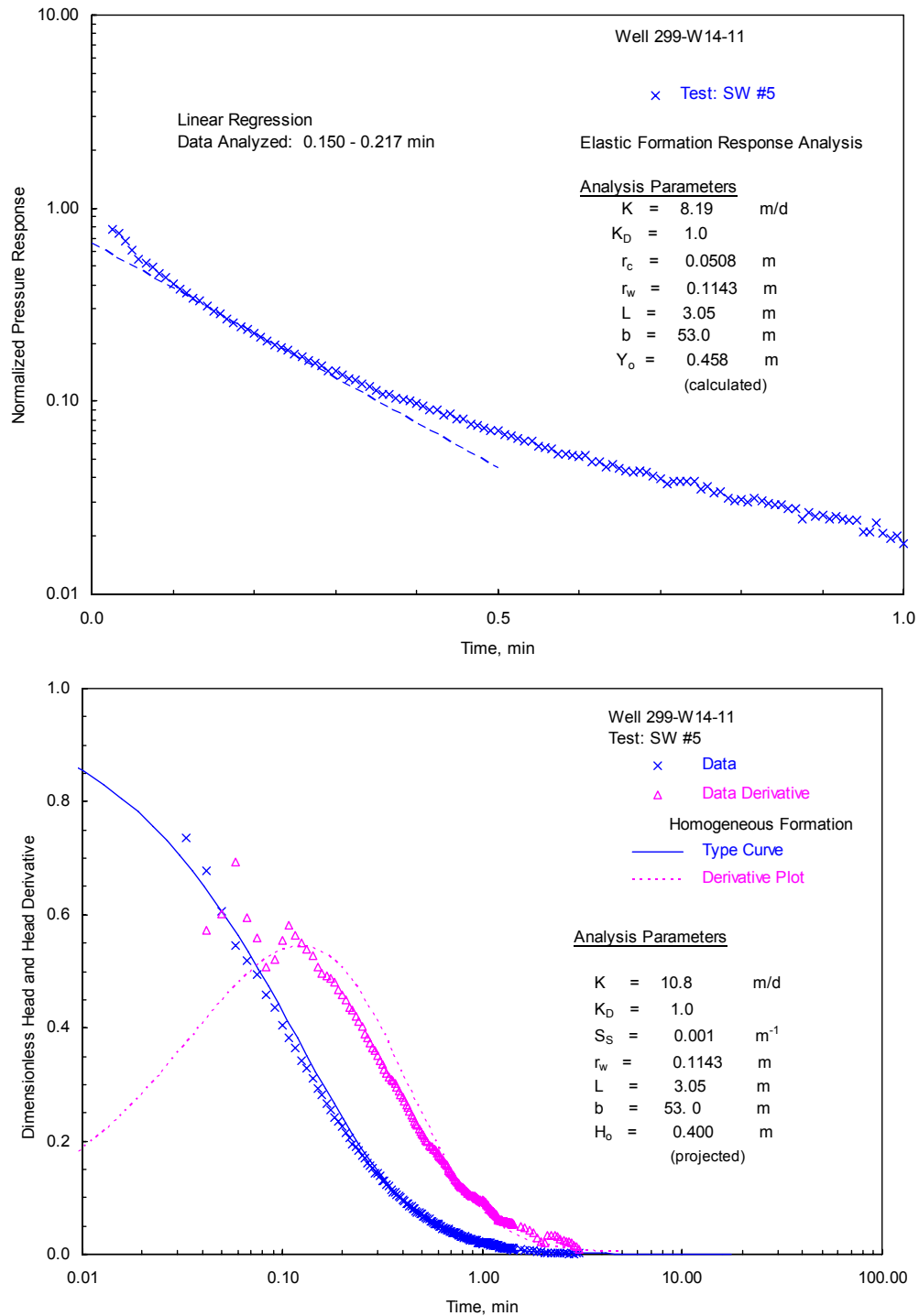


**Figure 4.3.** Selected Slug-Test Analysis Plots for Well 299-W14-11 (Bouwer and Rice method [top] and type-curve method [bottom])

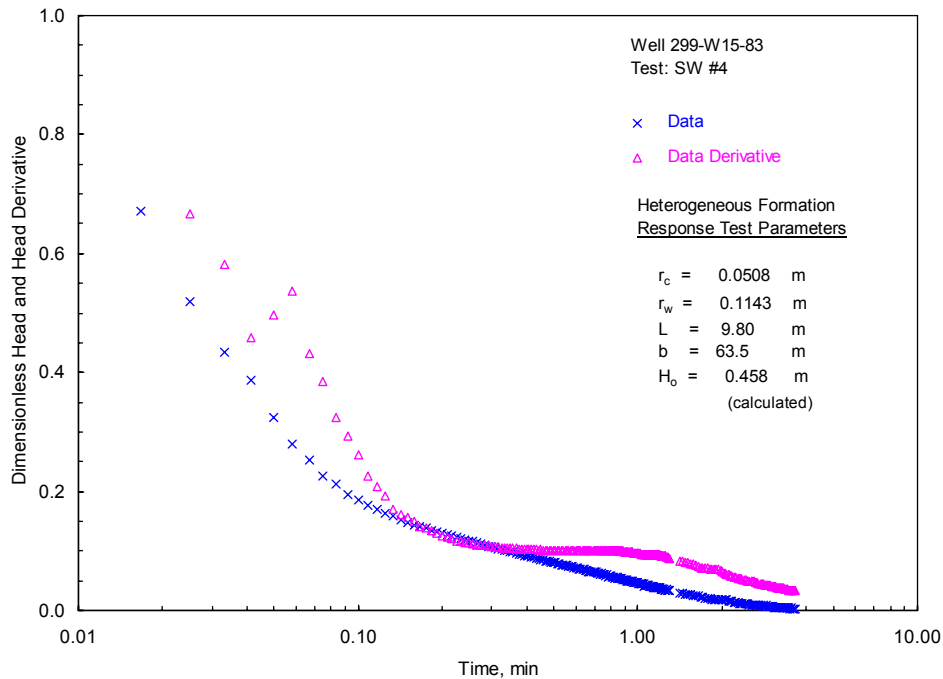


**Figure 4.4.** Heterogeneous Formation Slug-Test Response Exhibited for Well 299-W15-83

shown in Figure 4.5). For the outer lower permeability zone, a  $K$  estimate of 5.36 m/day was obtained for all tests. Results obtained from the Bouwer and Rice method are generally less definitive for tests exhibiting heterogeneous formation response behavior. However, for these tests, the Bouwer and Rice method produced comparable, but slightly lower  $K$  estimates as the type-curve method for the inner and outer permeability zones. For the Bouwer and Rice method, estimates of  $K$  for the high-permeability (inner) zone ranged from 9.34 to 11.7 m/day (average 10.5 m/day) for both stress-level tests. For the outer lower permeability zone, estimates of  $K$  ranged from 4.22 to 4.40 m/day (average 4.31 m/day). Selected examples of the analysis plots for this well are shown in Figure 4.6. As noted in Chapter 3, the inner-zone results are believed to be not representative of actual *in situ* formation conditions and may be attributable to a number of artificially imposed conditions (e.g., over well-development, high-permeability sandpack installation). For these reasons, only the outer-zone analysis results should be used to assess aquifer formation characteristics at this well location.

#### 4.1.5 Well 299-W15-94

At the time of testing, the well-screen interval included the upper 10.08 m of the unconfined aquifer and consisted of unconsolidated sediments of the Ringold Formation (Unit 5). The borehole geology log for this well indicates that the Ringold Formation test section (i.e., 72.55 to 82.63 m bgs) generally consists of a silty sandy gravel to sandy gravel unit, which varies in composition from 55 to 80% gravel, 20 to 35% sand, and 0 to 10% silt.

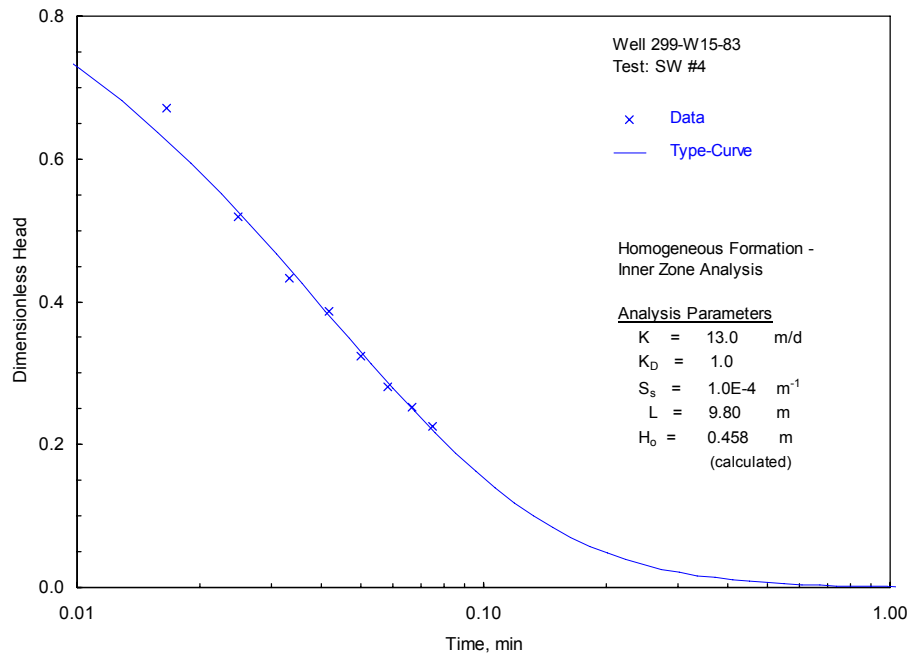


**Figure 4.5.** Selected Slug-Test Type-Curve Analysis Plots for Well 299-W15-83: Inner-Zone Analysis

A total of four slug tests (two high and two low stress) were conducted on October 13, 2005. All slug-test responses indicated a heterogeneous formation behavior, with a higher permeability zone located in proximity to the well screen, as indicated by a rapid recovery rate at early test times. This transitions to a slower recovery rate for the surrounding lower permeability material (exemplified on the type-curve response plot in Figure 4.7). A comparison of the normalized, high- and low-stress, slug-test responses indicates a slight delay in the early-test, time-response behavior for the high-stress tests, which is attributable to higher turbulence that occurred for these tests. For this reason, the low-stress test results are believed to provide more representative estimates for the inner-zone region close to the well screen. Nearly identical behavior was evident for tests conducted at a particular stress level, suggesting that the well had been developed sufficiently to establish stable skin conditions.

Slug tests exhibiting heterogeneous formation test response can be analyzed quantitatively using the homogeneous formation analysis approaches described in Chapter 3. For the homogeneous formation analysis, the type-curve method estimates for  $K$  ranged from 11.7 to 14.7 m/day (average 13.2 m/day) for both stress-level tests for the higher permeability inner zone (example analysis figure shown in Figure 4.8). For the outer lower permeability zone, a  $K$  estimate of 5.83 m/day was obtained for all tests. Results obtained from the Bouwer and Rice method are generally less definitive for tests exhibiting heterogeneous formation response behavior. However, for these tests, the Bouwer and Rice method produced comparable, but slightly lower,  $K$  estimates as the type-curve method for the inner and outer permeability zones. For the Bouwer and Rice method, estimates of  $K$  for the high-permeability (inner) zone ranged from 9.22 to 13.9 m/day (average 11.6 m/day) for both stress-level tests. For the outer lower permeability zone, estimates of  $K$  ranged from 4.44 to 4.54 m/day (average 4.49 m/day).



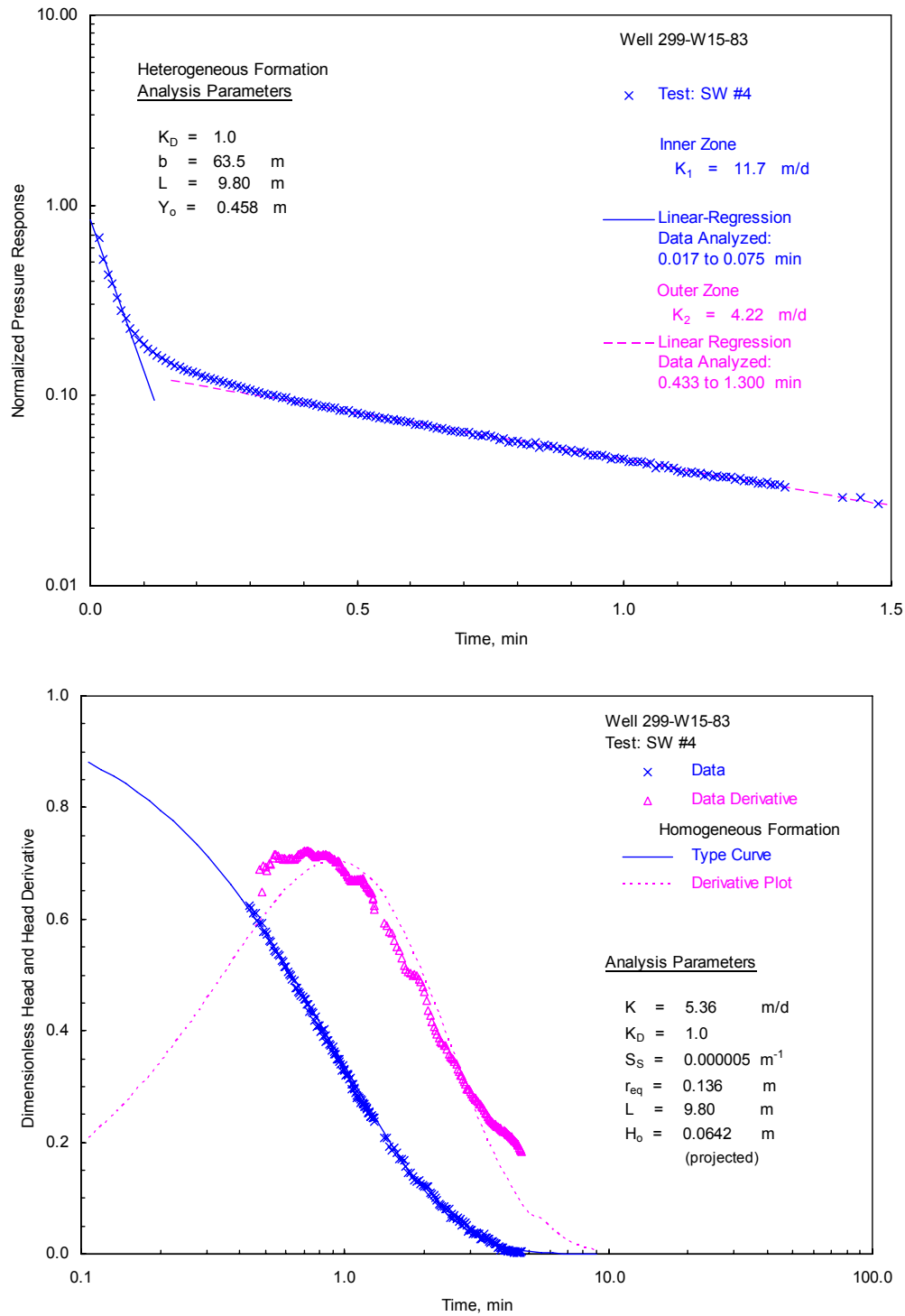


**Figure 4.6.** Selected Slug-Test Analysis Plots for Well 299-W15-83: Outer Zone Analysis (Bouwer and Rice method [top] and type-curve method [bottom])

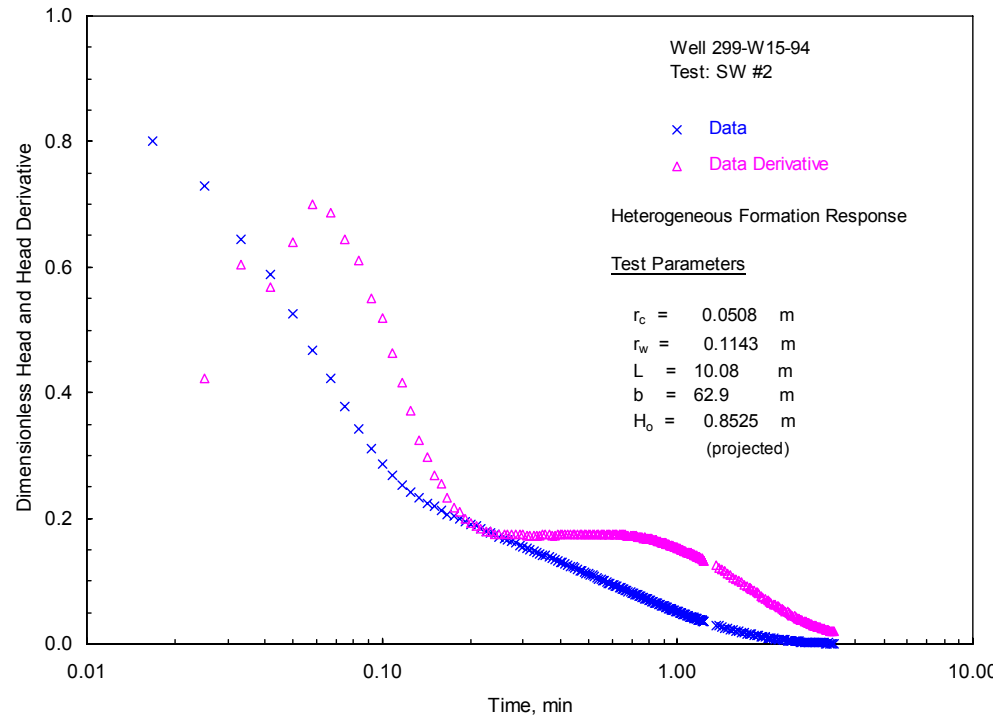


**Figure 4.7.** Heterogeneous Formation Slug-Test Response Exhibited for Well 299-W15-94

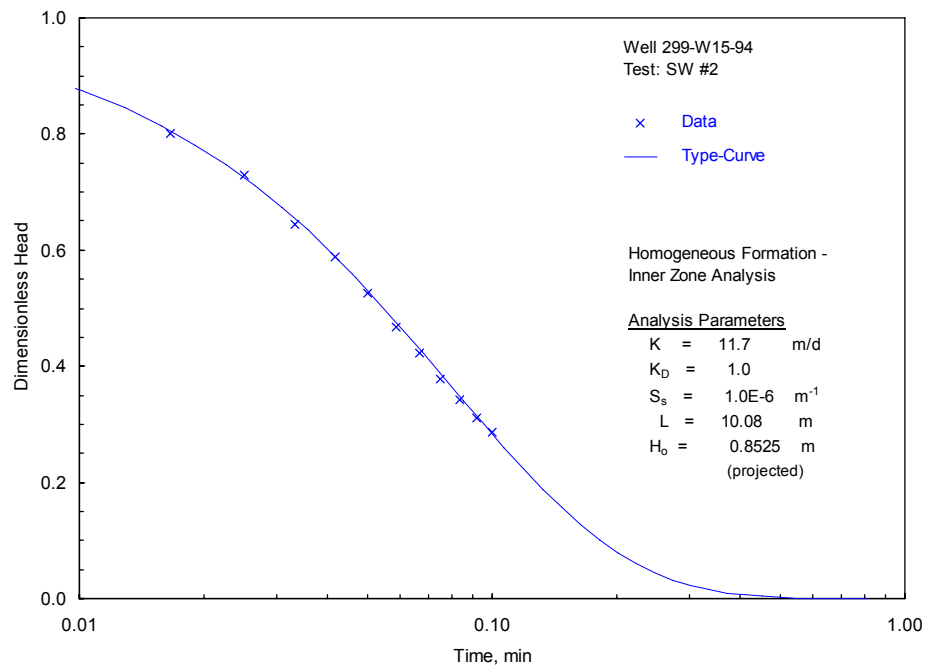


**Figure 4.8.** Selected Slug-Test Type-Curve Analysis Plots for Well 299-W15-94: Inner-Zone Analysis

Selected examples of the analysis plots for this well are shown in Figure 4.9. As noted in Chapter 3, the inner-zone results are believed to be not representative of actual *in situ* formation conditions and may be attributable to a number of artificially imposed conditions (e.g., over well-development, high-permeability sandpack installation). For these reasons, only the outer-zone analysis results should be used to assess aquifer-formation characteristics at this well location.

#### **4.1.6 Well 299-W15-152**

At the time of testing, the well-screen interval included the upper 10.10 m of the unconfined aquifer and consisted of unconsolidated sediments of the Ringold Formation (Unit 5). The borehole geology log for this well indicates that the Ringold Formation test section (i.e., 72.51 to 82.61 m bgs) generally consists of a silty sandy gravel to gravel unit, which varies in composition from 60 to 70% gravel, 20 to 40% sand, and 0 to 10% silt.

A total of four slug tests (two high and two low stress) were conducted on October 13, 2005. All slug-test responses indicated a heterogeneous formation behavior, with a higher permeability zone located in proximity to the well screen, as indicated by a rapid recovery rate at early test times. This transitions to a slower recovery rate for the surrounding lower permeability material (exemplified on the type-curve response plot in Figure 4.10). A comparison of the normalized, high- and low-stress, slug-test responses indicates nearly a slight delay in the early-test, time-response behavior for the high-stress tests, which is attributable to higher turbulence that occurred for these tests. For this reason, the low-stress test results are believed to provide more representative estimates for the inner-zone region close to the well screen. Nearly identical behavior was evident for tests conducted at a particular stress level, suggesting that the well had been developed sufficiently to establish stable skin conditions.

Slug tests exhibiting heterogeneous formation test response can be analyzed quantitatively using the homogeneous formation analysis approaches described in Chapter 3. For the homogeneous formation analysis, the type-curve method estimates for K ranged from 30.2 to 34.8 m/day (average 32.5 m/day) for both stress-level tests for the higher permeability inner zone (example analysis figure shown in Figure 4.11). For the outer lower permeability zone, a K estimate of 17.7 m/day was obtained for all tests. Results obtained from the Bouwer and Rice method are generally less definitive for tests exhibiting heterogeneous formation response behavior. However, for these tests, the Bouwer and Rice method produced comparable, but slightly lower, K estimates as the type-curve method for the inner and outer permeability zones. For the Bouwer and Rice method, estimates of K for the high-permeability (inner) zone ranged from 23.9 to 31.3 m/day (average 27.6 m/day) for both stress-level tests. For the outer lower permeability zone, estimates of K ranged from 11.4 to 13.6 m/day (average 12.5 m/day). Selected examples of the analysis plots for this well are shown in Figure 4.12. As noted in Chapter 3, the inner-zone results are believed to be not representative of actual *in situ* formation conditions and may be attributable to a number of artificially imposed conditions (e.g., over well-development, high-permeability sandpack installation). For these reasons, only the outer-zone analysis results should be used for assessing aquifer formation characteristics at this well location.

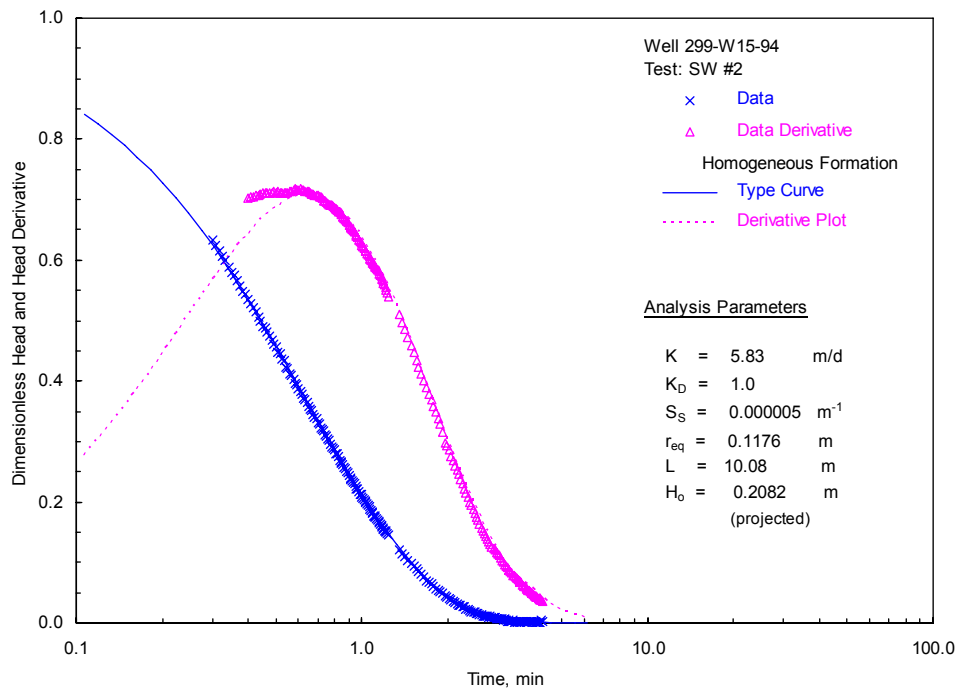
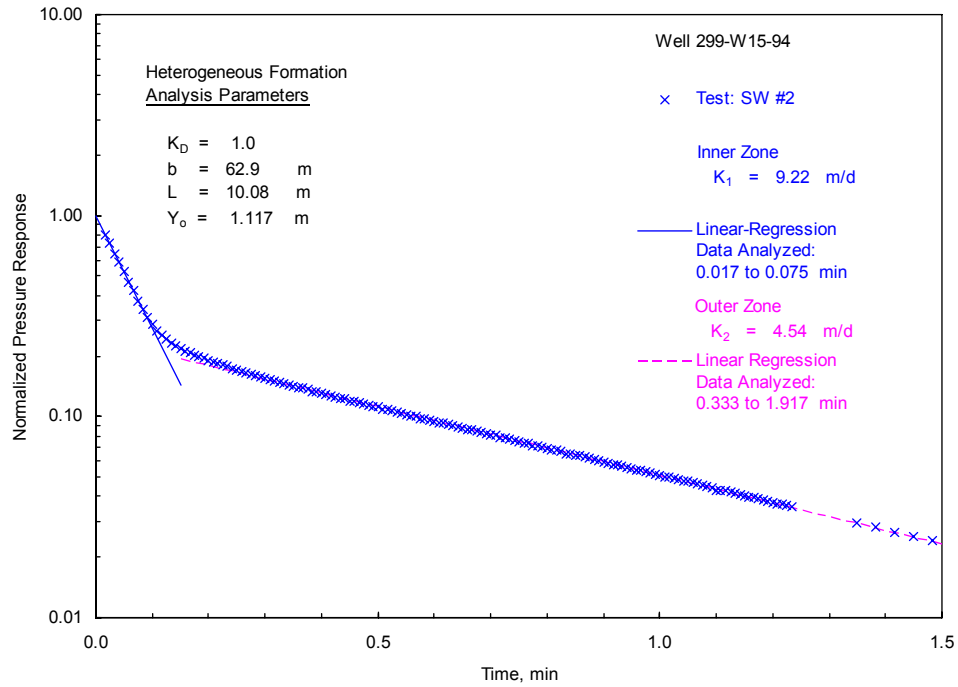


**Figure 4.9.** Selected Slug-Test Analysis Plots for Well 299-W15-94: Outer Zone Analysis (Bouwer and Rice method [top] and type-curve method [bottom])

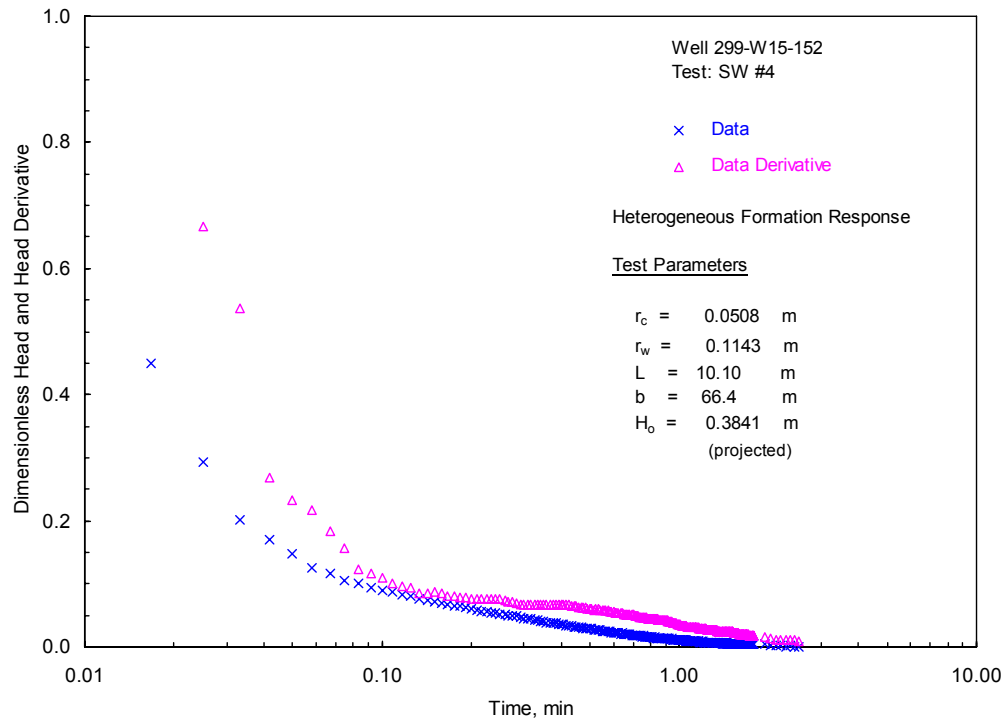


**Figure 4.10.** Heterogeneous Formation Slug-Test Response Exhibited for Well 299-W15-152

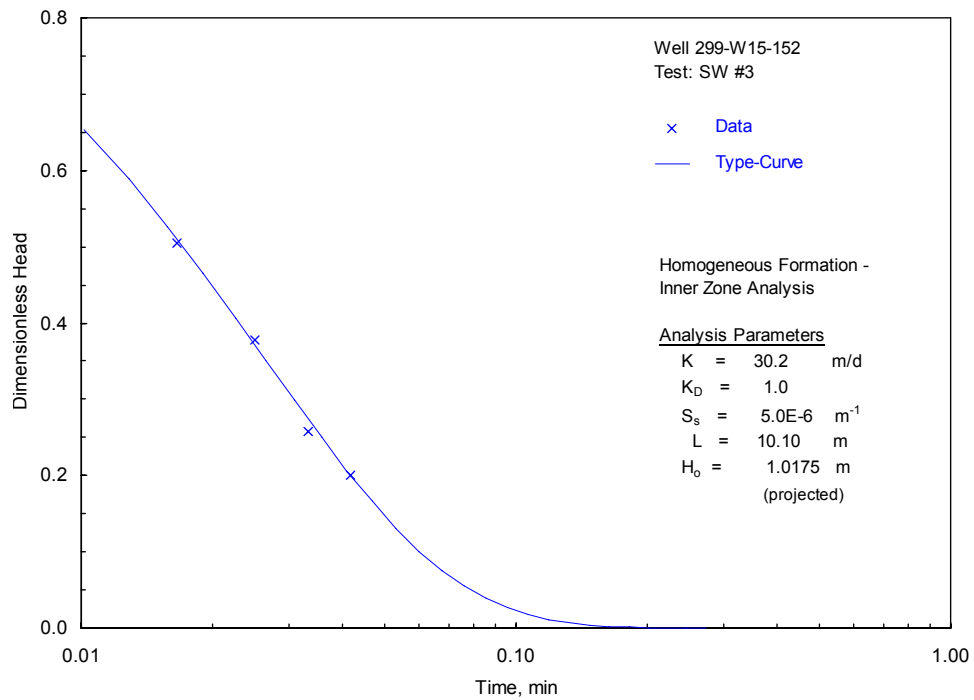


**Figure 4.11.** Selected Slug-Test Type-Curve Analysis Plots for Well 299-W15-152: Inner-Zone Analysis

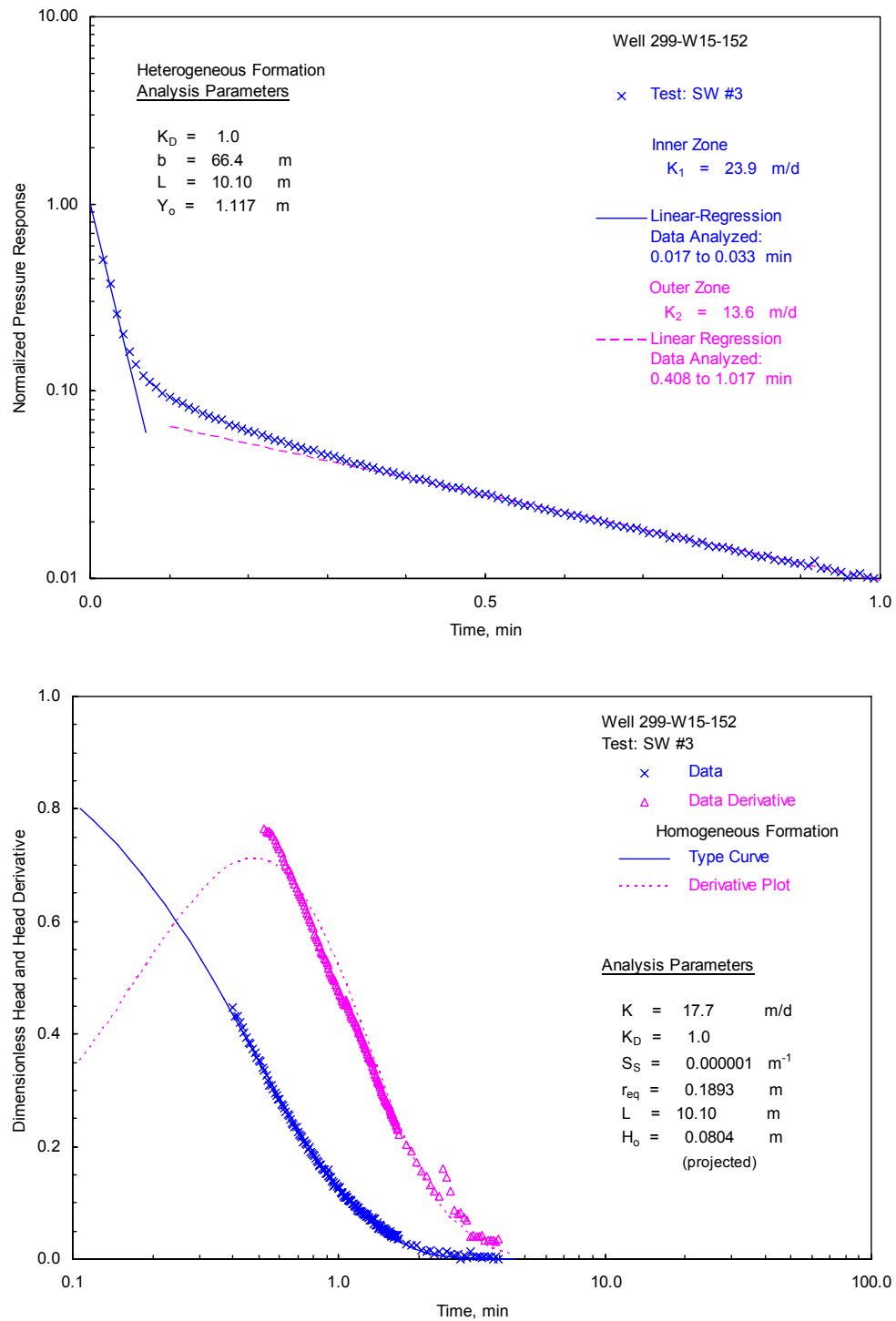


**Figure 4.12.** Selected Slug-Test Analysis Plots for Well 299-W15-152: Outer Zone Analysis (Bouwer and Rice method [top] and type-curve method [bottom])

#### 4.1.7 Well 299-W19-47

At the time of testing, the well-screen interval included the upper 10.19 m of the unconfined aquifer and consisted of unconsolidated sediments of the Ringold Formation (Unit 5). The borehole geology log for this well indicates that the Ringold Formation test section (i.e., 69.68 to 79.87 m bgs) generally consists of a silty sandy gravel to sandy gravel unit, which varies in composition from 60 to 70% gravel, 10 to 40% sand, and 0 to 15% silt and clay.

A total of four slug tests (two high and two low stress) were conducted on September 20, 2005. All slug-test responses indicated a heterogeneous formation behavior, with a higher permeability zone located in proximity to the well screen, as indicated by a rapid recovery rate at early test times. This transitions to a slower recovery rate for the surrounding lower permeability material (exemplified on the type-curve response plot in Figure 4.13). A comparison of the normalized, high- and low-stress, slug-test responses indicates nearly a slight delay in the early-test, time-response behavior for the high-stress tests, which is attributable to higher turbulence that occurred for these tests. For this reason, the low-stress test results are believed to provide more representative estimates for the inner-zone region close to the well screen. Nearly identical behavior was evident for tests conducted at a particular stress level, suggesting that the well had been developed sufficiently to establish stable skin conditions.

Slug tests exhibiting heterogeneous formation test response can be analyzed quantitatively using the homogeneous formation analysis approaches described in Chapter 3. For the homogeneous formation analysis, the type-curve method estimates for K ranged from 15.1 to 21.6 m/day (average 18.4 m/day) for both stress-level tests for the higher permeability inner zone (example analysis figure shown in Figure 4.14). For the outer lower permeability zone, a K estimate range of 4.10 to 4.75 m/day was obtained (average 4.43 m/day). Results obtained from the Bouwer and Rice method are generally less definitive for tests exhibiting heterogeneous formation response behavior. However, for these tests, the Bouwer and Rice method produced comparable, but slightly lower, K estimates as the type-curve method for the inner and outer permeability zones. For the Bouwer and Rice method, estimates of K for the high-permeability (inner) zone ranged from 11.4 to 17.1 m/day (average 14.3 m/day) for both stress-level tests. For the outer lower permeability zone, estimates of K ranged from 3.71 to 4.23 m/day (average 3.97 m/day). Selected examples of the analysis plots for this well are shown in Figure 4.15. As noted in Chapter 3, the inner-zone results are believed to be not representative of actual *in situ* formation conditions and may be attributable to a number of artificially imposed conditions (e.g., over well-development, high-permeability sandpack installation). For these reasons, only the outer-zone analysis results should be used for assessing aquifer formation characteristics at this well location.

#### 4.1.8 Well 299-W22-47

At the time of testing, the well-screen test interval included the upper 10.45 m of the unconfined aquifer and consisted of unconsolidated sediments of the Ringold Formation (Unit 5). The borehole geology log for this well indicates that the Ringold Formation test section (i.e., 69.92 to 80.37 m bgs) grades from a gravel in the upper-section to a sandy gravel unit over the remaining interval of the well-screen section.

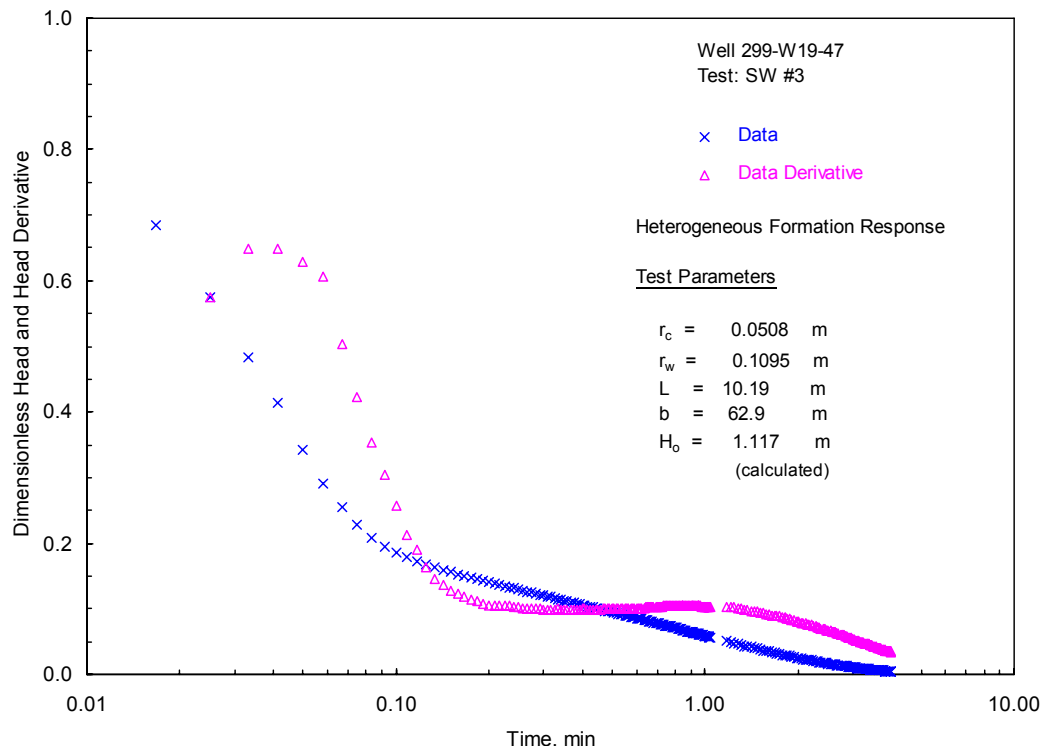


**Figure 4.13.** Heterogeneous Formation Slug-Test Response Exhibited for Well 299-W19-47

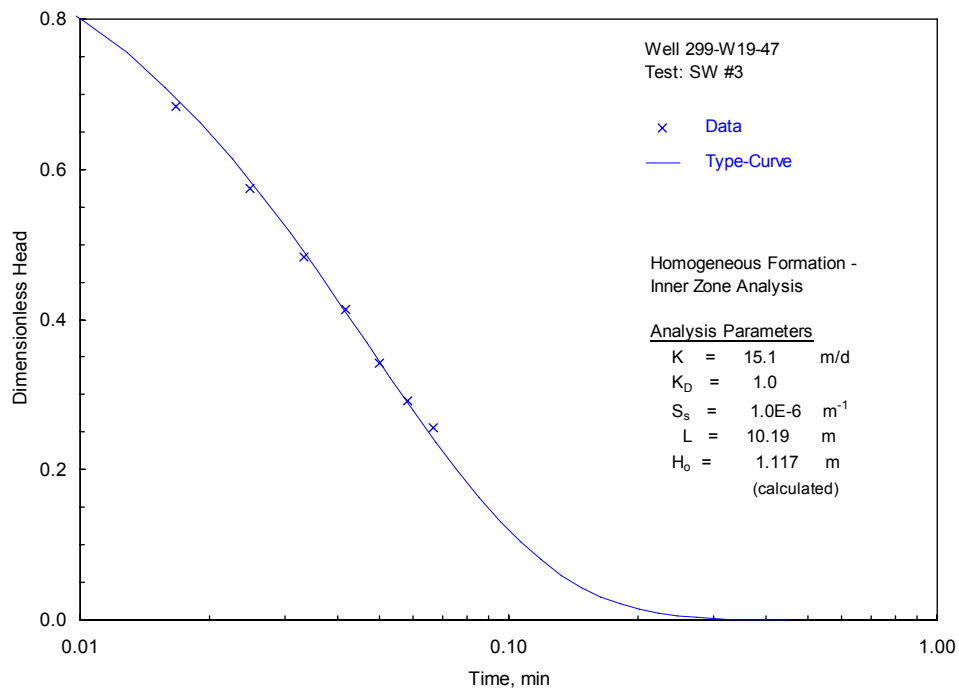


**Figure 4.14.** Selected Slug-Test Type-Curve Analysis Plots for Well 299-W19-47: Inner-Zone Analysis



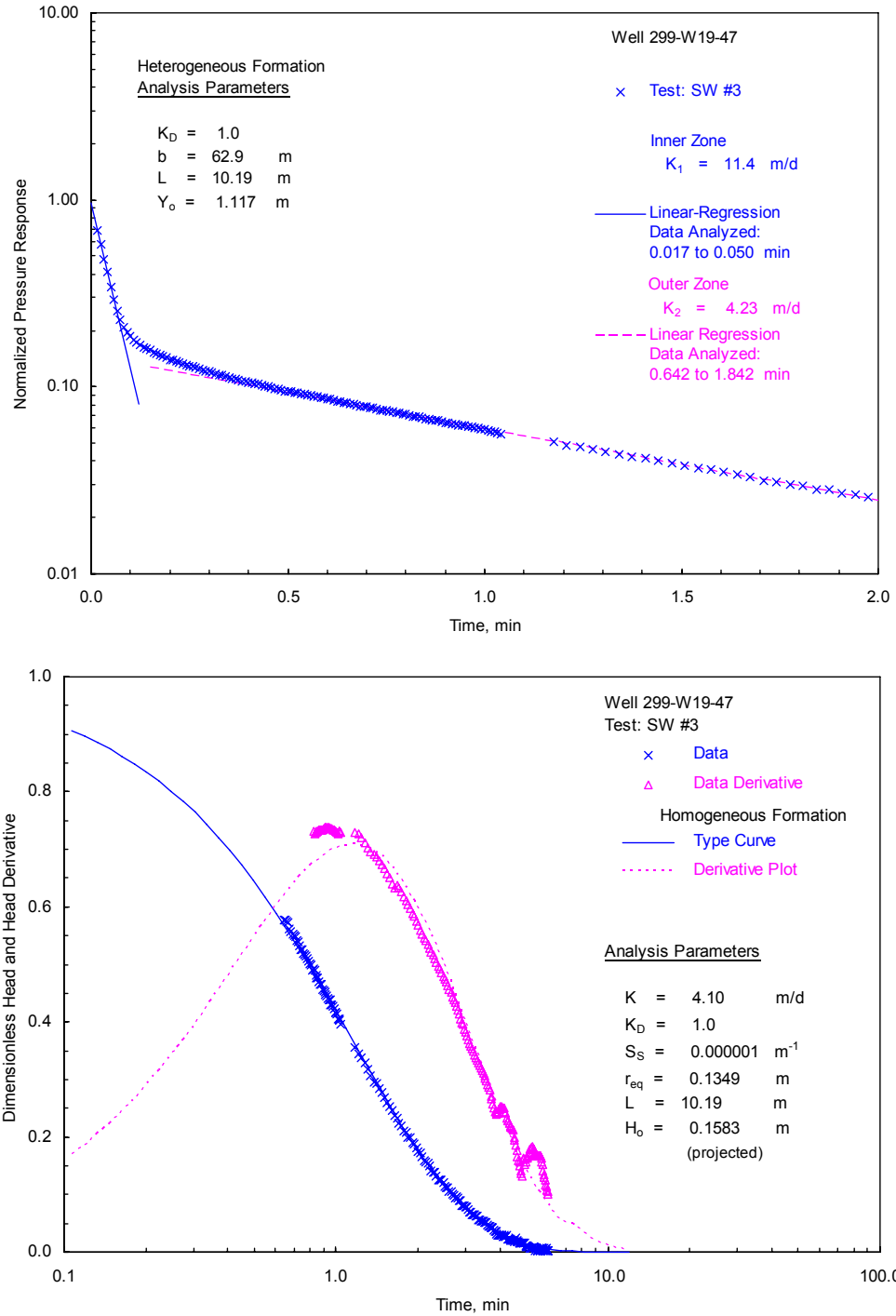


**Figure 4.15.** Selected Slug-Test Analysis Plots for Well 299-W19-47: Outer Zone Analysis (Bouwer and Rice method [top] and type-curve method [bottom])

A total of four slug tests (two high and two low stress) were conducted on September 27, 2005. All slug-test responses indicated rapid recoveries (>90% recovery within ~3 seconds) for all tests and are indicative of high-permeability conditions. Because of the existing high-permeability test interval conditions, very small test responses were exhibited during the low-stress tests. As a result, the hydraulic property estimates obtained for this well site were derived solely from the high-stress test results.

A comparison of the normalized, high-stress slug-test responses indicates nearly identical behavior, which suggests that the well had been fully developed. Examination of the individual slug-test responses did not indicate a nonlinear (concave downward), critically-damped slug-test response; however, the rapid recoveries suggest that the over-damped responses were close to the critically-damped threshold. Slug tests exhibiting this type of response behavior can be analyzed quantitatively either with standard, linear-response-based methods (i.e., using either the Bouwer and Rice or type-curve methods) or the High-K analysis method presented in Butler and Garnett (2000) (see Section 3.1.2). Because the test responses did not exhibit a distinguishingly clear, critically-damped response behavior, the standard over-damped analysis methods were used to analyze the slug tests at well 299-W22-47. In addition, because the test-response recoveries were nearly identical and recovered rapidly, the results from both high-stress tests were combined to facilitate the analysis process. Figure 4.16 shows the results of the combined analysis of high-stress tests. As indicated, an average estimate for K for the combined test plot yielded a value of 13.5 and 17.3 m/day using the Bouwer and Rice and type-curve methods, respectively.

#### **4.1.9 Well 299-W22-80**

Well 299-W22-80 was previously slug tested shortly after construction in October 2000 and was also tested using detailed hydraulic characterization methods (i.e., tracer-dilution, tracer pumpback testing) in June 2001. These test results are reported in Spane et al. (2002). To support additional hydrologic characterization at this well-site location (i.e., hydrochemical sampling and in-well flow assessment studies), the well was retested on September 27, 2005, by slug testing (one high and one low stress) to assess whether any changes in the well/aquifer response characteristics had occurred.

During the ~5 year period that occurred between slug testing, the surrounding water table had lowered, causing a 1.54 m decrease in the saturated well-screen section. This represents approximately a 15% percent reduction in the well test interval. If it is assumed that hydraulic conductivity is uniform within the well-screen section, then a discernable shift (i.e., slower test recovery) in slug-test response would be expected to be exhibited for the shorter well-screen tests. This is because slug-test response is largely controlled by the test interval transmissivity (i.e., hydraulic conductivity multiplied by the saturated well-screen length), as discussed in Section 3.1. For example, Figure 4.17 shows a comparison of predictive slug-test type-curve responses for well 299-W22-80 with longer (10.53 m; October 2000) and shorter (8.99 m; September 2005) saturated, well-screen conditions, based on the average hydrologic properties for this well site, previously reported in Spane et al. (2002). As shown, a discernable delayed response (i.e., shift to the right) would be expected for slug tests conducted with the shorter saturated well-screen length.

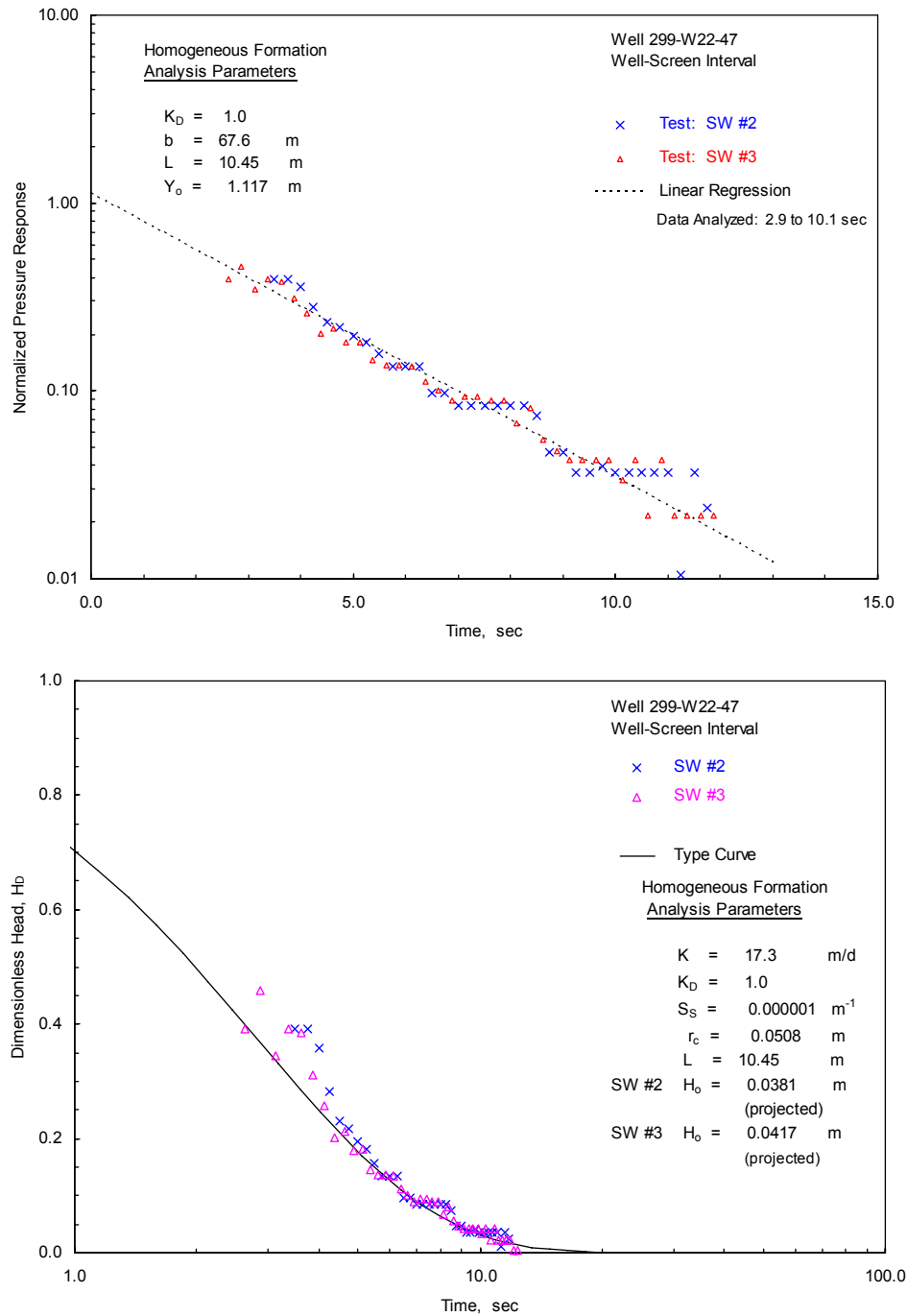


**Figure 4.16.** Combined Slug-Test Analysis Plots for Well 299-W22-47: (Bouwer and Rice method [top] and type-curve method [bottom])

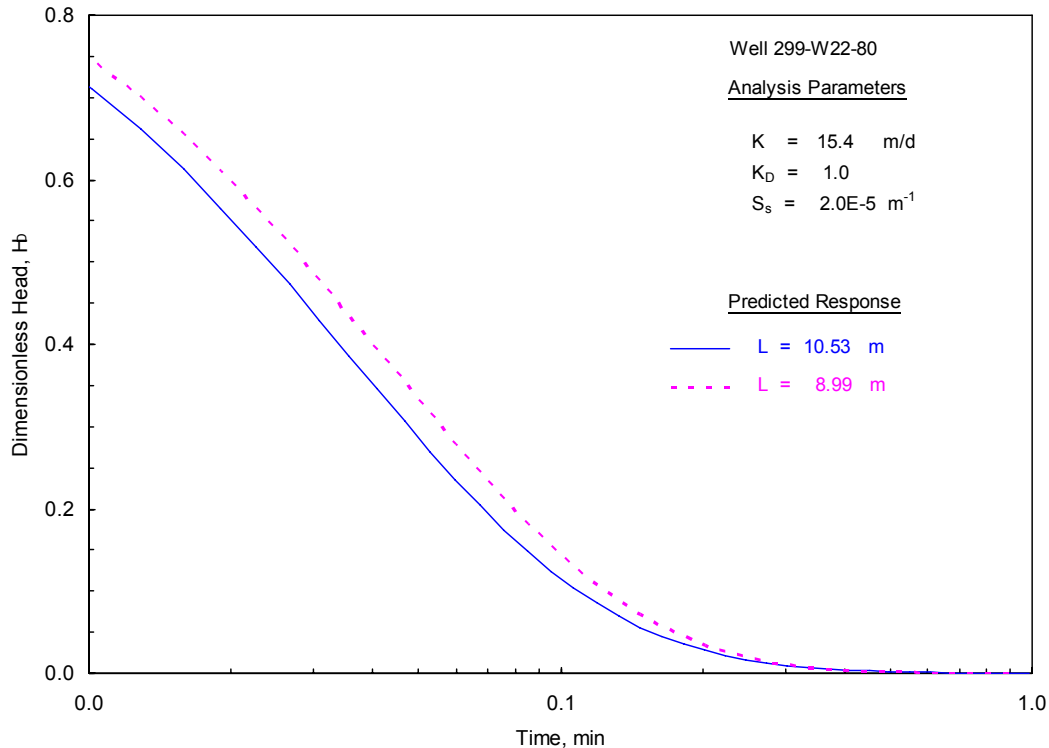


**Figure 4.17.** Predicted Slug-Test Type-Curve Response Plots for Well 299-W22-80

Figure 4.18 shows a comparison of low-stress slug tests conducted in October 2000 and September 2005. As shown, the 2005 recovery response is slower (i.e., offset to the right) than what was predicted in Figure 4.17, based on the smaller saturated well-screen length. This suggests that the upper 1.54 m of the 10.53 m saturated well-screen that was tested in October 2000 had a higher hydraulic conductivity than that exhibited for the lower 8.99-m section.

At the time of the September 2005 testing, the well-screen test interval included the upper 8.99 m of the unconfined aquifer and consisted of unconsolidated sediments of the Ringold Formation (Unit 5). The borehole geology log for this well indicates that the Ringold Formation test section (i.e., 64.18 to 73.17 m bgs) generally consists of a silty sandy gravel unit, which is composed of 60 % gravel, 25 to 30% sand, and 10 to 15% silt. It is of interest to note that the overlying 1.54 m of sediment that was previously saturated and included in the October 2000 testing is described as sandy gravel consisting of 60% gravel and 40% sand, with no discernable silt faction.

Because well 299-W22-80 had been a site of previous hydrologic test characterization, only two slug tests (one low and one high stress) were conducted on September 27, 2005. A comparison of the normalized, high- and low-stress slug-test responses indicates essentially identical behavior, which indicates linear test behavior and suggests that the well had been fully developed. Examination of the individual slug-test responses also indicates an over-damped homogeneous formation (linear) response displayed on the Bouwer and Rice analysis plot in Figure 4.19. A test method comparison of K estimates indicates that consistently lower results (~25% lower) were obtained for the Bouwer and Rice method.

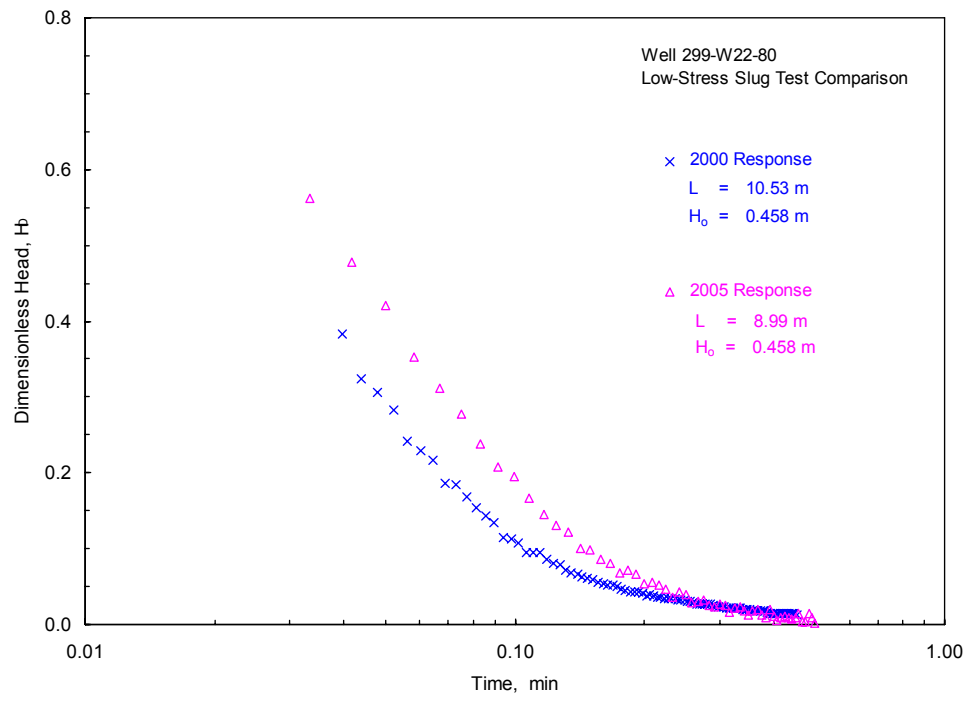


**Figure 4.18.** Comparison of Low-Stress, Slug-Test-Response Plots for Well 299-W22-80

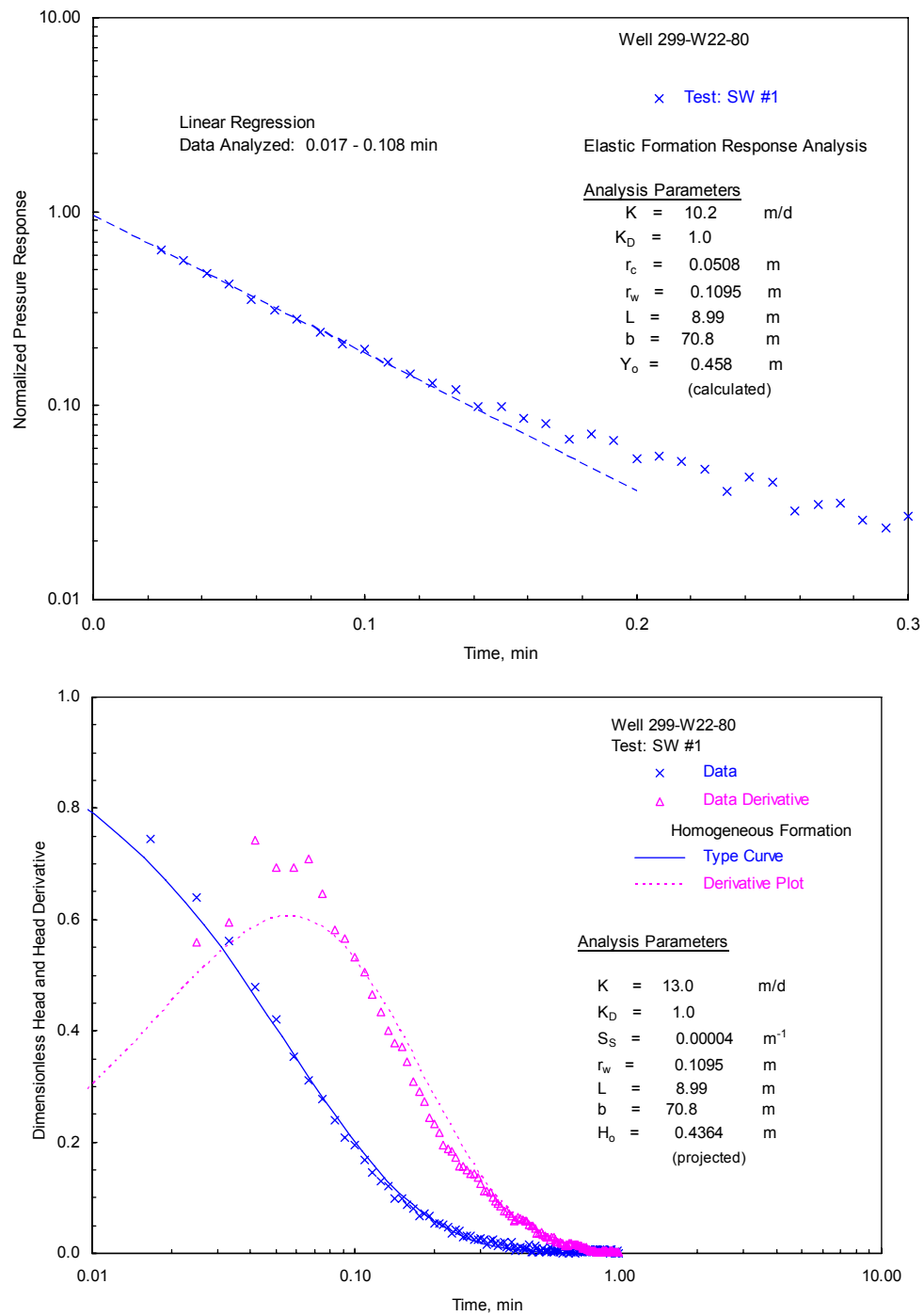


**Figure 4.19.** Combined Slug-Test Analysis Plots for Well 299-W22-80: (Bouwer and Rice method [top] and type-curve method [bottom])

For the Bouwer and Rice method, estimates for K ranged from 9.72 to 10.2 m/d (average 9.96 m/d), while the type-curve method provided an identical estimate value of 13.0 m/d for both stress-level tests. Selected examples of the analysis plots for this well are shown in Figure 4.19.

A comparison of the 2000 and 2005 type-curve method K estimates indicates a reduction in the average well-screen hydraulic conductivity from 15.4 to 13.0 m/day. This reduction in average hydraulic conductivity (and subsequent reduction in well-screen interval transmissivity) indicates that the overlying 1.54 m of formerly saturated Ringold unit sediments had an average K value of 29.4 m/day ( $T = 45.3 \text{ m}^2/\text{day}$ ). The estimated higher hydraulic conductivity value for the overlying 1.54 m of formerly saturated sediment is consistent with the geologic description ascribed to this section (i.e., sandy gravel unit) of the Ringold Formation. This suggests a discernable variation in hydraulic conductivity (i.e., by a factor of 2 to 3) with depth within the well-screen section at this well location.

## **4.2 Borehole Test/Depth Interval Characterizations**

Specific depth/interval slug-test characterization was conducted at three borehole sites during the course of drilling the test wells to assess the variation and vertical distribution of hydraulic conductivity and hydrochemical contamination with depth within the unconfined aquifer at these specific locations (note: results pertaining to hydrochemical contamination with depth are discussed in other reports). This type of characterization information is important for predicting/simulating contaminant migration (i.e., numerical flow/transport modeling) and designing proper monitor-well strategies for WMA locations. The specific borehole sites where detailed depth/interval slug-test characterization was conducted during FY and CY 2005 were as follows: well 299-W11-25B (WMA T); well 299-W14-11 (WMA TX-TY), and well 299-W22-47 (WMA S-SX). Analytical results and pertinent test information for the slug-tested borehole depth interval are discussed in the following section.

### **4.2.1 299-W11-25B**

As shown in Figure 4.20, borehole 299-W11-25B is located near the northeast boundary of WMA T. In all, five specific test/depth intervals were characterized between February 9 and 24, 2005, by slug testing as the borehole was advanced to its final depth at the top of the Ringold Lower Mud at ~124.7 m bgs. During the process of completing the borehole as a monitoring well facility, the well was lost and subsequently decommissioned.

Pneumatic slug tests were used for each test/depth interval. To conduct the pneumatic tests, compressed air was used to depress the fluid-column levels within the test-casing/test-interval system to the designed test stress levels. Actual stress levels applied for each test were determined by comparing pressure transducer readings below and above the borehole fluid-column surface. After the monitored fluid column stabilized for several minutes at the prescribed stress level, the slug test (slug-withdrawal test) was initiated by rapidly releasing the compressed gas used to depress the borehole fluid-column level. The compressed gas was released from the borehole column by opening valves (e.g., ball valves) mounted on the surface wellhead used to seal the casing system. As recommended in Spane et al. (1996), the gas release valves had a cross-sectional area that was greater (e.g., >1.5 times) than the cross-sectional area of the test system where fluid-level surface recovery took place during testing. For this test site, three or more multi-stress slug tests were conducted for each test zone. Individual slug tests were fully

recovered before depressing the fluid column to prepare the next slug test within the characterization sequence.

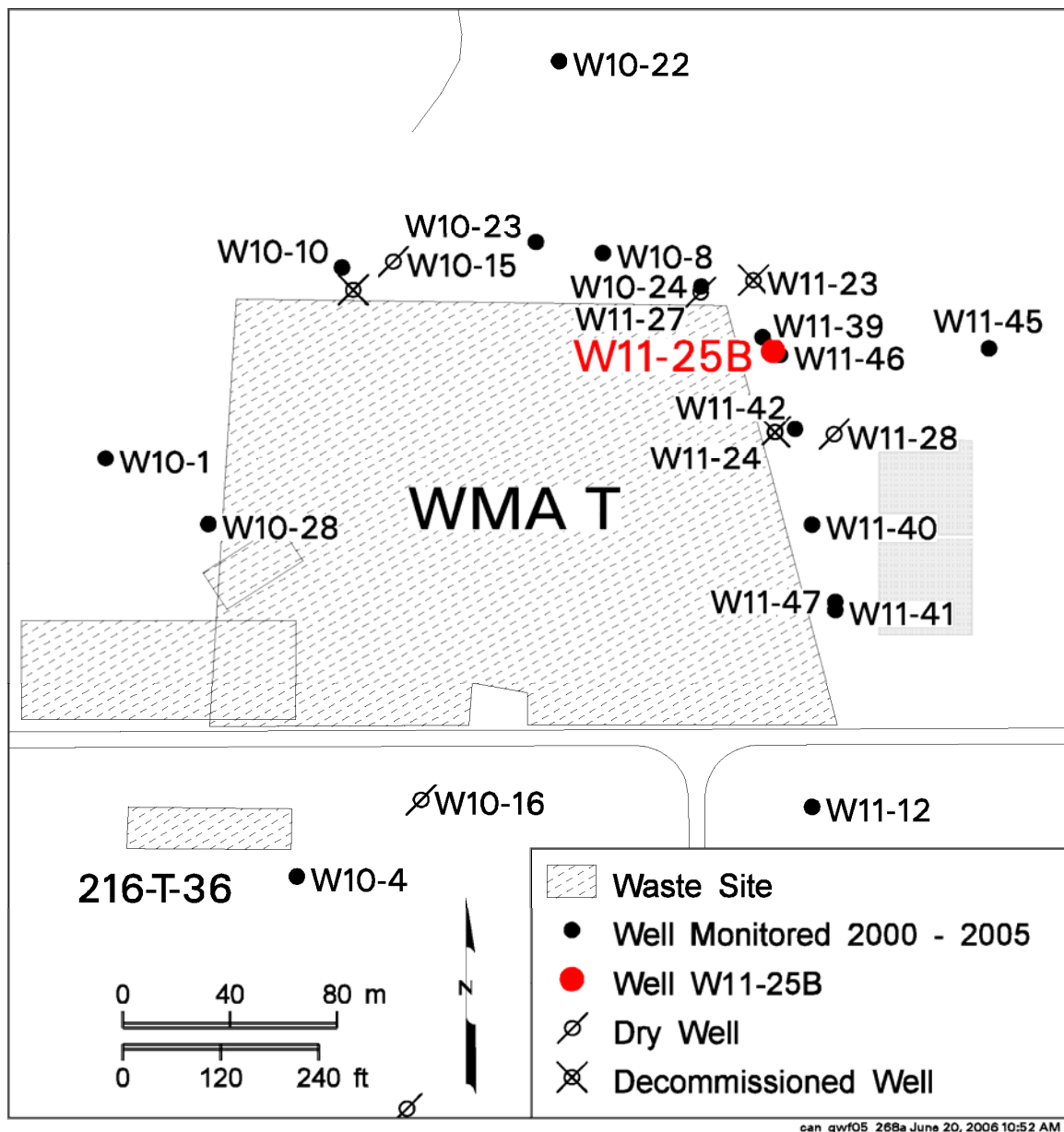


**Figure 4.20.** Well 299-W11-25B Location Map



Diagnostic analysis of slug tests conducted for the various test/depth intervals indicate expected exponential decay (over-damped) conditions for four of the five test depth intervals (Table 4.3). Heterogeneous formation/composite response conditions were indicated for one test/depth interval (Zone 4). This composite pattern exhibits a high-permeability (fast initial recovery), inner-zone response, which transitions to a lower permeability surrounding outer-zone formation response. The presence of a high-permeability inner-zone is believed to be reflective of artificially created conditions. These artificially created high-permeability conditions may be attributed to the setting of a smaller diameter packer/well-screen assembly and retraction of the larger diameter drill casing to expose the test/depth interval. It is believed that dislodged cobbles and gravel collapsing around the temporary well screen while the drill casing was being retracted created an artificial high-permeability inner-zone (surrounding the temporary well screen). An examination of the drilling log geologic description indicates the presence of 4- to 5-in. cobbles within a sandy gravel unit for this particular test depth interval.

**Table 4.3.** Slug-Test Characteristics for Selected Test/Depth Intervals at 299-W11-25B

Test Zone	Test Parameters				Diagnostic Slug-Test-Response Model	Hydrogeologic Unit Tested
	Test Date	# Slug Tests	Depth to Water, m bgs	Test/Depth Interval, m bgs		
Zone 1	2/9/05	3	73.75	82.29–85.34 (3.05)	Over-Damped (exponential decay)	Ringold Formation (Unit 5)
Zone 2	2/10/05	4	-	85.34–88.39 (3.05)	Composite: Test System Oscillations Superimposed on Formational Over-Damped Response (exponential decay)	Ringold Formation (Unit 5)
Zone 3	2/16/05	3	73.80	88.09–91.14 (3.05)	Composite: Test System Oscillations Superimposed on Formational Critically-Damped Response	Ringold Formation (Unit 5)
Zone 4	2/18/05	3	73.73	97.26–100.31 (3.05)	Over-Damped (exponential decay); Heterogenous Formation	Ringold Formation (Unit 5)
Zone 5	2/24/05	3	73.79	106.68–109.72 (3.05)	Over-Damped (exponential decay); note: test response affected by packer bypass	Ringold Formation (Unit 5)
Note: For all test wells, $r_c = 0.051$ meter; $r_w = 0.1143$ meter . Unit number in parentheses indicates the relevant groundwater-flow model layer, as described in Thorne et al. (1993).						

Two of the test zones (Zones 2 and 3) exhibited pronounced early-test time oscillations superimposed on exponential, over-damped recovery test responses. As discussed in Section 3.1.3, this superimposed oscillatory pattern is attributed to varying recovery rates that occur within the 0.1016 m I.D. test string and the annular zone between the dual-wall drill casing. The recovery rate imbalances within the two annular areas produce a test-system-induced oscillatory pattern, which is superimposed upon the general formation recovery slug-test pattern. An example of this type of superimposed response condition is shown in Figure 3.9.

Standard integrity stress testing of the packer/well-screen test system during slug-test characterizations indicated that significant packer bypass, and therefore lack of test-interval isolation, occurred for only one of the depth zones tested (Zone 5). For this reason, no quantitative characterization results can be ascribed for this test/depth interval.

Results from discrete test/depth interval slug-test characterization during drilling of borehole 299-W11-25B are representative of the Ringold Unit C/E sand and gravel (Unit 5). Hydraulic conductivity estimates range from 1.25 to 4.93 m/day (Table 4.4; average type-curve or High-K analysis results). Figure 4.21 shows the vertical depth distribution of hydraulic conductivity determined for the four depth intervals successfully tested at this well-site location. When combined with results obtained at nearby well 299-W11-39 (Spane et al. 2002), approximately 40% of the composite unconfined aquifer was characterized at this test-site location. As indicated in the figure, K values appear to be relatively uniform and vary only by a factor of four for the four test/depth intervals. The highest K value of 4.93 m/day was observed for the shallowest interval tested (Zone 1: 82.29 to 85.34 m bgs). This test zone is located approximately 8.5 to 11.5 m below the current water table. The hydraulic conductivity estimates shown in Figure 4.21 are based on the type-curve analysis method and do not include values determined for the non-formational, artificially induced, high-permeability inner-zones that were exhibited for test Zone 4. Results for the artificially produced high-K inner-zone are listed in Table 4.4 for simple comparison purposes. A brief description of the individual depth interval (Zone) tests is presented below. Selected analysis figures for the respective test zones are presented in Appendix A.

#### **4.2.1.1 Zone 1 (Depth: 82.29 to 85.34 m)**

After reaching a depth of 85.34 m bgs, the packer/well-screen assembly was lowered to the bottom of the borehole and the 0.229 m O.D. drill casing retracted 3.05 m, producing a test/depth interval for Zone 1 of 82.29 to 85.34 m bgs. The borehole geology log indicates that sediments within the test interval are highly variable and grade from a sandy gravel in the upper-section to a silty sandy gravel, which are composed of 65 to 70% gravel, 20 to 30% sand, and 5 to 10% silt. Near the base of the test interval, the silty sandy gravel unit grades into a medium sand.

A series of three pneumatic slug-withdrawal tests were conducted between 0906 hours and 1240 hours (Pacific Standard Time [PST]), February 9, 2005. The pneumatic slug tests were conducted by pressurizing the 4-in. testing-string casing (I.D. = 0.102 m) used to set the packer/well-screen assembly. The pneumatic tests used applied stress (compressed air) pressures that produced observed fluid-column depressions ranging from 4.9 to 5.4 m for individual tests. The pressure was rapidly released using the wellhead surface valves. The static depth-to-water for the test interval during testing was 73.75 m bgs.

**Table 4.4.** 299-W11-25B Test/Depth Interval Slug-Test Analysis Results

Test/Depth Interval	Bouwer and Rice Analysis Method	Type-Curve Analysis Method		High-K Analysis Method <sup>(b)</sup>	
	Hydraulic Conductivity, $K_h$ , <sup>(a)</sup> (m/day)	Hydraulic Conductivity, $K_h$ , <sup>(a)</sup> (m/day)	Specific Storage, $S_s$ (m <sup>-1</sup> )	Hydraulic Conductivity, $K_h$ , <sup>(a)</sup> (m/day)	Dimensionless Damping Parameter, $C_D$
Zone 1	4.60–4.86 (4.73)	4.67–5.18 (4.93)	3.0E-5–5.0E-5	NA	NA
Zone 2	1.23–1.28 (1.25)	1.25	1.0E-6–5.0E-6	NA	NA
Zone 3	NA	NA	NA	1.82–2.22 <sup>(c)</sup> (2.02)	2.75–2.85
Zone 4	Inner Zone: 21.2–27.8 (24.5) Outer Zone: 2.86–3.25 (3.10)	Inner Zone: 21.2–25.5 (23.4) Outer Zone: 2.89–3.24 (3.12)	1.0E-5  1.0E-5	NA	NA
Zone 5 <sup>(d)</sup>	-	-	-	-	-
NA Not applicable or applied analytical method. Number in parentheses is the average value for all tests. (a) Assumed to be uniform within the well-screen test section. For tests exhibiting a heterogeneous formation response, only outer zone analysis results are considered representative of <i>in situ</i> formation conditions. (b) When standard analytical methods are not valid, results are based on the High-K analysis method presented in Butler and Garnett (2000). (c) Outer zone exhibited critically-damped response characteristics. Results based on High-K analysis, type-curve method presented in Butler and Garnett (2000). (d) No quantitative analysis of test results possible due to packer bypass effects.					

All slug-test responses indicated a homogeneous formation, over-damped, test-response behavior. A very small oscillatory pattern is superimposed on the slug-test response during early test times. As discussed in Section 3.1.3, this superimposed oscillatory pattern is attributed to varying recovery rates that occur within the 0.1016 m I.D. test string and the annular zone between the dual-wall drill casing. A comparison of the normalized, higher and lower stress, slug-test responses indicates nearly identical behavior, suggesting linear test-response characteristics. Slug tests exhibiting this type of response behavior can be analyzed quantitatively following the procedure discussed in Section 3.1.3, using the homogeneous formation analysis approach as described in Butler (1998). For the homogeneous formation analysis, the type-curve method estimates for  $K$  ranged narrowly between 4.67 and 5.18 m/day (average 4.93 m/day) for all stress-level tests. Results obtained from the Bouwer and Rice method provided very similar estimates of  $K$ , which ranged from 4.60 to 4.86 m/day (average 4.73 m/day) for all tests. The  $K$  estimates are based on an average test-system-casing radius of 0.0685 m as discussed in Section 3.1.3. Selected examples of analysis plots for this test interval are shown in Appendix Figure A.1.

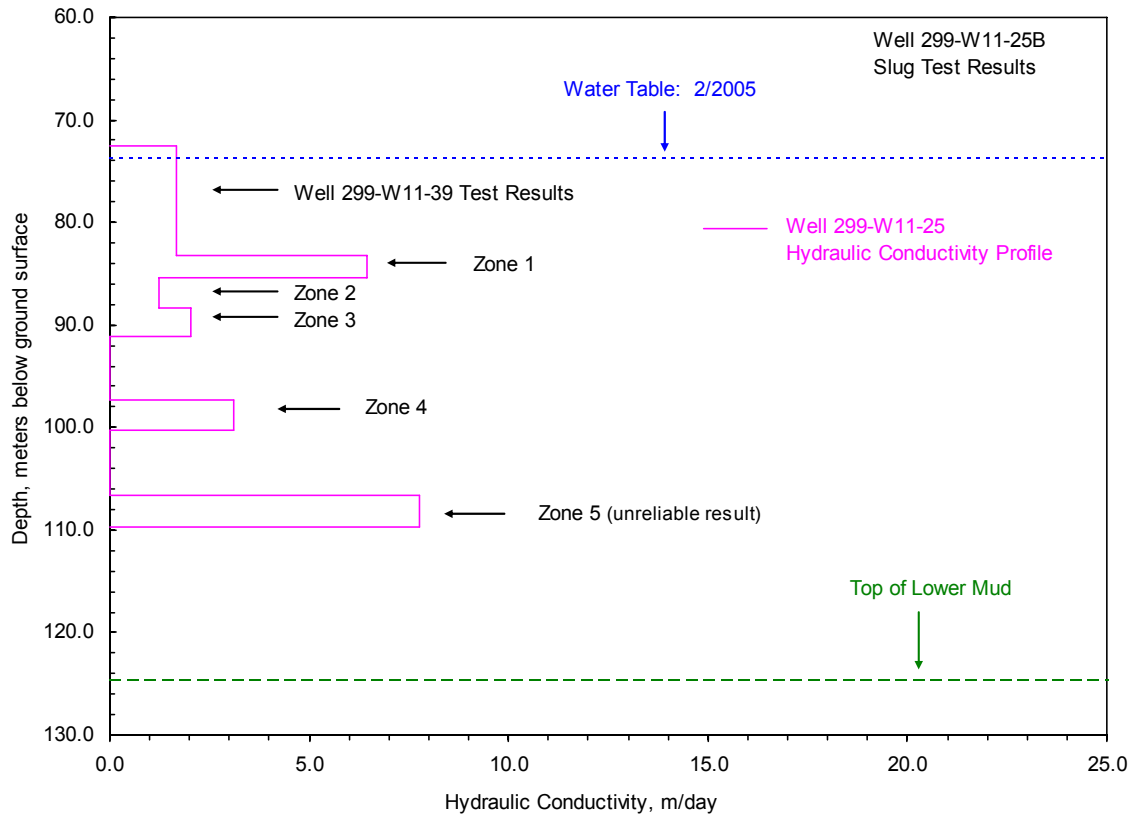


**Figure 4.21.** Hydraulic Conductivity Profile at Borehole 299-W11-25B

#### 4.2.1.2 Zone 2 (Depth: 85.34 to 88.39 m)

After reaching a depth of 88.39 m bgs, the packer/well-screen assembly was lowered to the bottom of the borehole, and the 0.229 m O.D. drill casing retracted 3.05 m, producing a test/depth interval for Zone 2 of 85.34 to 88.39 m bgs. The borehole geology log indicates that sediments within the test interval are primarily a medium sand, which grades to a sandy gravel over the lower section of the test zone. The lower sandy gravel unit is composed of 60 to 70% gravel and 30 to 40% sand.

A series of four pneumatic slug-withdrawal tests were conducted between 0905 hours and 1144 hours (PST), February 10, 2005. The pneumatic slug tests were conducted by pressurizing the 4-in. testing-string casing (I.D. = 0.102 m) used to set the packer/well-screen assembly. The pneumatic tests used applied stress (compressed air) pressures that produced observed fluid-column depressions ranging from 0.13 to 0.82 m for individual tests. The pressure was rapidly released using the wellhead surface valves. The static depth-to-water for the test interval during testing was not measured before or following testing, but is assumed to be approximately equal to the overlying Zone 1 test conditions (i.e., 73.75 m bgs).

All slug-test responses indicated a homogeneous formation, over-damped, test-response behavior. A very significant oscillatory pattern is superimposed on the slug-test response during early test times (<45 sec), similar to that shown in Figure 3.9. As discussed in Section 3.1.3, this superimposed

oscillatory pattern is attributed to varying recovery rates that occur within the 0.1016 m I.D. test string and the annular zone between the dual-wall drill casing. A comparison of the normalized, higher and lower stress, slug-test responses indicates nearly identical behavior, suggesting linear test-response characteristics. Slug tests exhibiting this type of response behavior can be analyzed quantitatively following the procedure discussed in Section 3.1.3, using the homogeneous formation analysis approach as described in Butler (1998). For the homogeneous formation analysis, the type-curve method provides a K estimate value of 1.25 m/day for all stress-level tests. Results obtained from the Bouwer and Rice method provided very similar estimates of K, which ranged narrowly between 1.23 and 1.28 m/day (average 1.25 m/day) for all tests. The K estimates are based on an average test-system-casing radius of 0.0685 m as discussed in Section 3.1.3. Selected examples of analysis plots for this test interval are shown in Appendix Figure A.2.

#### **4.2.1.3 Zone 3 (Depth: 88.09 to 91.14 m)**

After reaching a depth of 91.14 m bgs, the packer/well-screen assembly was lowered to the bottom of the borehole and the 0.229 m O.D. drill casing retracted 3.05 m, producing a test/depth interval for Zone 3 of 88.09 to 91.14 m bgs. The borehole geology log indicates that sediments within the test interval are primarily an unconsolidated to slightly cemented sandy gravel, which is composed of 60 to 70% gravel and 30 to 40% sand.

A series of three pneumatic slug-withdrawal tests were conducted between 1435 hours and 1613 hours (PST), February 16, 2005. The pneumatic slug tests were conducted by pressurizing the 4-in. testing-string casing (I.D. = 0.102 m) used to set the packer/well-screen assembly. The pneumatic tests used applied stress (compressed air) pressures that produced observed fluid-column depressions ranging from 0.26 to 1.17 m for individual tests. The pressure was rapidly released using the wellhead surface valves. The static depth-to-water for the test interval during testing was 73.80 m bgs.

All slug-test responses indicated critically-damped test-response behavior, with a significant oscillatory pattern superimposed on the slug-test response during early test times (< 45 sec), as shown previously in Figure 3.9. As discussed in Section 3.1.3, this superimposed oscillatory pattern is attributed to varying recovery rates that occur within the 0.1016 m I.D. test string and the annular zone between the dual-wall drill casing. A comparison of the normalized, higher and lower stress, slug-test responses indicates similar behavior, suggesting uniform test-response conditions. Examination of the individual slug-test responses also indicates consistent, slightly nonlinear (concave downward), critically-damped slug-test-response characteristics (see Bouwer and Rice analysis plot in Appendix Figure A.3). Slug tests exhibiting this type of response behavior cannot be analyzed quantitatively using standard, linear-response-based analytical methods (i.e., using either the Bouwer and Rice or standard type-curve methods—Section 3.1.1). The High-K analysis method presented in Butler and Garnett (2000) (see Section 3.1.2) was used to analyze these critically-damped slug-test responses. The High-K type-curve analysis method provided K estimates ranging from 1.82 to 2.22 m/day (average 2.02 m/day) for all tests. Selected examples of outer-zone analysis plots for this test/depth interval are shown in Appendix Figure A.3.

#### 4.2.1.4 Zone 4 (Depth: 97.26 to 100.31 m)

After reaching a depth of 100.31 m bgs, the packer/well-screen assembly was lowered to the bottom of the borehole and the 0.229 m O.D. drill casing retracted 3.05 m, producing a test/depth interval for Zone 4 of 97.26 to 100.31 m bgs. The borehole geology log indicates that sediments within the test interval are primarily an unconsolidated to slightly cemented sandy gravel, which is composed of 60 to 70% gravel and 30 to 40% sand. Included within the top of the test interval section is an ~0.9-m-thick medium sand unit that occurs between the depth of 97.54 and 98.45 m bgs.

A series of three pneumatic slug-withdrawal tests were conducted between 1230 hours and 1510 hours (PST), February 18, 2005. The pneumatic slug tests were conducted by pressurizing the 4-in. testing-string casing (I.D. = 0.102 m) used to set the packer/well-screen assembly. The pneumatic tests used applied stress (compressed air) pressures that produced observed fluid-column depressions ranging from 0.49 to 1.95 m for individual tests. The pressure was rapidly released using the wellhead surface valves. The static depth-to-water for the test interval during testing was 73.73 m bgs.

All slug-test responses indicated a heterogeneous formation behavior, with a higher permeability zone located in proximity to the well screen, as indicated by a rapid recovery rate at early test times. This transitions to a slower recovery rate for the surrounding lower permeability material (shown in test-response plots in Appendix Figure A.4). A very small oscillatory pattern is superimposed on the slug-test response during early test times (note: not shown in figures because of data smoothing). As discussed in Section 3.1.3, this superimposed oscillatory pattern is attributed to varying recovery rates that occur within the 0.1016 m I.D. test string and the annular zone between the dual-wall drill casing. A comparison of the smoothed (using a central moving-average scheme), normalized slug-test responses indicates nearly identical behavior, suggesting linear test-response behavior. Slug tests exhibiting linear, heterogeneous formation test-response characteristics can be analyzed quantitatively using the homogeneous formation analysis approaches described in Chapter 3. For the homogeneous formation analysis, the type-curve method estimates for K ranged from 21.2 to 25.5 m/day (average 23.4 m/day) for the various stress-level tests for the higher permeability inner zone (example analysis figure shown in Appendix Figure A.4). For the outer permeability zone, a K estimate range from 2.89 to 3.24 m/day (average 3.12 m/day) was obtained for all tests. Results obtained from the Bouwer and Rice method are generally less definitive for tests exhibiting heterogeneous formation response behavior. However, for these tests, the Bouwer and Rice method produced very comparable estimates as the type-curve method for the inner and outer permeability zones. For the Bouwer and Rice method, estimates of K for the high-permeability (inner) zone ranged from 21.2 to 27.8 m/day (average 24.5 m/day) for both stress-level tests. For the outer lower permeability zone, estimates of K ranged from 2.86 to 3.25 m/day (average 3.10 m/day). Selected examples of the outer-zone analysis plots for this borehole are shown in Appendix Figure A.5. As noted in Chapter 3, the inner-zone results are believed to be not representative of actual *in situ* formation conditions and may be attributable to a number of localized, artificially imposed, test interval conditions (e.g., borehole/gravel zone collapse around the smaller-diameter well screen). For these reasons, only the outer-zone analysis results should be used to assess aquifer formation characteristics at this test/depth interval location.

#### **4.2.1.5 Zone 5 (Depth: 106.68 to 109.73 m)**

After reaching a depth of 109.73 m bgs, the packer/well-screen assembly was lowered to the bottom of the borehole and the 0.229 m O.D. drill casing retracted 3.05 m, producing a test/depth interval for Zone 5 of 106.68 to 109.73 m bgs. The borehole geology log indicates that sediments within the test interval are primarily an unconsolidated to slightly cemented sandy gravel, which is composed of 70% gravel and 30 % medium to coarse sand.

A series of three pneumatic slug-withdrawal tests were conducted between 1041 hours and 1257 hours (PST), February 24, 2005. The pneumatic slug tests were conducted by pressurizing the 4-in. testing-string casing (I.D. = 0.102 m) used to set the packer/well-screen assembly. The pneumatic tests used applied stress (compressed air) pressures that produced observed fluid-column depressions ranging from 0.28 to 0.78 m for individual tests. The pressure was rapidly released using the wellhead surface valves. The static depth-to-water for the test interval during testing was 73.79 m bgs.

Before, during, and following completion of the slug-test characterization, standard packer integrity was tested by adding a known volume of water (a pressure stress) to the annular zone above the packer and between the inside of the drill casing and test system tubing string. Unlike the overlying test/depth intervals, direct associated pressure responses were observed during the packer stress tests, indicating a lack of test-interval isolation during testing. Repeated efforts to improve the packer/test interval sealing conditions and test-interval isolation were unsuccessful. As a result, the test results are not considered suitable for quantitative hydraulic property characterization for this particular test/depth interval.

#### **4.2.2 299-W14-11**

As shown in Figure 4.22, borehole 299-W14-11 is located near the northeast boundary of WMA TX-TY. In all, five specific test/depth intervals were characterized between April 19 and 28, 2005, by slug testing as the borehole was advanced to its final depth 105.8 m bgs. Following advancing the borehole to its final depth, the borehole was completed as a monitoring well with a well-screen located between 79.76 and 82.81 m bgs.

Pneumatic slug tests were used for each depth interval tested during borehole advancement. The pneumatic slug tests were conducted in the same manner as discussed in Section 4.2.1 for borehole 299-W11-25B. Diagnostic analysis of slug tests conducted for the various test/depth intervals indicate expected exponential decay (over-damped) conditions for all five borehole 299-W14-11 test depth intervals (Table 4.5). Heterogeneous formation/composite response conditions were indicated for the top two test/depth intervals (Zones 1 and 2). This composite pattern exhibits a high-permeability (fast initial recovery), inner-zone response, which transitions to a lower permeability surrounding outer-zone formation response. The presence of a high-permeability inner-zone is believed to be reflective of artificially created conditions. These artificially created high-permeability conditions may be attributed to the setting of a smaller-diameter packer/well-screen assembly and retraction of the larger diameter drill casing to expose the test/depth interval. It is believed that dislodged cobbles and gravel collapsing around the temporary well screen while the drill casing was retracted created an artificial high-permeability

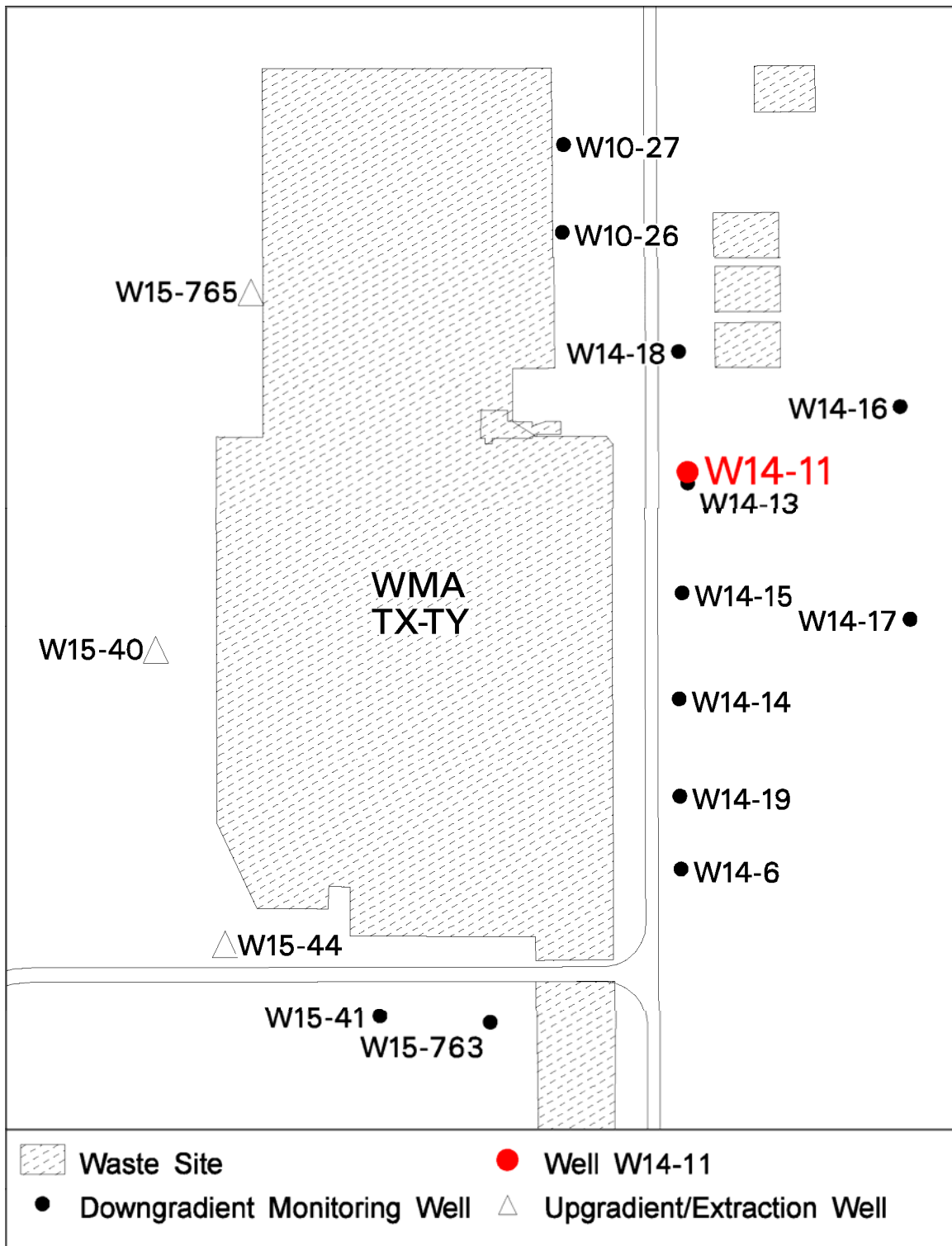


Figure 4.22. Well 299-W14-11 Location Map



**Table 4.5.** Slug-Test Characteristics for Selected Test/Depth Intervals at 299-W14-11

Test Zone	Test Parameters				Diagnostic Slug-Test-Response Model	Hydrogeologic Unit Tested
	Test Date	# Slug Tests	Depth to Water, m bgs	Test/Depth Interval, m bgs		
Zone 1	4/19/05	4	68.49	75.38–78.43 (3.05)	Over-Damped (exponential decay); Heterogeneous Formation	Ringold Formation (Unit 5)
Zone 2	4/21/05	4	68.49	84.55–87.60 (3.05)	Over-Damped (exponential decay); Heterogeneous Formation	Ringold Formation (Unit 5)
Zone 3	4/22/05	5	68.49	87.48–90.53 (3.05)	Composite: Test System Oscillations Superimposed on Formational Over- Damped Response	Ringold Formation (Unit 5)
Zone 4	4/26/05	4	68.34	96.62–99.67 (3.05)	Composite: Test System Oscillations Superimposed on Formational Over- Damped Response	Ringold Formation (Unit 5)
Zone 5	4/28/05	3	68.34	102.72–105.77 (3.05)	Composite: Test System Oscillations Superimposed on Formational Over- Damped Response	Ringold Formation (Unit 5)
Note: For all test wells, $r_c = 0.051$ meter; $r_w = 0.1143$ meter . Unit number in parentheses indicates the relevant groundwater-flow model layer, as described in Thorne et al. (1993).						

inner-zone (surrounding the temporary well screen). A similar heterogeneous formation/composite response condition was also exhibited for one of the test/depth intervals characterized at borehole 299-W11-25B.

Three of the test zones (Zones 3, 4, and 5) exhibited pronounced early-test time oscillations superimposed on exponential, over-damped recovery test responses. As discussed in Section 3.1.3, this superimposed oscillatory pattern is attributed to varying recovery rates that occur within the 0.1016 m I.D. test string and the annular zone between the dual-wall drill casing. The recovery rate imbalances within the two annular areas produce a test-system-induced oscillatory pattern, which is superimposed upon the general formation recovery slug-test pattern. An example of this type of superimposed response condition is shown in Figure 3.9. Similar oscillatory test responses were exhibited for depth intervals characterized during the borehole advancement of borehole 299-W11-25B, which also employed a dual-wall drill casing.

Results from discrete test/depth interval slug-test characterization during drilling of borehole 299-W14-11 are representative of the Ringold Unit C/E sand and gravel (Unit 5). Hydraulic conductivity estimates range from 1.43 to 4.71 m/day (Table 4.6; average type-curve results). Figure 4.23 shows the vertical depth distribution of hydraulic conductivity determined for the five depth intervals successfully tested at this well-site location. When combined with results for the completed well-screen section (Section 4.1.3) and results obtained at nearby well 299-W14-13 (Spane et al. 2001a), approximately 50% of the composite unconfined aquifer was characterized at this test-site location. As indicated in the figure, K values appear to be relatively uniform and vary only by a factor of four for the five test/depth intervals tested during borehole advancement. The lowest K value of 1.43 m/day was observed for the shallowest interval tested (Zone 1: 75.38 to 78.43 m bgs). This test zone is located approximately 7 to 10 m below the current water table. The highest K value of 4.93 m/day was observed for the deepest interval tested (Zone 5: 102.72 to 105.77 m bgs). The hydraulic conductivity estimates shown in Figure 4.23 are based on the type-curve analysis method and do not include values determined for the non-formational, artificially induced, high-permeability inner-zones that were exhibited for Test Zones 1 and 2. Results for the artificially produced high-K inner-zone are listed in Table 4.6 for simple comparison purposes.

The K estimate value for the completed well-screen test provided the highest K value (Section 4.1.3; K = 10.8 m/day) observed at well 299-W14-11. The completed well-screen test depth interval (79.76 to 82.81 m) occurs between Zones 1 and 2, which were tested during borehole advancement. The borehole geology log does not indicate a significant difference in gravel, sand, and silt percentages, in comparison to the test interval zones tested during borehole advancement. This higher K value at well 299-W14-11 is within the range reported previously in Spane et al. (2001a, 2001b, 2002, 2003) and Spane and Newcomer (2004) for the Ringold Unit C/E sand and gravel within the WMA TX-TY vicinity.

A brief description of the individual depth interval (Zone) tested during borehole advancement is presented below. Selected analysis figures for the respective test zones are presented in Appendix A.

#### **4.2.2.1 Zone 1 (Depth: 75.38 to 78.43 m)**

After reaching a depth of 78.43 m bgs, the packer/well-screen assembly was lowered to the bottom of the borehole and the 0.229 m O.D. drill casing retracted 3.05 m, producing a test/depth interval for Zone 1 of 75.38 to 78.43 m bgs. The borehole geology log indicates that the interval tested is primarily a sandy gravel unit, consisting of 60% gravel, 30% sand, and 10% silt. The sandy gravel unit is highly cemented and consolidated in the bottom 1.01 m of the test interval.

A series of four pneumatic slug-withdrawal tests were conducted between 0743 hours and 1114 hours (Pacific Daylight Time [PDT]), April 19, 2005. The pneumatic slug tests were conducted by pressurizing the 4-in. testing-string casing (I.D. = 0.102 m) used to set the packer/well-screen assembly. The pneumatic tests used applied stress (compressed air) pressures that produced observed fluid-column depressions ranging from 2.77 to 4.38 m for individual tests. The pressure was rapidly released using the wellhead surface valves. The static depth-to-water for the test interval during testing was 68.49 m bgs.

**Table 4.6.** 299-W14-11 Test/Depth Interval Slug-Test Analysis Results

Test/Depth Interval	Bouwer and Rice Analysis Method	Type-Curve Analysis Method		High-K Analysis Method <sup>(b)</sup>	
	Hydraulic Conductivity, $K_h^{(a)}$ (m/day)	Hydraulic Conductivity, $K_h^{(a)}$ (m/day)	Specific Storage, $S_s$ (m <sup>-1</sup> )	Hydraulic Conductivity, $K_h^{(a)}$ (m/day)	Dimensionless Damping Parameter, $C_D$
Zone 1	Inner Zone: 6.92–8.05 (7.49)	Inner Zone: 7.39–7.73 (7.56)	1.0E-5	NA	NA
	Outer Zone: 1.23–1.61 (1.42)	Outer Zone: 1.38–1.47 (1.43)	1.0E-5		
Zone 2	Inner Zone: 16.3–18.4 (17.4)	Inner Zone: 16.4–19.4 (17.9)	5.0E-5	NA	NA
	Outer Zone: 3.17–3.38 (3.28)	Outer Zone: 3.37–3.67 (3.52)	1.0E-5		
Zone 3	3.48–3.79 (3.64)	3.54–3.89 (3.72)	1.0E-5–5.0E-5	NA	NA
Zone 4	4.13–4.68 (4.41)	4.06–4.58 (4.32)	5.0E-5	NA	NA
Zone 5	4.64–5.10 (4.87)	4.58–4.84 (4.71)	1.0E-5	NA	NA
NA Not applicable or applied analytical method Number in parentheses is the average value for all tests. (a) Assumed to be uniform within the well-screen test section. For tests exhibiting a heterogeneous formation response, only outer zone analysis results are considered representative of <i>in situ</i> formation conditions. (b) When standard analytical methods are not valid, results are based on the High-K analysis method presented in Butler and Garnett (2000).					

All slug-test responses indicated a heterogeneous formation behavior, with a higher permeability zone located in proximity to the well screen, as indicated by a rapid recovery rate at early test times. This transitions to a slower recovery rate for the surrounding lower permeability material (shown in test-response plots in Appendix Figure A.6). A very small oscillatory pattern is superimposed on the slug-test response during early test times (note: not shown in figures because of data smoothing). As discussed in Section 3.1.3, this superimposed oscillatory pattern is attributed to varying recovery rates that occur within the 0.1016 m I.D. test string and the annular zone between the dual-wall drill casing. To facilitate test analysis, the oscillatory test-response behavior was smoothed, using a central moving-average method.

A comparison of the smoothed, normalized slug-test responses indicates nearly identical behavior, suggesting linear test-response behavior. Slug tests exhibiting linear, heterogeneous formation test-response characteristics can be analyzed quantitatively following the procedure discussed in Section 3.1.3, using the homogeneous formation analysis approaches described in Butler (1998). For the homogeneous formation analysis, the type-curve method estimates for  $K$  ranged from 7.39 to 7.73 m/day (average 7.56 m/day) for the various stress-level tests for the higher permeability inner zone (example analysis figure shown in Appendix Figure A.7). For the outer permeability zone, a  $K$  estimate range

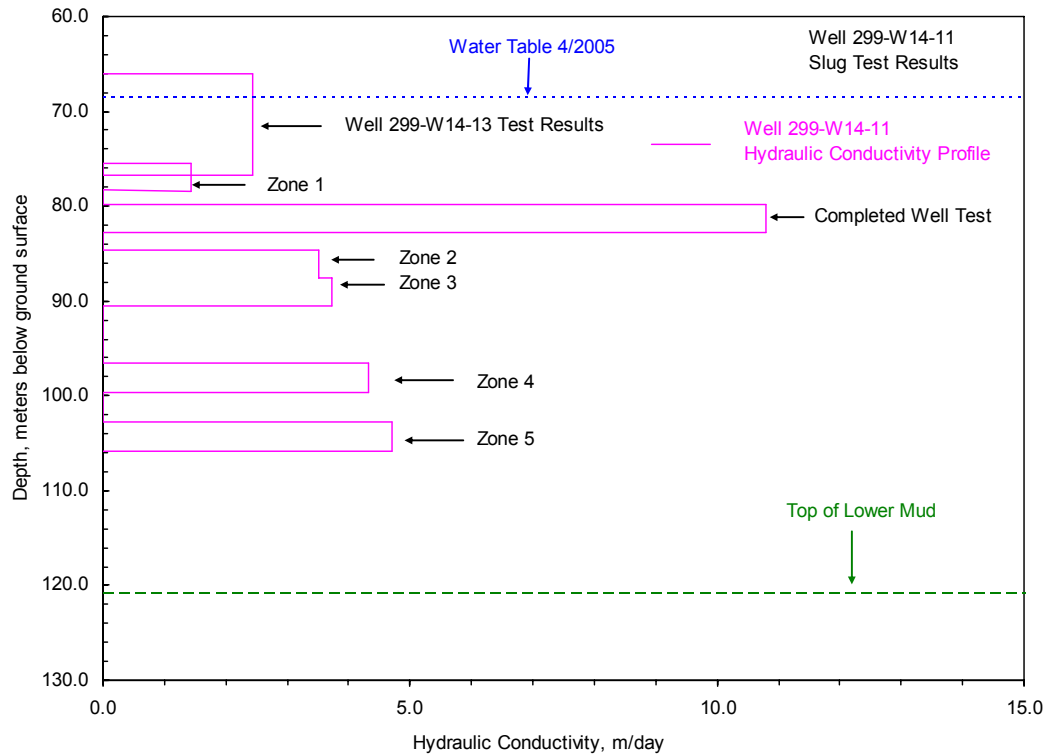


**Figure 4.23.** Hydraulic Conductivity Profile at Borehole 299-W14-11

between 1.38 and 1.47 m/day (average 1.43 m/day) was obtained for all tests. Results obtained from the Bouwer and Rice method are generally less definitive for tests exhibiting heterogeneous formation response behavior. However, for these tests, the Bouwer and Rice method produced very comparable estimates as the type-curve method for the inner and outer permeability zones. For the Bouwer and Rice method, estimates of  $K$  for the high-permeability (inner) zone ranged from 6.92 to 8.05 m/day (average 7.49 m/day) for all stress-level tests. For the outer lower permeability zone, estimates of  $K$  ranged from 1.23 to 1.61 m/day (average 1.42 m/day). Selected examples of the analysis plots for this borehole are shown in Appendix Figure A.7. As noted in Chapter 3, the inner-zone results are believed to be not representative of actual *in situ* formation conditions and may be attributable to a number of localized, artificially imposed, test interval conditions (e.g., borehole/gravel zone collapse around the smaller-diameter well screen). For these reasons, only the outer-zone analysis results should be used for assessing aquifer formation characteristics at this test/depth interval location.

#### 4.2.2.2 Zone 2 (Depth: 84.55 to 87.60 m)

After reaching a depth of 87.60 m bgs, the packer/well-screen assembly was lowered to the bottom of the borehole, and the 0.229 m O.D. drill casing retracted 3.05 m, producing a test/depth interval for Zone 2 of 84.55 to 87.60 m bgs. The borehole geology log indicates that the interval tested is primarily a sandy gravel unit, consisting of 50 to 60% gravel, 35 to 40% sand, and 5 to 10% silt.

A series of four pneumatic slug-withdrawal tests were conducted between 0631 hours and 0958 hours (PDT), April 21, 2005. The pneumatic slug tests were conducted by pressurizing the 4-in. testing-string casing (I.D. = 0.102 m) used to set the packer/well-screen assembly. The pneumatic tests used applied stress (compressed air) pressures that produced observed fluid-column depressions ranging from 0.19 to 4.02 m for individual tests. The pressure was rapidly released using the wellhead surface valves. The static depth-to-water for the test interval during testing was 68.49 m bgs.

All slug-test responses indicated a heterogeneous formation behavior, with a higher permeability zone located in proximity to the well screen, as indicated by a rapid recovery rate at early test times. This transitions to a slower recovery rate for the surrounding lower permeability material (shown in test-response plots in Appendix Figure A.8). A very small oscillatory pattern is superimposed on the slug-test response during early test times. As discussed in Section 3.1.3, this superimposed oscillatory pattern is attributed to varying recovery rates that occur within the 0.1016 m I.D. test string and the annular zone between the dual-wall drill casing. To facilitate test analysis, the oscillatory test-response behavior was smoothed, using a central moving-average method.

A comparison of the smoothed normalized slug-test responses indicates nearly identical behavior, suggesting linear test-response behavior. Slug tests exhibiting linear, heterogeneous formation test-response characteristics can be analyzed quantitatively using the homogeneous formation analysis approaches described in Chapter 3. For the homogeneous formation analysis, the type-curve method estimates for K ranged from 16.4 to 19.4 m/day (average 17.9 m/day) for the various stress-level tests for the higher permeability inner-zone (example analysis figure shown in Appendix Figure A.9). For the outer permeability zone, a K estimate range from 3.37 to 3.67 m/day (average 3.52 m/day) was obtained for all tests. Results obtained from the Bouwer and Rice method are generally less definitive for tests exhibiting heterogeneous formation response behavior. However, for these tests, the Bouwer and Rice method produced very comparable estimates as the type-curve method for the inner and outer permeability zones. For the Bouwer and Rice method, estimates of K for the high-permeability inner-zone ranged from 16.3 to 18.4 m/day (average 17.4 m/day) for all stress-level tests. For the outer lower permeability zone, estimates of K ranged from 3.17 to 3.38 m/day (average 3.28 m/day). Selected examples of the analysis plots for this borehole are shown in Appendix Figure A.9. As noted in Chapter 3, the inner-zone results are believed to be not representative of actual *in situ* formation conditions and may be attributable to a number of localized, artificially imposed, test-interval conditions (e.g., borehole/gravel zone collapse around the smaller-diameter well screen). For these reasons, only the outer-zone analysis results should be used for assessing aquifer formation characteristics at this test/depth interval location.

#### **4.2.2.3 Zone 3 (Depth: 87.48 to 90.53 m)**

After reaching a depth of 90.53 m bgs, the packer/well-screen assembly was lowered to the bottom of the borehole and the 0.229 m O.D. drill casing retracted 3.05 m, producing a test/depth interval for Zone 3 of 87.48 to 90.53 m bgs. The borehole geology log indicates that the interval tested is primarily a gravely sand unit, consisting of 75% sand, 15% gravel, and 10% silt. The sediments grade to a sandy gravel unit near the top and bottom of the test interval. The sandy gravel unit is composed of 40 to 50% gravel, 35 to 40% sand, and 10 to 25% silt.

A series of five pneumatic slug-withdrawal tests were conducted between 0715 hours and 1028 hours (PDT), April 22, 2005. The pneumatic slug tests were conducted by pressurizing the 4-in. testing-string casing (I.D. = 0.102 m) used to set the packer/well-screen assembly. The pneumatic tests used applied stress (compressed air) pressures that produced observed fluid-column depressions ranging from 0.27 to 1.14 m for individual tests. The pressure was rapidly released using the wellhead surface valves. The static depth-to-water for the test interval during testing was 68.49 m bgs.

All slug-test responses indicated a homogeneous formation, over-damped, test-response behavior. A very significant oscillatory pattern is superimposed on the slug-test response during early test times (<45 sec), similar to that shown in Figure 3.9. As discussed in Section 3.1.3, this superimposed oscillatory pattern is attributed to varying recovery rates that occur within the 0.1016 m I.D. test string and the annular zone between the dual-wall drill casing. To facilitate test analysis, the oscillatory test-response behavior was smoothed, using a polynomial-fit regression.

A comparison of the smoothed, normalized, higher and lower stress, slug-test responses indicates nearly identical behavior, suggesting linear test-response characteristics. Slug tests exhibiting this type of response behavior can be analyzed quantitatively using homogeneous formation analysis approaches, as described in Butler (1998). For the homogeneous formation analysis, the type-curve method estimates for K ranged from 3.54 to 3.89 m/day (average 3.72 m/day) for the various stress-level tests (example analysis figure shown in Appendix Figure A.10). Results obtained from the Bouwer and Rice method provided very similar estimates of K, which ranged narrowly between 3.48 and 3.79 m/day (average 3.64 m/day) for all tests. The K estimates are based on an average test-system-casing radius of 0.0685 m as discussed in Section 3.1.3. Selected examples of analysis plots for this test interval are shown in Appendix Figure A.10.

#### **4.2.2.4 Zone 4 (Depth: 96.62 to 99.67 m)**

After reaching a depth of 99.67 m bgs, the packer/well-screen assembly was lowered to the bottom of the borehole and the 0.229 m O.D. drill casing retracted 3.05 m, producing a test/depth interval for Zone 4 of 96.62 to 99.67 m bgs. The borehole geology log indicates that the interval tested is primarily a sandy gravel unit, consisting of 70% gravel, 25% sand, and 5% silt.

A series of four pneumatic slug-withdrawal tests were conducted between 1200 hours and 1551 hours (PDT), April 26, 2005. The pneumatic slug tests were conducted by pressurizing the 4-in. testing-string casing (I.D. = 0.102 m) used to set the packer/well-screen assembly. The pneumatic tests used applied stress (compressed air) pressures that produced observed fluid-column depressions ranging from 0.22 to 0.78 m for individual tests. The pressure was rapidly released using the wellhead surface valves. The static depth-to-water for the test interval during testing was 68.34 m bgs.

All slug-test responses indicated a homogeneous formation, over-damped, test-response behavior. A very significant oscillatory pattern is superimposed on the slug-test response during early test times (<60 sec), similar to that shown in Figure 3.9. As discussed in Section 3.1.3, this superimposed oscillatory pattern is attributed to varying recovery rates that occur within the 0.1016 m I.D. test string and the annular zone between the dual-wall drill casing. To facilitate test analysis, the oscillatory test-response behavior was smoothed, using a polynomial-fit regression.

A comparison of the smoothed, normalized, higher and lower stress, slug-test responses indicates nearly identical behavior, suggesting linear test-response characteristics. Slug tests exhibiting this type of response behavior can be analyzed quantitatively using homogeneous formation analysis approaches, as described in Butler (1998). For the homogeneous formation analysis, the type-curve method estimates for K ranged from 4.06 to 4.58 m/day (average 4.32 m/day) for the various stress-level tests (example analysis figure shown in Appendix Figure A.11). Results obtained from the Bouwer and Rice method provided very similar estimates of K, which ranged narrowly between 4.13 and 4.68 m/day (average 4.41 m/day) for all tests. The K estimates are based on an average test-system-casing radius of 0.0685 m as discussed in Section 3.1.3. Selected examples of analysis plots for this test interval are shown in Appendix Figure A.11.

#### **4.2.2.5 Zone 5 (Depth: 102.72 to 105.77 m)**

After reaching a depth of 105.77 m bgs, the packer/well-screen assembly was lowered to the bottom of the borehole and the 0.229 m O.D. drill casing retracted 3.05 m, producing a test/depth interval for Zone 4 of 102.72 to 105.77 m bgs. The borehole geology log indicates that the interval tested is primarily a sandy gravel unit, consisting of 60% gravel, 30% sand, and 10% silt.

A series of three pneumatic slug-withdrawal tests were conducted between 0918 hours and 1158 hours (PDT), April 28, 2005. The pneumatic slug tests were conducted by pressurizing the 4-in. testing-string casing (I.D. = 0.102 m) used to set the packer/well-screen assembly. The pneumatic tests used applied stress (compressed air) pressures that produced observed fluid-column depressions ranging from 0.30 to 1.24 m for individual tests. The pressure was rapidly released using the wellhead surface valves. The static depth-to-water for the test interval during testing was 68.34 m bgs.

All slug-test responses indicated a homogeneous formation, over-damped, test-response behavior. A moderate oscillatory pattern was superimposed on the slug-test response during early test times (<30 sec), similar to that shown in Figure 3.9. As discussed in Section 3.1.3, this superimposed oscillatory pattern is attributed to varying recovery rates that occur within the 0.1016 m I.D. test string and the annular zone between the dual-wall drill casing. To facilitate test analysis, the oscillatory early-test, time-response behavior was smoothed, using a polynomial-fit regression.

A comparison of the smoothed, normalized, higher and lower stress, slug-test responses indicates nearly identical behavior, suggesting linear test-response characteristics. Slug tests exhibiting this type of response behavior can be analyzed quantitatively following the procedure discussed in Section 3.1.3, using homogeneous formation analysis approaches, as described in Butler (1998). For the homogeneous formation analysis, the type-curve method estimates for K ranged from 4.58 to 4.84 m/day (average 4.71 m/day) for the various stress-level tests (example analysis figure shown in Appendix Figure A.12). Results obtained from the Bouwer and Rice method provided very similar estimates of K, which ranged narrowly between 4.64 and 5.10 m/day (average 4.87 m/day) for all tests. The K estimates are based on an average test-system-casing radius of 0.0685 m as discussed in Section 3.1.3. Selected examples of analysis plots for this test interval are shown in Appendix Figure A.12

### 4.2.3 299-W22-47

As shown in Figure 4.24, borehole 299-W22-47 is located near the southeast boundary of WMA S-SX. In all, four specific test/depth intervals were characterized between January 7 and 24, 2005, by slug testing as the borehole was advanced to its final depth 106.3 m bgs. Following advancing the borehole to its final depth, the borehole was completed as a monitoring well with a well-screen located between 69.70 and 80.37 m bgs.

Mechanical slug tests, using slugging rods of known displacement, were used for test characterization of the two top test/depth intervals (Zones 1 and 2) during borehole advancement, while pneumatic slug tests were used for the bottom two test/depth intervals (Zones 3 and 4). The pneumatic slug tests were conducted in the same manner as discussed in Section 4.2.1 and performed at boreholes 299-W11-25B and 299-W14-11. Diagnostic analysis of slug tests conducted for the various test/depth intervals indicate expected exponential decay (over-damped) conditions for all four test zones (Table 4.7). Three of the test zones (Zones 2, 3, and 4) exhibited moderate to pronounced early-test time oscillations superimposed on exponential, over-damped recovery test responses. As discussed in Section 3.1.3, this superimposed oscillatory pattern is attributed to varying recovery rates that occur within the 0.1016 m I.D. test string and the annular zone between the dual-wall drill casing. The recovery rate imbalances within the two annular areas produce a test-system-induced oscillatory pattern, which is superimposed upon the general formation recovery slug-test pattern. An example of this type of superimposed response condition is shown in Figure 3.9. Similar oscillatory test responses were exhibited for depth intervals characterized during the borehole advancement of 299-W11-25B and 299-W14-11, which also employed a dual-wall drill casing.

Results from discrete test/depth interval slug-test characterization during the drilling of borehole 299-W22-47 are representative of the Ringold Unit C/E sand and gravel (Unit 5). Hydraulic conductivity estimates range from 10.8 to 22.3 m/day (Table 4.8; average type-curve results). Figure 4.25 shows the vertical depth distribution of hydraulic conductivity determined for the four depth intervals successfully tested at this borehole site location. When combined with results for the completed well-screen section (Section 4.1.8), approximately 30% of the composite unconfined aquifer was characterized at this test-site location. As indicated in the figure, K values appear to be relatively uniform and vary only by a factor of two for the four test/depth intervals tested during borehole advancement. The hydraulic conductivity estimates shown in Figure 4.25 are based on the type-curve analysis method, which are considered to consistently provide representative estimates of *in situ* formation conditions.

The K estimate value for the completed well-screen test provided a K value estimate of 17.3 m/day (Section 4.1.8). The completed well-screen test depth interval (69.70 to 80.37 m) encompasses both Zones 1 and 2, which were tested during borehole advancement. It is interesting to note that the completed well-screen test K value is close to the average value of 16.8 m/day for Zones 1 and 2 (i.e., Zone 1, K = 11.2 m/day; Zone 2, K = 22.3 m/day). This close correspondence also lends credence to the observation that higher permeability sediments occur in the lower-section of the completed well-screen section.



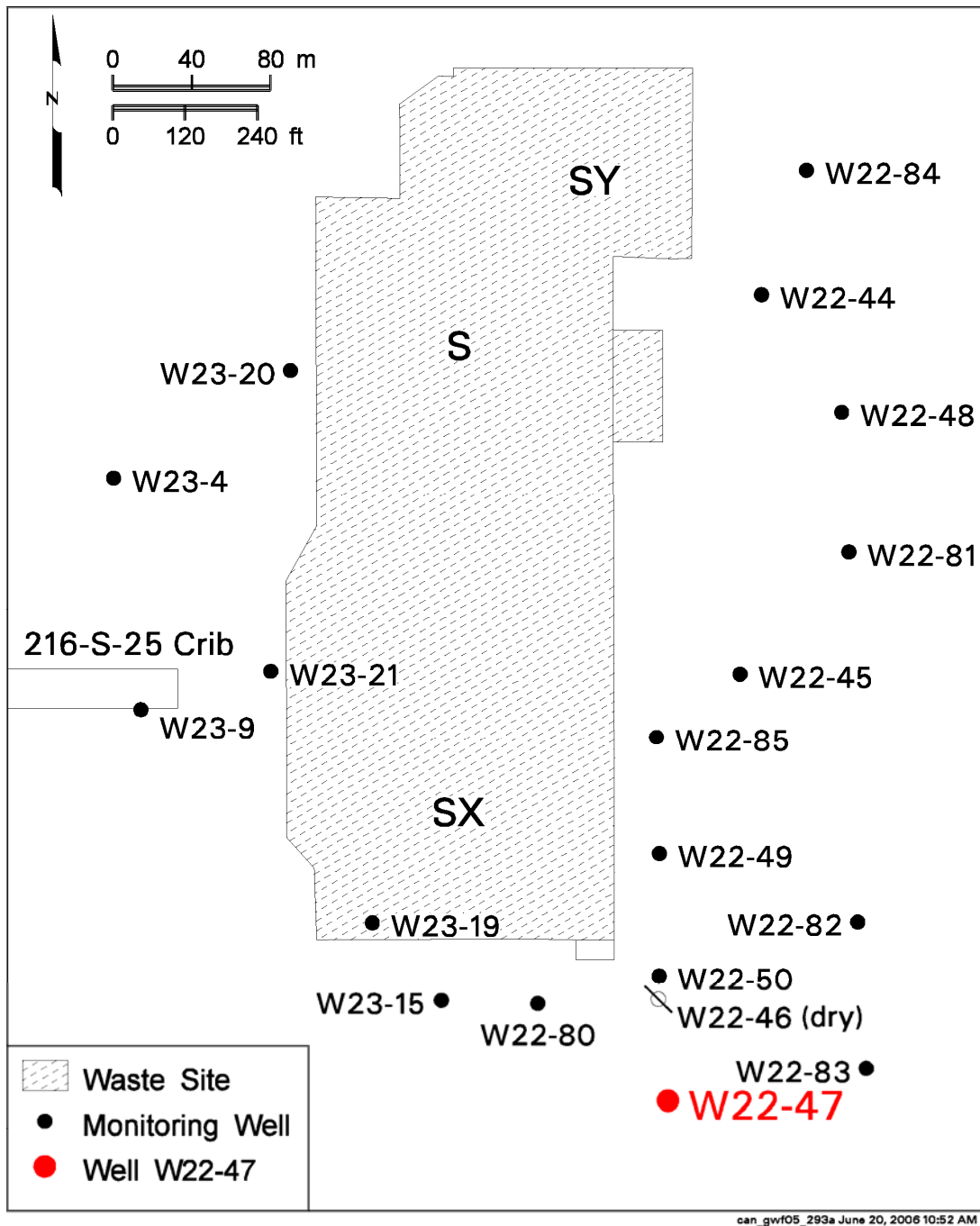


**Figure 4.24.** Well 299-W22-47 Location Map

**Table 4.7.** Slug-Test Characteristics for Selected Test/Depth Intervals at 299-W22-47

Test Zone	Test Parameters				Diagnostic Slug-Test-Response Model	Hydrogeologic Unit Tested
	Test Date	# Slug Tests	Depth to Water, m bgs	Test/Depth Interval, m bgs		
Zone 1	1/7/05	6	69.49	71.75–73.67 (1.92)	Over-Damped (exponential decay)	Ringold Formation (Unit 5)
Zone 2	1/11/05	6	69.74	75.89–78.95 (3.05)	Composite: Test System Oscillations Superimposed on Formational Over-Damped Response	Ringold Formation (Unit 5)
Zone 3	1/18/05	5	69.59	87.02–89.43 (2.41)	Composite: Test System Oscillations Superimposed on Formational Over-Damped Response	Ringold Formation (Unit 5)
Zone 4	1/24/05	4	69.58	102.96–106.47 (3.51)	Composite: Test System Oscillations Superimposed on Formational Over-Damped Response	Ringold Formation (Unit 5)
Note: For all test wells, $r_c = 0.051$ meter; $r_w = 0.1143$ meter . Unit number in parentheses indicates the relevant groundwater-flow model layer, as described in Thorne et al. (1993).						

A brief description of the individual depth interval (Zone) tested during borehole advancement is presented below. Selected analysis figures for the respective test zones are presented in Appendix A.

#### 4.2.3.1 Zone 1 (Depth: 75.38 to 78.43 m)

After reaching a depth of 73.67 m bgs, the packer/well-screen assembly was lowered to the bottom of the borehole and the 0.229 m O.D. drill casing retracted 1.92 m, producing a test/depth interval for Zone 1 of 71.75 to 73.67 m bgs. The borehole geology log indicates that the interval tested is primarily a sandy gravel unit with medium to coarse sand (note: no size-fraction percentages are indicated).

A series of three slug-injection and three slug-withdrawal tests were conducted between 1150 hours and 1412 hours (PST), January 7, 2005. The slug tests were conducted by using two different sized slugging rods. The stress levels for the two slugging rods are calculated to impose a slug-test response of 0.255 m (low-stress tests) and 0.458 m (high-stress tests) within a 0.1016-m inside diameter test string that was used to install the packer/well-screen assembly. The static depth-to-water for the test interval during testing was 69.49 m bgs.

**Table 4.8.** 299-W22-47 Test/Depth Interval Slug-Test Analysis Results

Test/Depth Interval	Bouwer and Rice Analysis Method	Type-Curve Analysis Method		High-K Analysis Method <sup>(b)</sup>	
	Hydraulic Conductivity, $K_h^{(a)}$ (m/day)	Hydraulic Conductivity, $K_h^{(a)}$ (m/day)	Specific Storage, $S_s$ (m <sup>-1</sup> )	Hydraulic Conductivity, $K_h^{(a)}$ (m/day)	Dimensionless Damping Parameter, $C_D$
Zone 1	8.36–8.75 (8.56)	11.2	3.0E-5	NA	NA
Zone 2	18.2–20.4 (19.3)	21.2–23.3 (22.3)	1.0E-5	NA	NA
Zone 3	9.36–11.9 (10.6)	9.54–12.1 (10.8)	1.0E-5	NA	NA
Zone 4	10.5–12.4 (11.5)	10.4–12.1 (11.2)	3.0E-5	NA	NA
NA Not applicable or applied analytical method Number in parentheses is the average value for all tests (a) Assumed to be uniform within the well-screen test section. For tests exhibiting a heterogeneous formation response, only outer zone analysis results are considered representative of <i>in situ</i> formation conditions (b) When standard analytical methods are not valid, results are based on the High-K analysis method presented in Butler and Garnett (2000).					

All slug-test responses indicated a homogeneous formation, over-damped, test-response behavior. Even though a dual-wall drill casing system was used at this borehole site, no significant imposed oscillatory pattern was superimposed on the over-damped, slug-test response during early test times. A comparison of the normalized, high- and low-stress, slug-test responses indicates essentially identical behavior, suggesting linear test-response characteristics. Slug tests exhibiting this type of response behavior can be analyzed quantitatively using homogeneous formation analysis approaches, as described in Butler (1998). For the homogeneous formation analysis, the type-curve method estimate for K was 11.2 m/day for low- and high-stress-level tests. Results obtained from the Bouwer and Rice method provided lower estimates of K, which ranged narrowly between 8.36 and 8.75 m/day (average 8.56 m/day) for all tests. The K estimates are based on an average test-system-casing radius of 0.0685 m as discussed in Section 3.1.3. Selected examples of analysis plots for this test interval are shown in Appendix Figure A.13

#### 4.2.3.2 Zone 2 (Depth: 75.89 to 78.94 m)

After reaching a depth of 78.94 m bgs, the packer/well-screen assembly was lowered to the bottom of the borehole and the 0.229 m O.D. drill casing retracted 3.05 m, producing a test/depth interval for Zone 2 of 75.89 to 78.94 m bgs. The borehole geology log indicates that the interval tested is primarily a sandy gravel unit with medium to coarse sand (note: no size-fraction percentages are indicated).

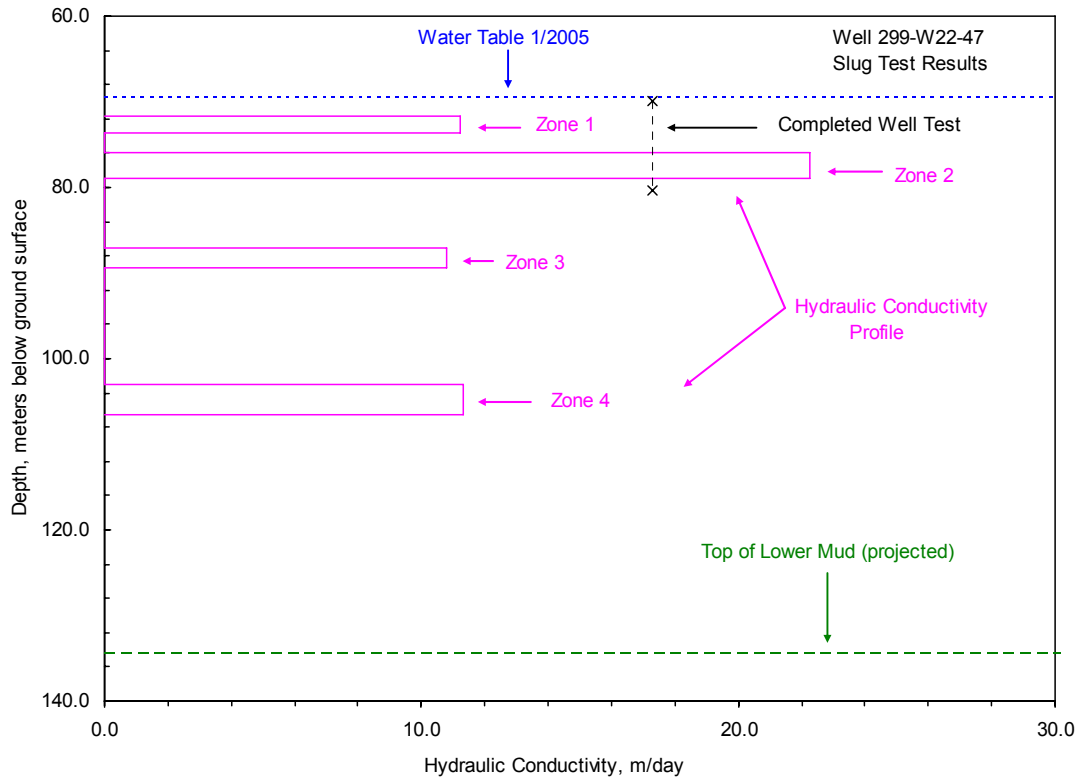


**Figure 4.25.** Hydraulic Conductivity Profile at Borehole 299-W22-47

A series of four slug-injection and two slug-withdrawal tests were conducted between 1023 hours and 1253 hours (PST), January 11, 2005. The slug tests were conducted by using two different sized slugging rods. The stress levels for the two slugging rods are calculated to impose a slug-test response of 0.458 m (low-stress tests) and 1.117 m (high-stress tests) within a 0.1016-m inside diameter test string that was used to install the packer/well-screen assembly. The static depth-to-water for the test interval during testing was 69.72 m bgs.

All slug-test responses indicated a homogeneous formation, over-damped, test-response behavior. A moderate oscillatory pattern was superimposed on the slug-test response during early test times (<20 sec), similar to that shown in Figure 3.9. As discussed in Section 3.1.3, this superimposed oscillatory pattern is attributed to varying recovery rates that occur within the 0.1016 m I.D. test string and the annular zone between the dual-wall drill casing. To facilitate test analysis, the oscillatory early-test, time-response behavior was smoothed, using a central, moving-average statistical method.

A comparison of the smoothed, normalized, higher and lower stress, slug-test responses indicates nearly identical behavior, suggesting linear test-response characteristics. Slug tests exhibiting this type of response behavior can be analyzed quantitatively following the procedure discussed in Section 3.1.3, using homogeneous formation analysis approaches as described in Butler (1998). For the homogeneous formation analysis, the type-curve method estimates for K ranged from 21.2 to 23.3 m/day (average 22.3 m/day) for the various stress-level tests (example analysis figure shown in Appendix Figure A.14).

Results obtained from the Bouwer and Rice method provided slightly lower estimates of K, which ranged from 18.2 to 20.4 m/day (average 19.3 m/day) for all tests. The K estimates are based on an average test-system-casing radius of 0.0685 m as discussed in Section 3.1.3. Selected examples of analysis plots for this test interval are shown in Appendix Figure A.14.

#### **4.2.3.3 Zone 3 (Depth: 87.48 to 90.53 m)**

After reaching a depth of 89.43 m bgs, the packer/well-screen assembly was lowered to the bottom of the borehole and the 0.229 m O.D. drill casing retracted 2.41 m, producing a test/depth interval for Zone 3 of 87.02 to 89.43 m bgs. The borehole geology log indicates that the interval tested is primarily a sandy gravel unit with medium to coarse sand (note: no size-fraction percentages are indicated).

A series of five pneumatic slug-withdrawal tests were conducted between 0933 hours and 1452 hours (PST), January 18, 2005. The pneumatic slug tests were conducted by pressurizing the 4-in. testing-string casing (I.D. = 0.102 m) used to set the packer/well-screen assembly. The pneumatic tests used applied stress (compressed air) pressures that produced observed fluid-column depressions ranging from 0.49 to 2.40 m for individual tests. The pressure was rapidly released using the wellhead surface valves. The static depth-to-water for the test interval during testing was 69.59 m bgs.

All slug-test responses indicated a homogeneous formation, over-damped, test-response behavior. A moderate oscillatory pattern was superimposed on the slug-test response during early test times (<30 sec), similar to that shown in Figure 3.9. As discussed in Section 3.1.3, this superimposed oscillatory pattern is attributed to varying recovery rates that occur within the 0.1016 m I.D. test string and the annular zone between the dual-wall drill casing. To facilitate test analysis, the oscillatory early-test, time-response behavior was smoothed, using a polynomial fit regression.

A comparison of the normalized, high- and low-stress, slug-test responses indicates very similar test-response behavior, suggesting linear test-response characteristics. Slug tests exhibiting this type of response behavior can be analyzed quantitatively following the procedure discussed in Section 3.1.3, using homogeneous formation analysis approaches as described in Butler (1998). For the homogeneous formation analysis, the type-curve method estimates for K ranged from 9.50 to 12.1 m/day (average 10.8 m/day) for low- and high-stress-level tests. Results obtained from the Bouwer and Rice method provided similar estimates of K, which ranged from 9.36 to 11.9 m/day (average 10.6 m/day) for all tests. The K estimates are based on an average test-system-casing radius of 0.0685 m as discussed in Section 3.1.3. Selected examples of analysis plots for this test interval are shown in Appendix Figure A.15.

#### **4.2.3.4 Zone 4 (Depth: 102.96 to 106.47 m)**

After reaching a depth of 106.47 m bgs, the packer/well-screen assembly was lowered to the bottom of the borehole and the 0.229 m O.D. drill casing retracted 3.51 m, producing a test/depth interval for Zone 4 of 102.96 to 106.47 m bgs. The borehole geology log indicates that the interval tested is primarily a sandy gravel unit with medium to coarse sand (note: no size-fraction percentages are indicated) that is moderately to well-cemented.

A series of four pneumatic slug-withdrawal tests were conducted between 0933 hours and 1452 hours (PST), January 24, 2005. The pneumatic slug tests were conducted by pressurizing the 4-in. testing-string casing (I.D. = 0.102 m) used to set the packer/well-screen assembly. The pneumatic tests used applied stress (compressed air) pressures that produced observed fluid-column depressions ranging from 0.49 to 2.40 m for individual tests. The pressure was rapidly released using the wellhead surface valves. The static depth-to-water for the test interval during testing was 69.58 m bgs.

All slug-test responses indicated a homogeneous formation, over-damped, test-response behavior. A moderate oscillatory pattern was superimposed on the slug-test response during early test times (<30 sec), similar to that shown in Figure 3.9. As discussed in Section 3.1.3, this superimposed oscillatory pattern is attributed to varying recovery rates that occur within the 0.1016 m I.D. test string and the annular zone between the dual-wall drill casing. To facilitate test analysis, the oscillatory early-test, time-response behavior was smoothed, using a polynomial fit regression.

A comparison of the normalized, high- and low-stress, slug-test responses indicates very similar test-response behavior, suggesting linear test-response characteristics. Slug tests exhibiting this type of response behavior can be analyzed quantitatively following the procedure discussed in Section 3.1.3, using homogeneous formation analysis approaches as described in Butler (1998). For the homogeneous formation analysis, the type-curve method estimates for K ranged from 10.4 to 12.1 m/day (average 11.2 m/day) for low- and high-stress-level tests. Results obtained from the Bouwer and Rice method provided very similar estimates of K, which ranged from 10.5 to 12.4 m/day (average 11.5 m/day) for all tests. The K estimates are based on an average test-system-casing radius of 0.0685 m as discussed in Section 3.1.3. Selected examples of analysis plots for this test interval are shown in Appendix Figure A.16.

## 5.0 Tracer-Dilution Test Results: Well 299-W22-47

Well 299-W22-47 was selected for detailed tracer test characterization during CY 2005. Results from the tracer-dilution phase of the single-well tracer testing were analyzed using the methods described in Section 3.2.1. To be strictly valid, the analytical assumptions require that the dilution occurs only as the result of lateral groundwater inflow (i.e., no vertical groundwater flow). As noted in Section 8.1.2, evidence provided by ambient electromagnetic flow-meter surveys conducted within the well suggested very slight upward flow conditions over several limited depth intervals within the well-screen section. For wells exhibiting low in-well vertical flow, determination of the vertical distribution of hydraulic conductivity within the well screen cannot be quantitatively evaluated from the tracer-dilution patterns observed vs. depth. In these situations, however, Spane et al. (2001a, 2001b) reports that an average well-column dilutionary pattern can be used to determine average in-well lateral flow velocity,  $v_w$ . A description of the performance and analysis of the tracer-dilution test conducted in well 299-W22-47 using the tracer-dilution characterization method is provided below.

A single well tracer-dilution test was initiated on November 14, 2005 (1012 hour, PST) by administering 5.3 liters of tracer solution (containing 16.944 grams of bromide) within the 10.45 m saturated well-screen section (69.92 to 80.37 m below brass cap). The tracer was introduced into the well using a 2.54-centimeter-diameter polypropylene tube that was open at a depth setting of 80.12 m below the brass cap. Following tracer introduction, an equilibration time of approximately 13 minutes was observed to allow the displaced non-tracer water to dissipate from the 2.54-centimeter tracer tube into the surrounding well-screen column. After the prescribed equilibration period, the tracer tube was slowly raised out of the well water column, causing emplacement of the 5.3 liters of prepared tracer into the well water column. The tracer tube then was slowly lowered and raised three times within the water column over a 5-minute period to mix the tracer within the well-screen section. As noted in Spane et al. (2001b, 2002), this method of tracer mixing provides a low-stress means of dispersing the administered tracer within the well-screen section.

Following mixing of the tracer solution, an assembly of five bromide probe sensors spaced individually at a separation distance of 2.1 m was lowered into the well. Final depth settings for the five bromide probes were 79.3, 77.2, 75.1, 73.0, and 70.9 m below the brass cap. Each probe had an attached plastic centralizer to keep the probe approximately centered within the well-screen section. The probe assembly was installed in approximately 28 minutes following the mixing of the tracer within the well screen. The bromide concentration within the borehole following emplacement and equilibration of the probes was approximately 80 mg/liter, with a small amount of variability in tracer concentration evident between the five probe depth settings (i.e., ~70 to 100 mg/L). The observed tracer concentration within the well after probe installation is less than half of the original designed concentration. Rapid dilution during the initial stages of tracer emplacement within well screens exposed to test formations of moderate to high-permeability conditions, however, is commonly observed during tracer testing at the Hanford Site.

Dilution of the tracer was rapid, reflecting the moderately high hydraulic conductivity conditions within the well-screen/test interval (see Section 4.1.8). The dilution and dissipation of bromide tracer within the well screen was observed for a period of approximately 2 days (2,854 min). Recovery of the

tracer from well 299-W22-47 and the surrounding aquifer was initiated with a constant-rate pumping test beginning on November 16, 2005 (1004 hours PST).

Visual examination of the dilution patterns for the various sensor-depth settings during the test indicates considerable noise for two of the probe depth settings, which is thought to be attributable to metal well-screen interference effects with the probe sensing surface (i.e., probe sensing surface in proximity to the metal well screen). In addition, there are indications within the various tracer probe-dilution patterns that corroborate the presence of a slight upward, vertical, in-well flow condition that was characterized using the EBF survey conducted within this well (Section 8.1.2). The tracer-dilution pattern exhibited a progressive decreasing rate with depth within the well-screen section (i.e., fastest dilution rate exhibited for the top probe depth setting of 70.9 m and slowest dilution rate exhibited for the lowest probe depth setting of 79.3 m).

As discussed in Section 3.2.1, to be strictly valid, tracer-dilution tests require that no vertical flow conditions exist within the well and that the tracer is continually mixed within the test section. To “simulate” a continuously mixed condition, an average well-screen tracer concentration was calculated, based on averaging all five sensor-depth readings recorded with time (i.e., 70.9 to 79.3 m below the brass cap). It is not known whether the vertical flow conditions observed within the well are significant enough to adversely affect these results. The analysis results, therefore, should be viewed as being qualitative estimates.

The observed, average dilution pattern versus time can be analyzed to calculate  $v_w$ , using Equation 3.3. Linear-regression analysis of the average dilution response (shown in Figure 5.1) within the well screen ( $r^2 = 0.99$ ) indicates a slope on the natural log of concentration versus time of  $-0.001265 \text{ minutes}^{-1}$ . The calculated average A/V relationship for the test interval, taking into account the presence of the sensor instrumentation/cable test system cross-sectional area, is  $13.505 \text{ m}^{-1}$ . Based on these observed and measured parameters, an average lateral groundwater-flow velocity within the well,  $v_w$ , is calculated at 0.13 m/day.



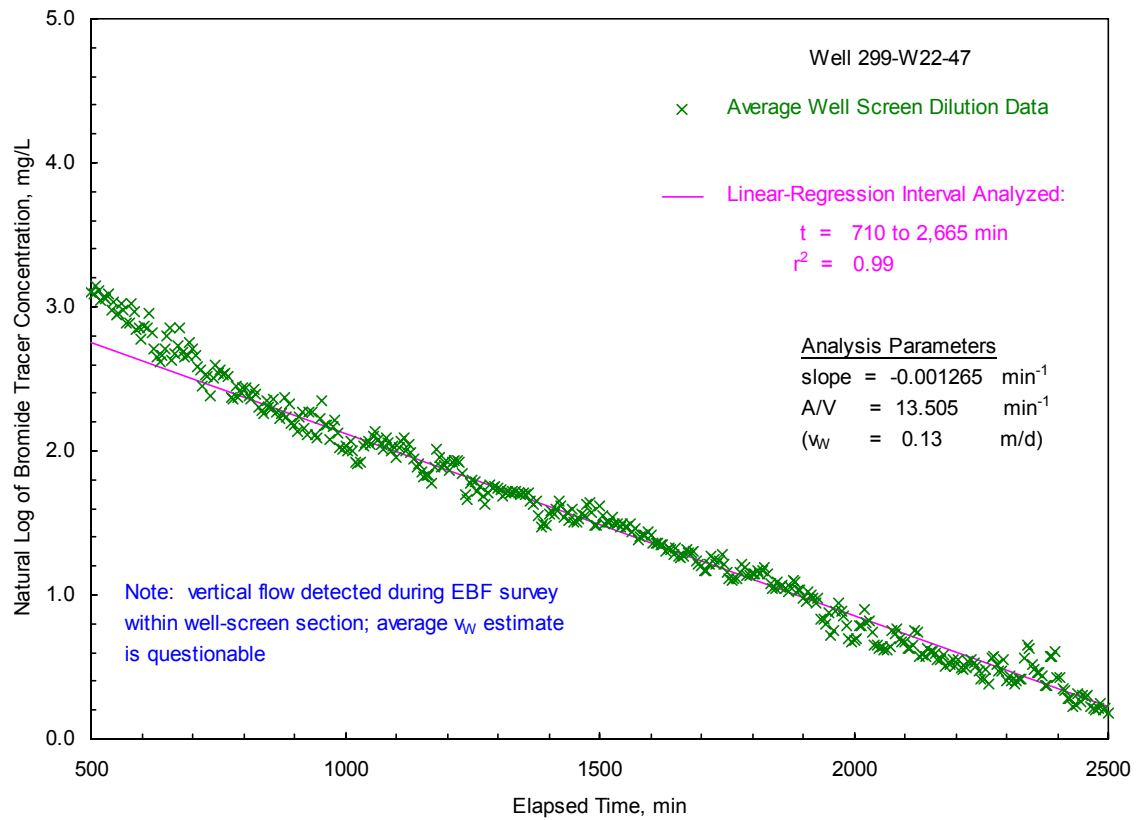


**Figure 5.1.** Average Tracer-Dilution Test Results Within Well 299-W22-47

## 6.0 Tracer-Pumpback Test Results: Well 299-W22-47

Results from the bromide tracer-pumpback phase conducted at well 299-W22-47 were analyzed using the methods described in Section 3.2.2. The analytical assumptions of full aquifer penetration and rapid pulse injection into the aquifer were not met with the given field test conditions. Because of these test deficiencies, the estimates derived from the pumpback test for effective porosity,  $n_e$ , and average ground-water-flow velocity within the aquifer,  $v_a$ , should only be used qualitatively. Future efforts should be directed to improve the estimates for  $n_e$  and  $v_a$  by accounting for these effects. A description of the information pertinent to the tracer-pumpback test performed in well 299-W22-47 is provided below.

After allowing tracer-drift for approximately 2 days (2,854 min), recovery of the tracer from well 299-W22-47 and the surrounding aquifer was initiated with a constant-rate pumping test beginning on November 16, 2005 (1004 hours PST). Tracer recovery was terminated after 244 minutes of pumping. The average tracer concentration within the well at the beginning of pumpback is estimated at 0.81 milligrams/liter. This estimate is based on late-time projection of the average dilution regression line (Figure 5.1) to the time of tracer pumpback initiation. Given the calculated well screen and sandpack volumes of 84.7 and 91.2 liters, respectively, 16.84 grams of the 16.94 grams of tracer initially emplaced in the well are estimated to have been transported from the well into the surrounding aquifer. After minor flow adjustments were completed during the first 2.67 minutes of the test, pumping rates remained relatively constant during tracer pumpback, ranging from 52.20 to 55.12 liters/min (average = 53.03 liters/min) for the entire test as shown in Figure 6.1. An estimated 14.17 grams of the total 16.94 grams of tracer (i.e., ~84%) emplaced in the well were recovered during the constant-rate pumping test. The pumping time,  $t_p$ , to recover 50% of the tracer emplaced within the aquifer (accounting for transit time during pumping from the well screen to land surface) is estimated at 40.84 minutes. The time required to recover the center of the tracer mass that was transported within the aquifer was used in Equations 3.10 and 3.11 to calculate  $n_e$  and  $v_a$ . As indicated in the equations, information pertaining to hydraulic conductivity,  $K$ , hydraulic gradient,  $I$ , aquifer thickness,  $b$ , and pumping rate,  $Q$ , must also be known for the test well site.

A  $K$  value of 16.5 m/day was used, which is based on results from the constant-rate pumping test for the test well (i.e., during tracer pumpback; Section 7.1). The calculated local  $I$  value of 0.00165 m/m represents the average hydraulic gradient conditions (i.e., November 14 and 16, 2005) based on trend-surface analysis for water-level elevation measurement periods for well 299-W22-47 and five nearby monitor wells, 299-W22-46, W22-49, -W22-50, -W22-82, -W22-83, and -W23-15, as indicated in Section 8.2. The  $b$  value of 67.6 m was calculated directly from the observed water-table elevation at the time of testing and projected geologic depth information obtained at nearby test wells.

Based on these input parameters and tracer-pumpback results,  $n_e$  and  $v_a$  are estimated to be 0.294 and 0.093 m/day, respectively. Based on the observed tracer-pumpback profile (see Figure 6.1) and calculated radial distance traveled within the aquifer by the tracer's center of mass (i.e., product of  $v_a$  and  $t_d = 0.2$  m), the results of pumpback reflect local, near-well, aquifer conditions and may be susceptible to the adverse wellbore effects discussed in Section 3.2.2. Table 6.1 summarizes the pertinent information associated with the tracer-pumpback results for well 299-W22-47.

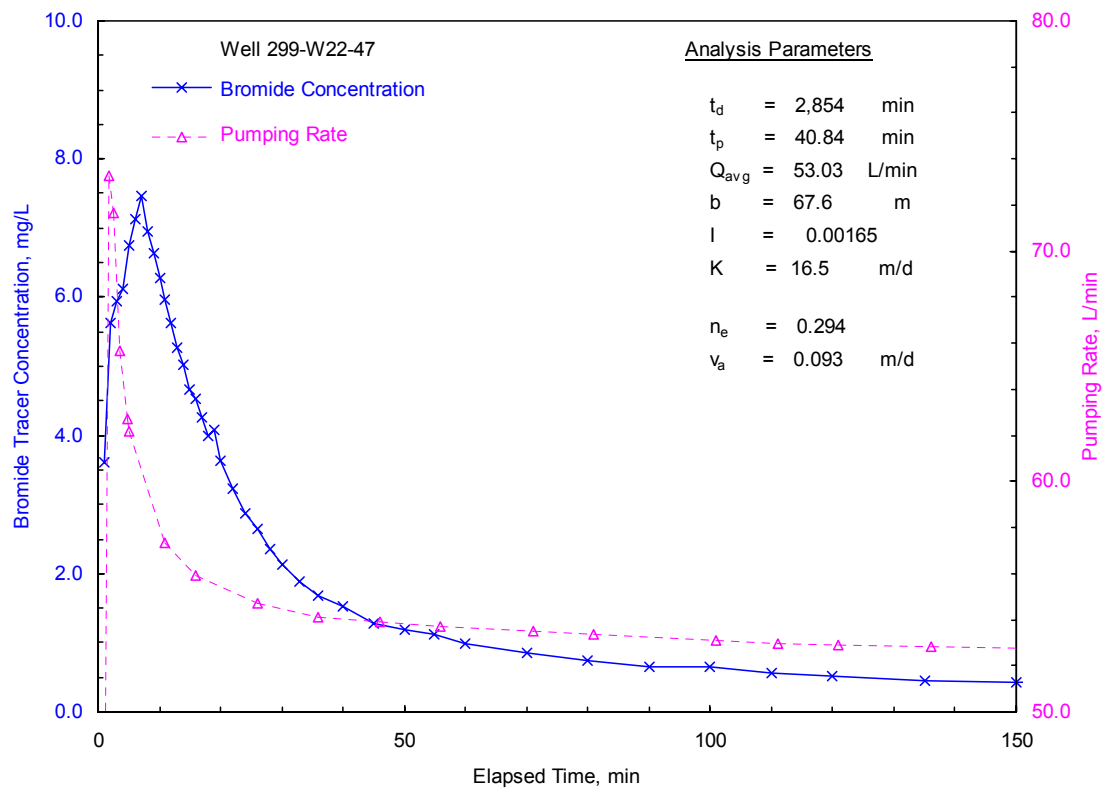


**Figure 6.1.** Tracer-Pumpback Test Results for Well 299-W22-47

**Table 6.1.** Tracer-Pumpback Test Summary for Well 299-W22-47

Waste Management Area	Well	Hydrologic Characterization Data				Tracer-Pumpback Test			
		Aquifer Thickness, $b$ (m)	Pumping Rate, $Q$ (liters/min)	Hydraulic Gradient, $I$ (m/m)	Hydraulic Conductivity, $K$ (m/day)	Tracer Drift Time, $t_d$ (min)	Tracer Recovery Time, $t_p$ (min) <sup>(a)</sup>	Effective Porosity, $n_e$	Groundwater-Flow Velocity, $v_a$ (m/day)
SST S-SX	299-W22-47	67.6	53.03	0.00165	16.5	2,854	40.84	0.294	0.093

(a) Time required to recover 50% of tracer from the aquifer.

## 7.0 Constant-Rate Pumping Test Results: Well 299-W22-47

Only one well site was selected for detailed hydrologic characterization during FY and CY 2005. As part of the detailed hydrologic characterization, a constant-rate pumping test was conducted and extended during the tracer-pumpback following the tracer-dilution test. Analysis of the resulting drawdown and recovery test data at the pumped well provides intermediate-scale estimates for transmissivity (T), hydraulic conductivity (K), vertical anisotropy ( $K_D$ ), storativity (S), and specific yield ( $S_y$ ). Barometric responses at the pumped well were monitored over an extended baseline period immediately following termination to tracer-pumpback when other hydraulic stresses were minimal. These baseline water-level data were analyzed to assess the effects of barometric pressure fluctuations on well water-level responses and remove barometric fluctuations from water levels recorded during the constant-rate pumping test, as discussed in Section 3.3.2. Derivative techniques (see Section 3.3.3) were applied diagnostically to identify aquifer conditions and select the appropriate analysis method. Combined type-curve analysis of both the test responses and the derivative plots was then used to calculate hydraulic properties. The type-curves were generated using the WTAQ3 computer program (Moench 1997) and account for a wide range of test and aquifer conditions, including partial penetration, vertical anisotropy, wellbore storage, unconfined aquifer drainage, and well-skin effects. A more detailed description of the various components of the constant-rate pumping-test analysis is provided in Section 3.2.

A description of the performance and analysis of the constant-rate pumping test is provided below, and a summary of results is presented in Table 7.1. The estimate for K was calculated by dividing T by the total aquifer thickness, b, rather than the length of the well-screen section at the pumping well. This is appropriate because the analysis type curves account for partial penetration of the aquifer and vertical anisotropy. Estimates of S and  $S_y$  resulting from the test analysis are considered less reliable than the estimates of T and K because of the lack of analyzable observation well data. Responses at the pumping well are also much less sensitive to storage parameters, and these parameter estimates are more likely to be affected by near-well heterogeneity.

**Table 7.1.** Constant-Rate Pumping Test Summary

Pumping Well	Well Analyzed	Transmissivity, T, m <sup>2</sup> /day	Horizontal Hydraulic Conductivity, $K_h$ , m/day	Vertical Anisotropy, $K_D$	Storativity, S	Specific Yield, $S_y$
299-W22-47	299-W22-47	1,116	16.5	0.3	0.00005	0.300

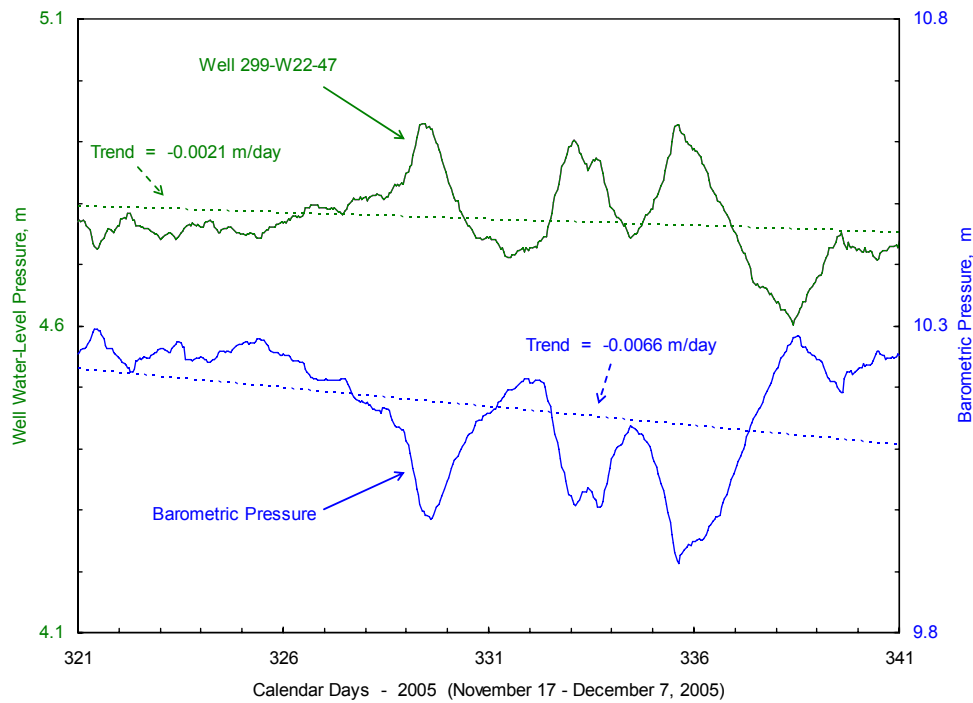
At the time of testing, the well screen at 299-W22-47 penetrated the upper 10.39 m of the unconfined aquifer, which has a total estimated thickness of approximately 67.6 m. The aquifer is within Ringold Unit E and is composed of sandy gravel with a medium to coarse sand matrix. The Ringold lower mud unit forms an aquitard at the bottom of the tested aquifer. No observation wells were located near enough to this new well to be affected by the aquifer test. The constant-rate discharge test was conducted from 1004 to 1408 Pacific Standard Time on November 16, 2005. The average flow rate during the test was 53.03 L/minute over the 244-minute pumping period.

Barometric and well water-level response characteristics were monitored for an ~21-d period (November 17 to December 7, 2005; 2005 Calendar Days: 321 to 341) immediately after the pumping test at the well was terminated (Figure 7.1). Based on the observed barometric and associated well water-level response characteristics, the multiple-regression deconvolution technique described in Section 3.3.2 was used to remove barometric pressure effects from the water levels measured during the test. A total time-lag dependence of 110 hr provided the best match of well water levels associated with barometric responses during the baseline monitoring period. Figure 7.2 shows the associated diagnostic barometric/well water-level response plot based on the multiple-regression analysis. This response pattern is characteristic of unconfined aquifer conditions as discussed in Rasmussen and Crawford (1997) and Spane (1999, 2002). Because of the relatively stable barometric pressure conditions preceding, during, and immediately following the pumping test, removing barometric pressure effects did not significantly improve the test data analysis.

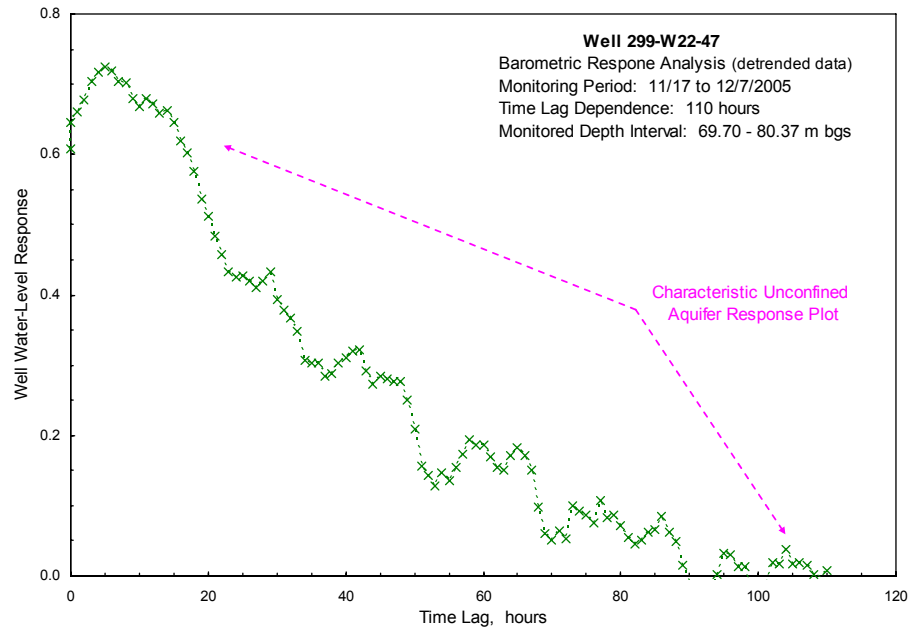
Figure 7.3 shows a log-log comparison plot of the drawdown and recovery data for pumping well 299-W22-47. The effects of frequent pumping-rate changes during the initial 2 minutes of the pumping test are readily exhibited in the drawdown data. Following pumping-rate stabilization, the drawdown and recovery data exhibit nearly identical behavior. Because the drawdown derivative is drastically affected by pumping-rate adjustments, it is not shown in the figure. The increasing recovery-data derivative pattern shown in Figure 7.3 for later test times indicates that the recovery test data are approaching infinite-acting radial flow conditions. However, the pumping and associated recovery periods would have had to be extended to reach these hydrologic test conditions. Because infinite-acting radial flow conditions were not established during the test, straight-line analysis techniques cannot be used to analyze the test data.

Figure 7.4 shows an analysis plot for the recovery data, with a type-curve match and a derivative plot. As shown, the type-curve and derivative plots provide a reasonable match to the observed test data except during the initial minute of recovery. The reason for this early-time matching discrepancy is not known, but may be attributable to a small amount of return flow from the test system back into the well at the time of test termination. The type-curve match shown in Figure 7.4 provided the following results for the unconfined aquifer at this well location:  $T = 1,116 \text{ m}^2/\text{day}$ ,  $S = 5.0\text{E-}05$ , and  $S_y = 0.30$ . The best-estimate  $K$  value of 16.5 m/day was calculated by dividing  $T$  by the total aquifer thickness,  $b$ , because partial penetration is accounted for in the analysis. The type-curve displayed is based on a vertical anisotropy ( $K_D$ ) of 0.3. This value for  $K_D$  provided the best composite fit for the test data and derivative than higher and lower values of  $K_D$ , although the differences in fit were relatively minor. The values of  $T$  and  $K$  for well 299-W22-47 may be higher than calculated if significant head losses occurred at the pumping rates used in this test. However, because the pumping rates were relatively low and other new (similarly constructed) RCRA wells installed in the 200 West Area have exhibited very low head-loss characteristics

(Spane et al. 2001a, 2001b), results of the type-curve-fitting analysis for pumping well 299-W22-47 are considered to provide representative estimates of aquifer hydraulic properties. Additionally, a relatively close correspondence for  $K$  estimates obtained from the slug and pumping tests (i.e.,  $K = 17.3$  m/day vs. 16.5 m/day), which were conducted under different hydrologic stress levels, also suggests that head losses did not have a significant effect on the pumping test results.



**Figure 7.1.** Barometric Pressure and Associated Well Water-Level Response during a 21-Day Baseline Monitoring Period at Well 299-W22-47



**Figure 7.2.** Barometric Response Analysis Plot for Well 299-W22-47

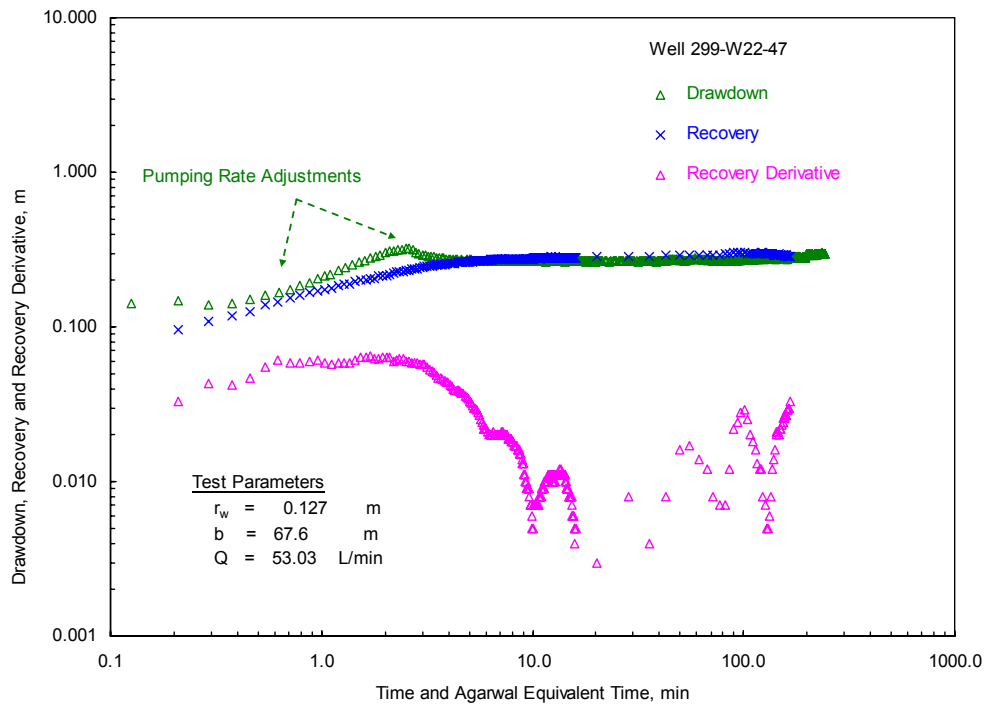


**Figure 7.3.** Drawdown and Recovery Test Data Comparison for Pumping Well 299-W22-47

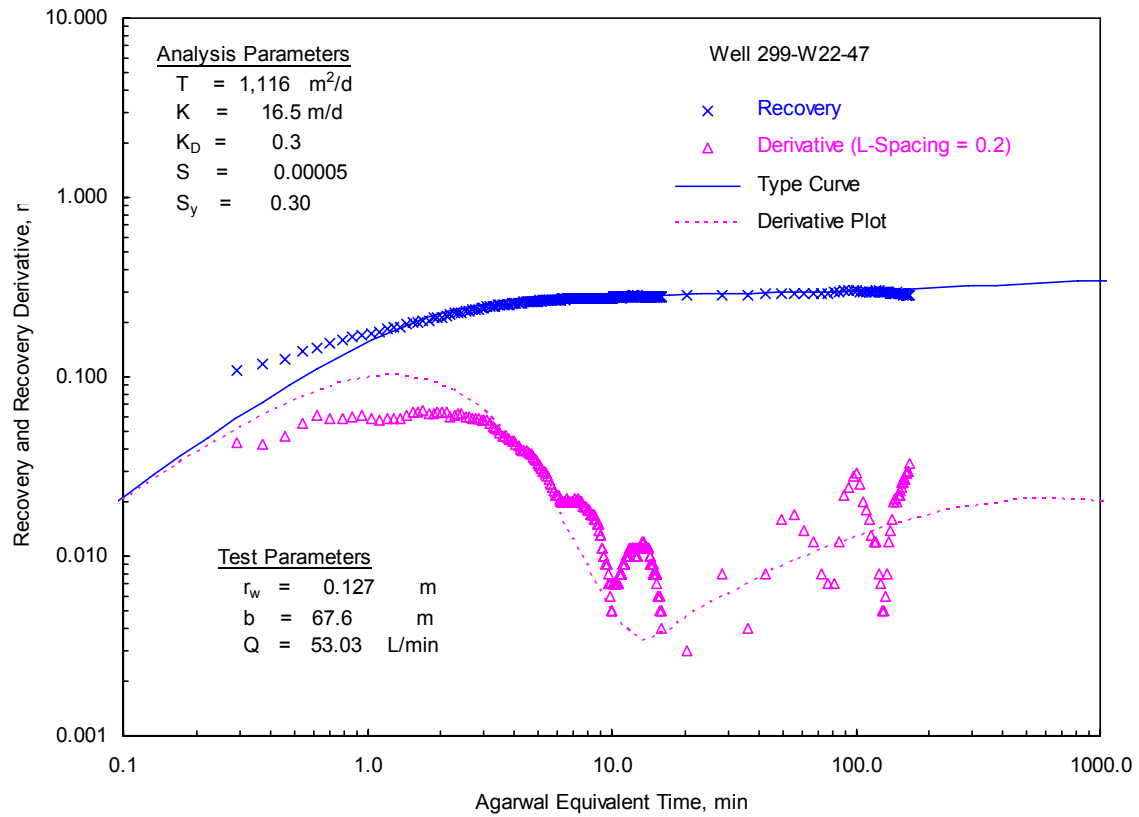


**Figure 7.4.** Type-Curve and Derivative Plot Analysis of Recovery Test Data for Pumping Well 299-W22-47



## **8.0 Groundwater-Flow Characterization Results**

Groundwater-flow characterization activities performed during FY and CY 2005 included ambient, in-well EBF surveys and a lateral groundwater-flow characterization for the well 299-W22-47 vicinity. This well location was the focus of tracer-dilution, tracer pumpback, and constant-rate pumping tests that are discussed in Chapters 5, 6 and 7, respectively. A detailed discussion of these groundwater-flow characterization activities is presented in the following report sections.

### **8.1 Ambient, In-Well Vertical Flow Characterization**

Three wells located in the Hanford Site's 200-West Area (299-W14-11, 299-W22-47, and 299-W22-80; Figure 8.1), were characterized using EBF surveys during FY and CY 2005. The primary objective of the EBF surveys was to characterize the ambient (i.e., static), in-well vertical flow conditions (i.e., vertical flow-velocity magnitude and direction) within the saturated well-screen section for each well. Wells with no or extremely low vertical-flow conditions can be used for conducting tracer-dilution and pumpback tests for detailed hydrologic characterization purposes, as discussed in Chapter 3.

A summary of the analytical results for the ambient vertical flow surveys conducted in FY and CY 2005 is presented in Table 8.1. As shown in the table, upward vertical in-well flow was detected within sections of the well screens of all wells surveyed. The cause of the observed, in-well vertical flow conditions is not known, but as noted previously in Spane et al. (2001a, 2001b, 2002, and 2003), it may be the result of either 1) proximity to local discharge, 2) heterogeneous formation conditions along the well screen, or 3) effects from neighboring well-pumping/-sampling or remedial action activities. The existence of vertical flow is not necessarily reflective of actual groundwater-flow conditions within the surrounding aquifer, but its presence implies a vertical hydraulic head gradient and has implications pertaining to the representativeness of groundwater samples collected from such monitor-well facilities. Instructive numerical model studies that examine the effects of vertical flow imposed by well-screen completions, in the presence of extremely low hydraulic gradients, are presented in Reilly et al. (1989) and Elci et al. (2001). A discussion of the performance and results for the EBF flowmeter surveys is provided below.

#### **8.1.1 Well 299-W14-11**

An ambient flowmeter survey was performed in well 299-W14-11 on October 6, 2005. Well 299-W14-11 is completed with a 3.05-m (10-ft) long, 4-in. I.D. wire-wrap screen with no solid joints and a 0.6-m sump below the bottom of the screen. The top of the well screen was approximately 11.16 m below the water table at the time of ambient flowmeter testing, and the screened section extends over the depth interval of 79.76 to 82.81 m bgs (Table 1.2). The measured static depth-to-water before beginning the flowmeter survey was 68.6 m bgs. The in-well vertical flow rate was measured every 0.3 m within the well-screen interval, beginning at a depth of 82.7 m bgs and ending at a depth of 80.2 m bgs. For EBF calibration purposes, points of zero flow were measured both within the well-screen sump, at a depth of 83.4 m bgs, and near the top of the water column above the well-screen interval at a depth of 69.0 m bgs.

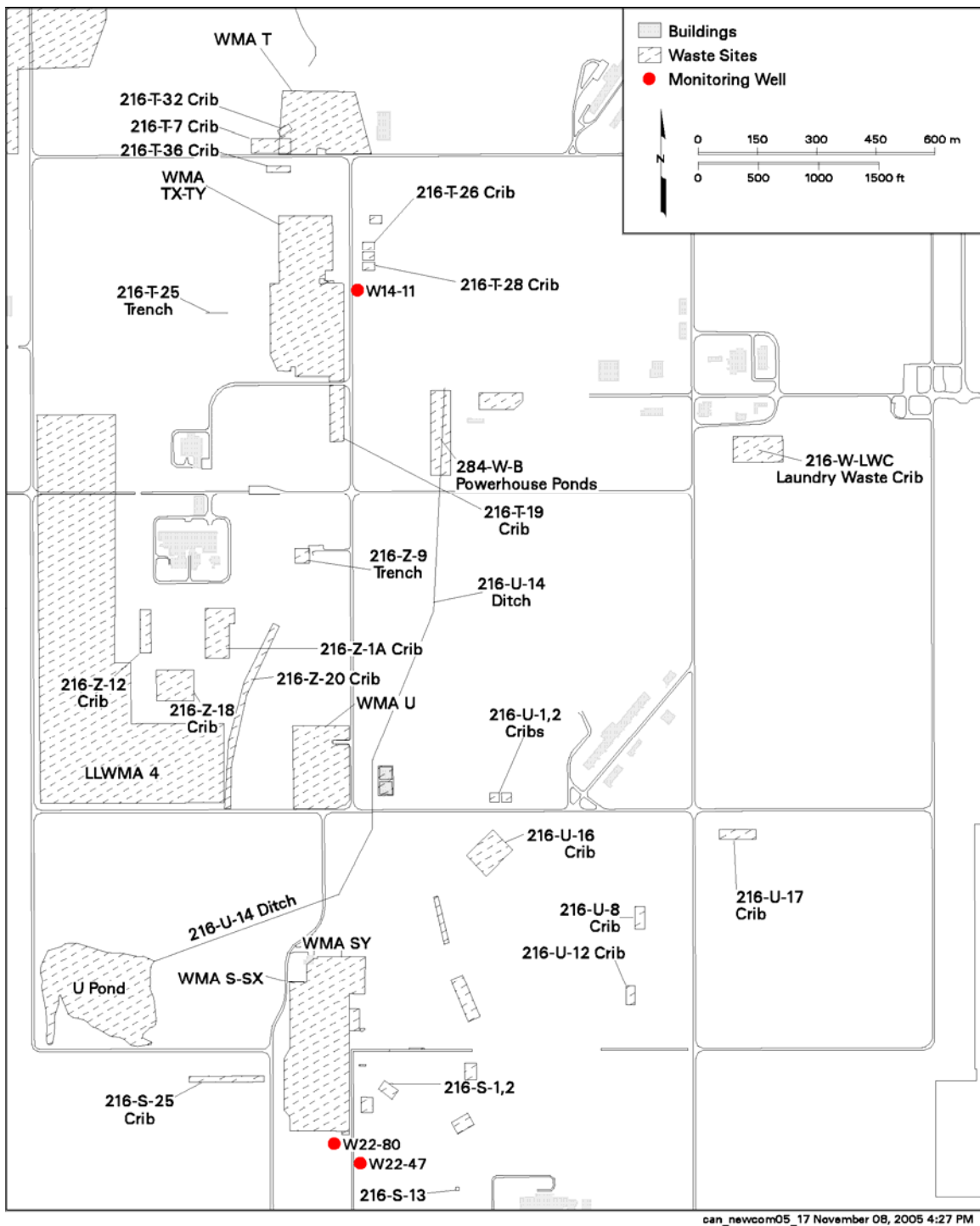


**Figure 8.1.** Map of 200-West Area Wells Surveyed with the Electromagnetic Borehole Flowmeter

**Table 8.1.** Summary of Ambient EBF Flowmeter Survey Results

Well	Measurement Date	Maximum Vertical Flow-Rate Range (L/min)	Maximum Vertical Flow Velocity Range (m/min)	Corresponding Depth <sup>(a)</sup> (m bgs)
299-W14-11	10/6/05	0.11 to 0.22 upward	0.014 to 0.027 (upward)	81.8 to 82.8
299-W22-47	10/7/05	0.04 to 0.09 upward	0.005 to 0.011 (upward)	72.4 to 74.4; 77.4 to 79.9
299-W22-80	9/23/05	0.23 to 0.35 upward	0.028 to 0.043 (upward)	66.7 to 71.6
(a) Corresponding depth where maximum vertical flow was measured.				

The profile of ambient vertical flow rate indicates measurable upward flow in the bottom 1 m of the screen interval and less than detectable flow in the upper 2 m of the screen interval (Figure 8.2, top). The maximum detectable upward flow rate ranged from 0.20 to 0.22 L/min, which was observed near the bottom of the well screen. The minimum detectable upward flow rate ranged from 0.11 to 0.13 L/min, which was measured at a depth of 1 m above the bottom of the well screen. These measured flow rates indicate equivalent upward in-well vertical flow velocities (i.e., within the 4-in. I.D. well screen) ranging from 0.014 to 0.027 m/min over the bottom 1-m well-screen interval. Vertical flow within the upper 2 m of the well screen was below the reported detection limit of the EBF flowmeter (i.e.,  $\geq 0.04$  L/min).

The calculated ambient differential lateral flow-rate profile is shown in Figure 8.2 (bottom). Positive differential lateral flow represents flow into the well while negative differential flow represents flow out of the well into the surrounding sandpack/formation. Examination of the figure indicates that the majority of lateral inflow to the well occurs near the bottom of the well-screen interval (i.e., between 82.7 and 82.8 m bgs) at a rate of 0.22 L/min. Above this depth interval, lateral flow exits the well screen over an ~1-m interval. The majority of flow exiting the well screen occurs at ~1 m above the bottom of the screen interval within the depth interval of 81.5 to 81.8 m bgs. As noted above, in-well flow measurements within the upper 2 m of the well screen were below the detection limit of the EBF flowmeter. Calculated differential lateral flow-rates indicated in the figure for this depth section, therefore, are not considered to be representative of actual *in situ* conditions.

### 8.1.2 Well 299-W22-47

An ambient flowmeter survey was performed in well 299-W22-47 on October 7, 2005. Well 299-W22-47 is completed with a 10.7-m (35-ft) long, 4-in. I.D. wire-wrap screen with two solid joints connecting three 3.05-m (10-ft) sections of screen. A third solid joint connects a 1.5-m (5-ft) section at the top of the well screen. The well-screen depth interval at well 299-W22-47 is 69.7 to 80.4 m bgs

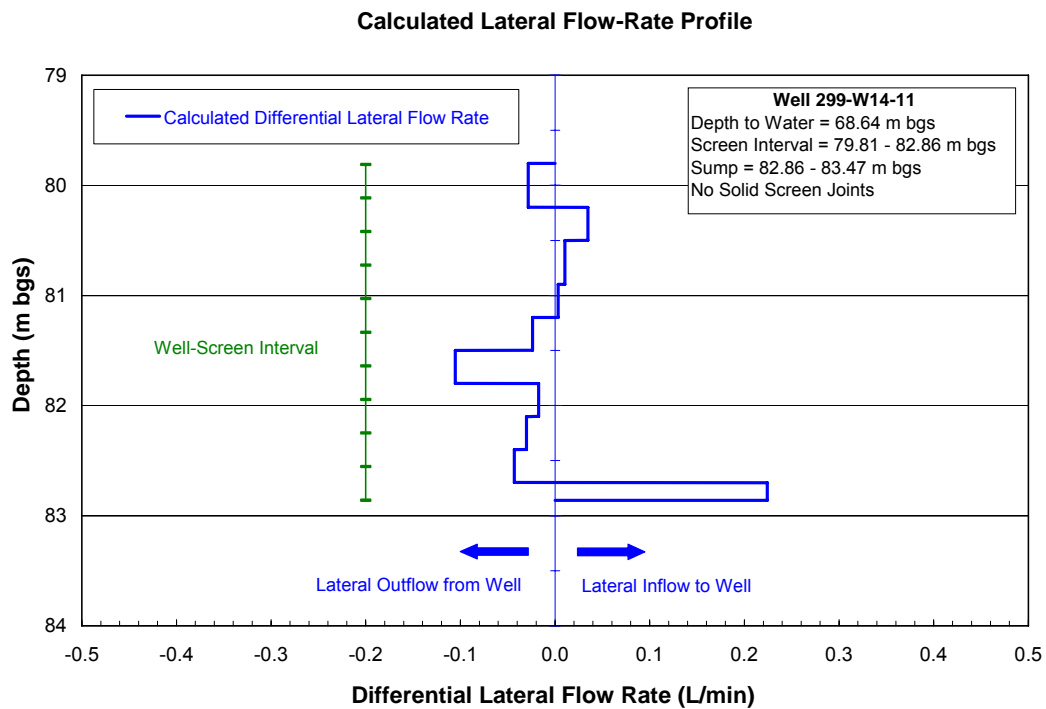
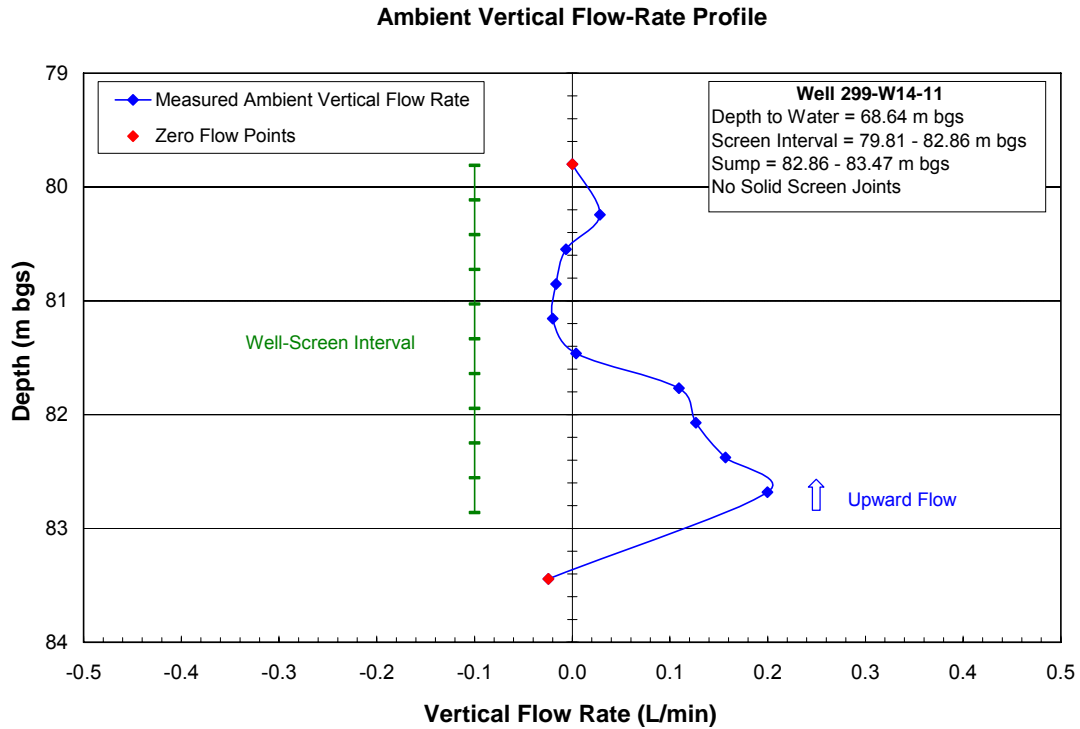


**Figure 8.2.** Well 299-W14-11 EBF Ambient Survey Results: Measured Vertical Flow-Rate Profile (top), and Calculated Differential Lateral Flow-Rate Profile (bottom)

(Table 1.2). A 0.6-m sump is attached to the bottom of the well screen. The measured static depth-to-water before beginning the flowmeter survey was 69.7 m bgs, which is at the top of the well-screen interval. The in-well vertical flow rate was measured every 0.6 m within the screen interval, beginning at a depth of 79.9 m bgs and ending at a depth of 70.1 m bgs. The vertical flow was also measured in the two upper solid joints at depths of 71.0 m and 74.1 m bgs. For EBF calibration purposes, points of zero flow were measured both within the sump at a depth of 80.6 m bgs and near the top of the water column at a depth of 69.9 m bgs.

The profile of ambient vertical flow rate indicates two measurable contributing intervals of upward flow within the saturated well-screen section (Figure 8.3, top). These zones of measurable flow, however, are at or near the minimum detectable level of the flowmeter (i.e., 0.04 L/min). Upward vertical flow rates ranged from 0.04 to 0.08 L/min near the bottom portion of the well screen (i.e., depth of 77.4 to 79.9 m bgs) and ranged from 0.04 to 0.09 L/min in the upper-section of the screened interval (i.e., depth of 72.6 to 74.4 m bgs). These measured flowrates correspond to an equivalent upward flow velocity range (i.e., in a 4-in. I.D. well screen) of 0.005 to 0.011 m/min over both depth intervals. Ambient vertical flow-rate measurements at all other depths ranged from less than detectable flow (i.e., <0.04 L/min) to 0.06 L/min upward flow. Because differences between the zero flow calibration points exhibit an uncertainty of 0.03 L/min, flow velocities over the remaining low-flow well-screen sections cannot be resolved with certainty. Ambient vertical flow-rate measurements at two of the screen solid joints (i.e., at depths of 71.0 and 74.1 m bgs) were consistent with the profile exhibited by the flow-rate measurements within the well screen. This correspondence in flow rates indicates that no significant vertical flow bypass occurred during the EBF survey (i.e., between the flowmeter inflatable packer and well screen).

The calculated ambient differential lateral flow-rate profile is shown in Figure 8.3 (bottom). A positive differential lateral flow represents flow into the well, while a negative differential flow represents flow out of the well into the surrounding sandpack/formation. Examination of the figure indicates that very little flow was entering or leaving the well over the well-screen interval. The calculated differential lateral flow indicates that in the lower portion of the well screen (i.e., between 76.2 and 80.1 m bgs), inflow enters the well at a flow rate ranging from 0.02 to 0.04 L/min, with the majority of the outflow from the well occurring at a flow rate of 0.03 L/min, occurring primarily within the middle to upper section of the screened interval (i.e., between 69.9 and 76.2 m bgs). As noted above, in-well flow measurements within the well screen were below the detection limit of the EBF flowmeter. The calculated differential lateral flow-rates indicated in the figure, therefore, are considered to be highly uncertain and should only be used for qualitative purposes.

### **8.1.3 Well 299-W22-80**

An ambient flowmeter survey was performed in well 299-W22-80 on September 23, 2005. Well 299-W22-80 is completed with a 10.7-m (35-ft) long, 4-in. I.D. wire-wrap screen with one solid joint connecting the bottom 4.6-m (15 ft) of the screen with the top 6.1-m (20 ft) of screen section. The well-screen depth interval at well 299-W22-80 is 62.5 to 73.2 m bgs (Table 1.2). A 0.6-m sump is attached to the bottom of the well screen. The measured static depth-to-water before beginning the flowmeter survey was 64.1 m bgs, which is below the top of the well-screen interval (saturated well-screen interval = 64.1

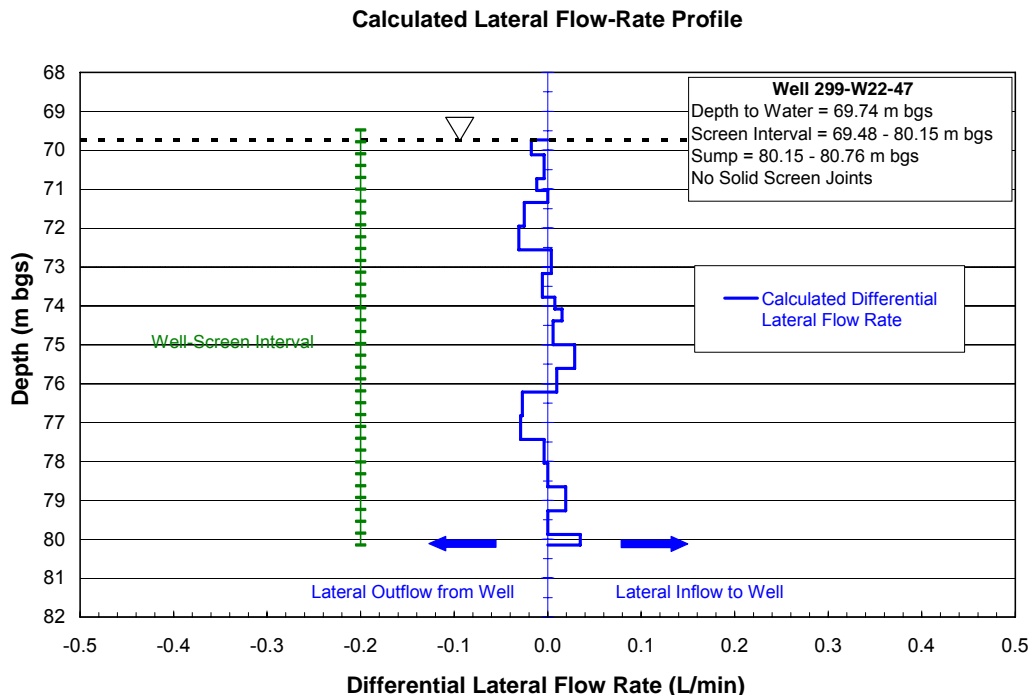
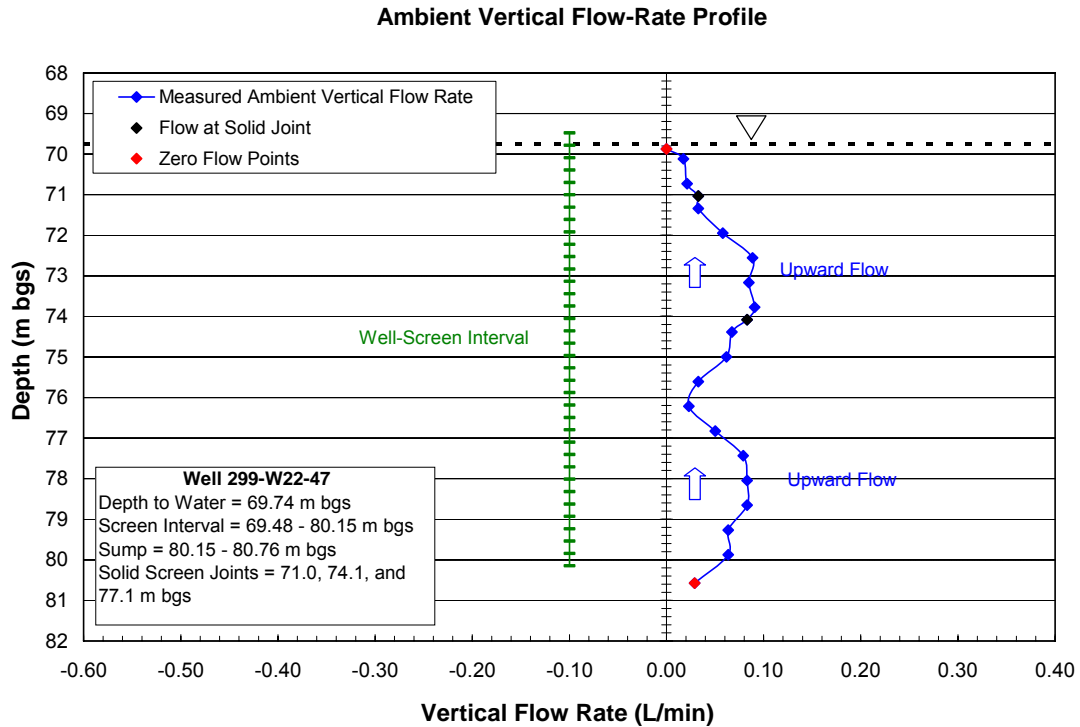


**Figure 8.3.** Well 299-W22-47 EBF Ambient Survey Results: Measured Vertical Flow-Rate Profile (top), and Calculated Differential Lateral Flow-Rate Profile (bottom)

to 73.2 m bgs). The in-well vertical flow rate was measured generally every 0.6 m within the screen interval, beginning at a depth of 71.6 m bgs and ending at a depth of 64.9 m bgs. A few measurements were also obtained at several 0.9 m spacings because of a difficulty in seating the inflatable flowmeter packer at a few depth settings. Vertical flow was also measured at the solid joint connection for the two well-screen sections at a depth of 67.9 m bgs. For EBF calibration purposes, points of zero flow were measured both within the sump vicinity at a depth of 73.0 m bgs and near the top of the water column at a depth of 64.2 m bgs.

The profile of ambient vertical flow rate indicates measurable upward flow over nearly the entire saturated well-screen section (Figure 8.4, top). The observed upward flow rate over the surveyed well-screen depth interval (66.7 to 71.6 m bgs) ranged from 0.23 to 0.35 L/min. Above 66.7 m bgs, upward flow decreased near the top of the saturated screen interval (i.e., at a depth of 64.9 to 66.1 m bgs) to a minimum of 0.04 L/min. These measured flow rates indicate equivalent upward in-well vertical flow velocities (i.e., in a 4-in. I.D. well screen) ranging from 0.005 to 0.043 m/min over the entire saturated screen interval, with a maximum flow-velocity range of 0.028 to 0.043 m/min occurring over the bottom ~2/3 of the saturated screen interval. Ambient vertical flow-rate measurements at the screen solid joint connection (i.e., at depth of 67.9 m bgs) were consistent with the profile exhibited by the flow-rate measurements within the well screen. This correspondence in flow rates indicates that no significant vertical flow bypass occurred during the EBF survey (i.e., between the flowmeter inflatable packer and well screen). It should be noted that the measured velocity range is nearly identical to the vertical flow velocities of 0.023 to 0.044 m/min calculated from an earlier tracer-dilution test conducted in well 299-W22-80 in 2001 (Spane et al. 2002). This indicates that the dominant upward vertical in-well flow is a persistent condition for this well-site location. For neighboring comparison purposes, it should also be recognized that a similar upward vertical flow pattern was exhibited at well 299-W22-47 (Chapter 8.1.2), which is located approximately 82 m southeast of well 299-0W22-47. However, the measured upward flow velocities for this well site were considerably lower as indicated in Table 8.1.

The calculated ambient differential lateral flow-rate profile for well 299-W22-80 is shown in Figure 8.4 (bottom). Positive differential lateral flow represents flow into the well, while negative differential flow represents flow out of the well into the surrounding sandpack/formation. Examination of the figure indicates that the majority of lateral inflow to the well occurs near the bottom of the well-screen interval (i.e., between 71.6 and 72.4 m bgs) at a rate of 0.35 L/min. Above this depth interval, lateral flow exits at the well screen over a broad interval, with the majority of flow exiting near the top of the screen interval between 64.2 and 66.7 m bgs.

## **8.2 Lateral Groundwater-Flow Conditions: Well 299-W22-47**

Table 8.2 lists results pertaining to the determination of groundwater-flow direction and hydraulic gradient conditions in the vicinity of well 299-W22-47 during the period of tracer test characterization. Groundwater-flow direction and hydraulic gradient were calculated using the commercially available WATER-VEL (In-Situ, Inc. 1991) software program. Water-level elevations from neighboring, representative wells were used as input to the WATER-VEL program to calculate groundwater-flow direction and hydraulic gradient conditions during the detailed characterization period. The program uses

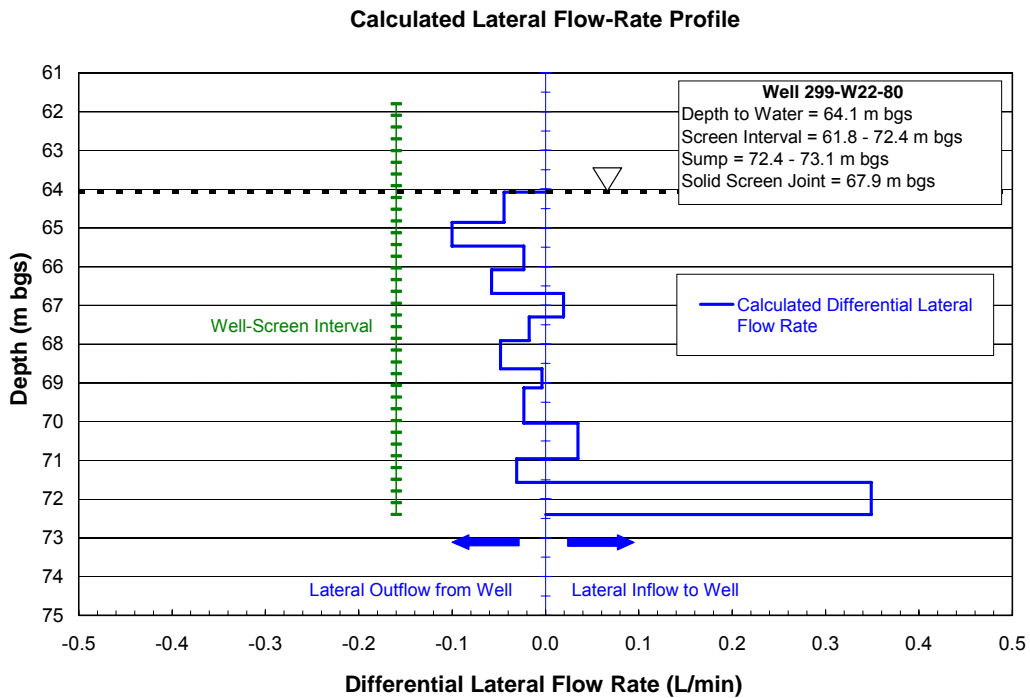
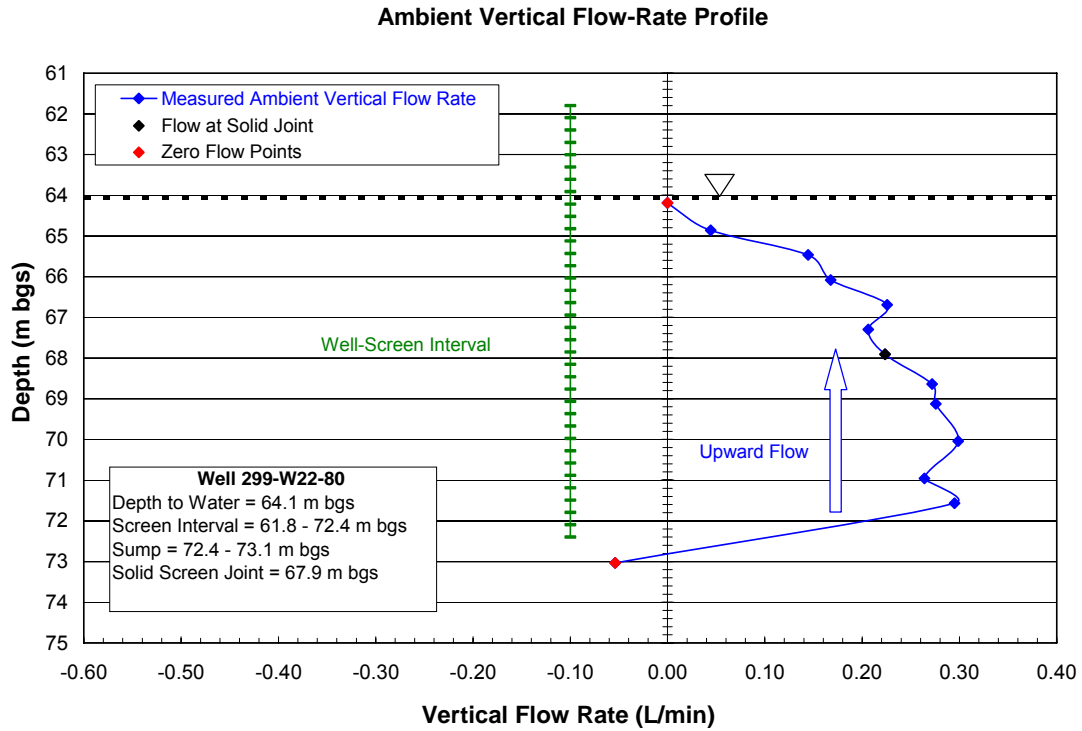


**Figure 8.4.** Well 299-W22-80 EBF Ambient Survey Results: Measured Vertical Flow-Rate Profile (top), and Calculated Differential Lateral Flow-Rate Profile (bottom)



a linear, two-dimensional trend surface (least squares) to randomly located hydraulic head or water-level elevation input data. This method is similar also to the linear approximation technique described by Abriola and Pinder (1982) and Kelly and Bogardi (1989). Reports that demonstrate the use of the WATER-VEL program to calculate groundwater-flow velocity and direction on the Hanford Site include Gilmore et al. (1992), Spane (1999), Spane et al. (2001a, 2001b, 2002, 2003), and Spane and Newcomer (2004).

**Table 8.2.** Groundwater-Flow Characterization Analysis Results

Well	Measurement Date	Groundwater-Flow Direction <sup>(a)</sup>	Hydraulic Gradient (m/m)	Wells Used in Analysis
299-W22-47	11/14/05	326°	0.00164	299-W22-46 299-W22-47 299-W22-49 299-W22-50
	11/16/05	325°	0.00166	299-W22-82 299-W22-83 299-W23-15
(a) 0 degrees East; 90 degrees North.				

The hydraulic gradient calculations listed in Table 8.2 were used to calculate the estimates of effective porosity and groundwater-flow velocity shown in Table 6.1. The indicated easterly and southeasterly groundwater-flow directions are consistent with generalizations presented in Hartman et al. (2006) for this area of the Hanford Site.

## 9.0 Conclusions

The detailed hydrologic characterization of the Hanford Site's unconfined aquifer system conducted during FY and CY 2005 included slug tests, a single-well tracer test (i.e., including tracer-dilution and tracer-pumpback), a constant-rate pumping test, and in-well vertical groundwater-flow surveys. Hydraulic property estimates obtained from the detailed tests include hydraulic conductivity, transmissivity, specific yield, effective porosity, in-well lateral and vertical groundwater-flow velocity, and aquifer groundwater-flow velocity. In addition, the characteristics of local groundwater flow (i.e., hydraulic gradient, flow direction) were determined for the general vicinity surrounding well 299-W22-47, which was the location for tracer test characterization.

### 9.1 Slug and Pumping Test Results

Slug-test results conducted within completed wells located near the top of the unconfined aquifer provided hydraulic conductivity estimates that ranged from 3.8 to 17.7 m/day for eight 200-West Area wells tested during FY and CY 2005. These tests are representative of the Ringold gravel Unit E. For general statistical comparison purposes, Figure 9.1 shows a summary histogram for hydraulic conductivity values based on 45 recent slug-test well characterizations (i.e.,  $\geq$ FY 1999) of the Ringold Formation within the 200-West Area, which is based on completed RCRA monitor-well tests (as reported in Spane et al. (2001a, 2001b, 2002, 2003) and Spane and Newcomer (2004)), slug-test characterizations performed in support of Hanford Site Comprehensive Environmental Response, Compensation, and Liability Act (CERCLA) well test investigations, and results presented in this report for slug tests conducted during FY and CY 2005. This summary data set is presented in Appendix B and is primarily reflective of conditions within the upper 10 m of the unconfined aquifer (i.e., Ringold Formation).

As indicated in Figure 9.1, estimates of hydraulic conductivity for these recent forty-five 200-West Area Ringold Formation well tests appear to conform to a log-normal distribution and range from 0.05 to 64.1 m/day, with a geometric mean of 3.43 m/day (note: based on type-curve slug-test analysis results). These estimates are surprisingly consistent with previously cited historical hydraulic conductivity values listed for this hydrogeologic unit in the 200-West Area (e.g., DOE/RL 1993; 200-West Area, 0.02 to 61 m/day) when water-table elevations within the unconfined aquifer were significantly higher (i.e.,  $\geq$ 3 m) than current hydrologic conditions. This close reported similarity in the hydraulic conductivity range suggests that the overlying (now de-saturated) Ringold Formation units may possess similar areal hydraulic property characteristics as currently exhibited by the current upper 10 m of the unconfined aquifer; although some local differences may exist (e.g., well 299-W22-80; Section 4.1.9).

Slug-test results for the one 200-East Area well tested during FY and CY 2005 provided an average hydraulic conductivity estimate for the Hanford formation of 96.9 m/day. This hydraulic conductivity estimate is consistent with previously reported (Spane et al. 2001a, 2001b, 2002, 2003; Spane and Newcomer 2004) high hydraulic conductivity values for the 200-East Area. As noted in Section 2.2, these high K estimate values are reflective of the preponderance of higher permeability gravel and sand units within the Hanford formation. It should also be noted that these earlier reported estimates for slug

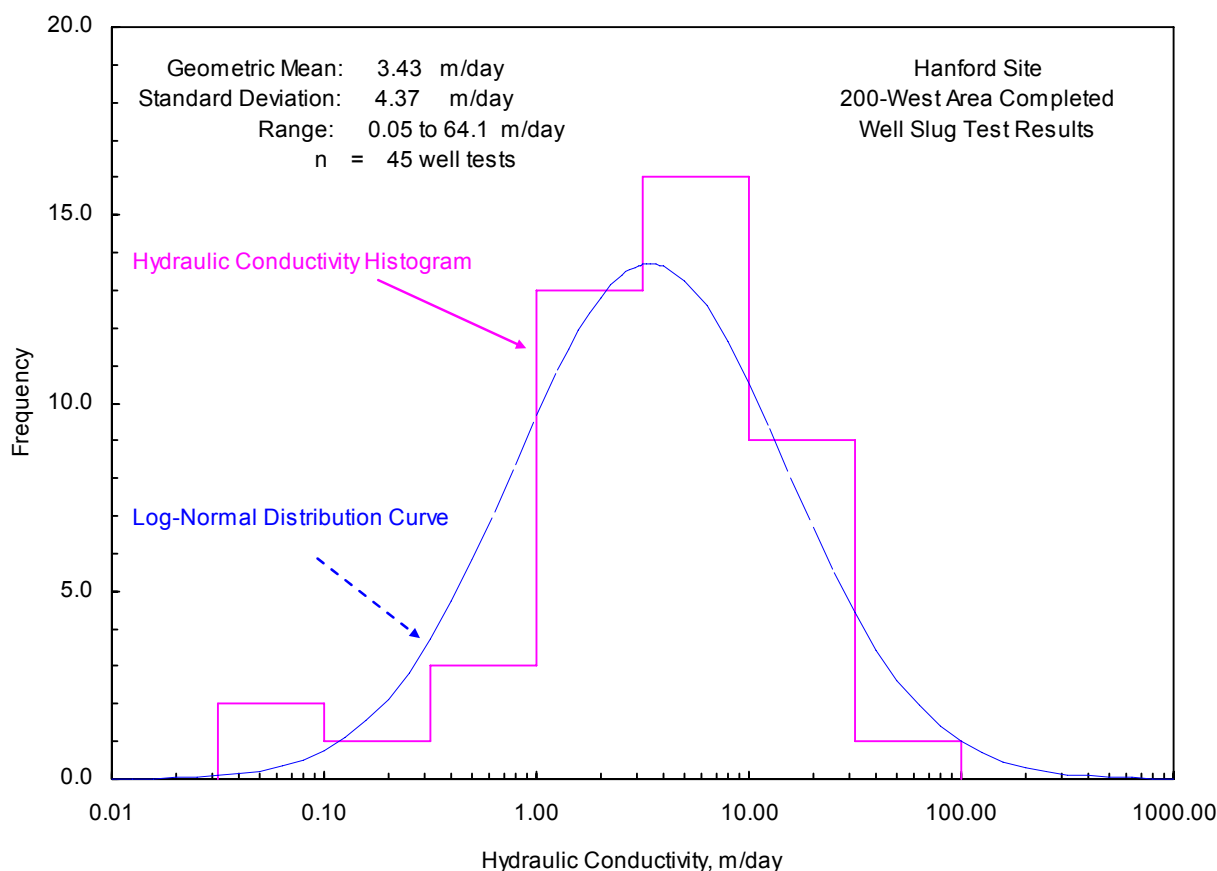


**Figure 9.1.** Hydraulic Conductivity Histogram for Recently Tested 200-West Area Wells

tests conducted in completed wells within the Hanford formation may actually underestimate the hydraulic conductivity for this highly permeable hydrogeologic unit. This is due to the requirement for pressure probe placement in proximity to the top of the well water column during slug testing, which was only recognized in more recent scientific publications (Section 3.1.2).

A comparison of the slug-test-derived hydraulic conductivity estimate at well 299-W22-47 (average type-curve analysis value;  $K = 17.3$  m/day) with the value obtained from the constant-rate pumping test ( $K = 16.5$  m/day) indicates a very close correspondence. This is well within previous, more extensive, comparisons between the two test methods (e.g., Spane et al. 2002). The general comparison relationship exhibited between slug- and pumping-test estimates also falls within the error range commonly reported for slug tests in aquifer characterization studies (i.e., within a factor of  $\sim 2$  or less [e.g. Butler 1996]).

Examination of selected depth-discrete slug-test characterization results for three 200-West Area locations (299-W11-25B, 299-W14-11, and 299-W22-47) indicate no distinct areal depth profile pattern for hydraulic conductivity that is consistent for all borehole sites. In most cases, a relatively uniform vertical distribution/depth profile was exhibited at each test location.

Analysis of the constant-rate pumping test results for well 299-W22-47 indicates a transmissivity and specific yield value of 1116 m<sup>2</sup>/day and 0.3, respectively. The specific yield estimate based on this well test, however, is considered to be less certain than the transmissivity estimate because of the relatively short duration (i.e., ~4-hr) for the pumping test (Chapter 7). Barometric response analysis of well water-level responses during a 21-day recovery period following termination of the pumping test indicated characteristic unconfined aquifer behavior, with a time-lag dependence reaching 110 hr. Removal of barometric pressure fluctuations from the observed drawdown and immediate recovery periods following termination of the pumping test did not significantly improve the pumping-test analysis. This is attributable, however, to the relatively small barometric pressure changes that occurred previous to, during, and immediately following the completion of the pumping test.

## 9.2 Single-Well Tracer Test Results

A detailed single-well tracer test was conducted at well 299-W22-47 for determining groundwater-flow velocity and effective porosity characteristics of the unconfined aquifer within this general area of the well-site location. The tracer test consisted of two components: a tracer-dilution/drift phase for determining in-well groundwater flow velocity conditions and the relative vertical distribution of hydraulic conductivity within the saturated well-screen section, and a tracer-pumpback component for determining the effective porosity and groundwater-flow velocity within the aquifer.

The tracer-dilution test results indicated an average in-well lateral groundwater-flow velocity ( $v_w = 0.13$  m/day) and a slight upward in-well vertical groundwater-flow condition that was evident in the tracer-dilution pattern. This upward, in-well groundwater-flow condition corroborates the earlier EBF survey results, which measured upward in-well flow velocities of 0.005 to 0.011 m/min (Section 8.1) for this Ringold Formation well-screen section. Results from the tracer-pumpback test provided estimates for effective porosity and aquifer groundwater-flow velocity of 0.294 and 0.093 m/day (~34 m/year), respectively. Because of the previously cited test site conditions and the fact that the calculated  $n_e$  and  $v_a$  values are reflective of a region ~0.2 m from the well (Chapter 6), these property values are considered to be only qualitative estimates.

Quantitative groundwater-flow characterization provided by trend-surface analysis of water-table elevation data for selected monitoring wells surrounding well 299-W22-47 provided groundwater-flow direction and hydraulic gradient information during the tracer-dilution monitoring period. The trend-surface analysis results indicated a consistent east-southeasterly groundwater-flow direction and a hydraulic gradient of 0.00165 m/m (Section 8.2). These groundwater-flow characteristics are consistent with conditions reported by Hartman et al. (2006) for this general area of the Hanford Site.

## 10.0 References

- Abriola LM and GF Pinder. 1982. "Calculation of velocity in three space dimensions from hydraulic head measurements." *Ground Water* 20(2):205-213.
- Bourdet DJ, A Ayoub, and YM Pirard. 1989. "Use of pressure derivative in well-test interpretation." *SPE Formation Evaluation* June 1989:293-302.
- Bouwer H. 1989. "The Bouwer and Rice slug test – an update." *Ground Water* 27(3):304-309.
- Bouwer H. 1996. "Discussion of Bouwer and Rice slug test review articles." *Ground Water* 34(1):171.
- Bouwer H, and RC Rice. 1976. "A slug test for determining hydraulic conductivity of unconfined aquifers with completely or partially penetrating wells." *Water Resources Research* 12(3):423-428.
- Brown DL, TN Narasimhan, and Z Demir. 1995. "An evaluation of the Bouwer and Rice method of slug test analysis." *Water Resources Research* 31(5):1239-1246.
- Butler JJ, Jr. 1990. "The role of pumping tests in site characterization: some theoretical considerations." *Ground Water* 28(3):394-402.
- Butler JJ, Jr. 1996. "Slug tests in site characterization: some practical considerations." *Environmental Geosciences* 3(3):154-163.
- Butler JJ, Jr. 1998. *The design, performance, and analysis of slug tests*. Lewis Publishers, CRC Press, Boca Raton, Florida.
- Butler, JJ, Jr. and EJ Garnett. 2000. *Simple procedures for analysis of slug tests in formations of high hydraulic conductivity using spreadsheet and Scientific Graphics Software*. Open-file Report 2000-40, Kansas Geological Survey, Lawrence, Kansas.
- Butler, JJ, Jr., GC Bohling, ZH Hyder, and CD McElwee. 1994. "The use of slug tests to describe vertical variations in hydraulic conductivity." *Journal of Hydrology* 156:137-162
- Butler JJ, CD McElwee, and W Liu. 1996. "Improving the quality of parameter estimates obtained from slug tests." *Ground Water* 34(3):480-490.
- Butler, JJ, Jr., EJ Garnett, and JM Healey. 2003. "Analysis of slug tests in formations of high hydraulic conductivity." *Ground Water* 41(5):620-630.
- Chen, C-S, and C-R Wu. 2006. "Analysis of depth-dependent pressure head of slug tests in highly permeable aquifers." *Ground Water* 44(3):472-482.

Church, PE and GE Granato. 1996. "Bias in ground-water data caused by well-bore flow in long-screen wells." *Ground Water* 34(2): 262-273.

Cole, C. R., M. P. Bergeron, C. J. Murray, P. D. Thorne, S. K. Wurstner, P. Rogers. 2001. *Uncertainty analysis framework Hanfords site-wide groundwater flow and transport model*. PNNL-13641, Pacific Northwest National Laboratory, Richland, Washington.

Connelly MP, JV Borghese, CD Delaney, BH Ford, JW Lindberg, and SJ Trent. 1992a. *Hydrogeologic model for the 200-East groundwater aggregate area*. WHC-SD-EN-TI-019, Rev. 0, Westinghouse Hanford Company, Richland, Washington.

Connelly MP, BH Ford, and JV Borghese. 1992b. *Hydrogeologic model for the 200-West groundwater aggregate area*. WHC-SD-EN-TI-014, Rev. 0, Westinghouse Hanford Company, Richland, Washington.

Cooper HH, Jr., and CE Jacob. 1946. "A generalized graphical method for evaluating formation constants and summarizing well-field history." *American Geophysical Union, Transactions* 27(4):526-534.

DOE/RL (see U.S. Department of Energy)

Drost W, D Klotz, A Koch, H Moser, F Neumaier, and W Rauert. 1968. "Point dilution methods of investigating groundwater flow by means of radioisotopes." *Water Resources Research* 4(1):125-146.

Elci A, FJ Molz III, and WR Waldrop. 2001. "Implications of observed and simulated ambient flow in monitoring wells." *Ground Water* 39(6):853-862.

Freeze RA and JA Cherry. 1979. *Groundwater*. Prentice-Hall, Englewood Cliffs, New Jersey.

Gephart RE, FA Spane, LS Leonhart, DA Palombo, and SR Strait. 1979. "Pasco Basin hydrology." In *Hydrologic studies within the Columbia plateau, Washington: An integration of current knowledge*, pp. III-1 to III-236. RHO-BWI-ST-5, Rockwell Hanford Operations, Richland, Washington.

Gilmore TJ, DR Newcomer, SK Wurstner, and FA Spane, Jr. 1992. *Calculation of groundwater discharge to the Columbia River in the 100-N area*. PNL-8057, Pacific Northwest Laboratory, Richland, Washington.

Graham MJ, GV Last, and KR Fecht. 1984. *An assessment of aquifer intercommunication in the B-Pond-Gable Mountain Pond area of the Hanford site*. RHO-RE-ST-12P, Rockwell Hanford Operations, Richland, Washington.

Güven O, RW Falta, FJ Molz, and JG Melville. 1985. "Analysis interpretation of single-well tracer tests in stratified aquifers." *Water Resources Research* 21(5):676-684.

Guyonnet D, S Mishra, and J McCord. 1993. "Evaluating the volume of porous medium investigated during slug tests." *Ground Water* 31(4):627-633.

- Halevy E, H Moser, O Zellhofer, and A Zuber. 1966. "Borehole dilution techniques – a critical review." In *Isotopes in Hydrology*, International Atomic Energy Agency, Vienna, Austria.
- Hall SH. 1993. "Single well tracer tests in aquifer characterization." *Ground Water Monitoring & Review* 13(2):118-124.
- Hall SH, SP Luttrell, and WE Cronin. 1991. "A method for estimating effective porosity and ground-water velocity." *Ground Water* 29(2):171-174.
- Hantush MS. 1964. "Hydraulics of wells." *Advances in Hydroscience* (VT Chow, ed) 1:282-433, Academic Press, New York.
- Hartman MJ, LF Morasch, and WD Webber (eds.). 2006. *Hanford Site groundwater monitoring for fiscal year 2005*. PNNL-15670, Pacific Northwest National Laboratory, Richland, Washington.
- Hyder Z and JJ. Butler, Jr. 1995. "Slug tests in unconfined formations: An assessment of the Bouwer and Rice technique." *Ground Water* 33(1):16-22.
- In-Situ Inc. 1991. *WATER-VEL<sup>TM</sup> Groundwater Velocity*. ISI-GWV-2.21-1, Laramie, Wyoming.
- Jacob, CE. 1963. "Determining the permeability of water-table aquifers." In *Methods of Determining Permeability, Transmissibility, and Drawdown*, U.S. Geological Survey, Water-Supply Paper 1536-I:245-271.
- Karasaki K, JCS Long, and PA Witherspoon. 1988. "Analytical Models of Slug Tests." *Water Resources Research* 24(1):115-126.
- Kearl PM, JJ Dexter, and JE Price. 1988. *Procedures, analysis, and comparison of groundwater velocity measurement methods for unconfined aquifers*. UNC/GJ-TMC-3, UNC Geotech, Grand Junction, Colorado.
- Kelly WE, and I Bogardi. 1989. "Flow directions with a spreadsheet." *Ground Water – Computer Notes* 27(2):245-247.
- Leap DI, and PG Kaplan. 1988. "A single-well tracing method for estimating regional advective velocity in a confined aquifer: Theory and preliminary laboratory verification." *Water Resources Research* 24(7):993-998.
- Lindsey KA. 1995. *Miocene- to Pliocene-aged suprabasalt sediments of the Hanford Site, south-central Washington*. BHI-00184, Bechtel Hanford Inc., Richland, Washington.
- Lindsey KA, BN Bjornstad, JW Lindberg, and KM Hoffman. 1992. *Geologic setting of the 200-East area: An update*. WHC-SD-EN-TI-012, Rev. 0, Westinghouse Hanford Company, Richland, Washington.

- Liu WZ, and JJ Butler, Jr. 1995. *The KGS model for slug tests in partially penetrating wells (Version 3.0)*. Kansas Geological Survey Computer Series Report 95-1, Lawrence, Kansas.
- McElwee CD. 2001. "Application of a nonlinear slug test model." *Ground Water* 39(5):737-744.
- McElwee CD, and MA Zenner. 1998. "A nonlinear model for analysis of slug-test data." *Water Resources Research* 34(1):55-66.
- Moench AF. 1997. "Flow to a well of finite diameter in a homogeneous, anisotropic water-table aquifer." *Water Resources Research* 33(6):1397-1407.
- Moench AF, and PA Hsieh. 1985. "Analysis of slug test data in a well with finite-thickness skin." In *Memoirs Hydrogeology of Rocks of Low Permeability, January 7-12, 1985, Tucson, Arizona*; International Association of Hydrogeologists 17(1):17-29.
- Molz FJ, JG Melville, O Güven, RD Crocker, and KT Matteson. 1985. "Design and performance of single-well tracer tests at the Mobile site." *Water Resources Research* 21(10):1497-1502.
- Neuman SP. 1972. "Theory of flow in unconfined aquifers considering delayed response of the water table." *Water Resources Research* 8(4):1031-1045.
- Neuman SP. 1974. "Effect of partial penetration on flow in unconfined aquifer considering delayed gravity response." *Water Resources Research* 10(2):303-312.
- Neuman SP. 1975. "Analysis of pumping test data from anisotropic unconfined aquifers considering delayed gravity response." *Water Resources Research* 11(2):329-342.
- Novakowski KS. 1989. "Analysis of pulse interference tests." *Water Resources Research* 25(11):2377-2387.
- Pickens JF, and GE Grisak. 1981. "Scale-dependent dispersion in a stratified granular aquifer." *Water Resources Research* 17(4):1191-1211.
- Rasmussen TC, and LA Crawford. 1997. "Identifying and removing barometric pressure effects in confined and unconfined aquifers." *Ground Water* 35(3):502-511.
- Reidel SP, and MA Chamness. 2007. *Geology Data Package for the Single-Shell Tank Waste Management Areas at the Hanford Site*. PNNL-15955 Rev. 1, Pacific Northwest National Laboratory, Richland, Washington.
- Reilly TE, OL Franke, and GD Bennett. 1989. "Bias in groundwater samples caused by wellbore flow." *Journal of Hydraulic Engineering* 115(2):270-276.
- Resource Conservation and Recovery Act of 1976*, as amended, Public Law 94-580, 90 Stat. 2795, 42 USC 6901 et seq.



Spane FA, Jr. 1993. *Selected hydraulic test analysis techniques for constant-rate discharge tests*. PNL-8539, Pacific Northwest Laboratory, Richland, Washington.

Spane FA, Jr. 1996. "Applicability of slug interference tests for hydraulic characterization of unconfined aquifer: (1) Analytical assessment." *Ground Water* 34(1):66-74.

Spane FA, Jr. 1999. *Effects of barometric fluctuations on well water-level measurements and aquifer test data*. PNNL-13078, Pacific Northwest National Laboratory, Richland, Washington.

Spane FA, Jr. 2002. "Considering barometric pressure in groundwater flow investigations." *Water Resources Research* 38(6), 14:1-18.

Spane FA, and DR Newcomer. 2004. *Results of detailed hydrologic characterization tests – FY 2003*. PNNL-14186, Pacific Northwest National Laboratory, Richland, Washington.

Spane FA, Jr. and WD Webber. 1995. *Hydrochemistry and hydrogeologic conditions within the Hanford Site upper basalt confined aquifer system*. PNL-10817, Pacific Northwest Laboratory, Richland, Washington.

Spane FA, Jr. and SK Wurstner. 1993. "DERIV: A program for calculating pressure derivatives for use in hydraulic test analysis." *Ground Water* 31(5):814-822.

Spane FA, Jr., PD Thorne, and LC Swanson. 1996. "Applicability of slug interference tests for hydraulic characterization of unconfined aquifer: (2) Field test examples." *Ground Water* 34(5):925-933.

Spane FA, Jr., PD Thorne, and DR Newcomer. 2001a. *Results of detailed hydrologic characterization tests – fiscal year 1999*. PNNL-13378, Pacific Northwest National Laboratory, Richland, Washington.

Spane FA, Jr., PD Thorne, and DR Newcomer. 2001b. *Results of detailed hydrologic characterization tests – fiscal year 2000*. PNNL-13514, Pacific Northwest National Laboratory, Richland, Washington.

Spane FA, Jr., PD Thorne, and DR Newcomer. 2002. *Results of detailed hydrologic characterization tests – fiscal year 2001*. PNNL-14113, Pacific Northwest National Laboratory, Richland, Washington.

Spane, FA, Jr., P.D. Thorne, and D.R. Newcomer. 2003. *Results of detailed hydrologic characterization tests – FY 2002*. PNNL-14186. Pacific Northwest National Laboratory, Richland, Washington

Springer RK, and LW Gelhar. 1991. "Characterization of large-scale aquifer heterogeneity in glacial outwash by analysis of slug tests with oscillatory response, Cape Cod, Massachusetts." In *U.S. Geological Survey Water Resources Investigations*. Report 91-4034:36-40.

Theis CV. 1935. "The relationship between the lowering of the piezometric surface and the rate and duration of discharge of a well using ground-water storage." *American Geophysical Union, Transactions*, 2:519-524; reprinted in Society of Petroleum Engineers, "Pressure Transient Testing Methods", SPE Reprint Series (14):27-32, Dallas, Texas.

Thorne PD, MA Chamness, FA Spane, Jr., VR Vermeul, and WD Webber. 1993. *Three-dimensional conceptual model for the Hanford Site unconfined aquifer system, FY 93 status report*. PNL-8971, Pacific Northwest Laboratory, Richland, Washington.

U.S. Department of Energy, Richland Operations Office, Richland, Washington (DOE/RL). 1993. *200 West groundwater aggregate area management study report*. DOE/RL-92-16, Rev. 0, Richland, Washington.

Waldrop WR, and HS Pearson. 2000. *Results of field tests with the electromagnetic borehole flowmeter at the Pacific Northwest National Laboratory, Richland, Washington*. QEC-T-132, Quantum Engineering Corporation, Loudon, Tennessee.

Williams BA, BN Bjornstad, R Schalla, and WD Webber. 2000. *Revised hydrogeology for the suprabasalt aquifer system, 200-East area and vicinity, Hanford Site, Washington*. PNNL-12261, Pacific Northwest National Laboratory, Richland, Washington.

Young, SC, HE Julian, HS Pearson, FJ Molz, and GK Boman. 1998. *Application of the Electromagnetic Borehole Flowmeter*. U.S. Environmental Protection Agency Research Report EPA/600/R-98/058, Ada, Oklahoma.

Zurbuchen BR, VA Zlotnik, and JJ Butler, Jr. 2002. "Dynamic interpretation of slug tests in highly permeable aquifers." *Water Resources Research* 38(3), 7:1-18.

## **Appendix A**

### **Selected Analysis Figures for Test/Depth Intervals: Boreholes 299-W11-25B, 299-W14-11, and 299-W22-47**

- A.1     Selected Slug-Test Analysis Plots for 299-W11-25B: Zone 1**
- A.2     Selected Slug-Test Analysis Plots for 299-W11-25B: Zone 2**
- A.3     Selected Slug-Test Analysis Plots for 299-W11-25B: Zone 3**
- A.4     Selected Slug-Test Analysis Plots for 299-W11-25B: Zone 4 - Inner Zone**
- A.5     Selected Slug-Test Analysis Plots for 299-W11-25B: Zone 4 - Outer Zone**
- A.6     Selected Slug-Test Analysis Plots for 299-W14-11: Zone 1 - Inner Zone**
- A.7     Selected Slug-Test Analysis Plots for 299-W14-11: Zone 1 - Outer Zone**
- A.8     Selected Slug-Test Analysis Plots for 299-W14-11: Zone 2 - Inner Zone**
- A.9     Selected Slug-Test Analysis Plots for 299-W14-11: Zone 2 - Outer Zone**
- A.10    Selected Slug-Test Analysis Plots for 299-W14-11: Zone 3**
- A.11    Selected Slug-Test Analysis Plots for 299-W14-11: Zone 4**
- A.12    Selected Slug-Test Analysis Plots for 299-W14-11: Zone 5**
- A.13    Selected Slug-Test Analysis Plots for 299-W22-47: Zone 1**
- A.14    Selected Slug-Test Analysis Plots for 299-W22-47: Zone 2**
- A.15    Selected Slug-Test Analysis Plots for 299-W22-47: Zone 3**
- A.16    Selected Slug-Test Analysis Plots for 299-W22-47: Zone 4**

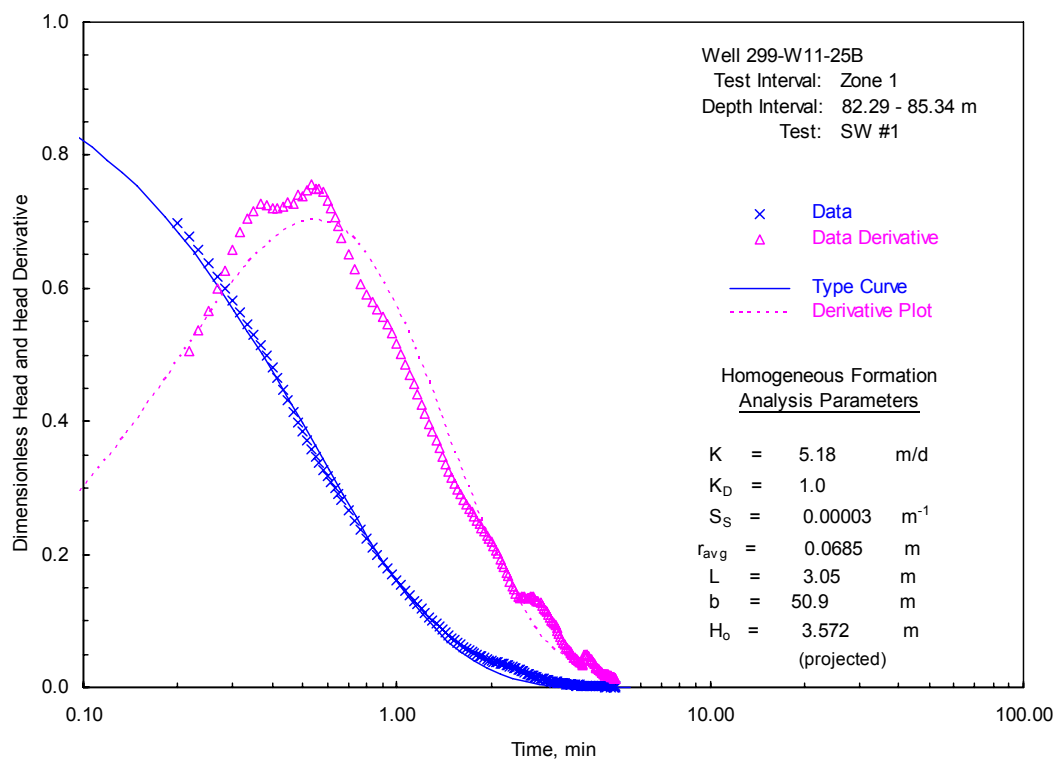
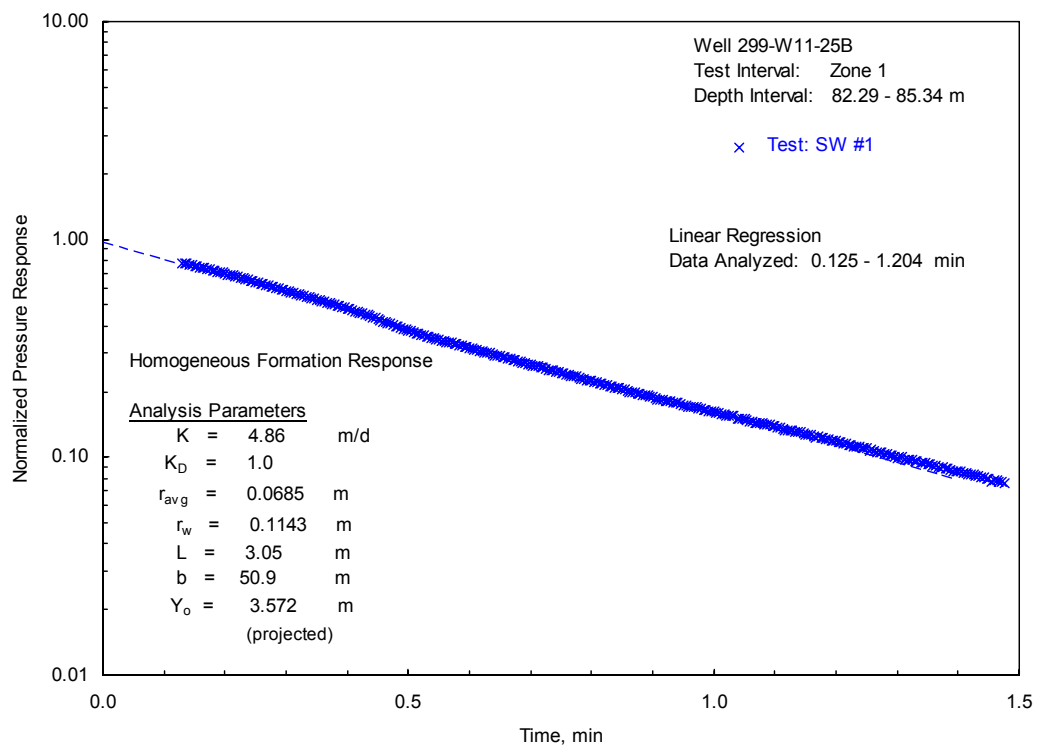


**Figure A.1.** Selected Slug-Test Analysis Plots for 299-W11-25B; Zone 1 (Bouwer and Rice method [top] and type-curve method [bottom])

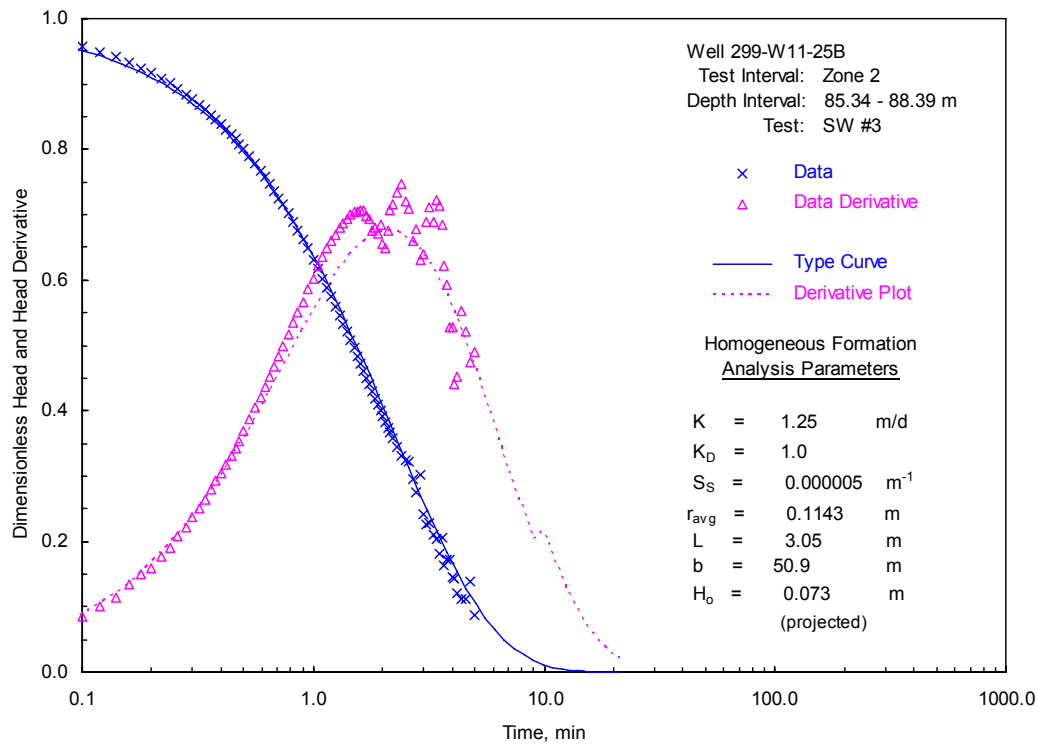
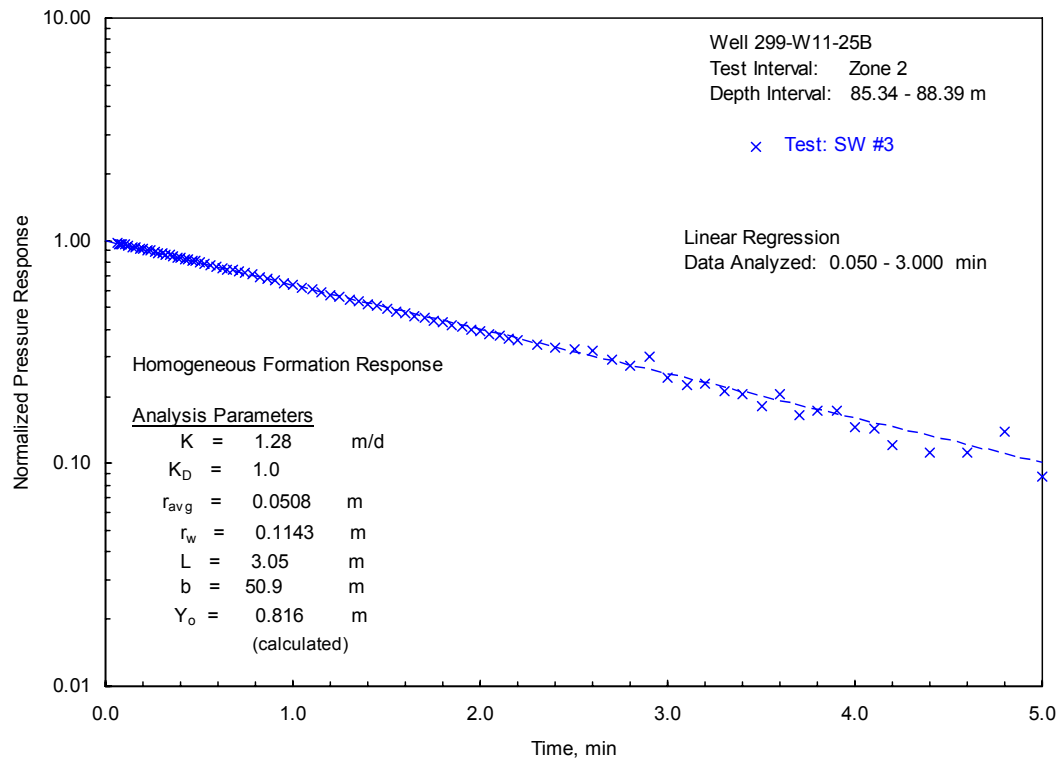


**Figure A.2.** Selected Slug-Test Analysis Plots for 299-W11-25B; Zone 2 (Bouwer and Rice method [top] and type-curve method [bottom])

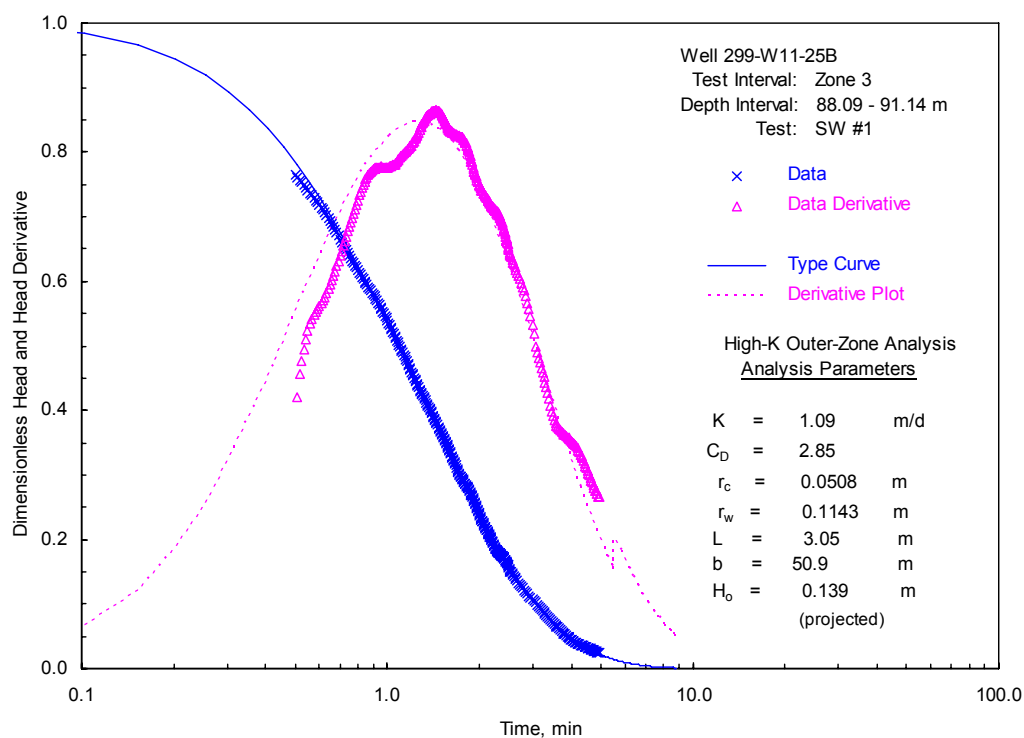
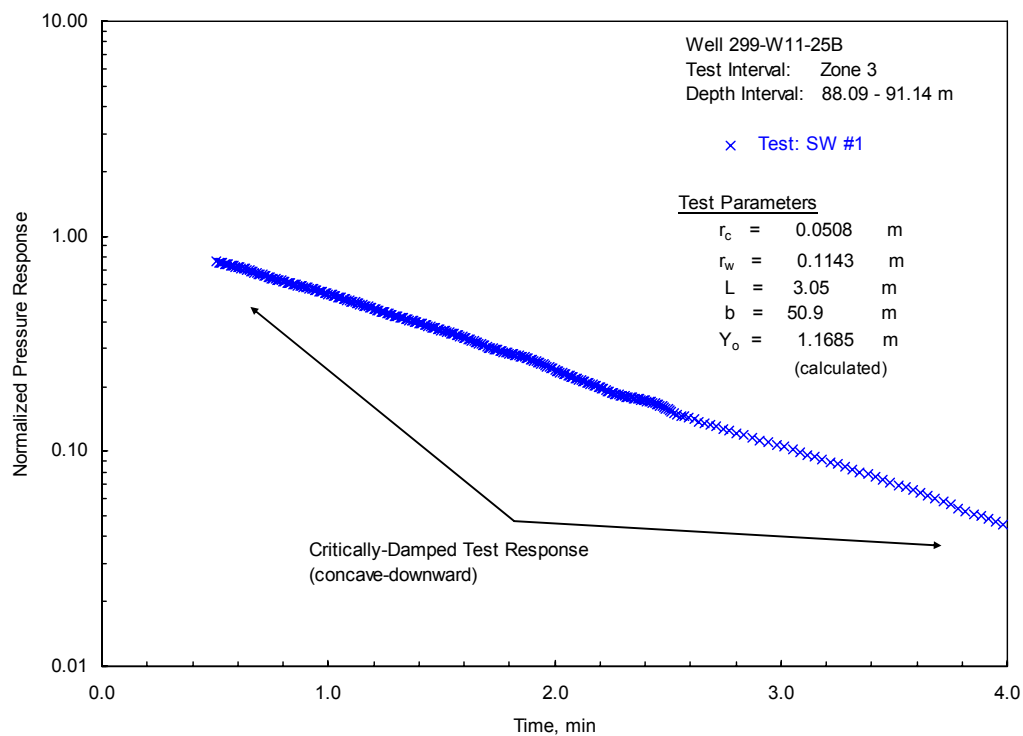


**Figure A.3.** Selected Slug-Test Analysis Plots for 299-W11-25B; Zone 3 (Bouwer and Rice method [top] and type-curve method [bottom])

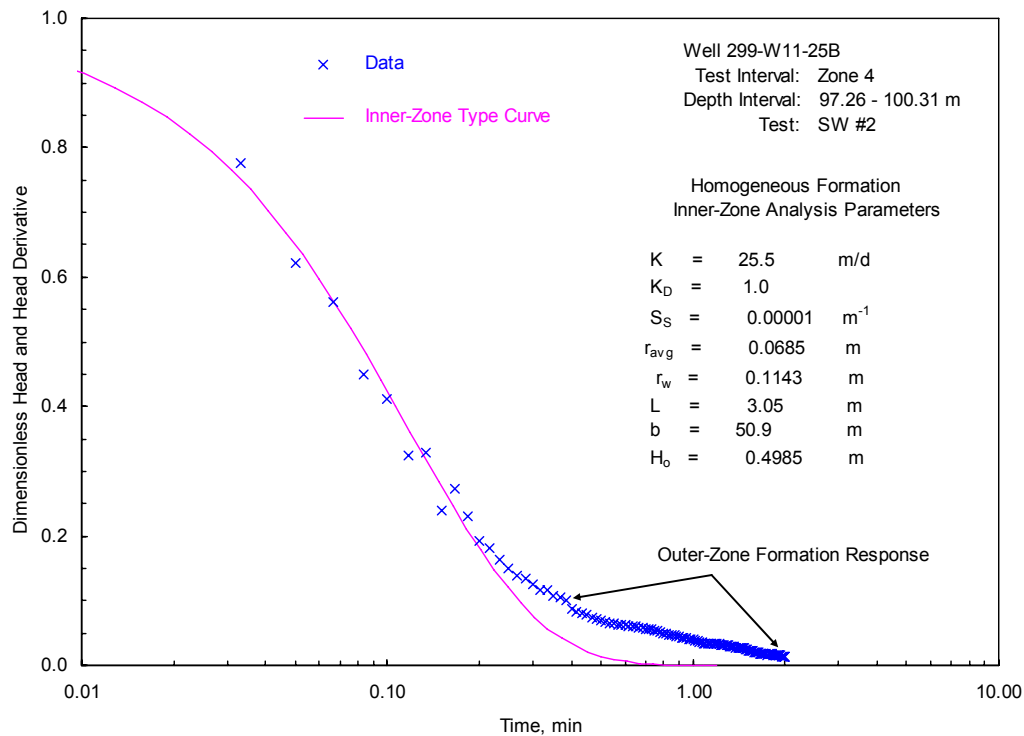
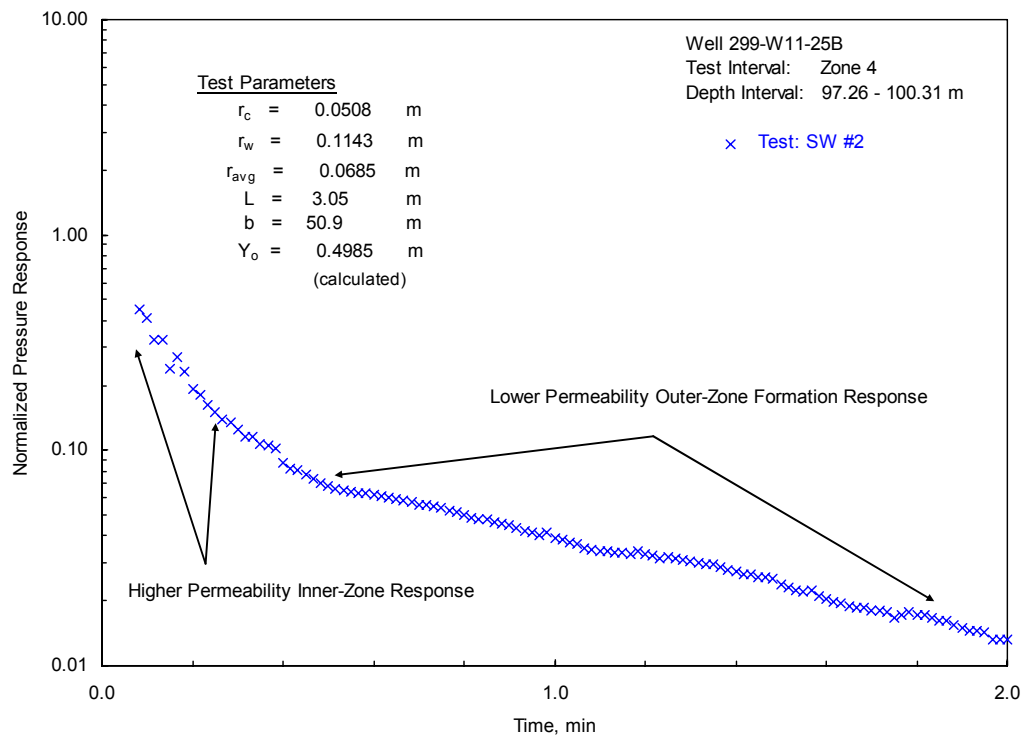


**Figure A.4.** Selected Slug-Test Analysis Plots for 299-W11-25B; Zone 4—Inner-Zone (Bouwer and Rice method [top] and type-curve method [bottom])

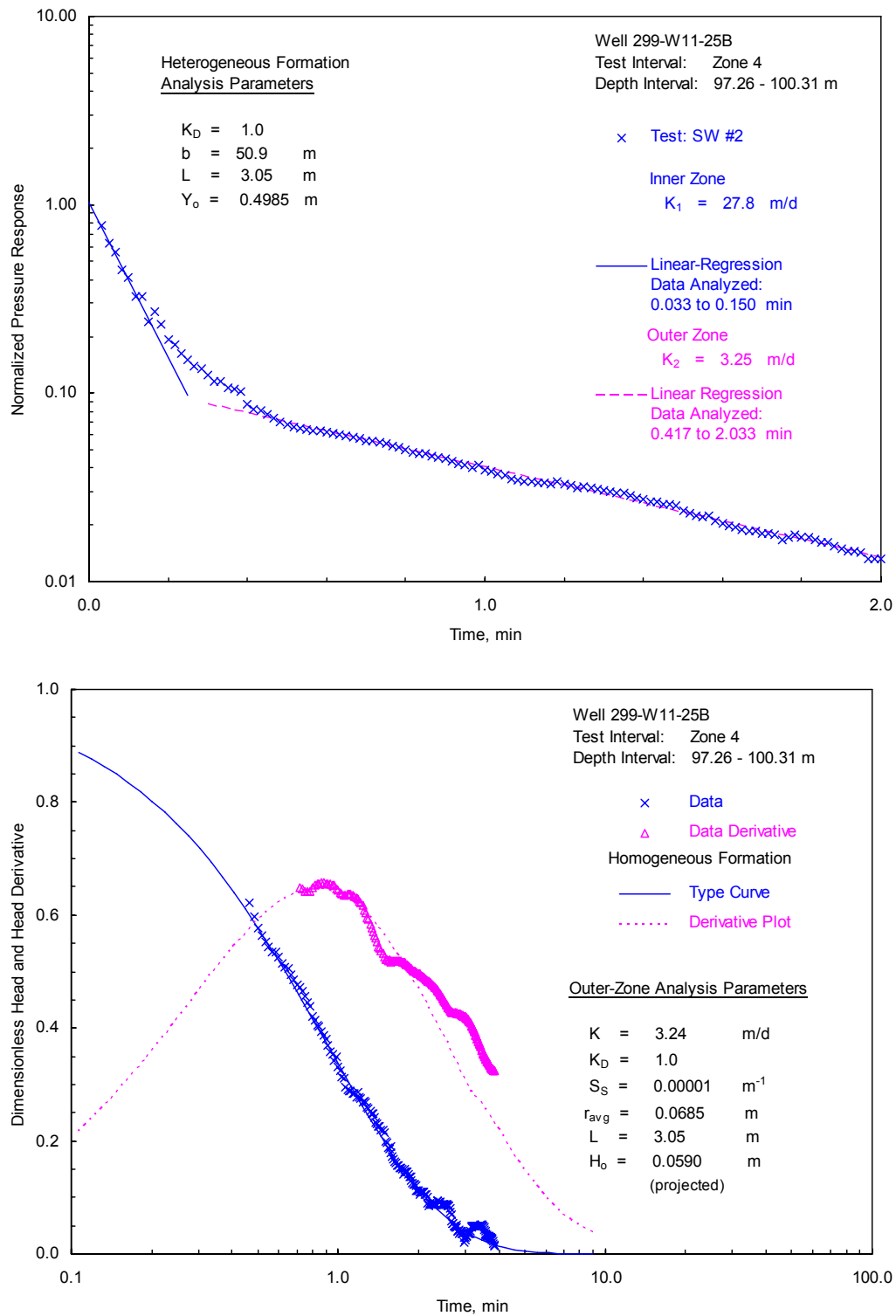


**Figure A.5.** Selected Slug-Test Analysis Plots for 299-W11-25B; Zone 4—Outer-Zone (Bouwer and Rice method [top] and type-curve method [bottom])



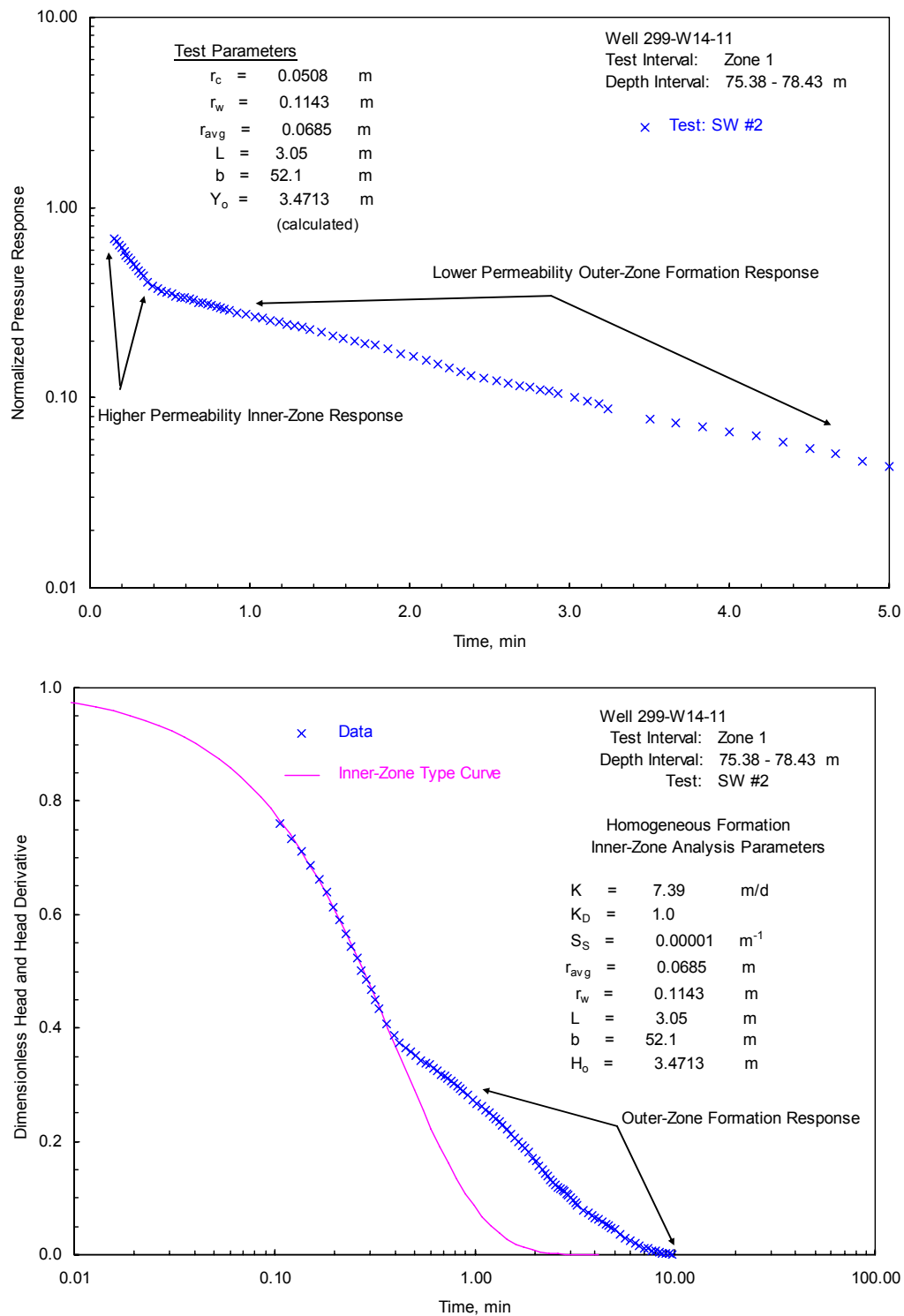


**Figure A.6.** Selected Slug-Test Analysis Plots for 299-W14-11; Zone 1—Inner Zone (Bouwer and Rice method [top] and type-curve method [bottom])

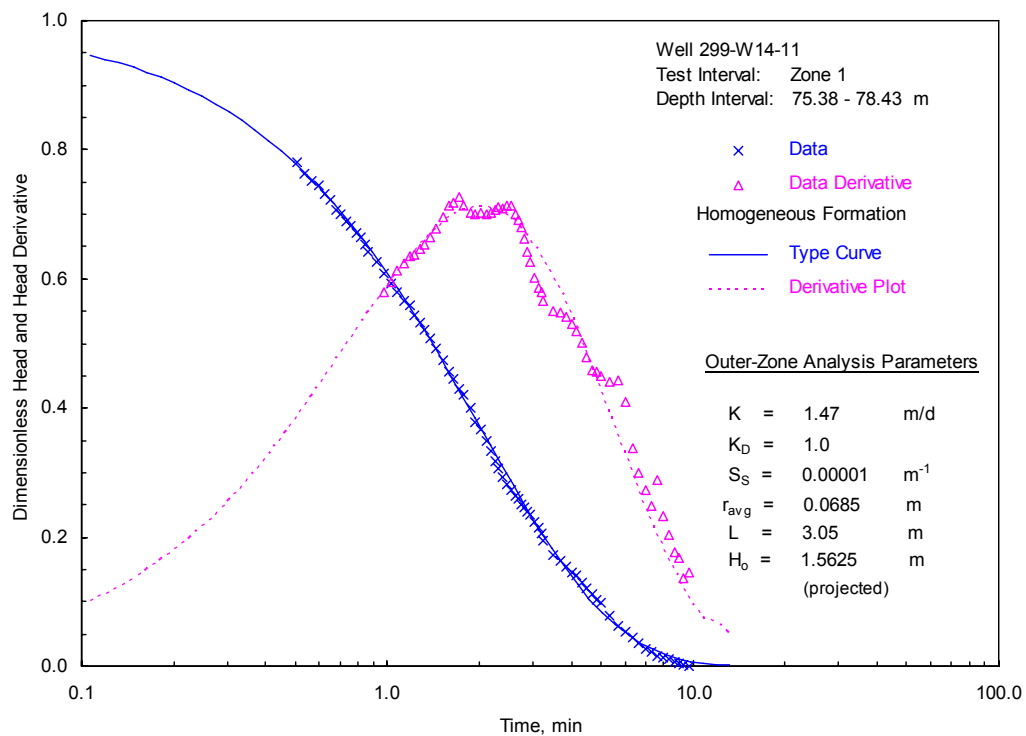
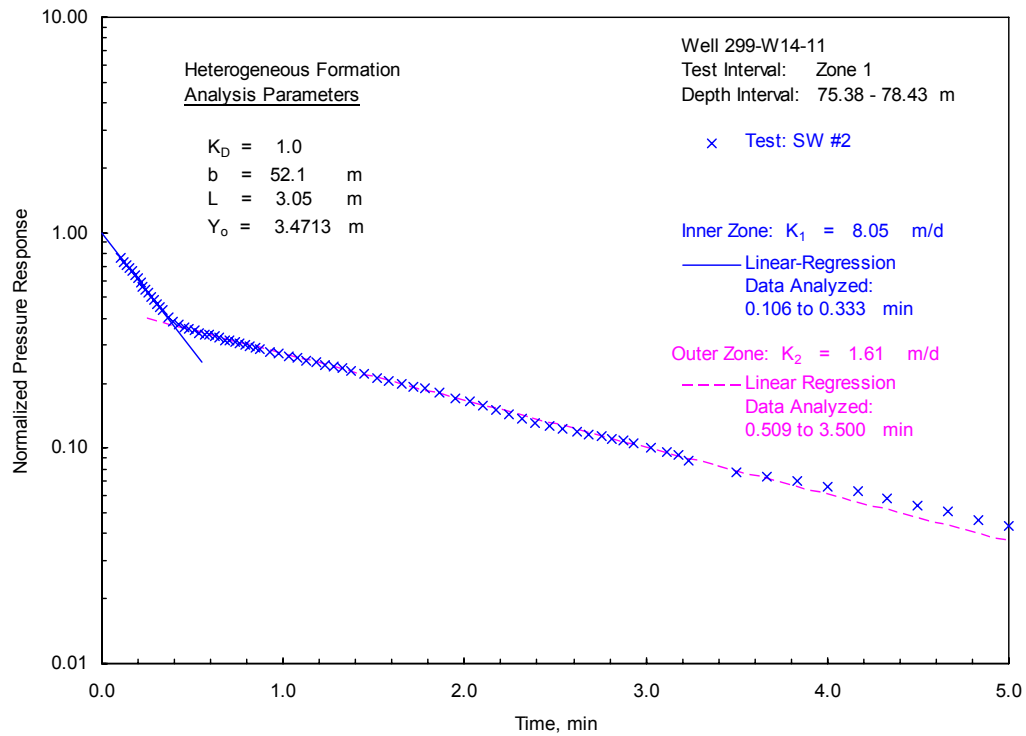


**Figure A.7.** Selected Slug-Test Analysis Plots for 299-W14-11; Zone 1—Outer Zone (Bouwer and Rice method [top] and type-curve method [bottom])

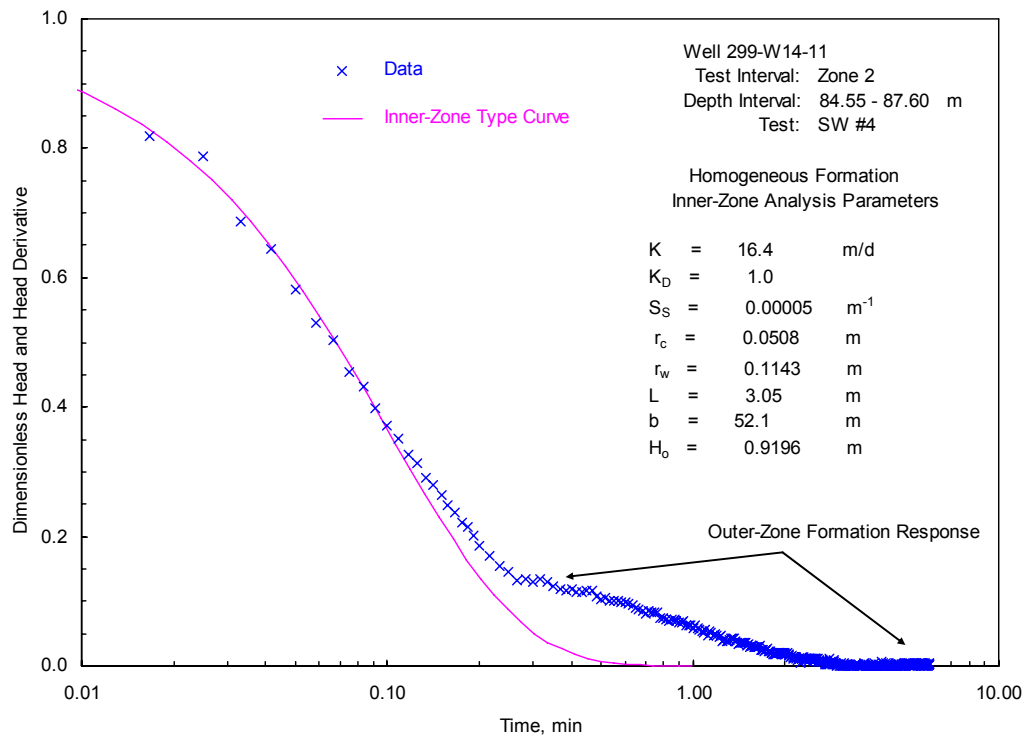
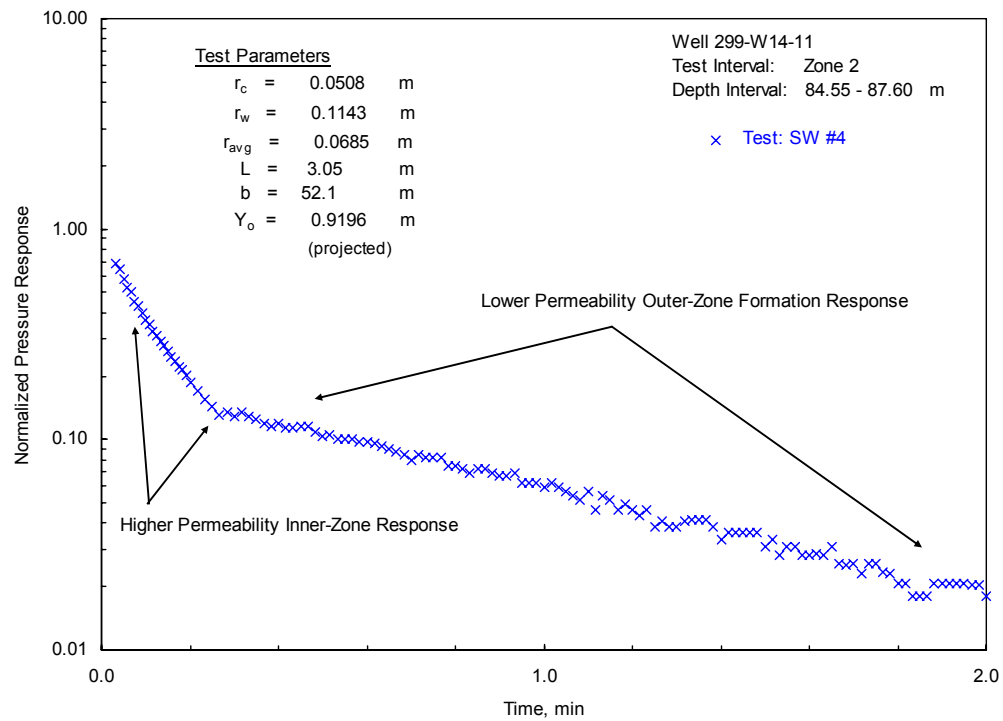


**Figure A.8.** Selected Slug-Test Analysis Plots for 299-W14-11; Zone 2—Inner Zone (Bouwer and Rice method [top] and type-curve method [bottom])

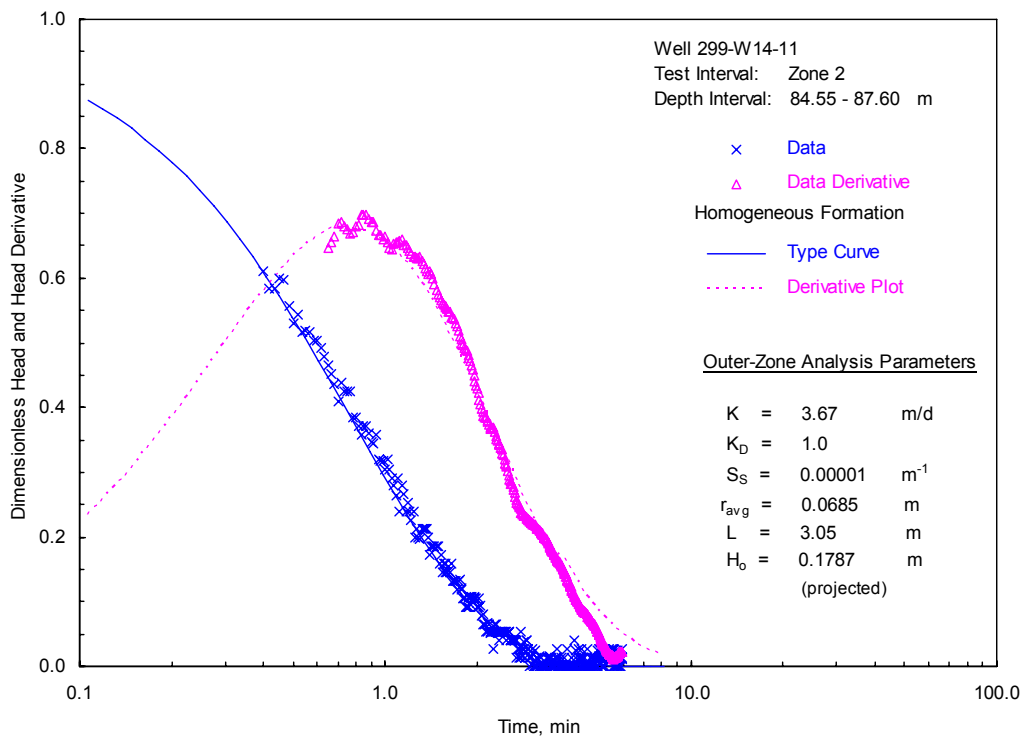
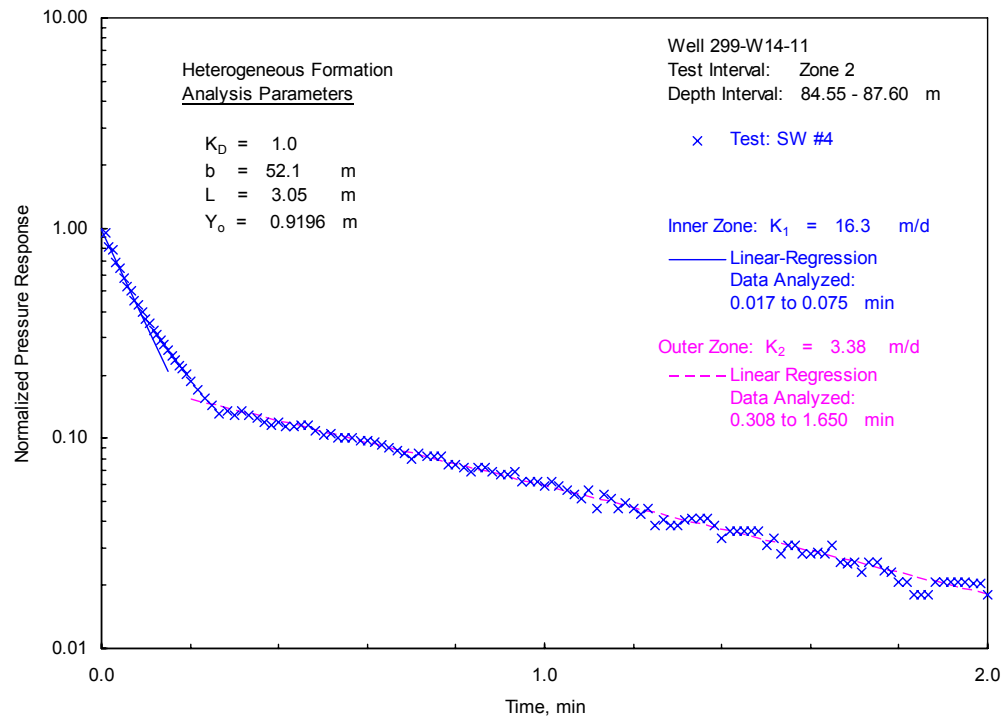


**Figure A.9.** Selected Slug-Test Analysis Plots for 299-W14-11; Zone 2—Outer Zone (Bouwer and Rice method [top] and type-curve method [bottom])

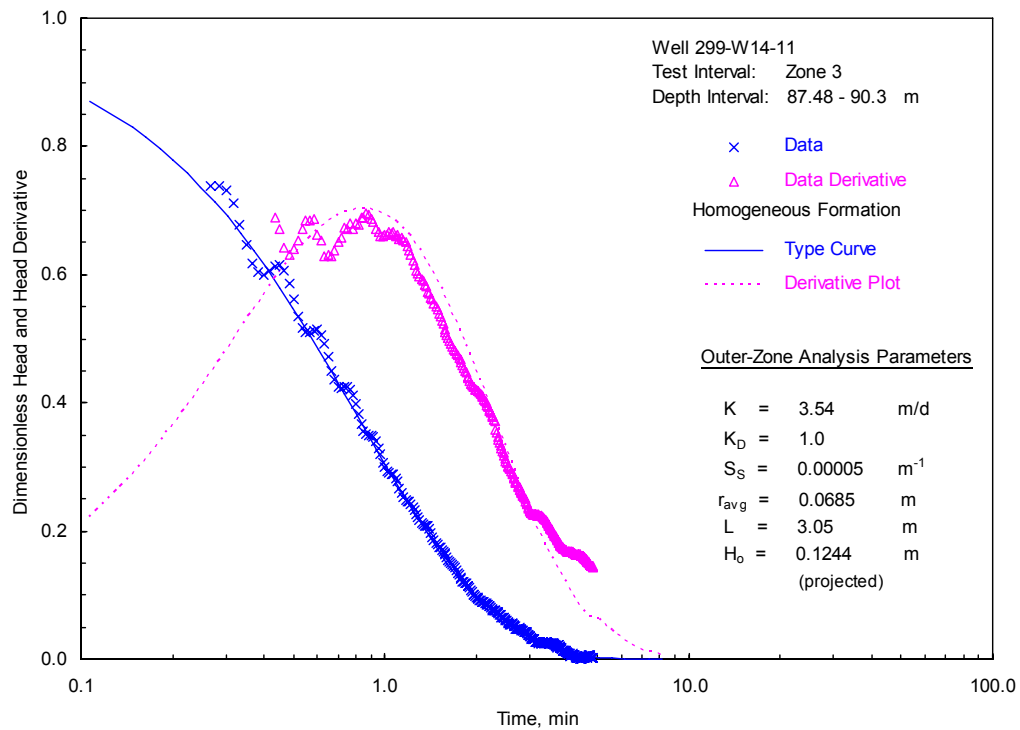
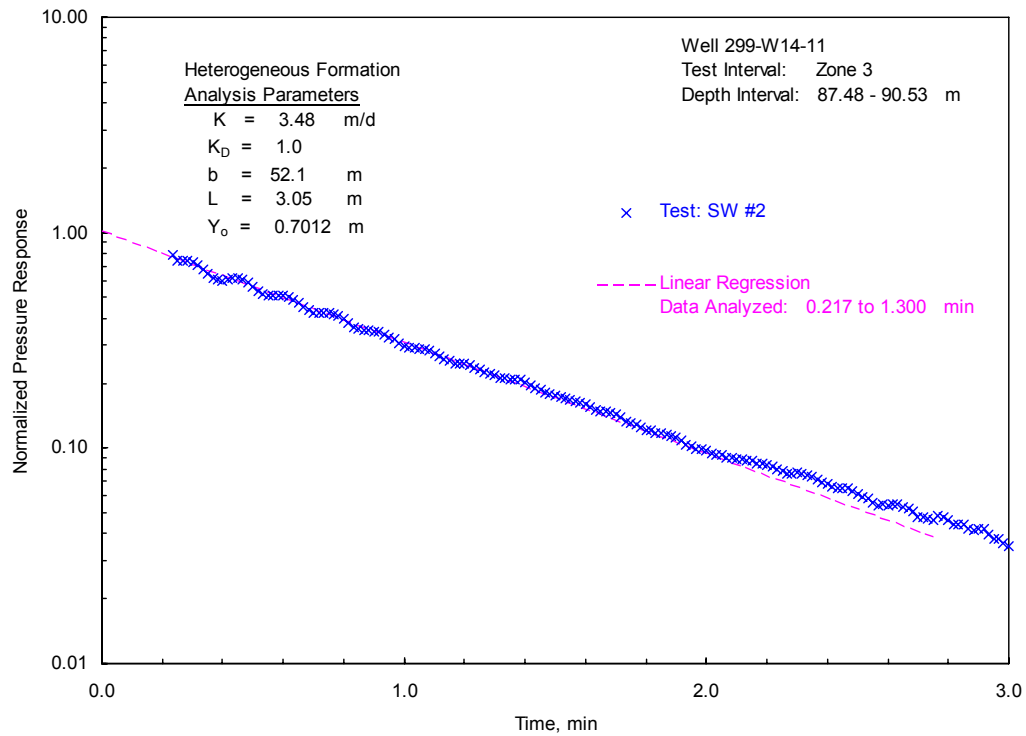


**Figure A.10.** Selected Slug-Test Analysis Plots for 299-W14-11; Zone 3 (Bouwer and Rice method [top] and type-curve method [bottom])

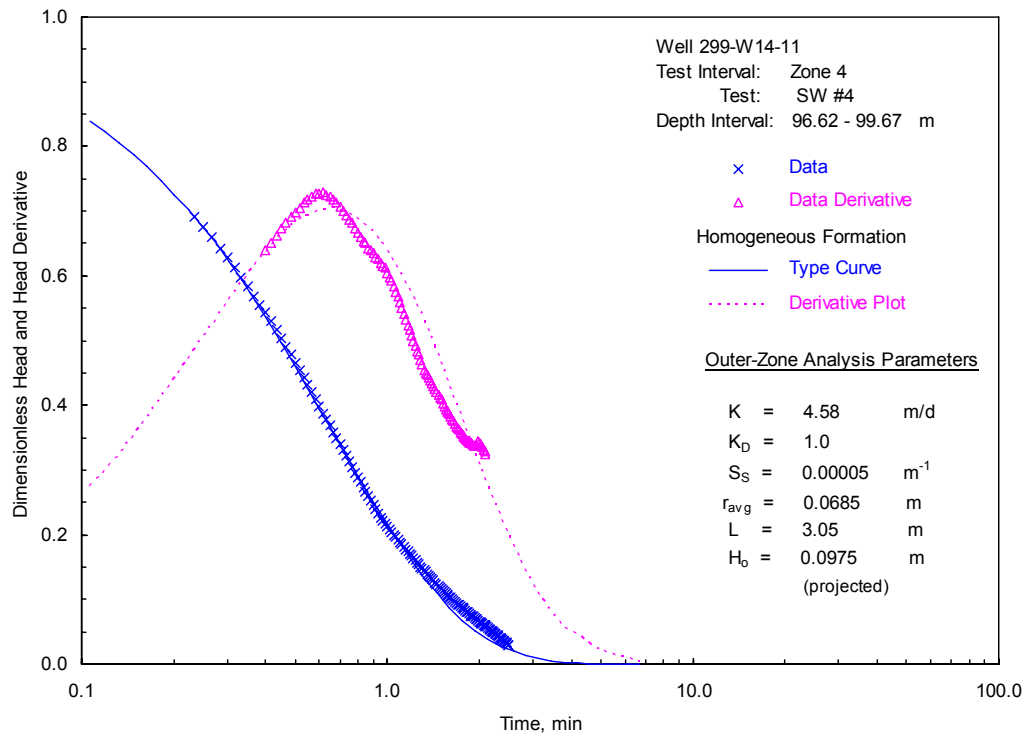
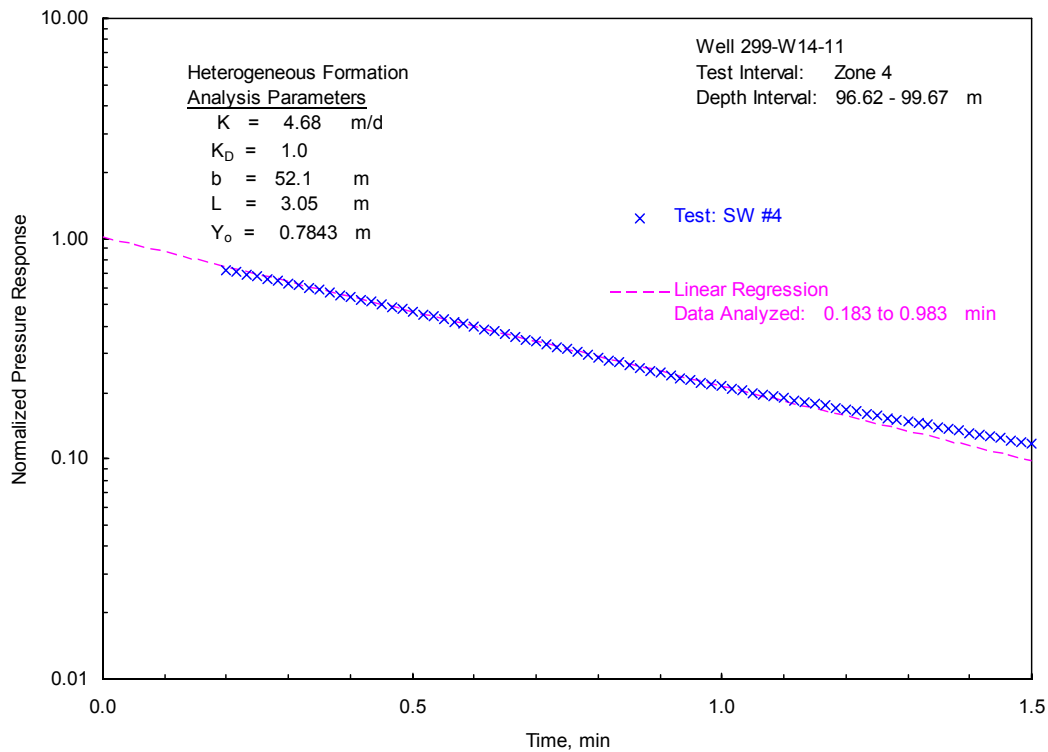


**Figure A.11.** Selected Slug-Test Analysis Plots for 299-W14-11; Zone 4 (Bouwer and Rice method [top] and type-curve method [bottom])

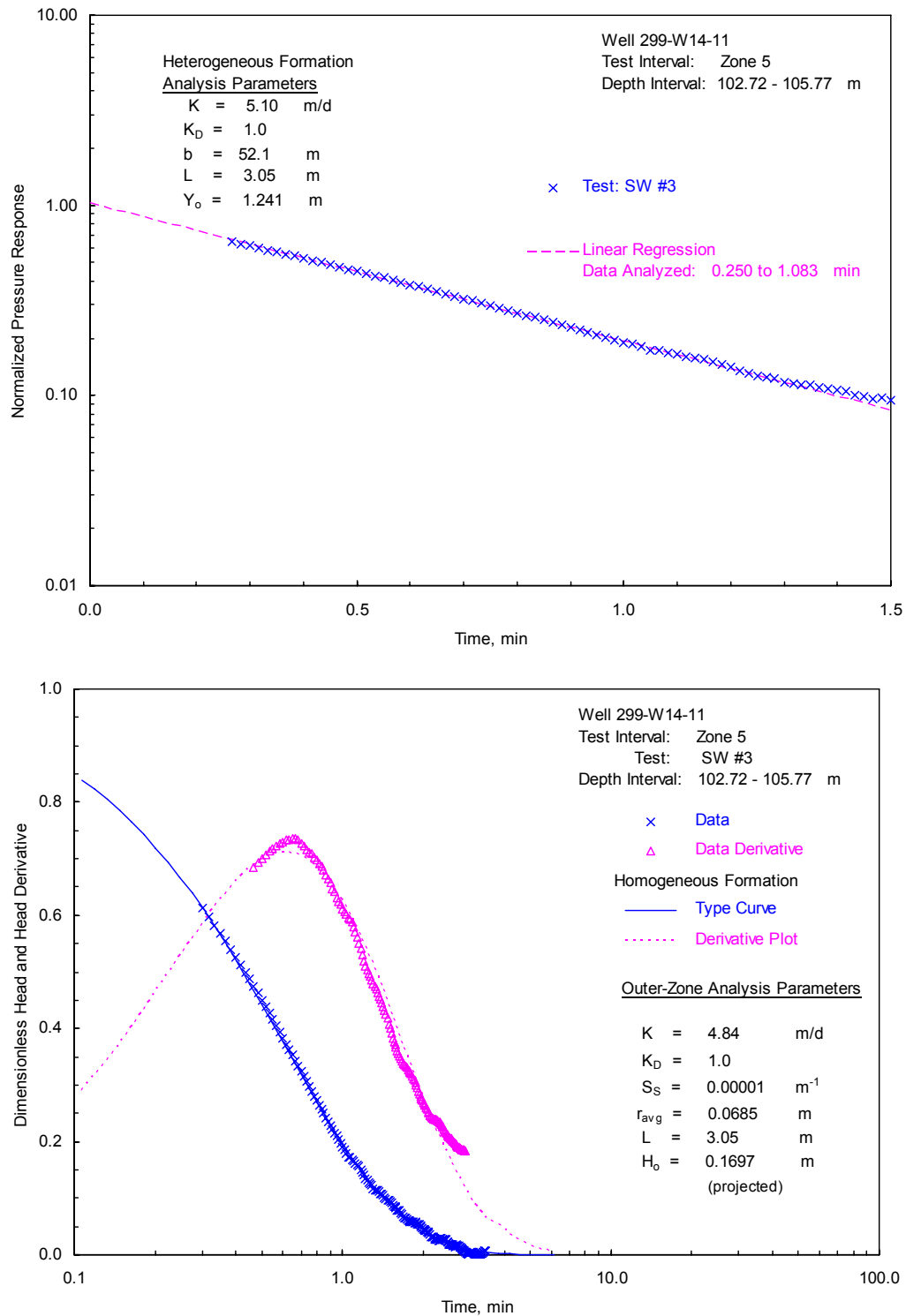


**Figure A.12.** Selected Slug-Test Analysis Plots for 299-W14-11; Zone 5 (Bouwer and Rice method [top] and type-curve method [bottom])

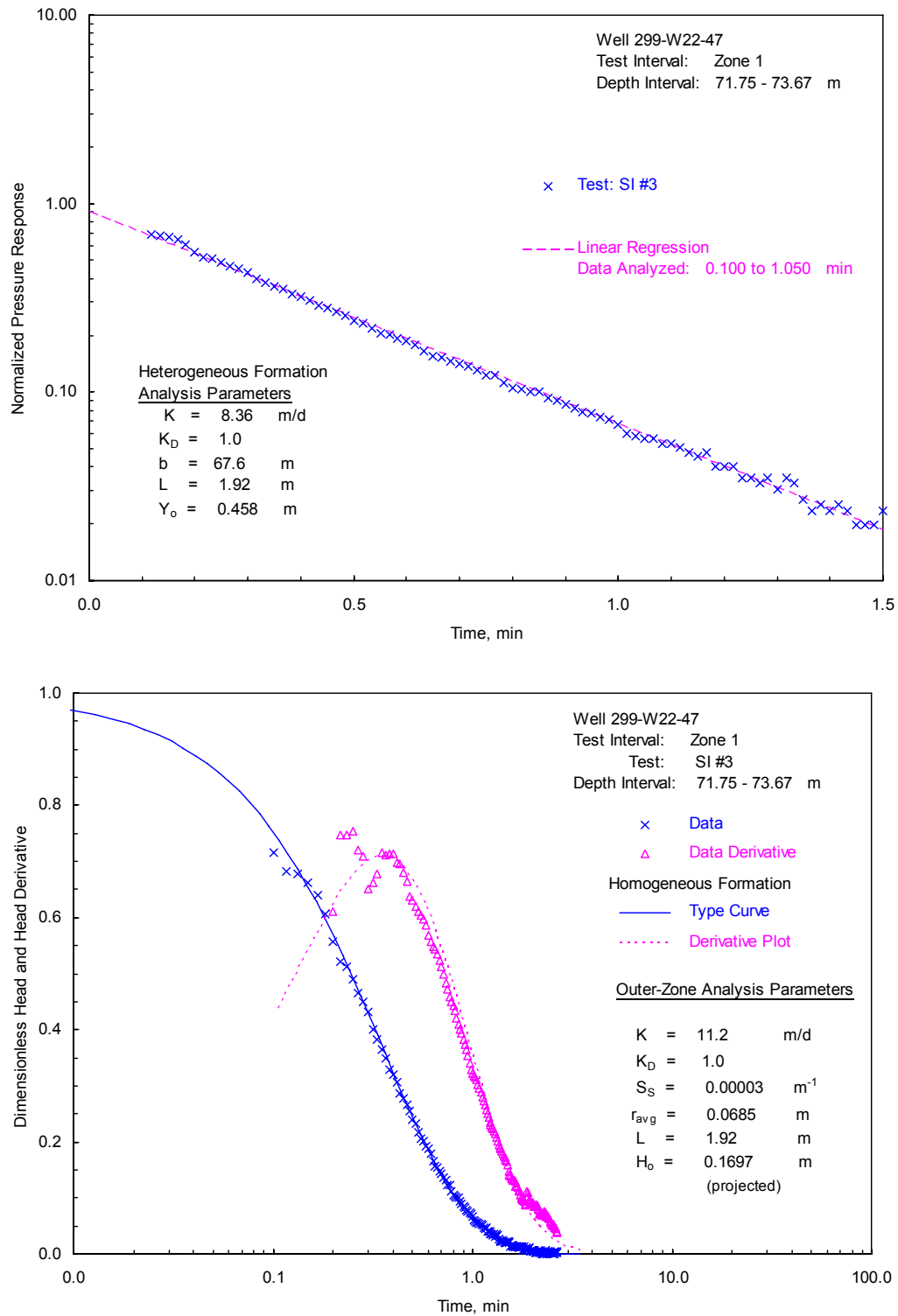


**Figure A.13.** Selected Slug-Test Analysis Plots for 299-W22-47; Zone 1 (Bouwer and Rice method [top] and type-curve method [bottom])



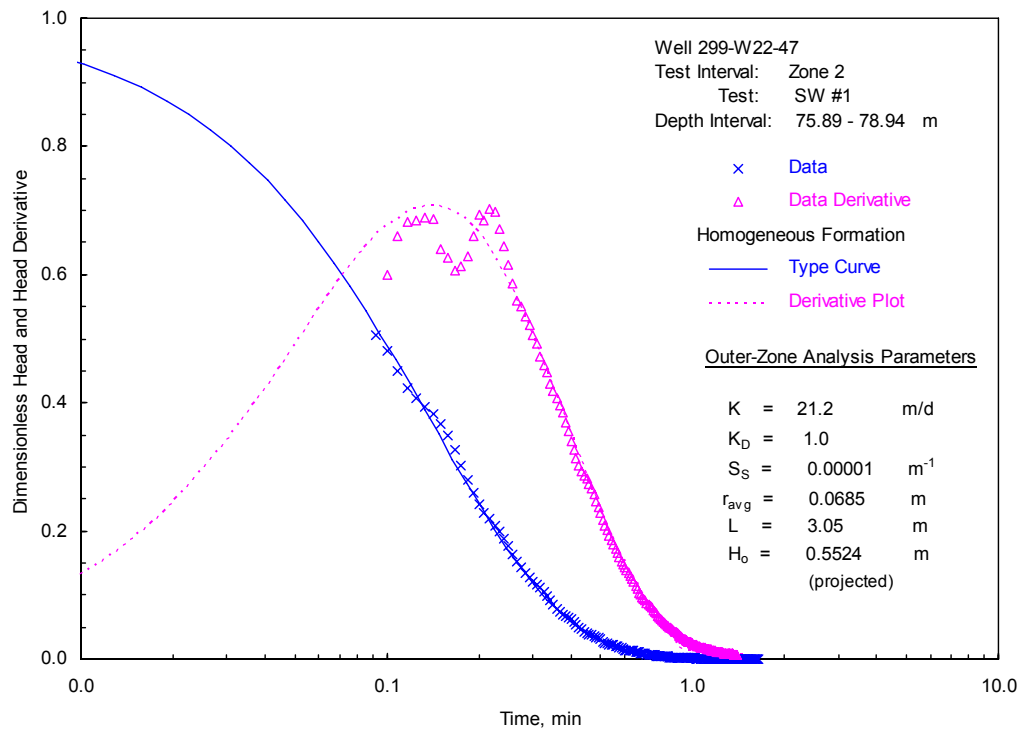
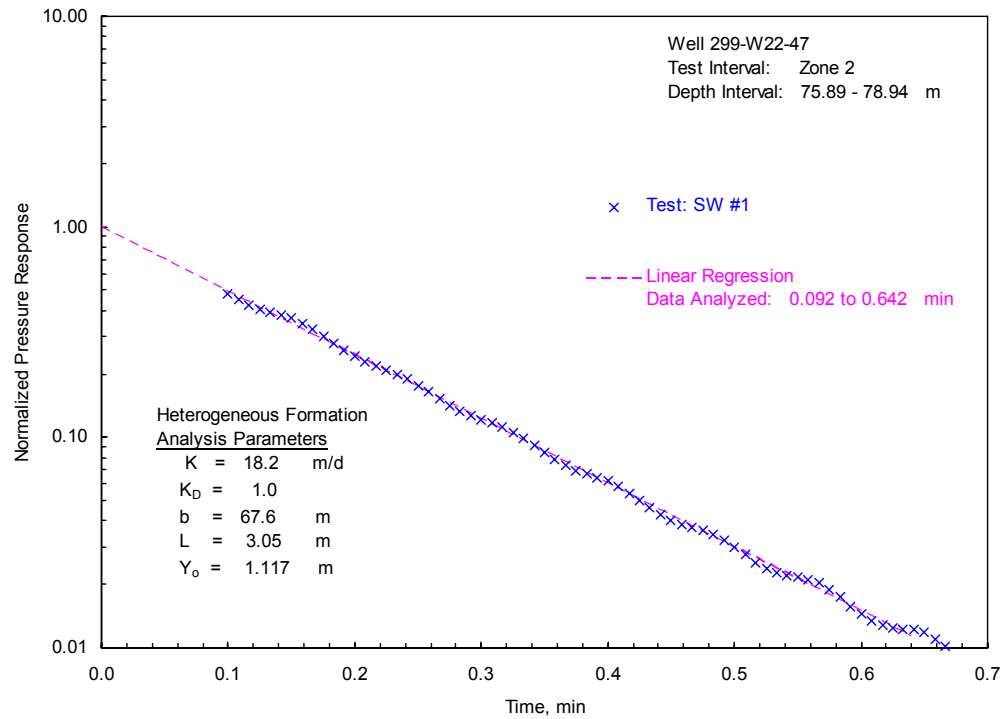


**Figure A.14.** Selected Slug-Test Analysis Plots for 299-W22-47; Zone 2 (Bouwer and Rice method [top] and type-curve method [bottom])

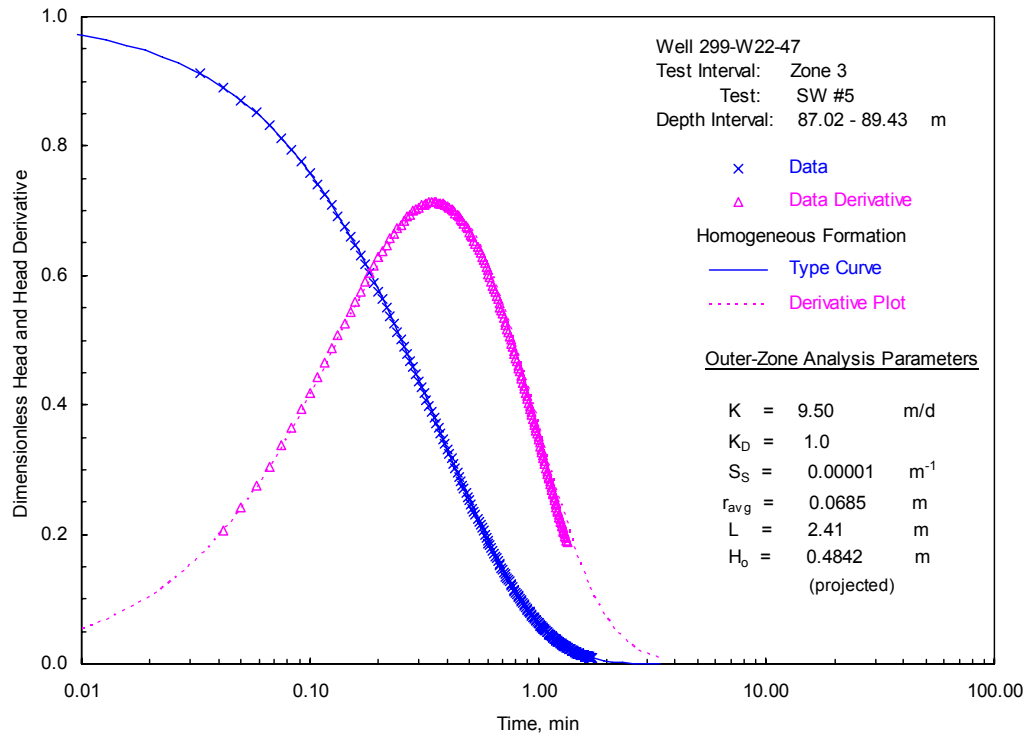
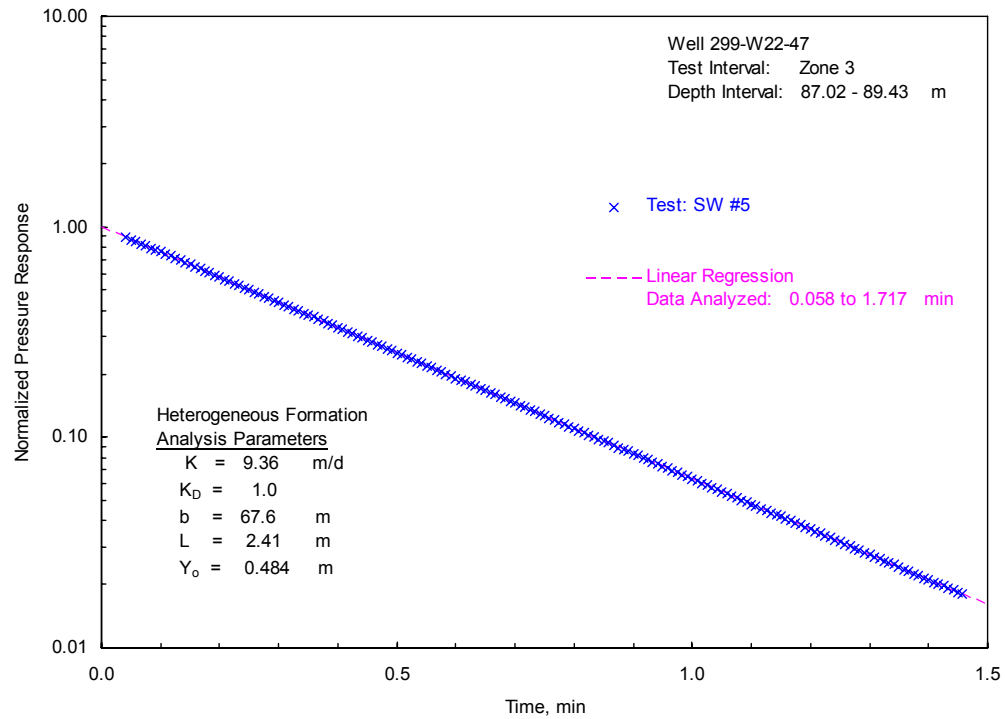


**Figure A.15.** Selected Slug-Test Analysis Plots for 299-W22-47; Zone 3 (Bouwer and Rice method [top] and type-curve method [bottom])

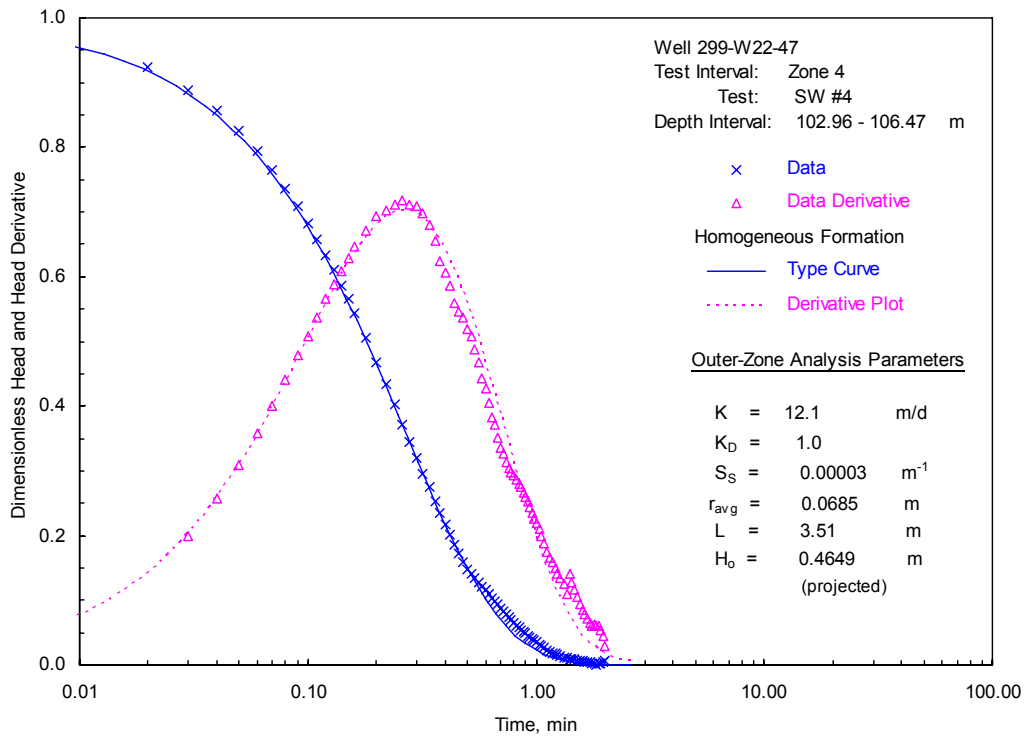
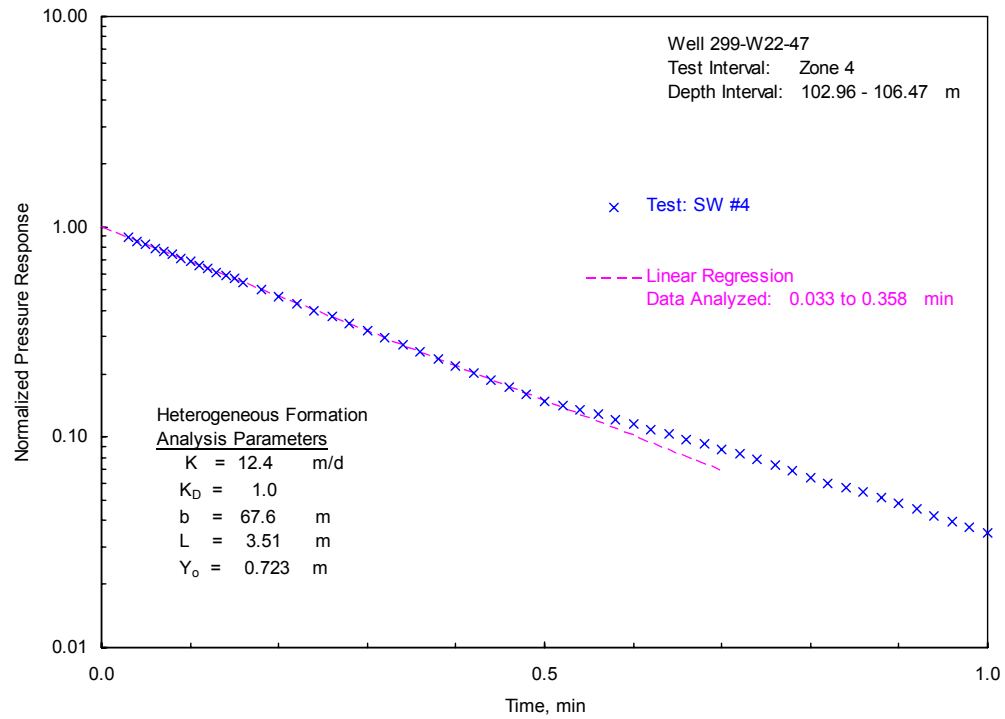


**Figure A.16.** Selected Slug-Test Analysis Plots for 299-W22-47; Zone 4 (Bouwer and Rice method [top] and type-curve method [bottom])

## **Appendix B**

### **Summary of Recent Slug-Test Characterization Results for Completed Wells Within the General 200-West Area**

**Table B.1.** Recent Slug-Test Characterization Results for Completed Wells within the General 200-West Area

Test Well	Date Tested	Well-Screen Depth, m bgs/bc*	Saturated Well-Screen Length, L m	Hydraulic Conductivity, $K_h^{(a)}$ (m/day)	Reference Source
2-W10-23	1/8/1999	68.82–79.52	10.70	2.35	Spane et al. (2001a)
2-W10-24	1/11/1999	71.00–81.70	10.70	1.68	Spane et al. (2001a)
2-W10-26	10/15/1998	66.15–76.85	10.42	1.95	Spane et al. (2001a)
2-W10-27	5/4/2001 5/7–8/2001	67.36–78.03	10.43	0.07	Spane et al. (2002)
2-W10-28	12/11–12/2001	68.64–79.31	10.42	27.9	Spane et al. (2003)
2-W11-39	2/13–15/2001	72.73–83.41	10.68	1.69	Spane et al. (2002)
2-W11-40	2/7/2001 2/13/2001	72.57–83.25	10.68	4.58	Spane et al. (2002)
2-W11-41	11/9/2000 11/13/2000	72.15–82.81	10.52	7.78	Spane et al. (2002)
2-W11-42	11/8/2000	72.16–82.84	10.19	28.1	Spane et al. (2002)
2-W11-46	9/21/2005	80.28–86.38	6.10	3.78	This Report
2-W14-11	9/20/2005	79.76–82.81	3.05	10.8	This Report
2-W14-13	10/14/1998	66.03–76.73	10.58	2.43	Spane et al. (2001a)
<p>* Depth reference point is considered to be below ground surface (bgs) or surface brass cap (bc) elevation datum.</p> <p>(a) K range based on multi-stress slug-test characterizations using the type-curve analysis method. Number in parentheses is the reported average or best estimate value for slug tests conducted.</p>					

**Table B.1. (contd)**

<b>Test Well</b>	<b>Date Tested</b>	<b>Well-Screen Depth, m bgs/bc*</b>	<b>Saturated Well-Screen Length, L m</b>	<b>Hydraulic Conductivity, <math>K_h^{(a)}</math> (m/day)</b>	<b>Reference Source</b>
2-W14-14	1/11/1999	66.14–76.81	10.67	2.64	Spane et al. (2001a)
	7/10/2002	66.14–76.81	8.92	3.22	Spane et al. (2003)
2-W14-15	11/13–14/2000	66.98–77.61	10.35	4.50	Spane et al. (2002)
2-W14-16	1/31/2001 2/5/2001	67.95–78.60	10.38	5.08	Spane et al. (2002)
2-W14-17	2/5/2001 2/7/2001	67.64–78.32	10.35	4.89	Spane et al. (2002)
2-W14-18	12/12/2001	66.46–77.13	9.92	0.54	Spane et al. (2003)
2-W15-40	10/14/1998	66.43–77.13	10.49	1.22	Spane et al. (2001a)
2-W15-41	3/29/2000	65.81–70.39	4.81	19.9	Spane et al. (2001b)
2-W15-83	10/5/2005	71.63–82.30	9.80	5.36	This Report
2-W15-94	10/13/2005	71.96–82.63	10.08	5.83	This Report
2-W15-152	10/13/2005	72.51–82.61	10.10	17.7	This Report
2-W15-763	5/3/2001	64.54–75.23	9.87	0.93	Spane et al. (2002)
<p>* Depth reference point is considered to be below ground surface (bgs) or surface brass cap (bc) elevation datum.</p> <p>(a) K range based on multi-stress slug-test characterizations using the type-curve analysis method. Number in parentheses is the reported average or best estimate value for slug tests conducted.</p>					

**Table B.1. (contd)**

<b>Test Well</b>	<b>Date Tested</b>	<b>Well-Screen Depth, m bgs/bc*</b>	<b>Saturated Well-Screen Length, L m</b>	<b>Hydraulic Conductivity, <math>K_h^{(a)}</math> (m/day)</b>	<b>Reference Source</b>
2-W19-41	10/19/1998	67.07–77.77	10.27	1.69	Spane et al. (2001a)
2-W19-42	10/15/1998	67.14–77.84	10.70	9.50	Spane et al. (2001a)
2-W19-46	7/22–23/2003	77.72–88.39	10.04	64.1	Spane and Newcomer (2004)
2-W19-47	9/20/2005	69.20–79.87	10.19	4.43	This Report
2-W22-45	1/27–28/2000	60.38–71.29	5.67	0.14	Spane et al. (2001b)
2-W22-46	4/13/2000	58.80–69.77	2.72	3.37	Spane et al. (2001b)
2-W22-47	9/27/2005	69.70–80.37	10.45	17.30	This Report
2-W22-48	1/26/2000	68.96–73.53	3.82	1.86	Spane et al. (2001b)
2-W22-49	1/27/2000	66.42–70.99	4.53	7.97	Spane et al. (2001b)
2-W22-50	4/10/2000	66.43–71.00	4.30	5.70	Spane et al. (2001b)
2-W22-79	10/19/1998	73.97–84.67	10.67	5.40	Spane et al. (2001a)
2-W22-80	10/25/2000 10/30/2000	62.49–73.17	10.53	15.4	Spane et al. (2002)
<p>* Depth reference point is considered to be below ground surface (bgs) or surface brass cap (bc) elevation datum.</p> <p>(a) K range based on multi-stress slug-test characterizations using the type-curve analysis method. Number in parentheses is the reported average or best estimate value for slug tests conducted.</p>					

**Table B.1. (contd)**

<b>Test Well</b>	<b>Date Tested</b>	<b>Well-Screen Depth, m bgs/bc*</b>	<b>Saturated Well-Screen Length, L m</b>	<b>Hydraulic Conductivity, <math>K_h^{(a)}</math> (m/day)</b>	<b>Reference Source</b>
2-W22-80	9/27/2005	62.49–73.17	8.99	13.0	This Report
2-W22-81	4/30/2001 5/1/2001	69.11–79.77	10.66	2.25	Spane et al. (2002)
2-W22-82	4/25–26/2001	68.92–79.61	10.40	1.45	Spane et al. (2002)
2-W22-83	4/26/2001	68.98–79.64	10.19	1.00	Spane et al. (2002)
2-W22-84	12/4/2001	70.71–81.38	10.40	1.51	Spane et al. (2003)
2-W22-85	12/5/2001	66.18 – 76.82	10.01	7.73	Spane et al. (2003)
2-W23-15	1/24/2000	56.60–67.79	5.73	0.05	Spane et al. (2001b)
2-W23-20	11/1/2000	65.68–76.35	10.67	16.9	Spane et al. (2002)
2-W23-21	1/30-31/2001	64.79–76.11	11.02	0.73	Spane et al. (2002)
<p>* Depth reference point is considered to be below ground surface (bgs) or surface brass cap (bc) elevation datum.</p> <p>(a) K range based on multi-stress slug-test characterizations using the type-curve analysis method. Number in parentheses is the reported average or best estimate value for slug tests conducted.</p>					



## Distribution

### No. of Copies

#### ONSITE

18	<u>Fluor Hanford</u>	
	Mark Byrnes	E6-44
	Dave Erb	E6-35
	John Smoot	E6-35
	Jon Lindberg	E6-35
	John McDonald	E6-35
	Stuart Luttrell (5)	E6-35
	Tony Knepp	E6-44
	Glen Triner	R3-62
	Duane Horton	E6-35
	Brent Barnett	E6-35
	Bruce Williams	E6-44
	Dave Miller	E6-44
	Chris Sutton	E6-44
	Craig Swanson	E6-35
4	<u>U.S. Department of Energy-Richland Operations</u>	
	Doug Hildebrand	A6-38
	Arlene Tortoso	A6-38
	John Morse	A6-38
	Public Reading Room	H2-53
2	<u>U.S. Department of Energy-Office of River Protection</u>	
	Robert Lober	H6-60
	Mary Beth Burandt	H6-60

### No. of Copies

#### ONSITE

1	<u>U.S. Environmental Protection Agency</u>	
	Dennis Faulk	B1-46
2	<u>Washington State Department of Ecology</u>	
	Dib Goswami	H0-57
	Zelma Jackson-Maine	H0-57
3	<u>CH2M Hill Hanford Group, Inc.</u>	
	Fred Mann	H6-03
	Dave Myers	H6-03
	Mike Connelly	H6-03
6	<u>Pacific Northwest National Laboratory</u>	
	D. Newcomer (2)	K6-96
	F. A. Spane (2)	K6-96
	Hanford Technical Library (2)	P8-55

## Electronic Distribution

### U.S. Department of Energy-Richland Operations

Matt Tonkin [matt@sspa.com](mailto:matt@sspa.com)

### Pacific Northwest National Laboratory

Mark D. Freshley	<a href="mailto:mark.freshley@pnl.gov">mark.freshley@pnl.gov</a>
Jonathan S. Fruchter	<a href="mailto:john.fruchter@pnl.gov">john.fruchter@pnl.gov</a>
George V. Last	<a href="mailto:george.last@pnl.gov">george.last@pnl.gov</a>
Philip E. Long	<a href="mailto:Philip.long@pnl.gov">Philip.long@pnl.gov</a>
Robert E. Peterson	<a href="mailto:Robert.Peterson@pnl.gov">Robert.Peterson@pnl.gov</a>
Mark L. Rockhold	<a href="mailto:Mark.Rockhold@pnl.gov">Mark.Rockhold@pnl.gov</a>
Ronald M. Smith	<a href="mailto:rmsmith@pnl.gov">rmsmith@pnl.gov</a>
Paul D. Throne	<a href="mailto:paul.thorne@pnl.gov">paul.thorne@pnl.gov</a>
Vince Vermeul	<a href="mailto:vince.vermeul@pnl.gov">vince.vermeul@pnl.gov</a>
Mark D. Williams	<a href="mailto:mark.d.williams@pnl.gov">mark.d.williams@pnl.gov</a>
DOE Public Reading Room	<a href="mailto:doe.reading.room@pnl.gov">doe.reading.room@pnl.gov</a>